Detoxification of heavy metal ions from aqueous solutions using a novel lignocellulosic multi–metal binding biosorbent

BY

Atefeh Abdolali

A Dissertation

Submitted in fulfilment for the degree of

DOCTOR OF PHILOSOPHY

In

Environmental Engineering

UTS
UNIVERSITY OF TECHNOLOGY SYDNEY

University of Technology, Sydney

New South Wales, Australia

July 2017

Certificate of original authorship

I certify that the work in this thesis has not previously been submitted for a degree nor has it been submitted as part of requirements for a degree except as fully acknowledged within the text.

I also certify that the thesis has been written by me. Any help that I have received in my research work and the preparation of the thesis itself has been acknowledged. In addition, I certify that all information sources and literature used are indicated in the thesis.

Signature of Student:

Atefeh Abdolali

Date:

ACKNOWLEDGMENTS

Firstly, I would like to express my sincere gratitude to my advisor Professor Huu Hao Ngo for the continuous support of my PhD study and related research, for his patience, motivation, and immense knowledge. His guidance helped me in all the time of research and writing of this thesis. I could not have imagined having a better advisor and mentor for my PhD study. Besides my advisor, I would like to thank my co–supervisor Dr Wenshan Guo for her mentor supports and useful comments on this dissertation. I appreciate Md Johir, UTS Environmental Engineering Laboratories Manager, for his patience guidance on the use of the laboratory equipment and for his supports in the lab.

This project would not have been possible without substantial help of Savo Grce and Brad Grief from Sydney Water providing me with municipal wastewater used in my experiments.

I gratefully acknowledge the funding sources that made my PhD work possible. I was funded by the Australian Government, under the Department of Innovation, Industry, Science and Research (DIISRTE) for Australian Postgraduate Award (APA) Scholarship. This research was also supported through an "Australian Government Research Training Program Scholarship". The financial support from Centre for Technology in Water and Wastewater (CTWW), UTS is highly appreciated as well.

Last but not the least, my most profound thanks, my most heartfelt appreciation, my deepest gratitude goes to my loving, supportive and encouraging family. I would like to thank my parents who raised me with a love of science and supported me in all my pursuits and to my brothers (Hamed and Ali) and my little sister (Mahshad) for supporting me spiritually throughout writing this thesis and my life in general. I would like to thank my husband, Ali, whose faithful support during my PhD study is so appreciated. Particularly in the last year by helping me to take care our beloved baby boy, Darian.

<div align="right">

Thank you

Atefeh Abdolali | July 2017

</div>

<div align="center">

———————

iii

</div>

DEDICATION

To my loveliest love, my most favourite boy in the world;

*My dearest **Darian***

Who spent whole days and nights of this project beside me!

JOURNAL PAPERS PUBLISHED

1. **Abdolali, A.**, Ngo, H.H., Guo, W.S., Zhou, J.L., Zhang, J., Liang, S., Chang, S.W., Nguyen , D.D., 2017. Application of a breakthrough biosorbent for removing heavy metals from synthetic and real wastewaters in a lab–scale continuous fixed–bed column. Bioresource Technology 229, 78–87.

2. **Abdolali, A.**, Ngo, H.H., Guo, W.S., Lu, S., Chen, S.S., Nguyen, N.C., Zhang, X., Wang, J., Wu, Y., 2016. A breakthrough biosorbent in removing heavy metals: equilibrium, kinetic, thermodynamic and mechanism analyses in a lab–scale study. Science of the Total Environment 542, 603–611.

3. **Abdolali, A.**, Ngo, H.H., Guo, W.S., Zhou, J.L., Du, B., Wei, Q., Wang, X.C., Nguyen, P.D., 2015. Characterization of a multi–metal binding biosorbent: chemical modification and desorption studies. Bioresource Technology 193, 477–487.

4. **Abdolali, A.**, Ngo, H.H., Guo, W.S., Lee, D.J., Tung, K.L., Wang, X.C., 2014. Development and evaluation of a new multi–metal binding biosorbent Bioresource Technology 160, 98–106.

5. **Abdolali, A.**, Guo, W.S., Ngo, H.H., Chen, S.S., Nguyen, N.C., Tung, K.L., 2014. Typical lignocellulosic wastes and by–products for biosorption process in water and wastewater treatment: A critical review. Bioresource Technology 160, 57–66.

CONFERENCE PRESENTATION

1. **Abdolali, A.**, Ngo, H.H., Guo, W.S., (2014). Standardized Preparation Method for a New Multi–Metal Binding Biosorbent for Cadmium, Copper, Lead and Zinc Biosorption. Presented poster at ESBES–IFIBiop Conference, Lille, France, 7th–10th September 2014.

2. **Abdolali, A.**, Ngo, H.H., Guo, W.S., (2013). Detoxification of heavy metal–bearing effluents on a novel multi–metal binding biosorbent, Accepted article in the 6thInternational Conference on the "Challenges in Environmental Science and Engineering" (CESE–2013), Daegu, Korea, 29th October–2nd November 2013.

TABLE OF CONTENTS

LIST OF TABLES

LIST OF ILLUSTRATIONS

NOMENCLATURES

Symbol	Description	Unit
a	Dose Response model exponent	
A	Column area	cm^2
Å	Angstrom	
a_S	Sips model constants	L/mg
b_L	Langmuir constant	L/mg
C=C–C	Asymmetric stretching aromatic rings	
$C_2H_4O_2S$	Mercapto–acetic acid	
$C_2H_4O_2S$	Thioglycolic acid	
C_2H_6O	Ethanol	
C_3H_6O	Acetone	
$C_6H_8O_7$	Citric acid	
$Ca(OH)_2$	Calcium hydroxide	
$CaCl_2$	Calcium chloride	
CaO	Calcium oxide	
C_{ads}	Adsorbed metal concentration	mg/L
C_b	Breakthrough concentration,	mg/L
$Cd(NO_3)_2 \cdot 4H_2O$	Cadmium nitrate tetrahydrate	
C_e	Effluent metal ion concentration	mg/L
C_{eq}	Equilibrium metal concentration	mg/L
C_f	Equilibrium metal concentrations	mg/L
CF_p	Overall sorption process concentration factor	
CH_2O	Formaldehyde	
CH_2O_2	Formic Acid	
CH_3COOH	Acetic Acid	
CH_3OH	Methanol	
C_i	Initial/ Influent metal concentrations	mg/L
–C–O–C=O	Symmetric stretching of ester groups	
–COOH	Carboxyl groups	
C_p	Eluted metal concentration at t_p	mg/L

Symbol	Description	Unit
CS_2	Carbon disulfide	
$Cu_3(NO)_2 \cdot 3H_2O$	Copper nitrate trihydrate	
D_i	Inner diameter	cm
E	Mean free energy of adsorption calculated by Dubinin–Radushkevich isotherm	kJ/mol
g	gram	
g/L	gram per litre	
H_2O_2	Hydrogen peroxide	
H_2SO_4	Sulphuric acid	
H_3PO_4	Phosphoric acid	
H–C–H	Asymmetric and symmetric stretch	
HCl	Hydrochloric acid	
HFO	Iron(III) oxy–hydroxide	
HNO_3	Nitric acid	
hr	hour(s)	
K	Kelvin	
K_1	The first–order reaction rate equilibrium constant	min^{-1}
K_2	The second–order reaction rate equilibrium constant	$g\ mg^{-1}\ min^{-1}$
K_2MnO_4	Potassium manganate	
k_{BDST}	BDST adsorption rate constant that describes the mass transfer from the liquid to the solid phase	L/mg h
K_F	Freundlich constant	L/g
K_p	Intra–particle diffusion kinetic model constant	$mg\ g^{-1}min^{-0.5}$
K_{RP}	Redlich–Peterson model constants	L/g
K_S	Sips model constants	L/g
k_{Th}	Thomas rate constant	mL/ mg min
k_{Y-N}	Yoon–Nelson proportionality constant	1/min

Symbol	Description	Unit
L	litre	
L	Bed height	cm
$L_{critical}$	Critical bed depth	cm
M	Molarity	mol/L
m	Mass of biosorbent in batch system	g
M	Total mass of the biosorbent in the column	g
m_{total}	Amount of metal ions sent to the column at different time	mg
mg/g	milligram of adsorbate per gram of adsorbent	
$MgCl_2$	Magnesium chloride	
$MgSO_4$	Magnesium sulphate	
min	minute(s)	
mol/g	mol per gram	
n	Freundlich exponent	
Na_2CO_3	Sodium carbonate	
NaCl	Sodium chloride	
$NaHCO_3$	Sodium bicarbonate	
$NaNO_3$	Sodium nitrate	
NaOH	Sodium hydroxide	
N_{BDST}	BDST biosorption capacity	mg/L
NH_4^+	Ammonium	
NH_4OH	Ammonium hydroxide	
$Pb(NO_3)_2$	Lead nitrate	
Q	Volumetric flow rate	mL/min
q_c	Column capacity (mg)	
q_{D-R}	Maximum adsorption capacity for heavy metal ions calculated by Dose Response model	mg/g
q_e	Metal adsorbed at equilibrium	mg/g
$q_{e,d}$	gram of desorbed metal per gram of adsorbent in column	mg/g

Symbol	Description	Unit
$q_{m,L}$	Langmuir maximum metal biosorption capacity	mg/g
q_t	Metal adsorbed at time t	mg/g
q_{Th}	Thomas maximum adsorption capacity for heavy metal ions	mg/g
rpm	round(s) per minute	
t	time	min
t_b	Breakthrough time ($C_e/C_i = 10\%$)	min
t_p	The time when the elution rate reaches the peak	min
t_{sat}	Saturation or exhaustion time ($C_e/C_i = 90\%$)	min
t_{total}	Total flow time	min
v	Solution volume in batch mode	L
v	Superficial velocity or the linear flow velocity of metal solution through the bed	cm/min
$V_{W,b}$	Treated water volume	L
$Zn(NO_3)_2 \cdot 6H_2O$	Zinc nitrate hexahydrate	
$ZnCl_2$	Zinc chloride	
$\Delta G°$	Gibbs free energy change	kJ/mol
$\Delta H°$	Enthalpy change	kJ/mol
$\Delta S°$	Entropy change	kJ/mol K
%E	Elution efficiency	%
%R	Metal removal (%)	%
$[H_3O]^+$	Hydronium	
°C	Degree Celsius	

ABBREVIATIONS

Symbol	Description
BDST	Bed Depth Service Time
CSTR	Continuous Stirred–Tank Reactor
AER	Adsorbent exhaustion rate in column
ANOVA	Analysis of Variance
AP	Apple peel
AV	Avocado peel
BET	Brunauer Emmett Teller
BOD	Biological Oxygen Demand
CC	Corncob
COD	Chemical Oxygen Demand
CP	Coir peat
CW	Coffee waste
EBCT	Empty Bed Contact Time (min)
EDTA	Ethylene diamine triacetic acid
EDTAD	Ethylene diamine tetraacetic dianhydride
EDX	Energy Dispersive X–Ray
ES	Egg shell
EU	Eucalyptus leave
FTIR	Fourier Transform Infrared Spectroscopy
GG	Garden grass
GS	Grape stalk
HLR	Hydraulic Loading Rate (m^3/m^2 hr)
LC	Lychee rind
MG	Mango skin
ML	Maple leave
MMBB	Multi–Metal Binding Biosorbent
MP	Mandarin peel
MP–AES	Microwave Plasma–Atomic Emission Spectrometer
MTZ	Mass Transfer Zone (cm)

Symbol	Description
OP	Orange peel
pH	potential Hydrogen
ppm	Part per million
PS	passion fruit skin
R^2	Coefficient of determination
RMSE	Residual Root Mean Square Error
RO	Reverse Osmosis
SC	Sugarcane bagasse
SD	Sawdust
SEM/EDS	Scanning electron microscopy with X–ray microanalysis
SSE	Error Sum of Square
TEM	Transmission Electron Microscopy
TOC	Total Organic Carbon
TSS	Total Suspended Solids
TW	Tea waste
WWTP	Water and Wastewater Treatment Plant
XPS	X–ray Photoelectron Spectroscopy

GREEK SYMBOLS

Symbol	Description	Unit
β_{RP}	Redlich–Peterson model exponent	
β_S	Sips model exponent	
μ	micro	
τ	the time required for retaining 50% of the initial adsorbate	min

PhD DISSERTATION ABSTRACT

Author: ATEFEH ABDOLALI

Date: July 2017

Thesis title: Detoxification of heavy metal ions from aqueous solutions using a novel lignocellulosic multi-metal binding biosorbent

Statistical data: 188 pages, 22 tables, 39 figures, and 188 references

School: Civil and Environmental Engineering

Supervisors: Prof. Dr Huu Hao Ngo (Principal supervisor)

Dr Wenshan Guo (Co-supervisor)

Keywords: Agro-industrial waste; Biosorption; Breakthrough curve; Chemical Modification; Fixed-bed column; Heavy metal; Kinetics; Modeling

Abstract

Since, the availability of a biomass at a low cost is a key factor dictating its selection for a biosorption, thus agro-industrial wastes and by-products are considered as alternatives for heavy metal biosorption development. Utilizing potentials of combination of common agro-industrial wastes and by-products let us have different kinds of active binding sites at same time in wastewater treatment. In order to make the biosorption process more suitable for heavy metal removal, both batch and continuous systems have been studied. Two breakthrough multi-metal binding biosorbent made from a combination of tea wastes, maple leaves and mandarin peel (MMBB1) and a mixture of tea waste, sawdust and corncob (MMBB2) were applied to evaluate their biosorptive potential of heavy metal removal from synthetic multi-metal solutions. FTIR and SEM were conducted, before and after biosorption, to explore the intensity and position of the available functional groups and changes in adsorbent surface morphology. Carboxylic and hydroxyl groups were found to be the principal

functional groups for the sorption of metals. MMBB1 exhibited better performance at pH 5.5 with maximum sorption capacities of 41.48, 39.48, 94.0 and 27.23 mg/g for Cd(II), Cu(II), Pb(II) and Zn(II), respectively. In batch system, MMBB1 was selected for further process optimization, modification, characterization and thermodynamic studies. The data indicated that Langmuir isotherm and pseudo–second order kinetics model describe the experimental data very well. The maximum amounts of biosorption capacity of modified MMBB increased to 69.56, 127.70, 345.20 and 70.55 mg/g for Cd(II), Cu(II), Pb(II) and Zn(II), respectively. Then a continuous fixed–bed study was carried out by utilizing the modified MMBB for cadmium, copper, lead and zinc removal from synthetic solution and real wastewater. The effect of operating conditions i.e. influent flow rate, metal concentration and bed depth was investigated at optimal pH (5.5±0.1) for a synthetic wastewater. Results confirmed that the total amount of metal adsorption decreased with increasing influent flow rate and also increased with increasing each metal concentration. The maximum biosorption capacity of 38.25, 63.37, 108.12 and 35.23 mg/g for Cd, Cu, Pb and Zn, respectively, were attained at 31 cm bed height, 10 mL/min flow rate and 20 mg/L initial concentration. The Thomas model found better describing the whole dynamic behaviour of the column. Finally, desorption studies indicated that metal–loaded biosorbent could be used after three consecutive sorption, desorption and regeneration cycles by applying a semi–simulated real wastewater.

Graphical abstract:

Biosrbent selection for Cd, Cu, Pb and Zn removal

Isothem, kinetic and thermodynamic studies

Multi–Metal Binding Biosorbent

Standardization and characterization of biosorbent combination in a batch system

Optimization of experimental conditions in a lab-scale column

XXX
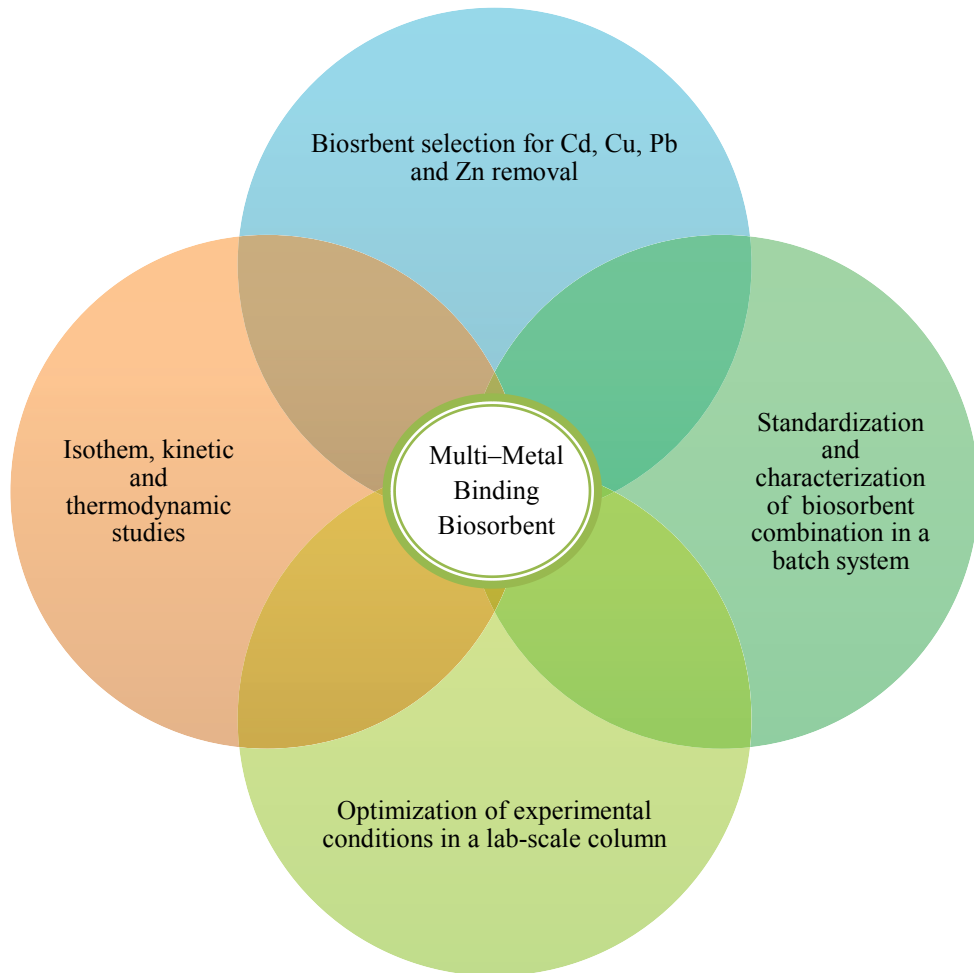
Chapter 1

Introduction

Chapter 1 Introduction

1.1 *Background of research*

As a consequence of global industrialisation and extensive use of machines in many industries, heavy metal ions, dyes, pesticides, humic substances, detergents and other persistent organic pollutants have been released into the aquatic environment. Besides, water sources shortage became a chronic worldwide environmental concern. Therefore, it is very urgent to treat industrial wastewater effluents, before they are discharged into the environment. It is essential that such action is in accordance with effective health and environmental regulations developed for various bodies of water (Shanmugaprakash and Sivakumar, 2015; Fu and Wang, 2011; Kalavathy and Miranda, 2010).

1.1.1 *Adverse effects of heavy metal ions and related environmental concerns*

Heavy metal ions such as cadmium, lead, zinc, nickel, copper, mercury and chromium or their compounds are now recognized as serious toxic pollutants due to their non–biodegradability, high environmental mobility and strong tendency for bioaccumulation in the food chain (Vargas–García et al., 2012; Akar et al., 2012). For instance, in latest decades, the annual global release of heavy metal reached 22,000 tons (metric tons) for cadmium, 939,000 tons for copper, 783,000 tons for lead and 1,350,000 tons for zinc (Ansari et al., 2014). The exposure to these toxic components causes both long term and acute illnesses in human and live stocks (Shanmugaprakash and Sivakumar, 2015; Kalavathy and Miranda, 2010).

1.1.2 *Removal technologies for heavy metal removal*

To remediate heavy metal polluted effluents, a wide range of physicochemical/ biological treatment technologies are currently employed in various industries (e.g. filtration, reverse osmosis (RO), membrane bioreactor, adsorption, chemical precipitation, coagulation, electroplating, evaporation, oxidation/ reduction, ion exchange, activated sludge, aerobic and anaerobic treatment, electrolysis, magnetic

separation, extraction, electrochemical techniques, etc.) (Patil et al., 2016; Fu et al., 2013; Bhatnagar and Sillanpää, 2010; Miretzky and Cirelli, 2010; Crini, 2006). Nonetheless, some of existing methods are very technically complicated and not effective enough especially in low concentrations when the target heavy metals concentration falls below 100 mg/L. Additionally, some methods also have disadvantages of high chemical reagent usage, high energy requirements, as well as the disposal problem of toxic secondary sludge (Montazer–Rahmati et al., 2011; Aksu et al. 2007). Recently, the attention has been addressed towards cheap agro–industrial wastes and by–products as biosorbents (Bhatnagar et al., 2015; Bhatnagar and Sillanpaa, 2010).

1.1.3   Biosorption

Among common and conventional methods for removing toxic metal ions from aqueous solution, biosorption on cheap, biodegradable, abundant and very available bio–wastes and by–products from agriculture and food industries cut the process cost significantly (Witek–Krowiak et al., 2011). Generally, biosorption process can reduce capital costs by 20%, operational costs by 36% and total treatment costs by 28% compared with the current systems (Bulut and Tez, 2007; Loukidou et al., 2004). Moreover, main advantages of these adsorbent are acceptably reasonable adsorption capacity even in very low traces of pollutants, high selectivity of metal ion wide range, high availability and low cost generation and regeneration (Wan Ngah and Hanafiah, 2008).

Over the past decades of studying heavy metal biosorption, many attempts have been carried out to reuse biosorbent for cycles by different eluents. A lot of them have been successfully for regeneration of biosorbent without tangible changes in biosorptive potential and a great number of papers have been published in this field. In view of importance of economy in process design there have been a few case studies focused on reutilizing and regeneration of the biosorbents as well as metal recovery (Carolin et al., 2017; Peng et al., 2017; Won et al., 2014). Particularly for precious metals such as Au, Pt, Pd, Rh, Os, Ir and Ru, because they are very expensive unlike heavy metals and biosorbents are much less costly than synthetic resins, biosorption–incineration combined process can be another option

for recovery of precious metals from the biosorbents. After desorption, the ionic form of metal ions can be reduced to metallic form along with oxidation of organic constituents during incineration (Cui and Zhang, 2008).

1.2 *Research gaps and needs*

The lignocellulosic materials have some negative sides such as low uptake capacity in raw form and releasing organic components in terms of high chemical oxygen demand (COD), biological oxygen demand (BOD) and total organic carbon (TOC), also they can cause secondary pollution as a sludge in water (Wan Ngah and Hanafiah, 2008). Many investigations have been carried out to improve the properties of the adsorbents and increase their capacity for metal ion uptake by chemically modification with mineral/organic acids, bases, organic compounds and oxidation agents (e.g. NaOH, CaO, $CaCl_2$, citric acid, acetic acid, formaldehyde, Na_2CO_3, $NaHCO_3$, HCl, H_2SO_4, HNO_3, H_2O_2, EDTA, methanol, etc.) (Velazquez–Jimenez et al., 2013; Wan Ngah and Hanafiah, 2008). The pre–treatments could modify the surface characteristics either by removing or masking the functional groups or by exposing more binding sites (Pehlivan et al., 2012).

Furthermore, though so many studies have been available on abundant and low–cost agro–industrial wastes and by–products as the adsorbents for heavy metal ions, all of them have been carried out to utilize a single adsorbent for this purpose. Hence, as each kind of lignocellulosic material has special functional groups and character, several types of appropriate biosorbents can be combined for gaining probable better detoxification efficiency.

In addition, the major disadvantage of biosorption process in heavy metal removal from aqueous solutions is producing a huge amount of solid biomasses to the environment. A few studies have considered regeneration after each desorption step to tackle the problem attributing to solid biosorbents by applying proper desorbing and regenerating agents without significant loss of adsorptive capacity. Last but not least, most studies on heavy metal removal by lignocellulosic biomasses have been performed in batch experiments and only a few have been reported in fixed–bed columns which are more relevant to real operating systems of wastewater treatment.

1.3   *Research hypotheses*

The primary hypothesis for this research is the development of a multi–metal binding biosorbent (MMBB) as an efficient, affordable and sustainable medium for the adsorption of Cd, Cu, Pb and Zn from aqueous solution. The secondary hypothesis is applying modified MMBB in a continuous column followed by investigating if its regeneration and reusability would be feasible.

1.4   *Objectives of the research*

The overall objective of this study is to develop a feasible process for heavy metal removal from industrial wastewater through biosorption on a combination of different lignocellulosic agro–industrial wastes and by–products.

The specific objectives of this study are as follows:

- To develop a multi–metal binding biosorbent (MMBB) combining various types of lignocellulosic agro–industrial wastes and by–products and select the best adsorbent for next experiments

- To investigate cadmium, copper, lead and zinc removal feasibility using the selected MMBB in batch experiments and then optimization of process and operation conditions

- To analyse the kinetic and equilibrium adsorption (pseudo–first–order, pseudo–second–order and intra–particle diffusion models) of these contaminants on different adsorbents

- To model batch equilibrium adsorption data by applying two–parameter isotherm equations of Langmuir, Freundlich, Dubinin–Radushkevich and Temkin and three–parameter models of Khan, Sips, Redlich–Peterson and Radke–Prausnitz adsorption isotherms

- To design and operate a lab–scale fixed–bed column for evaluating the applicability of selected and optimized MMBB for synthetic solution and real wastewater

- To study the effects of bed height, initial concentration and inlet flow rate in the column studies

- To display column adsorption data using the empirical models of Thomas, Yoon–Nelson, Dose Response model

- To develop a suitable method to desorption and regenerate the adsorbents in the continuous mode for three successive cycle

- To scale–up the MMBB packed bed column adsorption system by using BDST model data

1.5   *Research significance*

The reusing of lignocellulosic agro–industrial wastes and by–product such as tea waste, fruit peel and tree leaves as a heavy metal adsorbent results in double environmental benefits. Not only does it give a chance to reduce agricultural waste in a green way but also provides an efficient, beneficially low–cost technology and reusable alternatives for heavy metal ions from wastewater. The proposed process can be applied wherever industrial wastewater and agro–industrial waste and by–product are readily available enough for a practical application. The combination of different biosorbents might provide higher selectivity, as well.

Also the selected wastes have good results reported in other literatures for heavy metal removal and highly available in Australia and all over the world as well.

1.6   *Scopes of the research*

This study involves the development of a multi–metal binding biosorbent (MMBB) as a mixture of different selected biosorbents. Two selected MMBBs namely MMBB1 (tea waste, maple leaves and mandarin peels) and MMBB2 (tea waste, corncob and saw dust) are applied for the next experiments. Both MMBBs will be employed for batch experiments and characterization tests to evaluate and then compare their biosorptive capacities. The isotherm and kinetic studies are performed in the batch mode with synthetic wastewater solutions.

Multi–Metal Binding Biosorbent (MMBB) Development

Select the best adsorbents as two different combinations namely MMBB1 and MMBB2

Batch Experiments (Synthetic Solutions)

Effect of process operation conditions and phisico–chemical parameters	Isotherm, kinetic and thermodynamic studies Desorption and regeneration experiments

Optimization and Characterizations of Chemically Modified MMBB

Column Experiments (Synthetic Solutions and Real Wastewater)

Effect of culomn design parameters, and breakthrough modeling Scale–up calculation	Applicability of modified MMBB for real municipal wastewater Desorption and regeneration study

Figure 1.1 The main tasks and scope of this study

Isotherm data were described by two–parameter models of Langmuir, Freundlich, Dubinin–Radushkevich and Temkin and three–parameter models of Khan, Sips, Redlich–Peterson and Radke–Prausnitz adsorption isotherms while kinetic data were fitted with pseudo–first–order, pseudo–second–order and intra–particle diffusion models. After modification and optimization of MMBB whose metal biosorption capacity would be higher, desorption and regeneration potential will be tested and then characterized by SEM/EDS. The influences of different operating variables, process design conditions and also the breakthrough curve modeling are investigated in a mini–column with the synthetic wastewater. The modeling of the column data was done using Thomas, dose response, Yoon–Nelson, and Bed depth service time (BDST) models. A real wastewater is applied to validate the modified MMBB in real situation. The column adsorption, desorption and regeneration tests will be conducted with real wastewaters. The raw municipal wastewater was collected from Sydney Water Treatment Plant while the synthetic wastewater was prepared by dissolving nitrate salt of each metal ion in Milli–Q water.

1.7 *Outline and structure of this thesis*

A brief description of the contents of each chapter is presented herein below:

Chapter 1 introduces a context for this study and defines the research problem. The research objectives, main tasks and scope, and significance are highlighted. Chapter 1 comes to an end with the layout and structure of the thesis.

Chapter 2 (Literature review) presents: (i) characterization of lignocellulosic materials, (ii) application of lignocellulosic wastes and by–products as biosorbent in water and wastewater treatment for heavy metal ions, dyes, organic and nutrient removal, (iii) mechanism of biosorption and desorption process, (vi) reusability of heavy metal– loaded wastes and by–products and (v) conclusion, future perspectives and research gaps

Chapter 3 presents the materials and methods used in this study. All experiments in this study are described in detail. Contents of experiments, such as chemical

preparation, experimental setup, analytical methods as well as instruments used are introduced.

Chapter 4 investigates the competitive adsorption of Cd, Cu, Pb and Zn using two MMBBs, in batch system in regard with physico–chemical parameters such as pH, contact time, biosorbent dose and initial metal concentration. It also includes kinetic and isotherm modeling followed by characterization and desorption studies of these MMBBs.

Chapter 5 deals with optimization, chemical modification and characterization of the selected new biosorbent to find the principal surface functional groups and possible biosorption mechanisms. Desorption studies are carried out in terms of eluent type, concentration and contact time of desorption process. The effect of regeneration step by $CaCl_2$ will be then taken into consideration as well.

Chapter 6 aims to study chemically modified multi–metal binding biosorbent (MMBB) in a fixed–bed column. The effect of bed height, flow rate, biosorbent particle size, pH and initial metal concentration on packed bed reactors performance have been investigated and the possibility of regeneration and reuse has been studied. Moreover, Thomas and Dose Response models were applied for experimental data to simulate the breakthrough curves.

Chapter 7 evaluates the capability and applicability of MMBB in real situation, the MMBB packed–bed column was applied for a real wastewater stream. Bed Depth Service Time (BDST) model parameters were used to find the column capacity in order to predict the scale–up of a unit plant.

Chapter 8 summarizes key findings of this case study. Additionally, the unique contributions of this study to the field of Cd, Cu, Pb and Zn biosorption are highlighted. Chapter 8 ends with recommendations for future research.

Chapter 2

Literature Review

Chapter 2 Literature review

A major part of Chapter 2 was published in the following paper:

Abdolali, A., Guo, W.S., Ngo, H.H., Chen, S.S., Nguyen N.C., 2014. Typical lignocellulosic wastes and by–products for biosorption processes in water and wastewater treatment: a critical review. Bioresource Technology 160, 57–66.

2.1   ***Objectives***

At present, the interests in utilization of cheap alternatives have been significantly increased and many attempts have been made by researchers on feasibility of biosorption potential of lignocellulosic materials (either natural substances or agro–industrial wastes and by–products) as economic and eco–friendly options for toxic metal ion and dye removal from wastewater streams (Xu et al., 2017; Santos et al., 2015; Ahmed and Ahmaruzzaman, 2014; Raval et al., 2016). In this chapter, an overview of recent researches, the results and key finding on biosorption process by lignocellulosic agro–industrial wastes and by–products will be pointed out.

Chapter 2 (literature review) provides a research background for this study. As the main part of this literature review, Chapter 2 continues with the current state of studies on a wide variety of cheap biosorbents in natural and modified forms for heavy metal ions, dyes, organic and nutrient pollutants removal. The efficiency of each biosorbent has been also highlighted and discussed with respect to the operating conditions (e.g. initial pH value, temperature, hydraulic residence time, initial metal concentration, biosorbent particle size and its dosage), chemical modification on sorption capacity and preparation methods, thermodynamics and kinetics, as well as the applications.

The next section evaluates the potential of reusing and regenerating agricultural wastes and by–products used for heavy metal removal. This section provides deep insights into influential factors, desorbing and regenerating agents' properties and

desorption mechanisms as well. Additionally, Chapter 2 also justifies the selection of agro–industrial wastes and by–products for the development of cadmium, copper, lead and zinc adsorbents in this study. This Chapter ends with major findings and research gaps, which guide the present research.

2.2   *Characterization of lignocellulosic materials*

Lignocellulosic materials have been called photomass because they are a result of photosynthesis. Plant cell walls typically consist of three layers: the primary cell wall, the secondary cell wall and the middle lamella. The primary cell wall continuously extends with growing cells. The thick layer which is formed inside the primary cell wall after cell growth termination is known as secondary cell wall. The middle lamella forms an interface between secondary walls of adjacent plant cells and keeps them together as glue. The primary cell wall consists of the polysaccharides cellulose, hemicellulose and lignin. As shown in Figure 2.1, the cellulose aggregates to microfibrils which are covalently connected to hemicellulosic chains and form a cellulose–hemicellulose network that is embedded in the lignin matrix (Kubicek, 2012).

There are several types of cellulose in the cell wall of lignocellulosic materials. Cellulose (30–50%) is a linear polymer of β–D–glucopyranose sugar units whose average chain has a degree of polymerization of about 9,000–10,000 units. Approximately 65% of the cellulose is highly oriented and crystalline with no accessibility to water and other solvents, while the rest is composed of less oriented chains which have association with hemicellulose (20–40%) and lignin (15–25%). Hence, as its partial accessibility to water and other solvents, the molecular structure of cellulose gives a variety of characteristics such as hydrophilicity, chirality and degradability. Moreover, chemical reactivity is strongly a function of the high donor reactivity of the OH groups in cellulose molecules. In the crystalline structure of cellulose there are two parallel glucan chains that are bound by hydrogen bonding and Van der Waals forces. The bound sheets then stacked to needle-shaped fibres with the morphological hierarchy of elementary fibrils, microfibrils and microfibrillar bands (Kubicek, 2012).

With lower degree of polymerization than cellulose, the hemicellulose includes a group of polysaccharide polymers and the hemicelluloses which are not crystalline vary in structure and polymer composition depending on the source. In the primary cell wall of cereals and hardwood, xylan is the predominant hemicellulose polymer while in flowering plants, dicots and nongraminaceous monocots, xyloglucan is the major component. A rigid network structure of cellulose microfibrils is a result of cell wall extension via the length of the xyloglucan polymers which makes cross–link several cellulose microfibrils. In addition, hemicellulosic structure of the soft wood or gymnosperms cell walls consists galactomannans and galactoglucomannans (Kubicek, 2012).
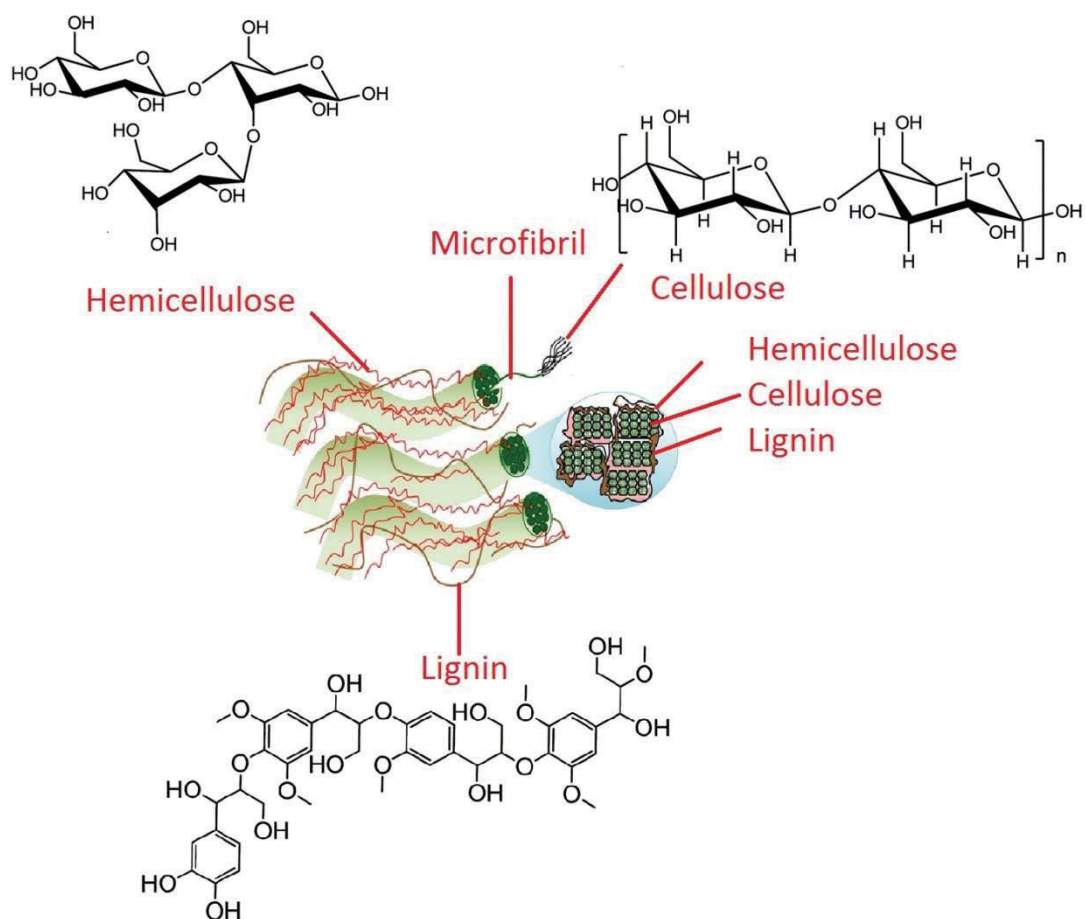
Figure 2.1 Lignocellulosic material wall and molecular structure (adapted from Xu et al., 2014)

Lignins are highly branched without crystalline–structure and are composed of nine carbon units derived from substituted cinnamyl alcohol of which the structure and chemical composition are a function of their source. A rigid structure which

strengthens the plant cell wall is also created by interaction between lignin and the cellulose fibrils. There are also small amounts of water, ash, cyclic hydrocarbons, organic and inorganic materials presented in lignocellulosic sources as extractives which contains a large number of both lipophilic and hydrophilic constituents (Kubicek, 2012; Cagnon et al., 2009; O'Connell et al., 2008). Chemical composition of some common lignocellulosic materials is presented in Table 2.1.

Table 2.1 Chemical composition of some common lignocellulosic materials

Type	Chemical Component (%)				
	Cellulose	Lignin	Hemicellulose	Ash	Silica
Rice straw	25–35	10–15	20–30	15–20	9–15
Wheat straw	30–35	16–21	26–32	4.5–9	3–7
Barley straw	30–35	14–15	24–29	5–7	3–6
Sugarcane bagasse	32–44	19–24	25–35	1.5–5	<4
Bamboo	26–43	21–31	15–26	1.7–5	<1
Grass	30–40	10–25	35–50	5–15	–
Corncob	35–45	5–15	35–45	1–2	<1
Leaves	15–25	5–10	70–80	<1	–
Cotton waste	80–95	–	5–20	<1	–
Hardwood	40–55	20–25	25–40	<1	–
Softwood	40–50	25–35	25–35	<1	–
Olive stone	30–35	20–25	20–30	<1	5–9
Nut shell and stone	25–35	30–40	25–30	–	–
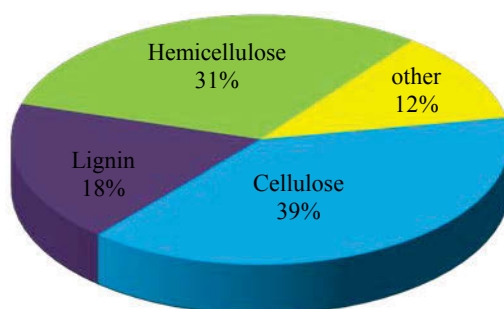
The type of functional groups and chemical components in lignocellulosic wastes and by–products are similar but in different amounts. They play an important role in heavy metal ions sorption (Asadi et al., 2008). Additionally, in order to enhance and reinforce the functional group potential and increase the number of active sites, some pre–treatment methods using different kinds of modifying agents are

applied within known protocols (Bhatnagar and Sillanpää, 2010; Wan Ngah and Hanafiah, 2008). As the agents include organic and mineral acids (HCl, HNO_3, H_2SO_4, acetic acid, citric acid and formic acid), bases and basic solutions (NaOH, Na_2CO_3, $Ca(OH)_2$ and $CaCl_2$), oxidizing agents (H_2O_2 and K_2MnO_4) and many other mineral and organic chemical compounds (formaldehyde, glutaraldehyde, CH_3OH, poly ethylene imine and epichlorohydrin).

According to the research carried out by O'Cannell et al. (2008), chemical modification can be applied to change certain properties of lignocellulosic biosorbents such as hydrophilic or hydrophobic characters, elasticity, water sorption ability, adsorptive or ion exchange capability, resistance to microbiological attack and thermal resistance.

In fact, chemical modification conducts two main approaches to enhance biosorptive capabilities: 1) the direct modification of the molecular structure through the introduction of chelating or metal binding functionalities through esterification (e.g. succinic anhydride and citric acid), etherification (e.g. sodium methylate, epichlorohydrin and polyethyleneimine), halogenation (e.g. 3–mercaptopropionic acid) and oxidation (e.g. sodium metaperiodate); and 2) grafting of selected monomers and adding to main chain of polymers so as to directly introduce metal binding capabilities or functionalization of grafted polymer chains by chelating agents. Different methodologies like photografting, high energy radiation and chemical initiation techniques have been applied to activate the backbone or main polymer. Amide, amine, carboxyl and hydroxyl binding ligands can be employed to form free radicals followed by copolymerization and functionalization. The carboxyl functional groups play a major role in metal removal using biosorbents (Tan and Xiao, 2009).

The variation in pH value can change the characterization and availability of metal ions as well as surface functional group chemistry. It can be said that the main parameters influencing pollutants removal are pH value of solution. Figure 2.2 shows the range of optimum pH of some different lignocellulosic biosorbents. In lower and higher pH values (pH<2 and pH>9), predominant competition between hydronium cation and metal ions, and soluble hydroxyl formation are the main

factors contributing to depletion of adsorption capacity (Pérez Marín et al., 2009). Recently, succinic, maleic and phtalic have been reported as good surface modification agents due to their specifications to increase carboxyl groups (–COOH) on the surface of biosorbent. Ethylene diamine tetraacetic dianhydride (EDTAD), as a biodegradable agent with two anhydride groups per molecules, is a proper option for surface modification through occurring esterification reaction, introducing carboxylic acid and amine groups, as well as enhancing chelating abilities and biosorption capacity (Pereira et al., 2010).
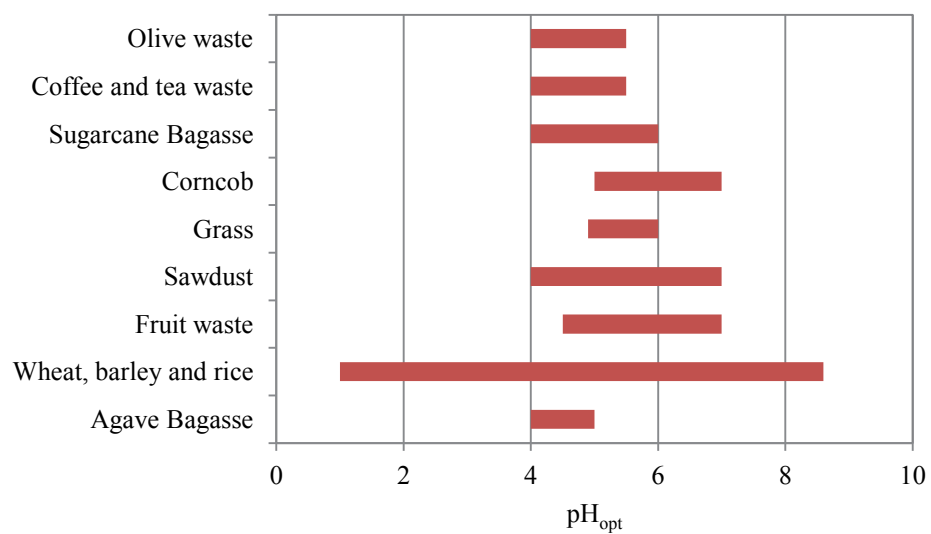
(a)
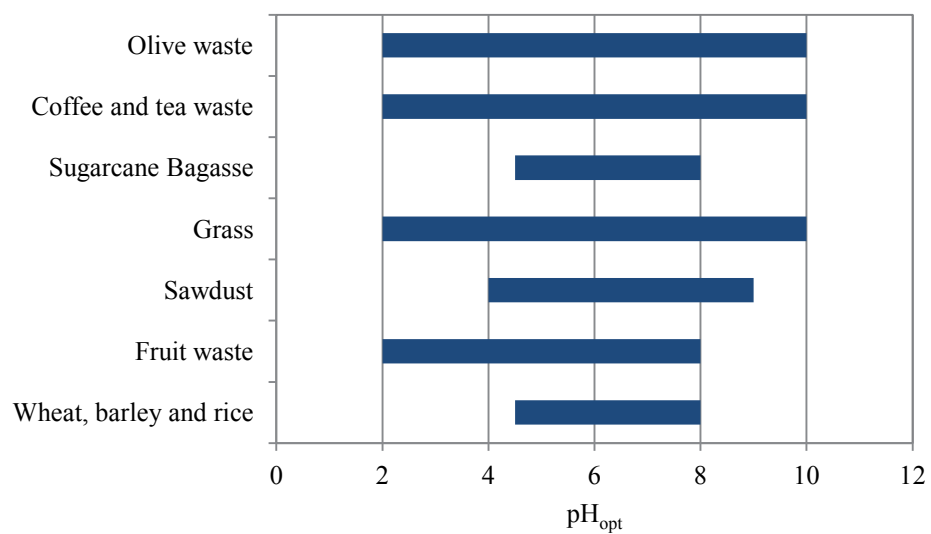
(b)

Figure 2.2 Optimum pH of some typical lignocellulosic agro–industrial wastes and by–product for (a) heavy metal and (b) dye removal

Velazquez–Jimenez et al. (2013) compared different types of modifying agents for agave bagasse treatment. They reported that organic acids like citric, oxalic and tartaric acid enforced weak and ineffective functional groups which were responsible for metal adsorption. Meanwhile, the analytical results indicated that concentration of oxygenated group like carboxyl group (–COOH) increased. This enhancement was probably obtained by modification via protonating unavailable functional groups with mineral acid like HNO_3 followed by transforming and oxidizing functional groups to carboxylic groups with NaOH. In another study, according to Fourier transform infrared spectroscopy (FTIR) analysis, the number of functional acid groups such as O–H and C–O (stretching vibrations of ethers and alcohols) increased through phosphoric acid treatment while titrable acid groups decreased through hydrogen peroxide treatment (Martín–Lara et al., 2012). Leyva–Ramos et al. (2012) also investigated the modification agent molarity to find the relationship between the capacity and acidic sites of corncob in natural and modified forms as well as the probable biosorption mechanism.

Nevertheless, it is generally difficult to compare the adsorptive properties of adsorbents directly, because there are considerable inconsistency in data presentation and differences in experimental conditions, materials and methodologies (e.g. different initial concentrations, pH value, temperature, adsorbent dose, particle size, etc).

2.3 *Application of lignocellulosic wastes and by–products as biosorbent in water and wastewater treatment*

2.3.1 *Lignocellulosic wastes and by–products for heavy metal ion removal*

Lignocellulosic waste materials have proper characteristics and structural compounds to adsorb heavy metal ions on their surface binding sites through interaction with the chemical functional groups (Abdel–Raouf and Abdul–Raheim, 2017; Bilal et al., 2013; Ding et al., 2013).

Without going into too much detail, the maximum biosorption capacities of different types of natural biosorbents, agro–industrial wastes and by–products for

heavy metal removal are summarised in Table 2.2 and some of the results are discussed hereinafter. Due to the different laboratory conditions (e.g. pH, temperature, adsorbent dose, particle size), materials and methodologies, it is not easy to conclude which biosorbent would be suitable for particular metal ion.

One of the main factors that sprightly influences whether an agro–industrial waste or by–product is practical or not is the availability. For example, sugarcane bagasse, an agro–waste from sugar industries has been extensively studied because of its low price and high availability all over the world. This biosorbent exhibited very high potential in heavy metal uptake during wastewater treatment (Alomá et al., 2012; Liu et al., 2012). The biosorption capacity of sugarcane bagasse could be noticeably improved by introducing carboxylic, amine and other functional groups into the surface materials (Pereira et al., 2010) or by removing soluble organic compounds and increasing efficiency of metal sorption (Martín–Lara et al., 2010). Based on the work of Pehlivan et al. (2013), the main factors determining the adsorption of As(V) on sugarcane bagasse modified by iron(III) oxy–hydroxide (HFO) were electrostatic interactions, ligand exchange and chelation between positively charged surface groups $\equiv FeOH^{2+}$ and negatively charged As(V) ions. Alomá et al. (2012) concluded that nickel ion biosorption on non–chemically modified sugarcane bagasse within temperature range of 25–65°C was exothermic and spontaneous. Moreover, Langmuir isotherm was able to simulate the experimental data better than Sips and Freundlich models.

Study on optimal preparation conditions for sugarcane bagasse, watermelon rind and banana peels to use in Cu(II) removing from water was carried out by Liu et al. (2012). The results demonstrated that 120 °C was the suitable drying temperature. The drying time for sugarcane bagasse, watermelon rind and banana peel was 1, 3 and 2 hr, respectively. They found that fine powder (<150 μm) was the most efficient size for Cu(II) removal. However, for continuous biosorption process in column, the mechanical strength should be considered as a result of biomass particle size.

In other study, when rice husk was subjected to 1.5% alkali treatment and used for Zn(II), Cu(II), Cd(II), Ni(II), Pb(II), Mn(II), Co(II), Hg(II) and Cr(VI) removal from

single ion and mixed solutions, the ultimate biosorption capacity calculated from Langmuir isotherm model was improved in the order of $Ni^{2+} < Zn^{2+} \approx Cd^{2+} \approx Mn^{2+} \approx Co^{2+} < Cu^{2+} \approx Hg^{2+} < Pb^{2+}$ at 32 ± 0.5 °C between pH range of 5.5 and 6.0 ± 0.1 (Krishnani et al., 2008). However, in other study, the pre–treatment of sugarcane bagasse using NaOH and HCl had no significant effect on mercury biosorption capacity (Khoramzadeh et al., 2013).

The other typical and abundantly available agro–industrial materials are wheat and barley wastes, as the main crops all over the world. The feasibility of utilization of these kinds of waste as very low–cost biosorbents were investigated by Pehlivan et al. (2012), Muhamad et al. (2010) and Aydin et al. (2008). Esterified barley straw was thermo–chemically modified with citric acid for copper adsorption (Pehlivan et al., 2012). Increasing the temperature improved the reaction efficiency but led to lower carboxyl content and increased cross–linking of modified barley straw. Increasing citric acid concentration enhanced free carboxyl groups on the biomass matrix. Besides, the results demonstrated that a significant amount of free COOH groups remained in the biomass structure up to 4 hr reaction time and then the increase in cross–linking occurred with more reaction time. On the contrary, some case studies suggested the acids as modifying agent should be used in lower concentrations due to prevention of cellulose structure damage and high toxicity. In addition, Miretzky and Cirelli (2010) reported that alkali treatments in comparison with acidic ones at the same conditions were more effective on metal ion removal by solving cell wall matrix. Therefore, alkali treatments could result in better diffusion through wall and make the functional groups denser and thermodynamically more stable. The increase in Cd(II) and Cu(II) uptake on wheat straw with temperature raise was attributed to the increase in the available active sites on the surface of the adsorbent by the opening up of the cellulose fibres when wheat straw was soaked in a warmer solution (Muhamad et al., 2010).

Sawdust has also been widely studied as an alternative adsorbent and has shown good stabilities (Asadi et al., 2008; Sud et al., 2008; Bulut and Tez, 2007; Prado et al., 2010). It has been identified that phenolic, hydroxyl and carboxylic functional groups of sawdust are responsible for heavy metal uptake, as heavy metal ions

could accumulate in secondary septum of wood in which the amount of lignin is very low. Palumbo et al. (2013) found that metal adsorption onto biosorbent is possibly a passive binding. They highlighted the effect of pH and natural organic matter on Zn removal. Metal uptake has been manipulated by pH stronger than the concentration of natural organic matter. Šćiban et al. (2007) investigated heavy metal biosorption capacity of sawdust during synthetic and real cable factory wastewater treatment. Heavy metal ion adsorption was influenced by the existence of other ions and organic materials in real wastewater through three phenomena, namely, synergism, antagonism and non–interaction. This study showed that copper was better adsorbed from wastewater with multiple heavy metal ions than from wastewater containing single Cu(II) ion, whereas Cd adsorption was inhibited by other metal ions and Zn removal were unaffected. As expected, some metal ions have better affinity towards lignocellulosic biosorbents than other ions and this fact ascertains the selectivity potential of functional group. The highest amount of correlation coefficients, BET, Langmuir and Freundlich models well described experimental data of zinc, copper and cadmium removal, respectively.

Bulut and Tez (2007) released that Ni, Cd and Pb biosorption on walnut tree sawdust was favourable at higher temperatures as the values of ΔG became more negative and positive ΔH suggested endothermic nature of adsorption. The randomness at solid–solution interface increased by temperature grows (positive ΔS), leading to enhancement of adsorption at higher temperatures. This may be related to adsorption surface activation and/or pore size enlargement. Reverse trend was obtained for Pb biosorption on different types of sawdust as an exothermic process (Prado et al., 2010).

As a pectin–rich by–product of fruit juice industry,the suitable chemical treatment (e.g. mercapto–acetic acid ($C_2H_4O_2S$) and carbon disulfide (CS_2))can make orange peels more favorable for metal adsorption due to the negativity amount of zeta potential, indicating higher physical stability and surface activity (Sha et al., 2009).

Martín–Lara et al. (2012) investigated the biosorption properties and mechanical strength of the olive stone modified by H_2SO_4 (1 M) for lead removal in a fixed–bed

column. The column was retained over 14 cycles of use and life factor revealed that biosorbent bed would be exhausted after 71.3 cycles. Furthermore, according to the work study mentioned above, all biosorption were found to achieve equilibrium in a very short contact time and all kinetic studies showed the applicability of pseudo–second–order kinetic model and the second–order nature of biosorption process of heavy metal ions onto raw and pre–treated biosorbents. This can be attributed to assumption of chemical adsorption rate–controlling step in biosorption process involving electron sharing or transferring between adsorbent and adsorbate (Pereira et al., 2010; Alomá et al., 2012; Bulut and Tez, 2007; Ding et al., 2012).

Table 2.2 The performance of different types of agro–industrial wastes for heavy metal ion removal from aqueous solutions

Adsorbent (modifying agent)	Adsorbate	q_{max} (mg/g)	Mechanism	Reference
Agave Bagasse (raw)	Cd	13.27	Ion exchange, complexation	Velazquez–Jimenez et al., 2013
Agave Bagasse (HCl)	Cd	13.5	Ion exchange, complexation	Velazquez–Jimenez et al., 2013
Agave Bagasse (HNO$_3$)	Cd	12.5	Ion exchange, complexation	Velazquez–Jimenez et al., 2013
Agave Bagasse (NaOH)	Cd	18.32	Ion exchange, complexation	Velazquez–Jimenez et al., 2013
Rice straw (raw)	Cd	13.89	Ion exchange, chelating	Ding et al., 2012
Grapefruit peel (raw)	Cd	42.09	Ion exchange	Torab–Mostaedi et al., 2013
Corncob (Citric acid)	Cd	49.2	Ion exchange	Leyva–Ramos et al., 2012
Wheat stem (raw)	Cd	11.6	Complexation	Tan and Xiao, 2009
Wheat stem (Methanol)	Cd	0.35	Complexation	Tan and Xiao, 2009
Wheat stem (NaOH)	Cd	21.84	Complexation	Tan and Xiao, 2009
Coconut shell [a] (raw)	Cd	37.78		Sousa et al., 2010
Coconut shell [b] (raw)	Cd	11.96		Sousa et al., 2010

Adsorbent (modifying agent)	Adsorbate	q_{max} (mg/g)	Mechanism	Reference
Rice husk (raw)	Cr	8.5	Complexation, ion exchange and surface precipitations	Bansal et al., 2009
Rice husk (Formaldehyde)	Cr	10.4	Complexation, ion exchange and surface precipitations	Bansal et al., 2009
Rice husk (Alkali–treated)	Cr	52.1	Ion exchange	Krishnani et al., 2008
Olive pomace (raw)	Cr	13.95	Ion exchange	Krishnani et al., 2008
Orange peel (raw)	Cu	50.94	Ion exchange, complexation	Sha et al., 2009
Orange peel ($C_2H_4O_2S$)	Cu	70.67		
Sunflower hull (raw)	Cu	57.14		Witek–Krowiak, 2012
Barley straw (raw)	Cu	4.64	Ion exchange, chelation	Pehlivan et al., 2012
Barley straw (Citric acid)	Cu	31.71	Ion exchange, chelation	Pehlivan et al., 2012
Garden grass (raw)	Cu	58.34		Hossain et al., 2012
Coconut shell (raw)	Cu	41.36		Sousa et al., 2010
Lentil shell (raw)	Cu	9.59		Aydin et al., 2008
Rice shell (raw)	Cu	2.95		Aydin et al., 2008
Wheat shell (raw)	Cu	17.42		Aydin et al., 2008
Sawdust (raw)	Cu	6.88		Šćiban et al., 2007
Rice straw (HNO_3–NaOH)	Cu	8.13		Rocha et al., 2009
Olive stone (raw)	Cu	20.2		Fiol et al., 2006
Coconut shell [a](raw)	Cu	41.36		Sousa et al., 2010
Coconut shell [b](raw)	Cu	20.26		Sousa et al., 2010
Agave Bagasse(raw)	Pb	35.6	Ion exchange, complexation	Velazquez–Jimenez et al., 2013
Agave Bagasse (HCl)	Pb	54.29	Ion exchange, complexation	Velazquez–Jimenez et al., 2013
Agave Bagasse (HNO_3)	Pb	42.31	Ion exchange,	Velazquez–Jimenez et

Adsorbent (modifying agent)	Adsorbate	q_{max} (mg/g)	Mechanism	Reference
			complexation	al., 2013
Agave Bagasse (NaOH)	Pb	50.12	Ion exchange, complexation	Velazquez–Jimenez et al., 2013
Rice husk (Alkali–treated)	Pb	58.1	Ion exchange	Krishnani et al., 2008
Corncob (raw)	Pb	16.22		Tan et al., 2010
Corncob (CH_3OH)	Pb	43.4		Tan et al., 2010
Corncob (NaOH)	Pb	7.89		Tan et al., 2010
Sawdust (raw)	Pb	15.9	Ion exchange, complexation	Bulut and Tez, 2007
Olive stone (raw)	Pb	92.6		Fiol et al., 2006
Coconut shell [a](raw)	Pb	54.62		Sousa et al., 2010
Coconut shell [b](raw)	Pb	17.9		Sousa et al., 2010
Agave Bagasse (raw)		2.23		Alomá et al., 2012
Sawdust (raw)	Ni	3.29	Ion exchange, complexation	Bulut and Tez, 2007
Rice husk (Alkali–treated)	Ni	5.52	Ion exchange	Krishnani et al., 2008
Grapefruit peel (raw)	Ni	46.13	Ion exchange	Torab–Mostaedi et al., 2013
Cashew nut shell (raw)	Ni	18.86		Kumar et al., 2011
Olive stone (raw)	Ni	21.3		Fiol et al., 2006
Coconut shell [a](raw)	Ni	16.34		Sousa et al., 2010
Coconut shell [b](raw)	Ni	3.12		Sousa et al., 2010
Agave Bagasse(raw)	Zn	7.84	Ion exchange, complexation	Velazquez–Jimenez et al., 2013
Agave Bagasse (HCl)	Zn	14.43	Ion exchange, complexation	Velazquez–Jimenez et al., 2013
Agave Bagasse (HNO_3)	Zn	12.4	Ion exchange, complexation	Velazquez–Jimenez et al., 2013
Agave Bagasse (NaOH)	Zn	20.24	Ion exchange, complexation	Velazquez–Jimenez et al., 2013
Agave Bagasse (EDTAD)[c]	Zn	105.26	Ion exchange	Pereira et al., 2010

Adsorbent (modifying agent)	Adsorbate	q_{max} (mg/g)	Mechanism	Reference
Agave Bagasse (EDTAD)[d]	Zn	45.45		Pereira et al., 2010
Sawdust (EDTAD)[c]	Zn	80	Ion exchange	Pereira et al., 2010
Sawdust (EDTAD)[d]	Zn	47.39		Pereira et al., 2010
Sawdust (raw)	Zn	0.96		Šćiban et al., 2007
Rice straw (HNO$_3$–NaOH)	Zn	8.63		Rocha et al., 2009
Rice husk (Alkali–treated)	Zn	8.14	Ion exchange	Krishnani et al., 2008
Coconut shell [a]	Zn	17.08		Sousa et al., 2010
Coconut shell [b]	Zn	7.32		Sousa et al., 2010
Rice straw (raw)	Hg	22.06		Rocha et al., 2009
Rice husk (raw)	Hg	36.1		Krishnani et al., 2008
Sugarcane Bagasse (raw)	Hg	35.71		Khoramzadeh et al., 2013

[a] single–component solution
[b] multi–component solution
[c] Synthetic wastewater
[d] Real wastewater

2.3.2   Lignocellulosic wastes and by–products for dye removal

Major pollutants in industrial wastewaters are high concentrations of TSS, COD, color, acidity and other soluble substances. Wastewater from dyeing operations is intense colored stream containing unfixed dyes along with salts and auxiliary chemicals such as emulsifying agents. Thus, the removal of color from textile industry and dyestuff manufacturing industry wastewaters represents a major environmental concern. In addition, resistance of dyes to biological degradation has made color removal from wastewaters more difficult, because most textile dyes have complex aromatic molecular structures that resist degradation (Guo and Ngo, 2012). Compared with other commercially used adsorbents such as activated carbon, inexpensive, locally available and effective materials can be used as a substitute for the removal of dyes from aqueous solution (Crini, 2006). An extensive list of biosorbents and the parameters affecting dye removal have been compiled in Table 2.3.

Table 2.3 The performance of different types of agro–industrial wastes for dye removal from aqueous solutions

Adsorbent	Modifying agent	Adsorbate	q_{max} (mg/g)	Reference
Sugarcane Bagasse	Succinic anhydride	Methylene blue	478.5	Guimarães Gusmão et al., 2012
		Gentian violet	1273.2	Guimarães Gusmão et al., 2012
Sugarcane Bagasse	raw	Crystal violet	10.44	Parab et al., 2009
Sugarcane	raw	Methyl red	5.66	Saad et al., 2010
Bagasse	H_3PO_4	Methyl red	10.98	Saad et al., 2010
Jute fibre	raw	Congo red	8.116	Roy et al., 2013
Rice husk	raw	Direct red–31	74.07	Safa et al., 2011
	Carboxymethyl cellulose sodium	Direct red–31	41.84	Safa et al., 2011
	Polyvinyl alcohol+sodium alginate	Direct red–31	11.44	Safa et al., 2011
	HCl	Direct red–31	74.63	Safa et al., 2011
	raw	Direct orange–26	53.19	Safa et al., 2011
	Carboxymethyl cellulose sodium	Direct orange	34.25	Safa et al., 2011
	Polyvinyl alcohol+sodium alginate	Direct orange	16.78	Safa et al., 2011
	HCl	Direct orange	46.95	Safa et al., 2011
Barley husk	raw	Solar red BA	400	Haq et al., 2011
Citrus waste	raw	Reactive blue 19	37.45	Asgher and Bhatti, 2012
	Sodium alginate immobilized	Reactive blue 19	400	Asgher and Bhatti, 2012
	Glacial acetic acid	Reactive blue 19	75.19	Asgher and Bhatti, 2012
	raw	Reactive blue 49	135.16	Asgher and Bhatti, 2012
	Sodium alginate immobilized	Reactive blue 49	80.00	Asgher and Bhatti, 2012
	Glacial acetic acid	Reactive blue 49	232.56	Asgher and Bhatti, 2012

Adsorbent	Modifying agent	Adsorbate	q_{max} (mg/g)	Reference
*Capsicum annuum*seed	Acetone	Reactive blue 49	96.35	Tunali Akar et al., 2011
*Oreganum*stalk	raw	Basic Red 18	172.41	Mavioglu Ayan et al., 2012
	HNO$_3$	Basic Red 18	272.92	Mavioglu Ayan et al., 2012
	H$_3$PO$_4$	Basic Red 18	280.73	Mavioglu Ayan et al., 2012
	raw	Methylene blue	94.34	Mavioglu Ayan et al., 2012
	HNO$_3$	Methylene blue	142.86	Mavioglu Ayan et al., 2012
	H$_3$PO$_4$	Methylene blue	147.06	Mavioglu Ayan et al., 2012
	raw	Acid Red 111	50.0	Mavioglu Ayan et al., 2012
	HNO$_3$	Acid Red 111	112.36	Mavioglu Ayan et al., 2012
	H$_3$PO$_4$	Acid Red 111	39.84	Mavioglu Ayan et al., 2012
Date stone	raw	Methylene blue	43.47	Belala et al.,
Palm tree waste	raw	Methylene blue	39.47	2011
Artocarpusheterophyllus (jackfruit) leaf powder	raw	Crystal violet	43.39	Saha et al., 2012
Sunflower seed hull	raw	Methylene violet	92.59	Hameed, 2008
Grass waste	raw	Methylene blue	457.64	Hameed, 2009a
Spent tea leaves	raw	Methylene blue	300.05	Hameed, 2009b
Olive pomace	raw	RR198	7.21×10^{-5} [a]	Akar et al., 2009
	raw	RR198	41.38	Akar et al., 2009
Beech sawdust	Calcium chloride	Methylene blue	12.2±1.8	Batzias and Sidiras, 2007

Adsorbent	Modifying agent	Adsorbate	q_{max} (mg/g)	Reference
	Zinc chloride		13.2±2.0	Batzias and Sidiras, 2007
	Magnesium chloride		15.6±2.4	Batzias and Sidiras, 2007
	Sodium chloride		9.7±0.6	Batzias and Sidiras, 2007
Mango seed	raw	Victazol Orange	44.8	Alencar et al., 2012
	HCl		71.6	Alencar et al., 2012
Tea waste	$FeCl_3.6H_2O+FeCl_2.4H_2O$	Janus green	129.87	Madrakian et al., 2012
		Methylene blue	119.05	Madrakian et al., 2012
		Thionine	128.21	Madrakian et al., 2012
		Crystal violet	113.64	Madrakian et al., 2012
		Congo red	82.64	Madrakian et al., 2012
		Neutral red	126.58	Madrakian et al., 2012
		Reactive blue 19	87.72	Madrakian et al., 2012

[a] mol/g

As the most commonly used dyes in textile and paper industries, the removal of methylene blue was conducted by Guimarães Gusmão et al. (2012) using succinylated sugarcane bagasse. The carboxylate functions in the sugarcane bagasse structure have negative charges to interact to cationic dyes and hence the functionality can be modified by succinic anhydride and sodium bicarbonate solution. After esterification, FTIR spectroscopy illustrated the presence of carboxylate group ($-COO^-Na^+$) and symmetric stretching of ester groups ($-C-O-C=O$) which were responsible to dye biosorption.In another similar study, adsorptive capability of sugarcane fibre to remove crystal violet was studied by Parab et al. (2009). Compared to sawdust and coir pith biosorption, the results revealed a good correlation of Freundlich and Redlich–Peterson (R–P) isotherm

models. The experimental data also indicated coir pith achieved the highest adsorption capacity followed by sawdust and sugarcane fibre.

Other researchers conducted batch and column experiments to simulate kinetics of methylene blue adsorption on calcium chloride, zinc chloride, magnesium chloride and sodium chloride treated beech sawdust. The Freundlich and Langmuir adsorption capacity in batch study remarkably increased by pre–treatments following the order of $NaCl>CaCl_2>MgCl_2>ZnCl_2$. In the case of column adsorption process, the adsorption capacity coefficient of the bed at different breakthrough values could be calculated by the Bed Depth Service Model developed by Bohart and Adams for all used modifying agents (Batzias and Sidiras, 2007). Han et al. (2007) conducted the similar study to investigate the effects of pH, adsorbate concentration, bed depth, flow rate and ionic strength and existed salt on methylene blue removal using rice husk in a continuous fixed–bed column system. The Thomas and Bed Depth Service Time models properly described the adsorption of methylene blue. Generally, breakthrough occurs faster at higher flow rate and dye concentration due to more mass transfer rate, whereas breakthrough time increases significantly with the decrease in the flow rate. The presence of other metal ions such as Na^+ and Ca^{2+} resulted in steeper slope and shorter breakthrough time. The effect of $CaCl_2$ was stronger than that of $NaCl$ at the same dye concentrations.

Acetone–treated capsicum seeds were used for reactive blue 49 uptake in batch and continuous column systems. According to FTIR spectra, –NH,–OH and C=C groups participated in dye removal through chemisorption mechanism. This process well described by Langmuir model in both batch and continuous modes. In batch biosorption experiments, ionic strength increase made a slight decrease in dye removal efficiency, while there were no significant changes obtained by increasing initial dye concentration (Tunali Akar et al., 2011).

Asgher and Bhatti (2012) compared raw, immobilized and acetic acid–treated citrus waste to remove reactive blue 19 and reactive blue 49 from aqueous solution. Very excellent performance was achieved for both dyes. Acidic pH range was the optimum condition under which dye molecules bound with surface active

sites of biomass (–NH,–OH and C=O groups) via hydrogen ions as bridging ligands. The physio–sorption was the predominant mechanism of removing reactive blue 19 and reactive blue 49 biosorption using citrus waste. The biosorption process of both dyes adequately followed all Langmuir, Freundlich and Temkin isotherms.

Hameed (2008, 2009a, 2009b) investigated the methyl viole removal using sunflower seed hull andmethylene blue removal using grass waste and spent tea leaves.The experimental data wereanalysed in terms of initial pH, initial dye concentration, biosorbent dose and contact time in order to find the best kinetic and isotherm model. For all dyes, the pseudo–second order–order kinetic model was better than pseudo–first–order and intra particle diffusion models. Methylen violet uptake on sunflower seed hull followed Freundlich while Langmuir equation was found to be in good agreement with sorption data ofmethylen blue on grass and tea waste. The dye removal is strongly dependant on pH, biosorbent dose, initial dye concentration as well as biosorbent typeaccording to the results of maximum dye biosorption capacitiesreported in literatures. In adition, the rough surface of these adsorbent provided a suitable bed for dye binding or entrappingaccording to SEM images.

The other study conducted by Madrakian et al. (2012) dealt with capability of magnetite nanoparticles loadedtea waste for adsorption of sevendyes (Janus green, methylene blue, thionine, crystal violet, Congo red, neutral red and reactive blue 19). In this study, cationic dyesindicated higher adsorptionremoval than anionic dyes. The authors suggested that the increase in intensity of some peaks (e.g. –OH, aliphatic C–H, C–O, NH_2 in amid bands) depicted in FTIR analysis could be attributed to the welleffectiveness ofmagnetite nanoparticles modification as a chemical modifier. They also reported very excellent biosorption removal(up to 98%) for all tested dyesunder optimum experimental conditions.

The possibility of using phosphoric acid ($H_3PO_4^-$) treated sugarcane bagasse to remove methyl red dye was explored by Saad et al. (2010). The efficiency of dye removal by H_3PO_4 treated bagasse was less than activated carbon and followed by untreated bagasse. Study on the effect of pH indicated that activated carbon decolourization remained 100% for all pH values, whereas for both treated and untreated bagasse, lowest percentage of dye removal was recorded at pH of 2. Dye

adsorption was significantly increased between the pH values of 3 and 6 and then gradually decreased in the pH range of 7–10. This trend illustrated that ion exchange mode and electrostatic attraction between dye anions and negatively charged surface of biosorbent. The kinetics of methyl red adsorption followed the pseudo–first–order kinetic expression and Langmuir isotherms model fit well the experimental data.

Safa et al. (2011) concluded that carbonyl, carboxyl and amide groups of rice husk were involved in Direct Red–31 and Direct Orange–26 removal at low pH values. Besides, at basic pH range, formation of more ionic species such as hydroxyl and carboxyl showed competition with dye anions for active sites and hence biosorption decreased.They also reported different biosorbent surface behaviours could be seen by different chemical modification agents. More positively charged active sites and stronger electrostatic attraction were created by acid treatment and surface protonation. Alkali treatment led to surface functional group deprotonation and interior biosorbent surface activation, and salt treatment could produce more binding sites for dyes. Additionally, cationic surfactant created positive charge impregnation on adsorbent surface. These several modification methods increased dye removal on rice husk in the following order:

Glutaraldehyde methanol< ethanol< NaOH< NH$_4$OH< boiling< native< Triton X–100< heat treated< cationic surfactant< MgSO$_4$< CaCl$_2$·H$_2$O< NaCl< HNO$_3$< H$_2$SO$_4$< HCl.

Akar et al. (2009) studied RR198 biosorption onto olive pomace in synthetic and real wastewater treatment. They found this process was spontaneous and endothermic in nature by calculating the thermodynamic parameters and well fitted by Langmuir isotherms better than both Freundlich and Dubinin–Radushkevich models. RR198 biosorption onto olive pomace was independent of ionic strength in the concentration range of 0.01–0.15 M, whereas, it decreased in the ionic strength over 0.15 M. Besides, there was no tangible decrease in biosorption capacity of olive pomace when it was utilized for treating real wastewater containing several interfering species.

The feasibility of barley husk to remove synthetic dye, namely direct solar red BA, was explored by Haq et al. (2011). The thermodynamic study suggested that

adsorption was physical and spontaneous due to the negative changes in free Gibbs energy. Similar to other biosorbents, biosorption capacity of barley husk either increased with the decrease of particle size or reduced with the increase of initial dye concentration (>100 mg/L) in the aqueous solution. The latter might be attributed to the fact that interactions between dye anions became prevalent and subsequently, resulting in lessening affinity of the dye binding sites on the biosorbent. The authors also reported that existence of salts and anionic or cationic surfactants (detergents) in wastewater could lead to lowering dye removal.

2.3.3   Lignocellulosic wastes and by–products for organic and nutrient removal

Recently, many attempts have been made for finding low–cost and effective anion/cation exchangers produced from agricultural by–products to remove organic pollutants and nutrients from aqueous solutions (Table 2.4). It is well known as the pH of the solution is one of the effective parameters on adsorptive potential of biomass and affects its surface charge as well as the degree of ionization of different pollutants (Ahmad et al., 2009; Stasinakis et al., 2008). At higher pH, negatively charged adsorbent sites increase, which enhance the adsorption of positively charged cations through electrostatic forces of attraction.

Ofomaja (2011) studied the kinetics, isotherm models and possible mechanism of biosorption process in terms of removing large organic pollutant molecule like 4–nitrophenol using mansonia (*Mansonia altissima*) wood sawdust. From calculated kinetic rates of pollutant sorption into macro–, meso– and micropores, the process mechanism was found to be complex, consisting of both external mass transfer and intra–particle diffusion. This process was quite well described by the pseudo second–order kinetic model and Freundlich isotherm.

Brandão et al. (2010) reported that natural sugarcane bagasse could adsorb up to 99% of gasoline and 90% of n–heptane in aqueous solutions within only 5 min. However, at low concentration of gasoline and n–heptane, monolayer biosorption could be simulated by Langmuir model. However, none of Langmuir, Freundlich, Temkin and Dubinin–Radushkevich models could well describe the process at high

concentration of n–heptane and for gasoline contaminated solution at concentration more than 0.04 mg/L. According to measured correlation coefficients, Freundlich presented the best simulations, followed by Dubinin–Radushkevich and Temkin isotherms and then Langmuir. The presence of ethanol in gasoline could enhance the solubility of gasoline in water, thereby improving the adsorptive capacity of sugarcane bagasse.

Table 2.4 The performance of different types of agro–industrial wastes for organic and nutrient removal from aqueous solutions

Adsorbent	Modifying agen	Adsorbate	q_{max} (mg/g)	Reference
Sugarcane Bagasse	raw	Gasoline	8.36	Brandão et al., 2010
		n–heptane	2.77	Brand ão et al., 2010
Sawdust	raw	Ammonium	1.7	Wahab et al., 2010
Sawdust	raw	4–nitrophenol	21.28	Ofomaja, 2011
Wheat straw	raw	Nitrate	0.14×10^{-3}[a]	Wang et al., 2007
	Epichlorohydrin	Nitrate	2.08×10^{-3}[a]	Wang et al., 2007
Wheat straw	Epichlorohydrin	Nitrate	52.8 ± 1.0	Xu et al., 2010
		Phosphate	45.7 ± 1.1	Xu et al., 2010
Wheat stalk	Epichlorohydrin	Phosphate	60.61	Xu et al., 2011
Cotton stalk	Epichlorohydrin	Phosphate	50.54	Xu et al., 2011
Banana peel	raw	Phenol	688.9	Achak et al., 2009

[a] mol/g

Achak et al. (2009) found that banana peel was a low–cost and efficient adsorbent for olive mill wastewater purification containing phenolic compounds with a high biosorptive capacity of 688.9 mg/g. Equilibrium state was attained within 3 hr and 96% of phenolic compounds were removed completely. Alkali condition was more favorable for phenol adsorption and lower pH value was more suitable for desorption process. They also explained that in case of using water for biosorbent recovery, if the cation or anion attached on biomass surface were very weak,

physiosorption via Van der Waals attraction was the main mechanism. If alkali water (pH 12) was used, adsorption mechanism could be ion exchange, while chemisorption was dominant mechanism if acetic acid was employed. Based on the results, since 0.17, 0.30 and 0.12 g/g of desorbed phenolic compounds could be obtained by neutral pH water (pH 7.3), acetic acid (pH 1.2) and alkaline water (pH 12), respectively, chemisorption might be the main mechanism of phenol removal.

Maximum biosorption capacity of NH_4^+ was obtained at pH of 8 using sawdust as biosorbent (Wahab et al., 2010). The biosorption was resulted from ammonium cation binding to negatively charged lignin and cellulose chains. Nevertheless, at range of acidic pH values, biosorption took place due to polar functional groups of lignin such as alcohols, aldehydes, ketones, acids and hydroxides. Equilibrium states were quickly reached within 20 min. The FTIR spectral characteristics of raw sawdust before and after ammonium biosorption illustrated that acidic groups of carboxyl and hydroxyl were predominant contributors in the complexation of ammonium ions and ion exchange processes.

Xu et al. (2010) applied a new method for preparation of wheat straw as an anion exchanger based on aminated intermediate (epoxypropyltriethylammonium chloride). Methanol solution was used as organic solvent to facilitate epichlorohydrin and triethylamine reaction, and pyridine was applied as a weak–base catalyst to open the strained epoxide rings. The maximum sorption capacities of modified wheat straw for nitrate and phosphate were approximately 52.8 and 45.7 mg/g, respectively, which could be comparable with the maximum biosorption capacity obtained from commercial anion exchange resin, activated carbon and other modified adsorbents. In addition, after four subsequent cycles of adsorption–desorption, both of eluting agents (HCl and NaCl) showed an excellent recovery performance without significant loss in biosorption capacity.

2.4 *Mechanism of biosorption and desorption process*

In fact, biosorption process includes a combination of several mechanisms including electrostatic attraction, complexation, ion exchange, covalent binding, Van der Waals attraction, adsorption and micro–precipitation (Montazer–Rahmati et al., 2011; Witek–Krowiak, 2012). Common mechanisms occurring in biosorption

process are illustrated in Figure 2.3. Physical adsorption takes place because of weak Van der Waals' attraction forces, whereas the so–called chemisorption is a result of relatively strong chemical bonding between adsorbates and adsorbent surface functional groups (Bhatnagar and Sillanpää, 2010).

The main mechanisms known for metal and dye adsorption on cellulosic biosorbents are chelating, ion exchanging and making complexion with functional groups and releasing $[H_3O]^+$ into aqueous solution. Ionic exchange is known as a mechanism which involves electrostatic interaction between positive cations and the negatively charged groups in the cell walls (Fiol et al., 2006). Many studies confirmed that ion exchange mechanism could be included in biosorption process rather than complexation with functional groups on the biosorbent surface. They also showed the role of sodium, potassium, calcium and magnesium present in the adsorbent during ion exchange (Ding et al., 2012; Tunali Akar et al., 2012; Krishnani et al., 2008).

The mechanisms also can be anticipated and verified through the understanding of the surface structure and functional groups, thermodynamic and kinetic studies as well as by combination of different methods of FTIR (Fourier Transform Infra–Red), SEM (Scanning Electron Microscopy), EDX (Energy Dispersive X–Ray), TEM (Transmission Electron Microscopy), Raman microscopy, XPS (X–ray photoelectron spectroscopy), and some conventional techniques like titration, chemical blocking of functional groups and concomitant release of cations from biosorbent during the sorption (Oliveira et al., 2014; Torab–Mostaedi et al., 2013; Witek–Krowiak, 2012; Ofomaja., 2011).

According to the results obtained from the intra–particle diffusion kinetic model, adsorption can be described as multiple sorption rates attributed to fast film diffusion, rate–limiting gradual adsorption stage (pore diffusion) and final slow equilibrium step of intra–particle transport.In batch systems, intra–particle diffusion was not the only rate controlling step but generally it is important in the biosorption kinetic process as adsorbent size was the main parameter of biosorption process(Ahmad et al. 2009). On the other hand, in continuous flow system, film diffusion is more likely the rate limiting step (Rangabhashiyam et al.,

2013). The mechanisms also can be anticipated and verified through the understanding of the surface structure, in order to make easier biosorption process design (Witek–Krowiak, 2012). The main mechanisms were usually found for biosorption process are ion exchange with other metal ions being in wastewater like Na^+, K^+, Ca^{2+} and Mg^{2+}, complexion with functional groups and releasing $[H_3O]^+$ into aqueous solution and chelating with surface functional groups (mainly—COOH, C=C, C—O and O—H) which was controlled by chemical sorption step regarding with pseudo–second–order kinetic model (Ding et al., 2012). Biosorption can be carried out by proton exchange using mineral and organic acids such as HCl, HNO_3, H_2SO_4 and acid acetic, by exchange with other ions like applying $CaCl_2$ or by chelating agents (for example EDTA). It is well known that under acidic conditions the adsorbent surface is protonated by $[H_3O]^+$ ions to make possible desorption of positively charged metal ions from the adsorbent surface (Ozdes et al. 2009).

The studies on Cr(VI) removal claimed that anionic chromium ion species could bind to the positively charged adsorbent surface and converted to Cr(III) through two mechanisms: 1) direct reduction by contact with the electron–donor groups of biosorbent; and 2) indirect mechanism consisting three steps of binding of anionic chromium(IV) ion to positively–charged surface of biosorbent, reduction to Cr(III) and then release the created Cr(III) ions. Low pH values could accelerate the rate of reduction reactions in both of two mechanisms (Blázquez et al., 2009; Krishnani et al., 2008). Besides, thermodynamic study and a good perception of temperature influence on biosorption process can help to understand the adsorption mechanism (Adamczuk and Kołodynska, 2015; Farooq et al., 2010).

In other study, Schiewer and Patil (2008) reported that the protonated citrus peels exhibited very good ability to Pb removal very similar to some ion exchange resins. They discovered, even at high ionic strength environment, Pb removal efficiency remained more than 90% which indicated that electrostatic attraction was not the main binding mechanism.

Along with kinetic and thermodynamic studies, isotherm models can also contribute to information about mechanism of adsorption. Blázquez et al. (2010)

described the types of Pb(II) biosorption on olive stone and two–phase olive mill solid. They highlighted that the type of biosorption is a function influences the shape of adsorption isotherm. This shape associates with formation of monomolecular or multimolecular layer adsorption via both strong and weak adsorbate–adsorbent interactions. Furthermore, based on hypothesis of Dubinin–Radushkevich isotherm, mean free energy of adsorption ($E = \frac{1}{\sqrt{2B_{D-R}}}$) calculated from Dubinin–Radushkevich isotherm can evaluate sorption properties and indicate if main mechanism is chemical reaction dominated by ion exchange (8<E<12 kJ/mol) or physical adsorption (E<8 kJ/mol) (Ding et al., 2012).

Desorption mechanism is similar to that of metal biosorption, therefore, desorbing agent or desorption conditions can be rationally selected (Rangabhashiyam et al., 2013). Heavy metal ions recovery cannot thoroughly fulfilled by desorption. This might be due to metal ions being trapped in the adsorbent porous structure of biosorbent and therefore difficult to release (Ozdes et al., 2009). Langmuir parameter amounts determine metal ion desorption being occurred in shorter or longer time because of metal ion affinity to surface functional groups.

Mata el al. (2009) reported that among cadmium, lead and cupper cadmium presented the lowest affinities for sugar–beet pulp and consequently recovered in shorter time (30 min) by 0.1M HNO_3 in comparison to lead (60 min) and copper (120 min). They also found that during desorption by mineral acid (HCl, HNO_3 and H_2SO_4), biosorbent can become swollen in the acid solution and the mass loss of biosorbent was the result of this damage that was observed between the first and last cycles. Hence, an efficient eluent is one that desorbs the metal completely without any damaging the biomass structure and functionality to be able to reuse.
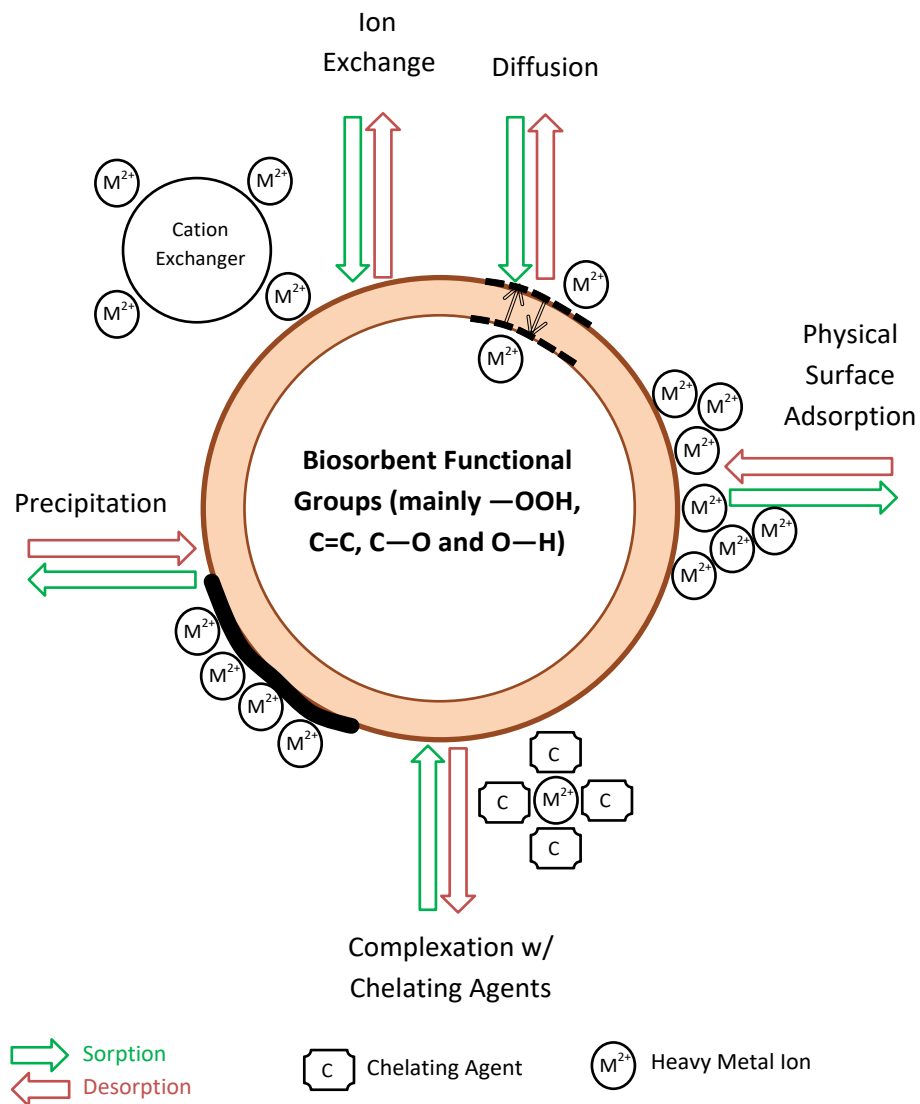
Figure 2.3 Common sorption/ desorption mechanisms

In other study, Njikam and Schiewer (2012) suggested that mineral acids such as HCl, which is cheap and relatively harmless are promising desorbing agents for efficient citrus peels regeneration. Rate–limiting step of desorption could be proposed by proper assuming of how the desorption rate depends on the quantity of metal ion–saturated binding sites. After each sorption and desorption cycle, the total amount of the newly adsorbed metal ions and that which could not be removed from the spent biosorbent by desorption increase. This can be explained as (i) surface functional group hydrolysis and decomposing, (ii) fewer number of unoccupied sites for further sorption and (iii) biosorbent mass loss during

successive sorption and desorption cycles (Gundogdu et al., 2009, Mehta and Gaur, 2005, Yao et al., 2009, Pan et al., 2009).

2.5 *Reusability of heavy metal– loaded wastes and by–products*

As mentioned before, the major disadvantage of biosorption is producing huge amount of solid biomass or aqueous solutions with high concentration of heavy metals to environment. To tackle the problem attributing to solid biomass discharge, applying proper desorbing and regenerating agent would be effective. Therefore, the biosorption process becomes economically and feasibly more attractive (Zafar et al., 2014, Das and Das, 2013, Gautam et al, 2014). On the other hand, for the problem of disposing outputs of desorption process, the metal ions can be removed or precipitated by low–cost chemicals and then recovered for using in industry. For this purpose, a lot of aspects such as process operation cost, biosorbent disponibility and value of recovery metal should be considered (Ronda et al., 2015).

The role of desorbing and regenerating agents implication can be improved in terms of biosorption capacity, desorption efficiency and also biosorbent stability after a number of sequential sorption, desorption and/or regeneration cycles. In many studies, it is very well known that under acidic conditions the adsorbent surface is protonated by $[H_3O]^+$ ions to make possible desorption of positively charged metal ions from the adsorbent surface (Asberry et al. 2015). Higher concentration of acids or bases used as desorbing agents might damage the biosorbent structure, hydrolyze polysaccharides on the surface of the biomass and subsequently decrease the sorption and desorption efficiency and biosorbent mass loss. On the other hand, as a result of excess amount of $[H_3O]^+$ ions on the biosorbent surface and reducing the metal biosorption capacity, regeneration step has been recommended. In some cases, after washing by deionized water, regenerating agent has been applied. Regeneration step could increase the stability and reusability of biosorbents and repairing the damage caused by the desorbing agents and removing the excess protons after each elution and providing new binding sites for next biosorption step. However, a complete desorption of heavy

metal ions could not be achieved which might be due to metal ions entrapped in the intra–pores (Ronda et al., 2015; Mata et al., 2010; Mata et al., 2009).

2.5.1   *Desorptive properties of different desorbing agents*

Desorbing agent must be low–cost, eco–friendly, non–toxic, non–damaging and effective for metal desorption (Kim et al., 2014; Das and Das, 2013; Singha and Das, 2011). Desorption experiments were usually carried out in a similar way to the biosorption studies (Gong et al., 2005). The metal–desorbed biomass was used in repeated sorption and desorption cycles with or without regeneration step to determine reusability potential of the adsorbent in batch system as illustrated in Figure 2.4. After adsorption step, metal–loaded biosorbent was filtered, dried, weighed and shaken with desorbing agents on an orbital shaker. Biosorbent–eluent suspension was centrifuged and the supernatant was filtered and analyzed for metal ions desorbed for further calculations. The biosorbent was repeatedly washed with distilled water after each desorption to eliminate any excess chemical. Biosorbent stability or any probable weight loss was controlled by weighing biomass after drying in oven. Desorption usually continued for enough time within that the outlet metal concentration remained constant and equal or close to zero.

Generally, desorption efficiency of metals adsorbed on biomass either in intact or chemically modified form was studied by many researchers to regenerate and reuse over a number of subsequent adsorption/ desorption cycles by acidic or alkali desorbing agents (Nguyen et al., 2014, Hossain et al., 2012, Liang et al., 2009a, Liang et al., 2009b).

HFO–treated sugarcane bagasse was applied for As(V) removal. Arsenic–loaded biosorbent was eluted by HCl and NaOH at different pH values. As(V) desorption by using 30% HCl, was 17%, whereas the highest recovery of 85% was reached with 1 M NaOH (Pehlivan et al., 2013).The biosorption properties and mechanical strength of olive mill solid waste modified by H_2SO_4 (1 M) for lead removal were studied in a fixed–bed column. This biosorbent retained over 14 cycles of use in continuous system and the life factor revealed that biosorbent bed would be exhausted after 71.3 cycles. Among CH_3COOH, HCl, H_2O, H_2SO_4, NaOH, NaCl and

Na_2CO_3, as the eluting agents, HCl presented the best desorption efficiency of Pb(II) from acid–treated olive stone (Martín–Lara et al., 2012).

Natural and modified orange peel after grafting of methyl acrylate was used to remove Cu, Cd, Pb and Ni. The adsorption and desorption experiments showed dilute HCl solution with concentration of 0.05 mol/L could be an appropriate elution agent for reuse orange peel for 5 cycles without tangible decrease in biosorption capacity (Feng et al., 2011; Feng et al., 2009a; Feng et al., 2009b). By applying HCl to regenerate similar adsorbent loaded with Cu^{2+} and Cd^{2+} ions, CS_2–treated orange peel can be used at least 5 cycles of adsorption–desorption without any changes in adsorptive ability (Schiewer and Patil, 2008).

Other study on wheat bran to lead uptake showed an endothermic and spontaneous adsorption process. To regenerate lead–loaded biosorbent, 0.5 M HCl showed better result in comparison with distilled water for three cycles of sorption/ desorption with no tangible change in biosorption capacity (Bulut and Baysal, 2006).

Zafar et al. (2014) explained the effect of chemical pretreatment and desorbing agent of nickel uptake by rice bran wastes. In terms of nickel biosorption capacity and economic efficiency pretreatment by nitric acid and hydrochloric acid were more effective than sodium hydroxide, aluminium hydroxide, sulphuric acid, formic acid, formaldehyde solution, acetic acid and methanol. Desorption studies revealed that biomass could be washed by nitric acid (0.1 M) more efficient rather than potassium hydroxide and calcium chloride (with same molarity). Nickel recovery slightly decreased with the increase in adsorption and desorption cycles. After three cycles, desorption efficiency of rice bran modified by nitric acid and hydrochloric acid reduced by about 20%. In this case nitric acid properly played the role of both chemical modification and desorbing agent as well. It may attribute to effectively release polysaccharides, also easily protonate pure amino sugar (namely ᴰ–glucosamine) and also increase the biomass porosity.
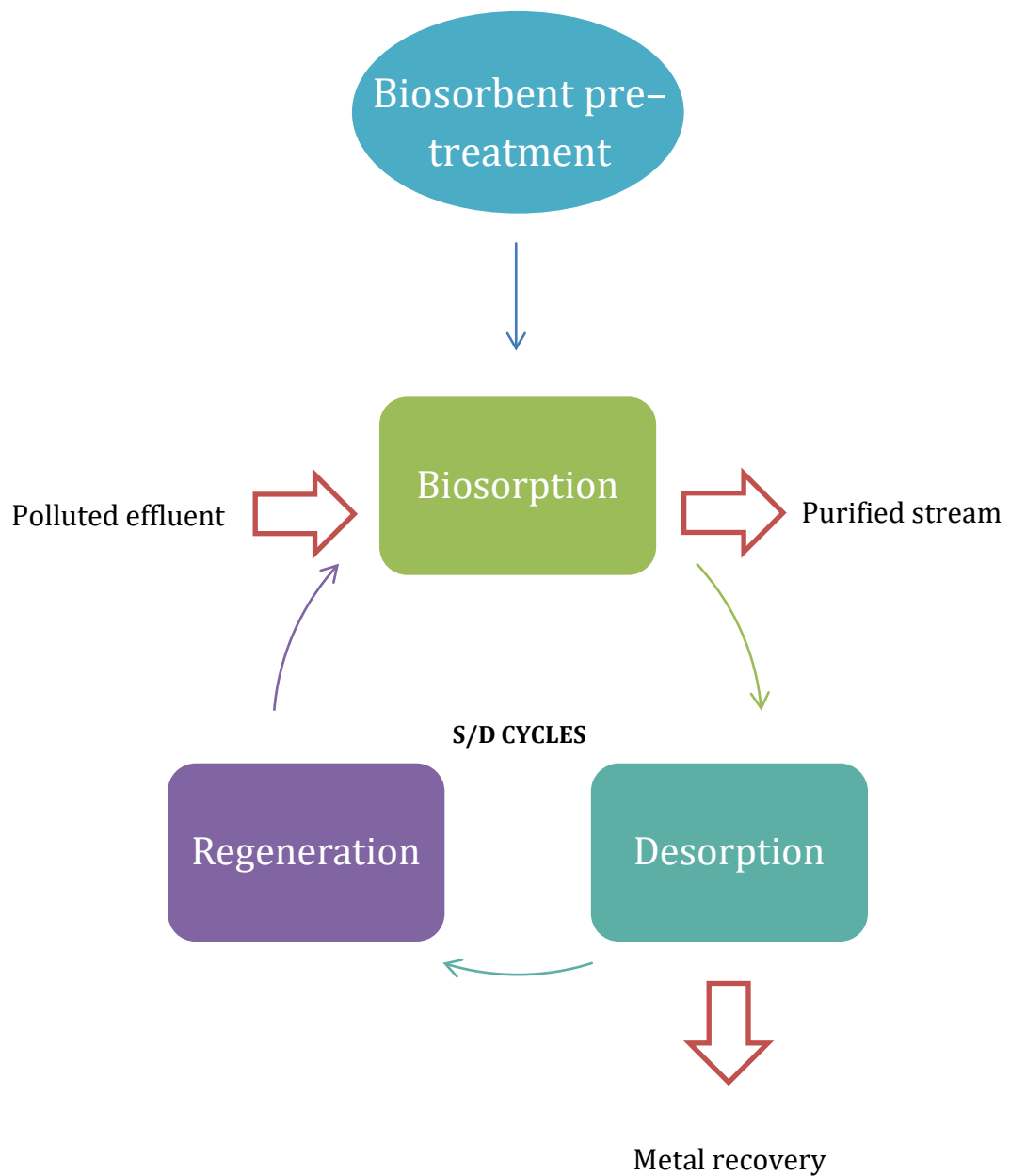
Figure 2.4 Batch experiment schematic diagram for sorption/ desorption/ regeneration cycles

Nitric acid has been used for washing the citrus peel saturated by cadmium in different concentrations. Cadmium desorption was very fast within the first 60 min and after 240 min, desorption efficiency reduced as a result of probable biomass structure damages. The same results could be achieved for higher concentrations of acid. However, desorption efficiency of EDTA reported in other studies showed that long exposure with complexing or chelating agents unlike mineral acids did

not make any biosorbent damage. Besides, chelating agents such as EDTA are more expensive than common mineral acids even in low concentrations. Therefore, applying cheap HCl with lower environmental concerns than other acids is recommended as industrial desorbent (Njikam and Schiewer, 2012, Pessoa de Franca et al., 2002, Schiewer and Volesky, 1997).

Khan et al. (2012) compared the leaching of Ni ions from mustard oil cake in single and multiple metal ion solutions. Adsorption efficiency of Ni(II) ions onto biosorbent in single metal and multi–metal system were 68.7% and 51.3%, respectively as expected. Saline and alkaline desorbents for releasing Ni ions binding to biosorbent were less effective than acidic medium. Among studied desorbents, nickel desorption efficiency by both 0.05M and 0.1M HCl in single metal ion system was reported almost 100% (99.4% and 99.8%, respectively) while in multi–metal system decreased to only 44.75%. In addition the biosorption efficiency in continuous process was comparatively less than batch process due to not enough contact time of the effluent with biosorbent. On the other hand desorption efficiency in batch system was slightly higher than continuous fixed–column in initial cycles (3 cycles) and then decreased from 66% to 59.6% at seventh cycle. This behaviour was basically due to continuous usage of the biosorbent.

Desorption process like biosorption is influenced by temperature and eluent concentration. Based on the study has been carried out by Bernardo et al. (2009) to investigate chromium desorption from metal–loaded agro–waste materials such as agave bagasse, oat and sorghum straws, the authors announced an interaction between Cr(III) ions and EDTA due to a chelate formation at 55 ℃ (not seen at lower temperatures of 25 and 35 ℃). Moreover, desorbing and regenerating properties of EDTA were more preferable than HNO_3 and NaOH because of less considerable biomass weight loss and not any biosorbent color change.

2.5.2   Regeneration of biosorbent

It is desirable to desorb and recovered the adsorbed metals and also regenerate the adsorbent materials for another cycle of application. The regeneration of the adsorbent can be achieved by washing loaded adsorbent with an appropriate

desorbing solution. Desorbing and regenerating agents must be cheap, effective, non–polluting and non–damaging to the adsorbent structure (Ozdes et al. 2009).

It is necessary to explain that the word of "regeneration" in different articles refers to applying metal–loaded biosorbents in several cycles of sorption and desorption steps in batch or continuous systems and in a few studies showed applying a chemical to make the surface mechanically stable, repair the surface damage by eluents or removing the protons of acidic desorbents before reutilizing in next sorption and desorption cycle. The other variable that affects the biosorption efficiency in a consecutive series of sorption and desorption is cell wall and the richness of polysaccharides. The progressive decrease of biosorptive potential of biomasses is as a direct result of both micro and macro restructuration. Therefore, some chemicals such as $CaCl_2$, $Ca(OH)_2$ and NaOH were suggested to be applied as regenerating agent based on biomass type (Mata et al., 2010).

Besides, in literature, a slight structural modification was reported for some chemical like EDTA rather than alkaline and acidic solution when they were used as desorbents. Therefore, for these materials both desorbing and regenerating potential can be simultaneously considered (Bernardo et al., 2009).

The reusability and economic feasibility of mustard oil cake to remove nickel ions was studied in seven cycles of sorption and desorption and the Ni ions leached to HCl solution in batch and continuous process. In spite of the fact that HCl could introduce some surface active sites on biosorbent surface it stopped at third cycles because of decomposition of surface functionalities (Khan et al., 2012).
Other similar study was completed by Reddy et al. (2012) to find the effect of HCl concentration varied from 0.1 to 0.6 M to regenerate *Moringa oleifera* leaves. The *M. oleifera* leaves powder was esterified by NaOH followed by citric acid modification and then applied for Cd, Ni and Cu removal.0.4M hydrochloric acid was chosen as a suitable concentration for five cycles of sorption and desorption. The results showed that esterified *M. oleifera* leaves powder can be used repeatedly at least four times without significantly losing the biosorption capacity for Cd(II), Cu(II) and Ni(II). The biosorption efficiency of fifth Sorption/ Desorption cycle was comparatively equivalent with first one (>90% for all metals).

Mata et al. (2009 and 2010) using 0.1M HNO_3 as desorbing agent and 1M $CaCl_2$ as regenerating agent for sugar–beet pectin gel beads in order to Cd, Cu and Pb uptake. It was very successful to reuse pectin gel beads after nine cycles of sorption/ desorption/ regeneration. The results were very promising. Calcium chloride can increase the stability and reusability of biomass and repairing the damage caused by the desorbing agents and removing the excess protons after each elution providing new binding sites. Pectin gel beads were successfully reused (9 cycles) without any significant loss in biosorbent mass (an average 20%). Metals uptake levelled off for lead and copper removal and increased for cadmium after using a 1M $CaCl_2$ regeneration step after each desorption. In contrast, without regenerating step, the biomass loss was more than 20%. It was obvious that the biosorbent appearance, coarse porosity and even visible structure and mechanical stability demolish completely. In other study, calcium chloride was successfully utilized as an eluent to desorbed cadmium, lead and nickel adsorbed on brown algae of *Cystoseira indica*. In that investigation, calcium chloride was compared with sodium chloride and acetic acid for five consecutive cycles of sorption and desorption (Montazer–Rahmati et al., 2011).

In Table 2.5, desorption efficiency and reusability of some common biosorbents are listed. According to these results, it can be concluded that the factors are responsible for selecting the adequate desorbent for metal recovery are biomass type, metal and concentration of eluent.

2.6   *Process costs and overall scheme of biosorption*

In order to estimate the costs of biosorption treatment process, capital investment and plant operating costs are excluded from discussion as they rely on the plant type and nature of wastewater and pollutants to be treated. The cost of collection, transportation, processing and pre–treatment of biosorbents, providing and maintaining optimal conditions along with biosorbents regeneration and then disposal of exhausted biosorbents are major aspects to be considered for the process cost estimation (Vijayaraghavan and Balasubramanian, 2015). Many researchers employed natural wastes and by–products generated from agricultural and food industries such as bacterial or fungal wastes from food

industries, activated sludge from wastewater treatment plants, seaweed and plant residues (Abbas et al., 2014). Most of these wastes or by–products are considered to have low commercial importance and cause disposal problems and extra costs; hence they can be obtained from respective industries for free or at low cost. The cost regarded to transportation can be minimized if the local source of wastes applies for wastewater treatment facilities (Volesky, 2007). As discussed earlier some sort of biosorbent pre–treatment is always necessary to obtain high biosorption efficiency and performance, consequently the major cost is usually associated with the biosorption process preparation including chemical costs as well as disposal costs of chemical wastes. In real wastewater treatment process, by considering the volume of wastewater, the pH control is practically possible for keeping optimum treatment conditions. Besides, once a biosorbent is completely utilized in repeated cycles, landfilling or chemical or thermal destruction techniques seem only practical and ultimate biosorbent disposal procedures, however they are not cost–effective and eco friendly. Landfilling is expensive due to high tax whereas destructive techniques such as incineration or exposure to strong acids/bases may lead to sludge disposal costs. Some exhausted biosorbents can also be reused as a renewable source of biofuels or compost for soils once heavy metal ions are completely removed from the exhausted biosorbents (Kumar et al., 2017; Vijayaraghavan and Balasubramanian, 2015).

2.7   *Conclusion, future perspectives and research gaps*

2.7.1   *Major findings and conclusions*

According to a substantial number of researches carried out on wastewater treatment via biosorption processes, a growing trend to use lignocellulosic agro–industrial wastes and by–products as an abundant alternative can be seen. The application of lignocellulosic–based biosorbents for removing various pollutants from water and wastewater offers many attractive features such as the outstanding adsorption capacity for a wide range of pollutants and the fact that these materials are low–cost, non–toxic and biocompatible.

It can be concluded that the obtained maximum adsorption capacity, selectivity and regeneration efficiency of lignocellulosic agro–industrial wastes and by–products provide some idea for selecting proper adsorbent for metallic and organic pollutants, dyes, and nutrients removal. There is a favourable pH range for aquatic pollutants in which maximum adsorption takes place.

Additionally, the research results can help to propose optimum operation conditions for future studies on water and wastewater detoxification, as well as to improve environmental issues of aquatic industrial waste disposal and to facilitate solid wastes minimization.

However, most of studies have focused on influential parameters, isotherm, thermodynamic and kinetic studies in batch mode. Thus, the main problems that currently exist with agro–industrial wastes and by–products are lack of informaion about the biosorption mechanism, material characterization, removal efficiency and reusability of adsorbents in continuous mode.

2.7.2   *Future perspectives and research gaps*

Although much work has been implemented on the biosorptive capabilities of different lignocellulosic wastes and by–products for wastewater purification, there are still significant research gaps as follows.

- It is desirable to develop sustainable biosorbents whose selectivity for pollutants removal varied by biosorbent type, operation conditions and physico–chemical parameters.

- Although lignocellulosic wastes and by–products have adsorption capacity limitation in comparison with current commercial adsorbents, a good adsorbent selection with proper chemical modification can considerably improve adsorptive properties of the material.

Table 2.5 Desorption efficiencies of different biosorbents at first and last sorption and desorption cycles

Biosorbent (modification)	Metal ion	Desorbing agent	S/D Cycles	Desorption efficiency (%)	Reference
Rice bran (HNO_3)	Ni(II)	HNO_3	3	89.4%[a] and 68.2%[b]	Zafar et al., 2014
Rice bran (HCl)	Ni(II)	HNO_3	3	86.5%[a] and 67.4%[b]	Zafar et al., 2014
Mustard oil cake	Ni(II)[c]	HCl	3	99.8%[a] and 59.6%[b]	Khan et al., 2012
Mustard oil cake	Ni(II)[d]	HCl	1	44.75%[a]	Khan et al., 2012
Grapefruit peels	Ni(II)	HCl	5	98%[a] and 95%[b]	Torab–Mostaedi et al., 2013
Grapefruit peels	Cd(II)	HCl	5	97%[a] and 93%[b]	Torab–Mostaedi et al., 2013
Pine bark	Pb(II)	HCl	5	86%[a] and 21%[b]	Gundogdu et al. 2009

[a]First cycle of sorption/ desorption

[b]Last cycle of sorption/ desorption

[c]Single metal system

[d]multi–metal system

- A notable disadvantage of employing agro wastes and by–products is leaching soluble organic compounds into water as secondary pollutions and weakening the mechanical structure stability during the treatment process. This might limit their use in large scale applications and in fixed–bed columns with high influent flow rate. Accordingly further research is needed in this regard.

- In the past decades, the effects of pH, metal ion concentration, biomass concentration, contact time, temperature and ion strength on biosorption have been widely studied, but information regarding desorption as one of the most important aspects of any successful biosorption–process development is still scanty. Hence, a breakthrough in adsorbent development is required to solve the critical problems of metal ion recovery along with biosorbent regeneration even for low–cost agro wastes and by–products to keep the process cost down and also to introduce green technologies for wastewater purification.

- To find the most economic and highly effective desorbing agent, along with determining optimum elution conditions, desorption kinetic models (e.g. Lagergren zero–order, pseudo–first and second order kinetic models) should be deliberately considered in future studies or modified for desorption process if required. Desorptive performance of many more chemicals can be studied to improve desorption efficiency and precious metal recovery by suitable eluents in the matter of the functional groups and characteristics of each type of lignocellulosic materials.

- The number of papers on batch biosorption and the current developed kinetic and isotherm models can provide proper explanation and simulation for most of the mechanism studies on biosorption process and continuous process in fixed–bed column or Continuous Stirred–Tank Reactor (CSTR).

- Despite the fact that many attempts have been made on wastewater treatment via biosorption process, but more researches are needed for industrial application in terms of economy and feasibility. The feasibility of using lignocellulosic wastes and by–products will be studied in pilot scale and then subsequently checked in commercial industrial scale. Besides, the disposal of

used adsorbent in safe and environmental friendly way and making the valuable end–use of these wastes should be deliberately considered in future studies.

Chapter 3

Experimental Investigation

Chapter 3 Experimental investigations

3.1   *Materials*

3.1.1   Preparation of heavy–metal–containing effluent

The stock solution containing Cd, Cu, Pb and Zn were prepared by dissolving cadmium, copper, lead and zinc nitrate salt, $Cd(NO_3)_2 \cdot 4H_2O$, $Cu_3(NO)_2 \cdot 3H_2O$, $Pb(NO_3)_2$ and $Zn(NO_3)_2 \cdot 6H_2O$ in Milli–Q water. For remove any inaccuracies in metal concentration, all stock solutions were chemically analyzed to correct their concentration to use in experiments with required amounts. The chemical analyses and concentration measurements were carried out by Microwave Plasma–Atomic Emission Spectrometer, MP–AES (Agilent Technologies, USA)

3.1.2   The raw municipal wastewater

The real wastewater used in this study was the primary effluent, downstream of the Malabar WWTP sedimentation tanks collected from Sydney Water Plant, NSW, Australia. Prior to the adsorption test, the sewage was settled for 24 hr, filtered using a 150 μm sieve, and used for column adsorption tests without any pH alterations. The concentrations of Cd, Cu, Pb and Zn and major quality parameters of the solutions before and after passing through the column were determined according to standard procedures. Since the concentrations of Cd, Cu, Pb and Zn were very low, an appropriate amount of metallic nitrate salts were added to provide the desired initial concentrations for each metal ions. Semi– simulated wastewater used in this content refers to this adapted municipal wastewater.

3.1.3   Preparation of adsorbents

The biosorbents applied in metal removal process for selecting the best ones in term of biosorption capacity were sawdust (SD), sugarcane (SC), corncob (CC), tea waste (TW), apple peel (AP), grape stalk (GS), mandarin peel (MP), orange peel (OP), maple leave (MP), passion fruit skin (PS), garden grass (GG), mango skin (MG), lychee rind (LC), avocado peel (AV), eucalyptus leave (EU), egg shell (ES), coffee waste (CW) and also coir peat (CP). All biosorbents were collected from

Sydney area or local markets. After using or removing their useable parts, they were washed by tap and distilled water to remove any dirt, color or impurity and then dried in the oven (Labec Laboratory Equipment Pty Ltd., Australia) at 105 ˚C overnight. Having ground and sieved (RETSCH AS–200, Germany) to different sizes (<75 μm, 75–150 μm, 150–300 μm 300–425 μm, 425–600 μm and 600–1000 μm), the natural biosorbents were kept in a desiccator prior to use in future experiments.

3.1.4 Preparation of modified adsorbents

Biosorbent was physical modified by heating (50–150 ˚C in a drying oven for 24 hr) and boiling (100 g biosorbent in 150 mL water). For chemical modification, HCl (1M), NaOH (1M), HNO_3 (1M), H_2SO_4 (1M), $CaCl_2$ (1M), formaldehyde (1%) and mixture of NaOH (0.5M) and $CaCl_2$ (1.5M) in ethanol were used as the modification agents. 10 g of each biosorbent was soaked in 1 L of each solution and thoroughly shaken (150 rpm) for 24 hr at room temperature. Pretreatment with sodium chloride and calcium chloride solution containing 500 mL ethanol, 250 mL NaOH (0.5M) and 250 mL $CaCl_2$ (1.5M) was same as the other chemicals. Afterwards, all materials were filtered and rinsed several times with distilled water to remove any free chemicals until the neutral pH to be obtained and dried in oven over night. All biosorbents were kept in a desiccator prior to use in future experiments.

3.1.5 Chemical reagents

All the reagents used for analysis were of analytical reagent grade from Scharlau (Spain) and Chem–Supply Pty Ltd (Australia). Solution pH was adjusted with 1M HCl and 1M NaOH solutions.

3.2 *Methods*

3.2.1 Biosorption studies in batch system

The batch experiments were performed with synthetic multi–metal solution with concentration of 3000 mg/L for each metal by dilution in Milli–Q water for predetermined metal concentration. A known weight of adsorbent (5 g/L) was

added to a series of 200 mL Erlenmeyer flasks containing 50 mL of metal solution on a shaker (Ratek, Australia) at room temperature and the flasks were shaken at 150 rpm for 24 hr. To avoid vaporizing aqueous solution, all flasks covered with the parafilm during biosorption process. Once equilibrium reached, to separate the biomasses from solutions, the solutions were filtered by Whatman™ GF/C–47 mm/circle (GE Healthcare, Buckinghamshire, UK) filter paper and final concentration of metal was measured using MP–AES. All the experiments were carried out in duplicates.

The amount of heavy metal ion adsorbed, q(mg/g) was calculated from the following Equation:

$$q = \frac{v(C_i - C_f)}{m}$$ (3.1)

where, C_f and C_i (mg/L) are the initial and equilibrium metal concentrations in the solution, respectively. v (L) the solution volume and m (g) is the mass of biosorbent. All the experiments were carried out in duplicates and the deviation within 5%.

3.2.1.1   Characterization of adsorbents by FTIR and SEM

To determine the functional groups involved in biosorption of Cd(II), Cu(II), Pb(II) and Zn(II) onto MMBB, a comparison between the Fourier Transform Infrared Spectroscopy (FTIR) before and after meal loading was done using SHIMADZU FTIR 8400S (Kyoto, Japan). Metal–loaded biosorbent were filtered and dried in the oven. The small amount of samples was placed in the FTIR chamber on the KBr plates for analysing the functional groups involving in biosorbent process by comparing with unused multi–metal biosorbent.

Scanning Electron Microscopy (SEM) and Energy Dispersive X– ray Spectrometry (EDS) of the free and loaded MMBB was performed on ZEISS EVO|LS15 (Germany) at an electron beam voltage of 15 kV, pressure of about 7×10^{-6} Torr, temperature of 20 ℃, spot size of 10–200 μm and with the working distance of 9–11mm. The MMBB samples were examined before and after modification, biosorption, desorption and regeneration to elucidate the porous properties of the biosorbents.

3.2.1.2 Effects of process parameter

Influence of pH

In order to study the effect of pH on heavy metal adsorption, the initial pH of the solutions varied from 2 to 5.5, by adding appropriate amount of NaOH or HCl solutions. The batch procedure at each pH was followed as above described using an initial concentration of 50 mg/L.

Influence of contact time

The contact time varied from 15 min to 24 hr for the biosorption of Cd(II), Cu(II), Pb(II) and Zn(II) adsorption on MMBB at different initial concentration of 50 mg/L and room temperature with similar procedure explained above.

Influence of adsorbent dose

The dependency of Cd(II), Cu(II), Pb(II) and Zn(II) adsorption on biosorbent dose was studied at room temperature and optimum pH by varying biosorbent dose (0.2, 1, 2, 5, 10 and 20 g/L).

Influence of particle size

In order to study the effect of particle size on adsorption, batch experiments as above described were carried out using the biosorbent with different particle sizes of <75 μm, 75–150 μm, 150–300 μm 300–425 μm, 425–600 μm, 600–1000 μm and 1–2 mm and an initial metal concentration of 50 mg/L, at room temperature.

Effect of biosorbent ratio

The effect of proportions for selected biosorbent for heavy metal removal was fulfilled with different proportions of the biosorbents. In order to test the significance and adequacy of the model, statistical testing of the model in the form of analysis of variance (ANOVA) was conducted. 1:1:1 ration is considered as reference ratio for any comparison.

Influence of temperature

The effect of temperature on the Cd, Cu, Pb, and Zn adsorption was investigated in the range 298–323 K (25–50 ℃) in batch experiments already described and initial concentration of 1–50 mg/L.

Influence ion strength

The effect of ionic strength on biosorption is studied by performing equilibrium sorption tests in batch systems. The flasks contained heavy Cd, Cu, Pb and Zn with initial concentrations of 10, 50 and 100 mg/L. Ionic strength of solutions varied by adding $NaNO_3$ with concentrations of 0.1 and 0.2 M. These relatively high concentrations were chosen for simulating the real wastewaters. For comparison with lower ionic strength level, there was a reference case with no addition of $NaNO_3$ to the heavy metal solution.

Effect of biosorbent drying temperature

All of biosorbents were dried at various temperatures to investigate the influence of drying temperature increasing from 50 to 150 ℃ on drying rate and remaining weight.

3.2.2   Biosorption kinetic studies

A series of contact time experiments for cadmium, copper, lead and zinc adsorption on modified MMBB from 0–3 hr were carried out at pH 5.5±0.1 and room temperature. Each sample was taken each 15 min from 1 L solution containing Cd, Cu, Pb and Zn ions with initial concentration of 10, 50 and 100 mg/L and 5 g of biosorbents. Experimental data of kinetic studies were fitted to the pseudo– first and pseudo– second order kinetic models.

3.2.3   Biosorption isotherm studies

The isotherm study was performed by mixing 5 g/L MMBB with 50 mL solution of various Cd, Cu, Pb and Zn concentrations (10–500 mg/L) in a series of Erlenmeyer flasks. The initial pH values were kept at optimal pH (5.5±0.1). The suspensions

were shaken at 150 rpm, room temperature for 3 hr on a rotary shaker to ensure the equilibrium was fully reached. The relationship between metal biosorption capacity and metal concentration at equilibrium has been described by very common Langmuir and Freundlich isotherm models. The kinetic and isotherm constants were evaluated by non–linear regression using MATLAB® software. Furthermore, residual root mean square error (RMSE), error sum of square (SSE) and coefficient of determination (R^2) were used to measure the goodness of fitting along with model parameters.

3.2.4   Biosorption thermodynamic studies

The impact of temperature on the Cd, Cu, Pb, and Zn adsorption was evaluated by performing experiments in the range 298–323 K (25–50 ˚C). The amount of 5 g/L MMBB was added to several 200 mL Erlenmeyer flasks containing 50 mL of solution with different initial heave metal concentration (1–50 mg/L). The pH of suspensions was kept at optimal pH (5.5±0.1). After being covered with parafilm, to keep the reaction constant, the flasks were shaken at 150 rpm in a thermostatic shaker. At the end of the contact time, the suspensions were filtered and the filtrates were analyzed to identify cadmium, copper, lead and zinc concentration.

3.2.5   Desorption studies in batch system

Desorption study was carried out in a similar way to the biosorption studies. After adsorption step, metal– loaded biosorbent (5 g/L) was filtered, dried, weighed and shaken with 50 mL of desorbing agents in 200 mL Erlenmeyer flasks at 150 rpm on an orbital shaker. The suspension of metal– loaded MMBB and eluent was centrifuged (Sigma203, Germany) at 4000 rpm for 15 min and the supernatant was filtered and analyzed for metal ions desorbed. Desorption of metal–loaded biosorbent was studied with different eluting agents including NaCl, $CaCl_2$, NaOH, CH_3COOH, HCl, HNO_3, H_2SO_4 and Milli–Q water. Following biosorption cycle with contact time of 3 hr, metal–loaded biosorbent was filtered and then added in 100 ml of above solutions and shaken at 150 rpm for 3 hr. After desorption, adsorbent was washed repeatedly with Milli–Q water to remove any residual eluting solution and used for the next biosorption cycle.

In order to evaluate the regeneration properties of 1M $CaCl_2$, desorption experiments were performed with and without regeneration step in five consecutive sorption/ desorption cycles.
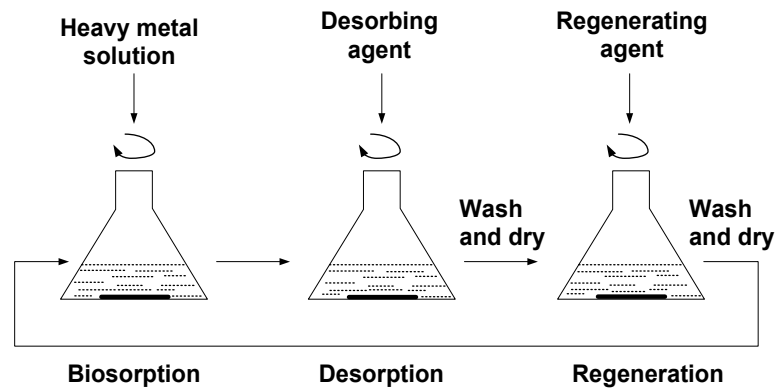
Figure 3.1 Schematic diagram of batch desorption study

3.2.6   Biosorption studies in continuous fixed–bed column

The continuous sorption of Cd(II), Cu(II), Pb(II) and Zn(II) by MMBB was performed in a mini glass column of 100 cm long and 22 mm of inner radius (Figure 3.2). 5, 10, 15 g of biosorbent (particle size distribution = 425–600 μm) mixture was uniformly packed into the column with respective bed heights of 9.5, 21 and 31 cm. A disk with a 150 μm pore was constructed on the bottom of the glass column to support the biosorbent and also prevent any loss. The column was first filled with glass beads (~5 cm) at the bottom. It was then packed with 2 g glass wool (about 2 cm), modified MMBB, 2 g of glass wool and this was followed by another layer of glass beads (~5 cm) for an even liquid flow across the column's cross–sectional area. The glass wool prevented venting of MMBB accompanied by effluent. The column was packed with a defined amount of MMBB (5, 10, 15 g) to achieve the desired bed height. Once the columns were filled, the biosorbent beds were fully immersed by distilled water, and then the bed was left to swell to ensure complete air bubbles expulsion. Following this the column was compacted by gravity. The fixed bed's packing was kept at a constant density. To ensure consistent packing porosity, the column was packed at varied bed heights using a constant bulk density of MMBB which was determined from the packing bulk density in a 0.5 m high column.

Column leaching experiments were conducted at room temperature, and the leaching rate was maintained at 10, 20 and 30 mL/min. In other word, the superficial velocity (v) also called hydraulic loading rate (HLR) was kept at 1.578 m^3/m^2 hr, 3.156 m^3/m^2 hr and 4.734 m^3/m^2 hr. The metal solutions were fed into the top of the column from a 20 L storage tank using a mechanical pump. The feed synthetic solution containing various Cd, Cu, Pb and Zn concentrations (10, 20, 30 mg/L) and semi– simulated wastewater passed through the column in a downward direction at different flow rates (10, 20, and 30 mL/min) or HLR of 1.578 m^3/m^2 hr, 3.156 m^3/m^2 hr and 4.734 m^3/m^2 hr.

The top of the column was connected to a peristaltic pump (Masterflex® Console Drive, Model No. 77521–47, Cole–Parmer Instrument Company) using a silicone tube to obtain a constant steady downward flow. These experimental parameter values were selected to be as close as possible to those derived from industrial electroplating processes which have been used by other researchers. A stream of synthetic or semi–simulated real wastewater was pumped through the column. 10 mL samples were collected at predefined time intervals to: firstly, assess the residual concentration of metals; and secondly, determine the retained amount of heavy metal by Microwave Plasma–Atomic Emission Spectrometer, MP–AES (Agilent Technologies, USA). In order to ensure the formation of a complete breakthrough curve, each experiment was run for approximately 10 hr. The samples were taken at 15min intervals in the first 4 hr and then at 30min intervals for the rest of the experiment.

The column capacity, q_c (mg), for a given inlet concentration and flow rate is equal to the area under the plot of the adsorbed metal concentration, where C_i and C_e (mg/L) are the influent and effluent metal ion concentrations, respectively, versus time (min) and is calculated as follows (Martín–Lara et al., 2016):

$$C_{ads} = C_i - C_e \qquad\qquad\qquad (3.2)$$

$$q_c = \frac{QA}{1000} = \frac{Q}{1000} \int_{t=0}^{t=t} C_{ads}\, dt \qquad\qquad\qquad (3.3)$$

where Q is the flow rate (mL/min), A is the area under the breakthrough curve and t (min) could be t_{total}, t_{sat} or t_b that represent the total flow time, the saturation or

exhaustion time (C_e/C_i = 90%), or the breakthrough time (C_e/C_i = 10%), respectively.

A Glass wool
B MMBB
C Glass beads
D Untreated wastewater tank
P Pump

Sample analysing in MPAES

Metal Conc. data
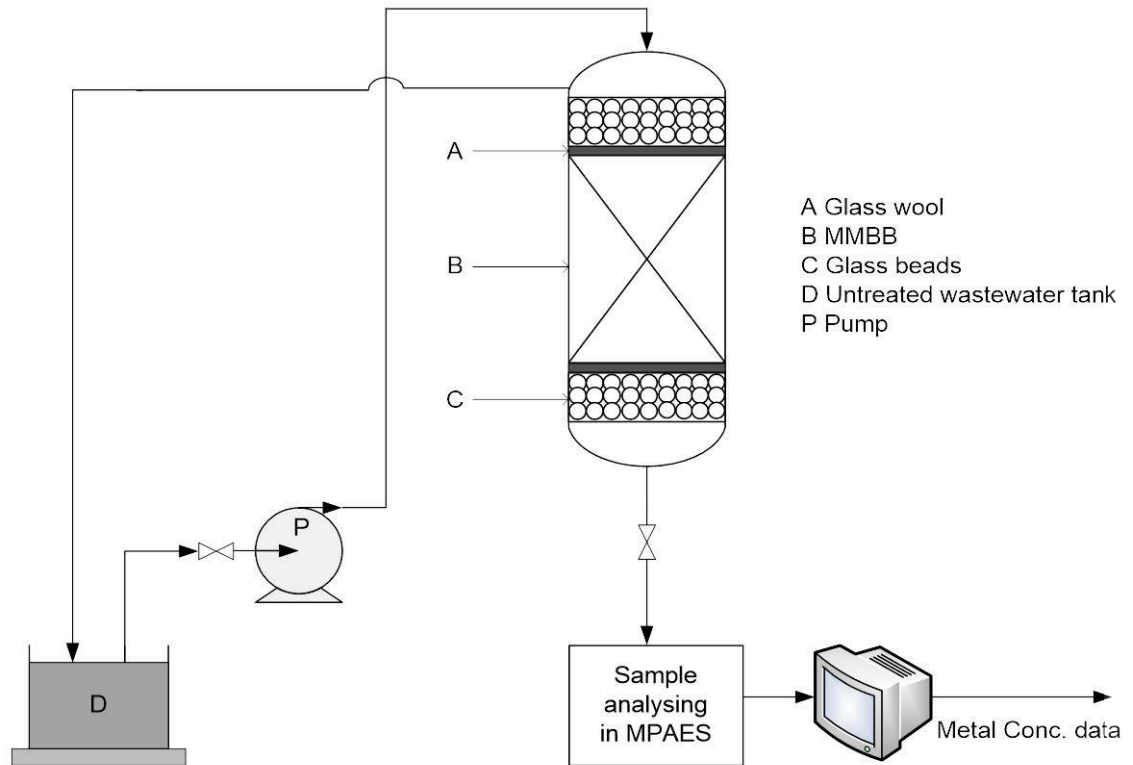
Figure 3.2 Schematic diagram of the experimental set up for a continuous process

The amount of metal ions sent to the column at different time, in mg, can be calculated from the following expression;

$$m_{total} = \frac{C_i Qt}{1000}$$ (3.4)

And the metal removal (%) can be calculated from the ratio of column capacity to the amount of metal ions sent to the column as;

$$\%R = \frac{q_c}{m_{total}} \times 100$$ (3.5)

The biosorption capacity, q, the weight of Cd(II), Cu(II), Pb(II) and Zn(II) adsorbed per unit dry weight of biosorbent (mg/g) can be determined as following;

$$q = \frac{q_c}{M}$$ (3.6)

where M is the total mass of the biosorbent in the column (g).

The equilibrium metal concentration, C_{eq} (mg/L);

$$C_{eq} = \frac{m_{total} - q_c}{V_{ef}} \tag{3.7}$$

$$V_{ef} = Qt \tag{3.8}$$

In each experiment the mass transfer zone, MTZ (cm) was calculated by:

$$MTZ = L(1 - \frac{t_b}{t_{sat}}) \tag{3.9}$$

where L is the bed height (cm).

The empty bed contact time (EBCT) in the column (min) is achieved from the ratio of bed volume (mL) to the flow rate (mL/min) as follows (Ohura et al., 2011):

$$EBCT = \frac{Bed\ volume}{Flow\ rate} \tag{3.10}$$

3.2.7 *Continuous desorption experiments*

The desorption study in batch experiments showed that 0.1 M HCl (5g/L) was the best desorption agent. Prior to conducting the desorption test, metal–loaded fixed–bed column was thoroughly washed with a large amount of distilled water for 30 min (20 mL/min) to eliminate unbound heavy metal ions. After each desorption cycle by passing 0.1M HCl (10 mg/L), the column was washed with distilled water for 30 min (20 mL/min) in order to eliminate the rest of the acid placed in the bed. Then 1 M CaCl$_2$ solution with flow rate of 10 mL/min passed through the column to regenerate the used biosorbent. The column was followed by rinsing again using distilled water for 30 min (20 mL/min) and then run for another biosorption cycle (10 mL/min).

The elution efficiency (%E) can be obtained by dividing the amount of metal desorbed by the amount of metal adsorbed in the previous biosorption stage and the amount of metal remaining on the biosorbent following desorption stage. As a result, the efficiency of metal ion removal was determined for each cycle using the following equations (Martín–Lara et al., 2016):

$$q_{total,d} = \frac{Q}{1000} \int_{t=0}^{t=t} C_e \, dt \tag{3.11}$$

$$q_{e,d} = \frac{q_{total,d}}{M} \tag{3.12}$$

$$\%E = \frac{q_{e,d}}{q_i + q_{e,d}} \times 100 \tag{3.13}$$

where $q_{e,d}$ is g of desorbed metal per g of adsorbent and M is the total mass of the biosorbent in the column. In the first cycle the adsorbent is free of heavy metal ions ($q_i = 0$), but in the consecutive cycles q_i (mg/g) is different from zero, as the desorbing agent was not completely efficient. Hence, some heavy metal ions were retained at the adsorbent binding sites.

3.3   *Calculations*

3.3.1   Batch biosorption process analysis and modeling

3.3.1.1   Adsorption kinetics in batch system

In batch systems, the adsorption kinetics was described by a number of models with varying degrees of complexity such as pseudo–first–order, pseudo–second–order and intra–particle diffusion kinetic model. The pseudo–first–order kinetic model known as the Lagergren equation and takes the form as Febrianto et al., 2009:

$$q_t = q_e[1 - \exp(-K_1 t)] \tag{3.14}$$

where, q_t and q_e are the metal adsorbed at time t and equilibrium, respectively, and K_1 (min^{-1}) is the first–order reaction rate equilibrium constant.

The pseudo–second–order kinetic model considered in this study is as follows:

$$\frac{t}{q_t} = \frac{1}{K_2 q_e^2} + \frac{t}{q_e} \tag{3.15}$$

where, K_2 (g mg^{-1} min^{-1}) is the second–order reaction rate equilibrium constant.

The intra–particle diffusion model follows:

$$q_t = K_P t^{1/2} + C \tag{3.16}$$

3.3.2   Adsorption isotherm in batch system

To optimize the design of biosorption process, it is necessary to acquire the appropriate correlation for equilibrium curve. In this study, the metal biosorption capacity as a function of metal concentration at equilibrium state has been described by very common two–parameter models of Langmuir, Freundlich, Dubinin–Radushkevich and Temkin and three–parameter models of Khan, Sips, Redlich–Peterson and Radke–Prausnitz adsorption isotherms. All the model parameters were evaluated by non–linear regression using MATLAB® software. Furthermore, residual root mean square error (RMSE), error sum of square (SSE) and coefficient of determination (R^2) were used to measure the goodness of fitting along with model parameters.

Langmuir isotherm model is as follows:

$$q_e = \frac{q_{m,L} b_L C_e}{1 + b_L C_e} \tag{3.17}$$

where, $q_{m,L}$ is the maximum metal biosorption and b_L(L/mg) the Langmuir constant. These constants related to monolayer adsorption capacity and energy of adsorption respectively (Montazer–Rahmati et al. 2011).

Freundlich isotherm model is an empirical equation presented as follows (Montazer–Rahmati et al., 2011):

$$q_e = K_F C_e^{1/n} \tag{3.18}$$

where K_F (L/g) is Freundlich constant and n the Freundlich exponent. It is assumed that the stronger binding sites on a heterogeneous surface are occupied first and binding strength decreases with increasing degree of site occupation.

The Dubinin–Radushkevich (D–R) equation is generally expressed as follows:

$$q_e = q_{D-R} \exp(-B_{D-R} \varepsilon_{D-R}^2) \tag{3.19}$$

$$\varepsilon_{D-R} = RT \ln(1 + \frac{1}{C_e}) \tag{3.20}$$

Where $\varepsilon_{D-R,}$ the Polanyi potential, is a constant related to the biosorption energy, R is the gas constant (8.314 kJ/mol) and T is the absolute temperature (K). q_{D-R} and B_{D-R} are the D–R isotherm constants in mg/g and mol^2/kJ^2, respectively.

According to Temkin isotherm, interactions between adsorbate and adsorbent make linear decrease in adsorption energy and heat of adsorption. The model is mathematically represented as (Febrianto et al., 2009):

$$q_e = \frac{RT}{b_{Te}}\ln(K_{Te}C_e) \qquad\qquad (3.21)$$

where b_{Te} (kJ/mol) and K_{Te} (L/g) are Temkin model constants.

Radke–Prausnitz isotherm can be represented as (Montazer–Rahmati et al., 2011):

$$q_e = \frac{a_{R-P}r_{R-P}C_e^{\beta_{R-P}}}{a_{R-P}+r_{R-P}C_e^{\beta_{R-P}-1}} \qquad\qquad (3.22)$$

where a_{R-P} and r_{R-P} are Radke–Prausnitz model constants and β_{R-P} the Radke–Prausnitz model exponent. Radke–Prausnitz isotherm constants, a_{R-P} and r_{R-P} for Cd(II), Cu(II), Pb(II) and Zn(II).

The Sips isotherm is a combination of the Langmuir and Freundlich isotherm models and is expected to describe heterogeneous surfaces much better. At high sorbate concentrations it predicts a monolayer adsorption capacity characteristic of the Langmuir isotherm whereas at low sorbate concentrations it reduces to the Freundlich isotherm. It is given as (Febrianto et al., 2009):

$$q_e = \frac{K_S C_e^{\beta_S}}{1+a_S C_e^{\beta_S}} \qquad\qquad (3.23)$$

where K_S and a_S are the Sips model constants in L/g and L/mg, respectively and β_S is the Sips model exponent. Cd(II), Cu(II) and Zn(II) biosorption data was

Unlike Sips model, the Redlich–Peterson isotherm behaves like the Freundlich isotherm at high adsorbate concentrations and comes close the Henry's law at low amounts of concentration. The model can be presented as (Febrianto et al., 2009; Montazer–Rahmati et al., 2011):

$$q_e = \frac{K_{RP}C_e}{1+a_{RP}C_e^{\beta_{RP}}} \tag{3.24}$$

where K_{RP} and a_{RP} are the Redlich–Peterson model constants in L/g and L/mg, respectively and β_{RP} is the Redlich–Peterson model exponent which lies between 0 and 1.

3.3.3 *Fixed–bed biosorption process analysis and modeling*

In continuous biosorption systems, the concentration profiles in the liquid and adsorbent phases vary in both space and time. The mathematical and quantitative modeling approaches are applied for design and optimization of fixed-bed columns. Consequently, from the perspective of process modeling, the dynamic behaviour of a fixed-bed column can be described in terms of the effluent concentration-time profile, i.e. the breakthrough curves (Chu, 2004). Several models have been applied to predict the breakthrough performance and also to calculate the column kinetic constants and evaluate the fixed–bed columns' adsorption capacity of the fixed-bed columns (Cruz–Olivares et al., 2013)

3.3.3.1 Thomas model (Th)

The Thomas model is the most model which is used in evaluation of the performance of a fixed–bed column and prediction of breakthrough curves. This model complies with the Langmuir kinetics of adsorption which means that the axial dispersion in the column adsorption can be assumed negligible (Gutiérrez–Segura et al., 2014). It is because of the rate of driving force follows the second–order reversible reaction kinetics.

$$\frac{C}{C_i} = \frac{1}{1+\exp\left[\left(\frac{k_{Th}}{Q}\right)(q_{Th}M-C_iQt)\right]} \tag{3.25}$$

where k_{Th} is the Thomas rate constant (mL/ mg min) and q_{Th} is the maximum adsorption capacity for heavy metal ions (mg/g).

3.3.3.2 Dose Response model (DR)

The Dose Response model has been widely applied in pharmacology to describe different types of processes. It can also be used to describe biosorption in columns (Cruz–Olivares et al., 2013). The DR model is represented by the equation:

$$\frac{C}{C_i} = 1 - \frac{1}{1+(\frac{C_i Q t}{q_{D-R}M})^a}$$

(3.26)

where a is a constant and q_{D-R} is the maximum adsorption capacity for heavy metal ions (mg/g) calculated by Dose Response model.

3.3.3.3 Yoon–Nelson model (YN)

The Yoon–Nelson model is a relatively simple model based on the adsorption of gases on activated charcoal. According to this model, the rate of decrease in the probability of adsorption for each adsorbate molecule is proportional to the probability of sorbate sorption and the probability of sorbate breakthrough on the sorbent. The equation is (Cruz–Olivares et al., 2013):

$$\frac{C}{C_i} = \frac{\exp(k_{Y-N}t - k_{Y-N}\tau)}{1 + \exp(k_{Y-N}t - k_{Y-N}\tau)}$$

(3.27)

where k_{Y-N} is the Yoon–Nelson proportionality constant (1/min) and τ is the time required for retaining 50% of the initial adsorbate (min).

3.3.3.4 Bed Depth Service Time (BDST) model

The BDST model was derived from the equation described by Adams–Bohart, but was modified by Hutchins (Izquierdo et al., 2010). It is one of the most widely used models that describes heavy metal adsorption in a fixed–bed column. BDST is a simple model able to predict the relationship between the depth and service time in terms of metal concentration and biosorption parameters. The model is based on physically measuring the capacity of the bed at different breakthrough values i.e. 10%, 30%, 60% and 90%. It ignores the intra–particle mass transfer resistance and also neglects the external film resistance. As a result, the adsorbate is directly adsorbed onto the biosorbent surface.

The BDST model estimates the required bed depth for a given service time by the following equation (Riazi et al., 2016):

$$\frac{C}{C_i} = \frac{1}{1+\exp\left[k_{BDST}C_i\left(\frac{N_{BDST}}{C_i v}L-t\right)\right]}$$

(3.28)

where N_{BDST} is the biosorption capacity (mg/L), v is the linear flow velocity of metal solution through the bed (cm/h), k_{BDST} is the adsorption rate constant that describes the mass transfer from the liquid to the solid phase (L/mg h) and L is the bed height (cm).

3.4 *Analytical methods and instruments*

Heavy metal ions (Cd^{2+}, Cu^{2+}, Pb^{2+} and Zn^{2+}) and other metal ions such as Na^+, K^+, Mg^{2+} and Ca^{2+} and were determined by 4100 MP–AES Spectrometer (Microwave Plasma–Atomic Emission Spectrometry), Agilent Technologies (USA). The pH and conductivity were measured by Hach HQ40d Multi meter. The chemical oxygen demand (COD) analysis was carried out with Hach DR/2000 Spectrophotometer. The total organic carbon (TOC) measurement was conducted using Multi N/C 3100, Analytik Jena AG. The total suspended solid (TSS) determination was done in accordance with the standard method.

3.5 *Statistical analysis*

Experiments were implemented in duplicate, and the data represented the mean values. The highest deviation was limited to 5%. The error bars indicating the standard deviation were shown in figures wherever possible.

Chapter 4

Feasibility Studies and Development of a Multi–Metal Binding Biosorbent

Chapter 4 Feasibility studies and development of a multi–metal binding biosorbent (MMBB)

A major part of Chapter 4 was published in the following papers:

Abdolali, A., Ngo, H.H., Guo, W.S., Lee, D.J., Tung, K.L., Wang, X.C., 2014. Development and evaluation of a new multi–metal binding biosorbent. Bioresource Technology 160, 98–106.

Abdolali, A., Ngo, H.H., Guo, W.S., Lu, S., Chen, S.S., Nguyen, N.C., Zhang, X., Wang, J., Wu, Y., 2016. A breakthrough biosorbent in removing heavy metals: equilibrium, kinetic, thermodynamic and mechanism analyses in a lab–scale study. Science of the Total Environment 542, 603–611.

4.1 *Introduction*

4.1.1 *Research background*

In recent years, biosorption has been considered as cost effective alternatives for removing metals and the interest in utilization of cheap alternatives has been significantly increased (Bulut and Tez, 2007; Gupta et al., 2009; Gadd, 2009a; Gadd, 2009b, Volesky, 2007). Many attempts have therefore been made by many researchers on feasibility of biosorption potential of lignocellulosic materials as economic and eco–friendly options, both natural substances and agro–industrial wastes and by–products. These adsorbents may be classified either on basis of their availability (natural materials and industrial/ agro–industrial/ domestic wastes or by–products and synthesized ones) or depending on their nature (organic and inorganic materials) (Tang et al., 2013; Gupta et al., 2009). Among inexpensive biosorbents, most of the studies have been engrossed in lignocellulosic wastes (as naturally intact or chemically modified) such as sawdust, weed and wood waste (Asadi et al., 2008; Bulut and Tez, 2007; Pereira et al., 2010), sugarcane bagasse (Homagai et al., 2010; Martín–Lara et al., 2010; Pereira et al., 2010), fruit rind, pulp and seeds (Feng et al., 2011; Liu et al., 2012; Martín–

Lara et al., 2010; Torab–Mostaedi et al., 2013), wheat or barley straw (Pehlivan et al., 2012), rice husk, hull and straw (Asadi et al., 2008; Kazemipour et al., 2008), olive pomace and stone (Blázquez et al., 2009; Martín–Lara et al., 2012), etc . The heavy metal bio–recovery can be affected by physico–chemical parameters of the solution such as pH, ion strength, initial metal concentration, temperature and by other characteristics of the adsorbent like concentration, presence of organic and inorganic functional groups and chemical modification (Gupta et al., 2009; Montazer–Rahmati et al., 2011; Pehlivan et al., 2012; Tan and Xiao, 2009; Tan et al., 2010; Velazquez–Jimenez et al., 2013).

All of the previous attempts have been made to study the agro–industrial wastes and by–products individually. The novelty of the present work is using combination of selected agro–industrial multi–metal binding biosorbents for removal of cadmium, copper, lead and zinc ions from synthetic aqueous multi–metal solutions. The significant difference between previous studies and current work is gaining the advantages and also using the biosorptive potentials of various biosorbents in a combination. The purpose of blending different lignocellulosic materials is having all potentials of biosorbents for heavy metal uptake (Martín–Lara et al., 2010; Martín–Lara et al., 2010). Also these wastes were selected because of the good results reported in other literatures for heavy metal removal (Feng et al., 2011; Amarasinghe and Williams, 2007). Additionally, they are properly available in Australia and also all over the world.

4.1.2   Objectives

The present work is a preliminary study on developing a new multi–metal binding biosorbent (MMBB) by combining a group of high biosorptive capability natural lignocellulosic agro–industrial wastes. Firstly, the adsorption studies were carried out to select the best combination of different biosorbents, selected from various types of biosorbents compared in similar conditions. These wastes were selected because of the good results reported in other literatures for heavy metal removal. Besides, they are properly available in Australia and also all over the world. Then the experiments were continued to compare the effect of different contact times, pH, initial metal concentration, and biosorbent dose on biosorptive potential of

selected combination. The results were mainly evaluated by two popular kinetic models of pseudo–first–order and pseudo–second–order correlations and three two–parameter and four three–parameter adsorption models (Langmuir, Freundlich, Dubinin–Radushkevich, Khan, Radke–Prausnitz, Sips and Redlich–Peterson). Finally, the appropriate isotherm and kinetic models were established. Also elution efficiency (sorption and adsorptions cycles) on adsorption capacity were then studied and the selected adsorbent was characterized using SEM and FTIR.

4.2   *Selection of adsorbents*

The most important factors for selecting an adsorbent are adsorption capacity, reusability, local availability, compatibility, kinetics and cost (Nguyen, 2015). Eighteen individual biosorbents, namely, sawdust (SD), sugarcane (SC), corncob (CC), tea waste (TW), apple peel (AP), grape stalk (GS), mandarin peel (MP), orange peel (OP), maple leave (MP), passion fruit skin (PS), garden grass (GG), mango skin (MG), lychee rind (LC), avocado peel (AV), eucalyptus leave (EU), egg shell (ES), coffee waste (CW) and also coir peat (CP), individually (biosorbent dose: 5 gr/L, 50 mg/L initial metal Conc. at room temperature and pH of 5.0–5.5, rotary speed of 150 rpm for 24 hr) were evaluated and compared in terms of biosorption capacity (Figure 4.1). As can be seen in Figure 4.1, the results indicate TW, ML, MP, OP and CP showed satisfying biosorptive capacity for all heavy metal ions (cadmium, copper, lead and zinc). SD and CC had quite less biosorptive potential in comparison with GG, AV, LC, GS and PS. AP, SC, ES and EU results for Pb, Zn, Cd and Cu were very unsatisfactory that this type of waste will not be considered for study in combination with other biosorbents. Two different combinations of TW:ML:MP (MMBB1) containing the best ones and TW:SD:CC (MMBB2) as a combination of TW with highest biosorption capacity with two low biosorption capacity were selected to apply for further batch experiments. The purpose of this selection was showing how influential the component of combination (with very different biosorptive potential) was. The equal ratio of each biosorbent in the MMBBs was chosen for the experiments.
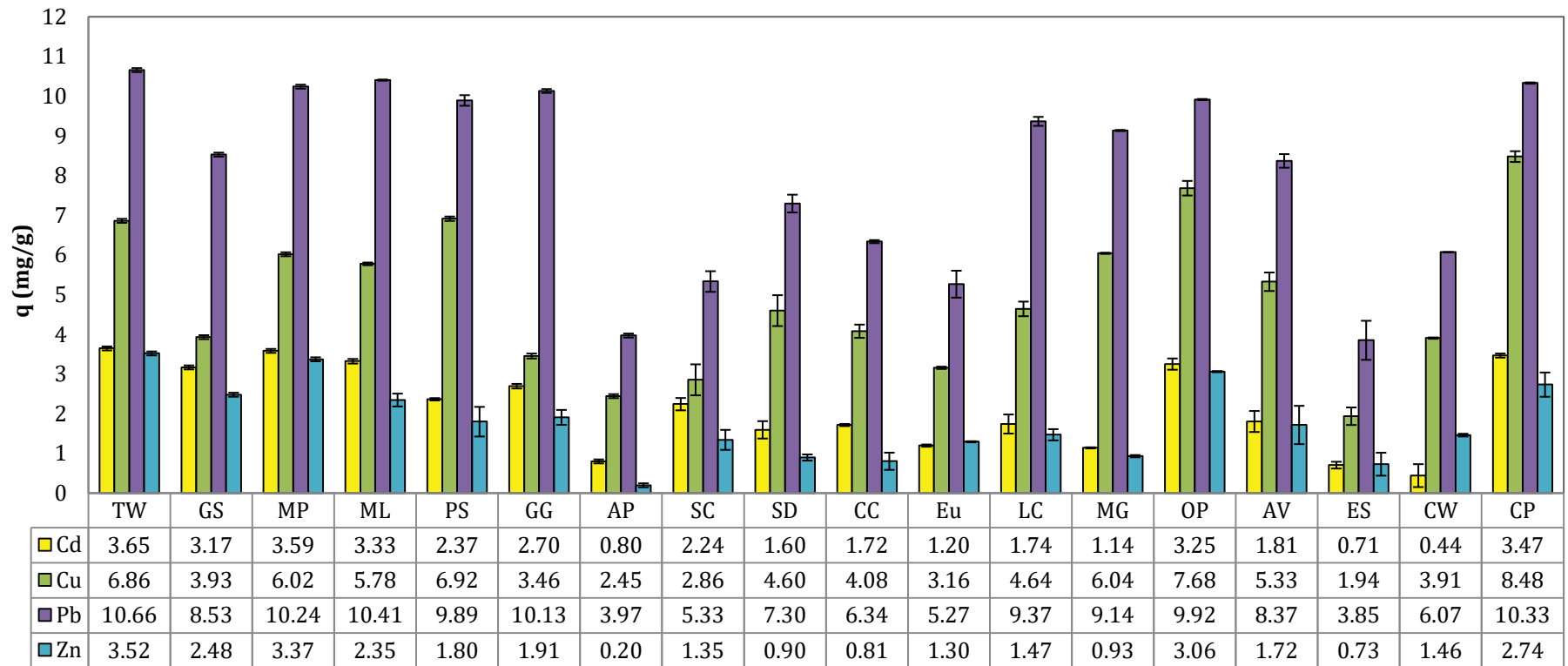
Figure 4.1 Comparison between different agro–industrial wastes and by–products for Cd(II), Cu(II), Pb(II) and Zn(II) adsorption(initial pH 5.5±0.1; room temperature, 22±1 ℃; contact time: 24 hr; initial metal conc.: 50 mg/L; biosorbent dose: 5g/L; rotary speed: 150 rpm, particle size: 75–150 μm)

	TW	GS	MP	ML	PS	GG	AP	SC	SD	CC	Eu	LC	MG	OP	AV	ES	CW	CP
Cd	3.65	3.17	3.59	3.33	2.37	2.70	0.80	2.24	1.60	1.72	1.20	1.74	1.14	3.25	1.81	0.71	0.44	3.47
Cu	6.86	3.93	6.02	5.78	6.92	3.46	2.45	2.86	4.60	4.08	3.16	4.64	6.04	7.68	5.33	1.94	3.91	8.48
Pb	10.66	8.53	10.24	10.41	9.89	10.13	3.97	5.33	7.30	6.34	5.27	9.37	9.14	9.92	8.37	3.85	6.07	10.33
Zn	3.52	2.48	3.37	2.35	1.80	1.91	0.20	1.35	0.90	0.81	1.30	1.47	0.93	3.06	1.72	0.73	1.46	2.74

4.3   *Characterization of adsorbents by FTIR*

To determine the functional groups involved in biosorption of Cd(II), Cu(II), Pb(II) and Zn(II) onto MMBB1 and MMBB2, a comparison between the FTIR spectra before and after meal loading was done using SHIMADZU FTIR 8400S (Kyoto, Japan). The FTIR spectrum of MMBB exhibited a large number of absorption peaks, indicating the complexity in nature of this adsorbent. It also confirmed changes in functional groups and surface properties of MMBBs. The shift of some functional groups bands and their intensity significantly changed after heavy metal biosorption (Table 4.1 and Table 4.2).

From Table 4.1 and Table 4.2, the shifts may be attributed to carboxylic (C=O) and hydroxylic (O–H) groups on both MMBB's surface. They were dominantly active groups in Cd(II), Cu(II), Pb(II) and Zn(II) biosorption process, suggesting that acidic groups, carboxyl and hydroxyl, are main contributors in the complexation of metal cations and ion exchange processes. For MMBB1, amine and amide groups were found between medium intensity peaks in the frequency range of 1640–1560 with 132.13 cm^{-1} shift after biosorption process. Meanwhile, for MMBB2, the medium intensity peaks relating to amine and amide groups were found between the frequency ranges of 3400–3250 with 4.9 cm^{-1} shift after biosorption process. The peaks detected in spectra of MMBB1 were laid between 1320–1000 cm^{-1}, which is related to C=O stretch in amides, ketones, aldehydes, carboxylic acids and esters (Feng et al., 2011). In addition, a shift of 32.79 cm^{-1} was in the range of 1500–1450, and is attributed to C=C–C asymmetric stretching aromatic rings. In Table 4.2, the strong peaks between 1320–1000 cm^{-1} and also 1820–1680 cm^{-1} present the existing of C–O stretch (COOH) and C=O stretch in amides, ketones, aldehydes, carboxylic acids and esters, respectively (Hossain et al., 2012).

A big change (78.12 cm^{-1}) occurred on MMBB1 after metal loading. This is reflected in the strong and broad band present between 3500–3200 cm^{-1}. This may be assigned to complexation of metal ions with the ionized O–H groups of polymeric compounds (i.e. alcohols, phenols and carboxylic acids) of cellulose and lignin of lignocellulosic materials (Hossain et al., 2012; Feng et al., 2011). The

changes of peaks in the range of 3000–2850 cm^{-1} and 3100–3000 cm^{-1} for MMBB1 and in the range of 3000–2850 cm^{-1} and 1470–1450 cm^{-1} for MMBB2. These variations indicated the involvement of H–C–H asymmetric and symmetric stretch and C–H stretch of aromatic rings on MMBB1 and H–C–H asymmetric and symmetric stretch and C–H stretch of alkanes which can be found in the molecular structure of MMBB2, respectively.

The other detected peaks in Table 4.1 represent existence of H–C=O:C–H stretch in aldehydes in the range of 2850–2700 cm^{-1} of MMBB1.

4.4   *SEM analysis*

From Table 4.1 and 4.2, SEM depicts the morphology changes of unloaded and loaded biosorbent. SEM images exhibited the morphological changes on the biosorbent surface before and after metal biosorption. After biosorption of heavy metal ions, the surface became smoother with less porosity with probable metal entrapping and adsorbing on biosorbent.

4.5   *Effect of different physico–chemical parameters*

4.5.1   Influence of pH

The adsorption of cadmium, copper, lead and zinc was studied as a function of pH altering in the range of 2.0–5.5±0.1. Heavy metal ions exhibit amphoteric property which means these substances can act as either an acid or a base, depending on the pH. Minimum solubility for Cd, Cu, Pb and Zn is about 11.0, 8.1, 10.0 and 10.1 (Huang et al., 2017; Rudnicki et al., 2014). In the synthetic solution containing multi–metal ions, copper and lead hydroxide significantly precipitated above pH 6.0. Therefore, the initial pH values above 5.5 are not preferable due to the observed presence of metal hydroxide precipitation, so as the experiments were not conducted beyond pH 5.5. Figure 4.2 represents the effect of pH of the adsorption of cadmium, copper, lead and zinc altering in the range of 2.0–5.5. It can be seen that the adsorption capacity of metals increased with increasing in pH values in all cases.

Table 4.1 FTIR spectra and SEM images of (a) unloaded and (b) metal–loaded MMBB1

Frequency (cm^{-1})		Transmittance (%)		Bond/Functional group	SEM images
Unloaded	Loaded	Unloaded	Loaded		
514.05	510.19	21.47	16.45	C–Br stretch/ Alkyl halides	
1005.92	1007.85	84.40	76.06	C=O stretch/ Alcohols, carboxylic acids, esters and ethers	
1491.04	1458.25	83.57	74.93	C–C stretch(In–ring)/ Aromatics	
1590.38	1458.25	84.23	74.93	N–H band/ 1° amines and amides	
1654.03	1654.03	78.75	72.34	–C=C– stretch/ Alkanes	
2721.68	2820.05	85.77	77.18	H–C=O: C–H stretch/ Aldehydes	
2958.93	2957	83.06	75.48	H–C–H Asymmetric and symmetric stretch/Alkanes	
3096.85	3096.85	82.54	75.04	C–H stretch/ Aromatics	
3348.57	3230.91	81.42	74.19	–C≡C–H: C–H stretch/ Alkynes	
3482.63	3404.51	81.61	74.24	O–H stretch, H–Bonded/ Alcohols and Phenols	
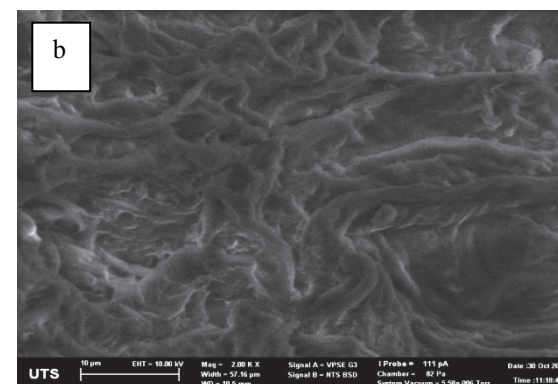
Table 4.2 FTIR spectra and SEM images of unloaded and metal–loaded MMBB2

Frequency (cm^{-1})		Transmittance (%)		Bond/Functional group	SEM images
Unloaded	Loaded	Unloaded	Loaded		
1185.2	1175.9	79.1	68.55	C–O stretch (COOH)/ Alcohols, carboxylic acids, esters and ethers	
3295.16	3290.26	64.5	53.5	N–H band/1° and 2° amines and amides	
2892.51	2882.11	73.26	65.70	H–C–H Asymmetric and symmetric stretch/Alkanes	
1503.12	1509.12	72.33	65.54	N–O asymmetric stretch/Nitro compounds	
1465.4	1461.8	62.75	61.13	C–H band/Alkanes	
1776.43	1767.33	69.3	64.3	C=O stretch/Amides, ketones, aldehydes, carboxylic acids and esters	
3381.64	3373.34	71.8	64.4	O–H stretch, H–Bonded/ Alcohols and Phenols	

Although all metal adsorption followed similar pattern, the adsorption capacity of Cu and Pb increased significantly by increase in pH values However, the changes of Cu and Pb adsorption on both MMBB1 and MMBB2 was much more obvious than that of Zn and Cd when the pH value increased from 2.0 to 5.5±0.1;

For MMBB1: Cu; 1.30 to 6.90 mg/g, Pb: 4.51 to 10.84 mg/g, Zn: 0.33 to 2.83 and Cd: 0.79 to 3.28 mg/g

For MMBB2: Cu; 1.07 to 5.70 mg/g, Pb: 2.50 to 8.53 mg/g, Zn: 0.29 to 1.83 and Cd: 1.30 to 1.72 mg/g).

The results indicated that the optimum pH value was 5.5 for all metals.
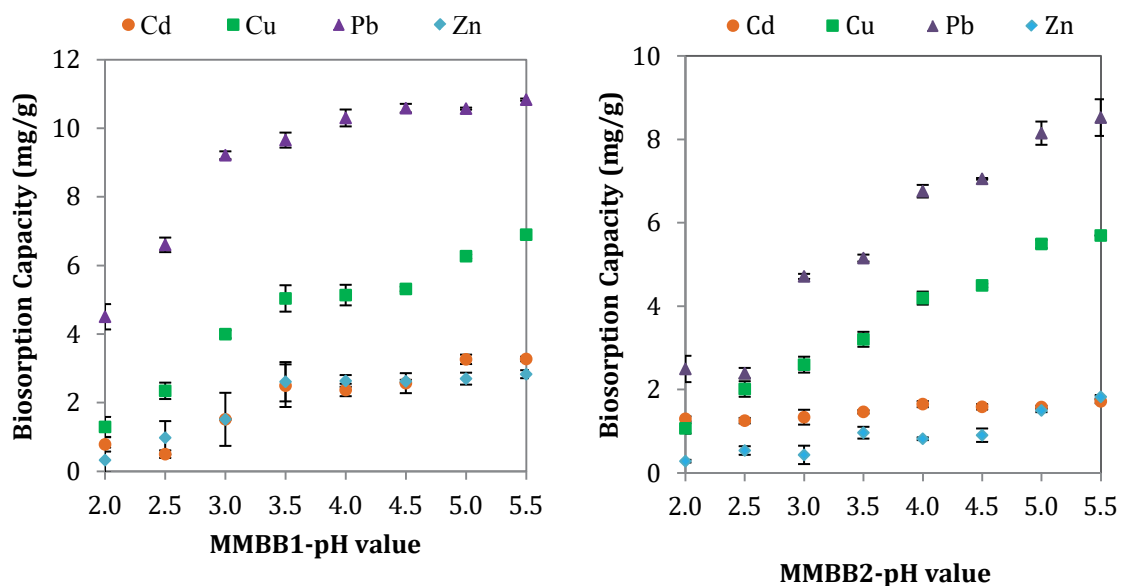
Figure 4.2 Effect of initial pH of solution on Cd(II), Cu(II), Pb(II) and Zn(II) adsorption (room temperature, 22±1 °C; contact time: 24 hr; initial metal conc.: 50 mg/L; biosorbent dose: 5g/L; rotary speed: 150 rpm, particle size: 75–150μm)

4.5.2   Influence of contact time

A series of contact time experiments for cadmium, copper, lead and zinc adsorption on MMBB1 and MMBB2 from 0–24 hr were carried out at 50 mg/L initial concentration and room temperature. It is evident from the Figure 4.3 that

the rate of metal uptake was very fast within first 30 min as a result of the exuberant number of available active sites on adsorbent surfaces and then decreased until equilibrium was reached. Biosorption capacity leveled off at equilibrium state within 180 min. Therefore, the biosorption time was set to 180 min in each experiment.
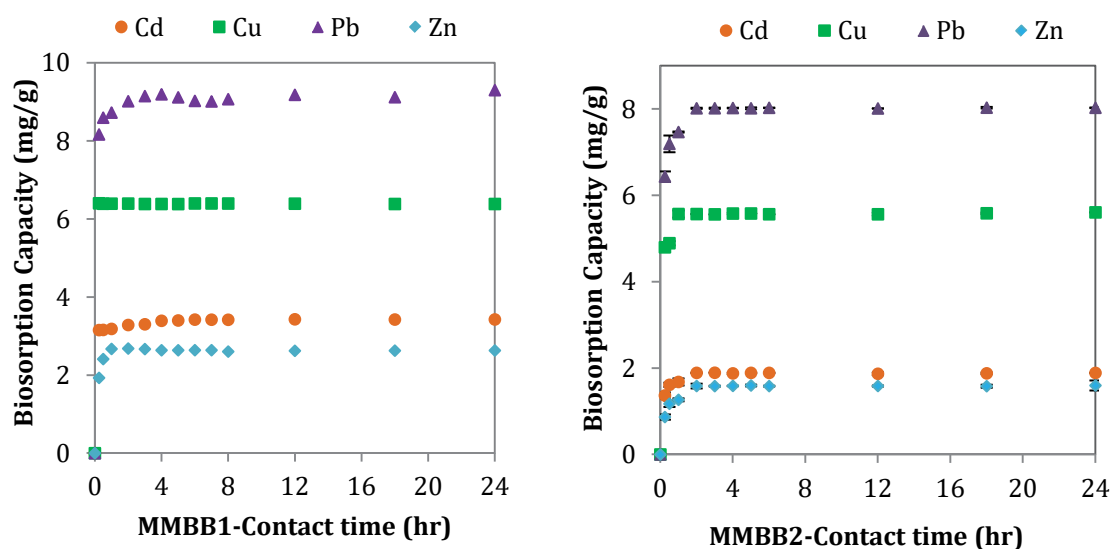
Figure 4.3 Effect of contact time on Cd(II), Cu(II), Pb(II) and Zn(II) adsorption (pH 5.5±0.1; room temperature, 22±1 ℃; initial metal conc.: 50 mg/L; biosorbent dose: 5g/L; rotary speed: 150 rpm, particle size: 75–150μm)

4.5.3   Influence of adsorbent dose

Biosorption capacity was also affected by biosorption dose and amount of available active sites and this effect is shown in Figure 4.4. There is a hike in removal efficiency of all heavy metal ions. The experimental results indicate that the percentage removal of all metal ions on MMBB1 and MMBB2 represents an equilibrium pattern for biosorbent amounts of 5 g/L and more. As it plateaued, the optimum amount of adsorbent for future study would be 5 g/L whose highest removal efficiencies were about 68 %, 75 %, 85 % and 55 % for Cd, Cu, Pb and Zn, respectively for MMBB2 and 70%, 84%, 98 % and 61% for Cd, Cu, Pb and Zn, respectively, on 5 g/L MMBB1.
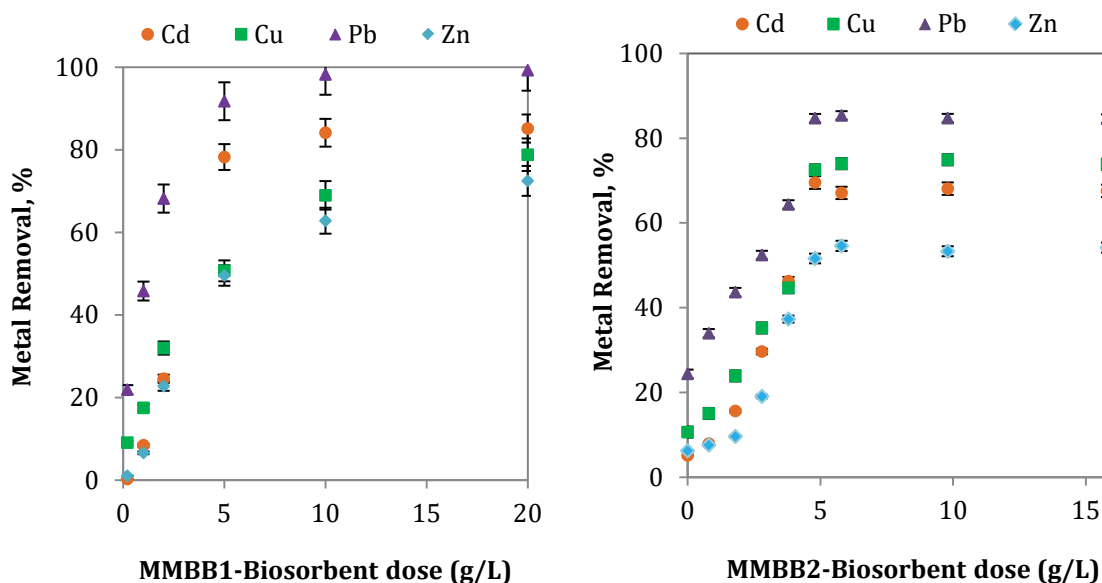
Figure 4.4 Effect of biosorbent dose on Cd(II), Cu(II), Pb(II) and Zn(II) adsorption (pH 5.5±0.1; room temperature, 22±1 °C; contact time: 3 hr; initial metal conc.: 50 mg/L; rotary speed: 150 rpm, particle size: 75–150μm)

4.6 *Adsorption kinetics*

In batch systems, the adsorption kinetics was described by a number of models with varying degrees of complexity such as pseudo–first–order, pseudo–second–order and intra–particle diffusion kinetic model.

A kinetic investigation was carried out to quantify the adsorption rate controlling steps in Cd(II), Cu(II), Pb(II) and Zn(II) uptake on MMBB. The pseudo–first–order and pseudo–second–order kinetic models were applied for kinetic study.

The experimental data and obtained parameters of these models were measured by MATLAB® and summarized in Table 4.3. These kinetic models were exploited to describe the probable mechanism of biosorption. As shown in Table 4.3, with comparison between adsorption rate constants, the estimated q_e and the coefficients of correlation associated with the Lagergren pseudo–first–order, the pseudo–second–order and intra–particle diffusion kinetic models at room temperature for MMBBs, it is obvious that both kinetic models of pseudo–first–

order and pseudo–second–order kinetic models well described all metal biosorption rather than intra–particle diffusion model. However, the coefficients of correlation (R^2) of pseudo–second–order kinetic model were slightly larger than those of pseudo–first–order kinetic model for copper and cadmium. For lead and zinc ions, the Lagergren pseudo–first–order described equilibrium state and experimental data better than the other kinetic model. Totally, the kinetic models indicated that chemical reaction would be presumably the rate limiting step of Cd, Cu, Pb and Zn biosorption on MMBB. The calculated q_e for pseudo–second–order kinetic model (1.92, 5.88, 8.06 and 1.60 mg/g for Cd(II), Cu(II), Pb(II) and Zn(II), respectively) are also close to the experimental values (1.89, 5.57, 8.04 and 1.60 mg/g).

The experimental data and obtained parameters of these models for MMBB2 are shown in Table 4.3. The results indicate that pseudo–second–order kinetic model can describe experimental data better than the two other kinetic models (R^2 = 0.99), suggesting that chemical reaction would be presumably the rate limiting step of Cd, Cu, Pb and Zn biosorption on MMBB2. The calculated value of q_e for pseudo–second–order kinetic model (3.40, 6.39, 8.99 and 2.68 mg/g for Cd(II), Cu(II), Pb(II) and Zn(II), respectively) are also close to the experimental values (3.30, 6.40, 9.02 and 2.88 mg/g).

Table 4.3 Comparison between adsorption rate constants, the estimated q_e and the coefficients of determination associated with the Lagergren pseudo–first–order, the pseudo–second order and intra–particle diffusion kinetic models (pH 5.5±0.1; room temperature, 22±1 ℃; initial metal conc.: 50 mg/L; biosorbent dose: 5g/L; rotary speed: 150 rpm, particle size: 75–150μm)

Model	Parameter	Metal			
		Cd	Cu	Pb	Zn
MMBB1					
Experimental	$q_{e,exp}$ (mg/g)	3.30	6.40	9.02	2.88
1st–order kinetic model	K_1 (min^{-1})	3.36	6.39	9.06	2.64
	$q_{e,cal}$ (mg/g)	10.70	8.047	8.93	5.17
	R^2	0.990	0.999	0.995	0.998
2nd–order kinetic model	$K_2 \times 10^3$ (gmg^{-1} min^{-1})	3.40	6.39	8.99	2.68

Model	Parameter	Metal			
		Cd	Cu	Pb	Zn
	$q_{e,cal}$ (mg/g)	11.08	3.32	0.72	0.08
	R^2	0.995	0.999	0.985	0.988
Intra–particle diffusion model	K_P (mg g^{-1}min$^{-0.5}$)	0.05	0.53	0.25	0.08
	C	1.73	5.35	8.96	0.79
	R^2	0.92	0.89	0.88	0.90
MMBB2					
Experimental	$q_{e,exp}$ (mg/g)	1.89	5.57	8.04	1.60
1st–order kinetic model	K_1 (min^{-1})	0.03	0.10	0.07	0.02
	$q_{e,cal}$ (mg/g)	1.19	5.98	8.39	1.21
	R^2	0.79	0.95	0.94	0.85
2nd–order kinetic model	$K_2 \times 10^3$ (gmg^{-1} min^{-1})	0.17	0.08	0.06	0.09
	$q_{e,cal}$ (mg/g)	1.92	5.88	8.06	1.60
	R^2	0.99	0.99	0.99	0.99
Intra–particle diffusion model	K_P (mg g^{-1}min$^{-0.5}$)	0.07	1.12	0.15	0.07
	C	1.16	4.35	6.19	0.68
	R^2	0.93	0.81	0.88	0.90

4.7 *Adsorption isotherm*

The correlation between the adsorbed and the aqueous metal concentrations at equilibrium has been described by the Langmuir, Freundlich, Dubinin–Radushkevich, Sips, Redlich–Peterson, Radke–Prausnitz and Khan adsorption isotherm models. All the model parameters which were evaluated by non–linear regression using MATLAB® software are presented in Table 4.4. Furthermore, residual root mean square error (RMSE), error sum of square (SSE) and correlation of determination (R^2) were used to measure the exactness of fitting.

The Langmuir equation describes the equilibrium condition better than the other models (R^2: 0.99 and small RMSE values). From Table 4.4, the maximum amounts of biosorption capacity of MMBB1 by monolayer adsorption assumption for Cd, Cu, Pb and Zn obtained from Langmuir equation are 41.48, 39.48, 94.00 and 27.23 mg/g, respectively. Some metal ions have better affinity towards biosorbents than other ions and this fact ascertains the selectivity potential of functional group (Šćiban et al., 2007). This phenomenon can be confirmed by calculating the

Langmuir parameter of b_L representing this attraction. b_L values for Pb (0.007 L/mg) was higher than Cu, Cd and Zn.

Furthermore, it was understood that the Langmuir isotherm corresponded to a dominant ion exchange mechanism while the Freundlich isotherm showed adsorption–complexation reactions taking place at the outer heterogeneous surface of the adsorbent (Asadi et al., 2008; Kazemipour et al., 2008).

Among three–parameter isotherm models, for Cu(II) and Zn(II), Khan isotherm describes biosorption conditions moderately better than Sips and Redlich–Peterson models, while for Cd(II) and Pb(II), the Sips model was found to provide the best correlation of the biosorption equilibrium data. The foregoing analysis of isotherm models shows that the better fit for Cd(II), Cu(II), Pb(II) and Zn(II) biosorption is produced by three–parameter isotherm models rather than two–parameter isotherm models.

Maximum monolayer adsorption capacities of MMBB2 ($q_{m,L}$) were 31.73, 41.06, 76.25 and 26.63 mg/g for Cd(II), Cu(II), Pb(II) and Zn(II) sorption, respectively.

The b_L values of Cd(II), Cu(II), Pb(II) and Zn(II) biosorption which were estimated from this isotherm are 0.005, 0.010, 0.034 and 0.005 L/mg, respectively and shows the steepest initial isotherm slope (the highest b_L) is for Pb(II) as can be expected.

From Table 4.5, it is apparent that equilibrium data of Cd(II), Cu(II) and Pb(II) biosorption onto MMBB2 fitted well by the Freundlich isotherm ($R^2 = 0.99$) and for Zn(II) the Langmuir isotherm was quite better fitted than Freundlich isotherm according to the values of R^2 of Langmuir isotherm model (0.97) being higher than that of Freundlich isotherm (0.95) as well as values of RMSE and SSE which are quite less than those of the other three models. Besides, it was understood that the Langmuir isotherm corresponded to a dominant ion exchange mechanism while the Freundlich isotherm showed adsorption–complexation reactions taking place in the adsorption process (Asadi et al., 2008).

Temkin model constants, b_{Te} (kJ/mol) and K_{Te} (L/g), were 0.77, 0.55, 0.31 and 0.77 kJ/mol and 0.15, 0.21, 1.16 and 0.08 L/g, for for Cd(II), Cu(II), Pb(II) and Zn(II),

respectively. This model is not a proper correlation for examined heavy metals according to R², RMSE and SSE values.

Radke–Prausnitz isotherm constants, a_{R-P} and r_{R-P} for Cd(II), Cu(II), Pb(II) and Zn(II) were calculated as 5.10, 9.24, 3.25 and 4.10 L/mg, 0.21, 0.63, 2.57 and 0.18 L/g, respectively.

As the results listed in Table 4.5, among two–parameter isotherms, both Freundlich and Langmuir models agreed very well with experimental data rather than the other two–parameter isotherm models and these are confirmed by small values of RMSE and SSE and R² amounts closed to 1.0, too. This result indicates the formation of monolayer coverage of metal ions at the outer heterogeneous surface of the sorbent.

Table 4.4 Isotherm constants of two– and three–parameter models for Cd(II), Cu(II), Pb(II) and Zn(II) adsorption onto MMBB1 (Initial pH 5.5±0.1, initial metal Conc.: 1–500 mg/L, contact time: 3 hr, rotary speed: 150 rpm, biosorbent dose: 5 g/L, particle size: 75–150μm)

Models		Metal			
		Cadmium	Copper	Lead	Zinc
Two–parameter models					
Langmuir $q_e = \frac{q_{m,L}b_L C_e}{1+b_L C_e}$					
	$q_{m,L}$(mg/g)	41.48	39.48	94.00	27.23
	b_L (L/mg)	0.001	0.004	0.007	0.002
	SSE	35.74	62.35	13.50	0.84
	R²	0.99	0.99	0.99	0.99
	RMSE	3.45	4.56	2.12	0.53
Freundlich $q_e = K_F C_e^{1/n}$					
	K_F	0.92	1.64	7.80	0.46
	n	1.88	1.96	2.38	1.80
	SSE	50.37	44.37	50.11	2.92
	R²	0.79	0.92	0.98	0.97
	RMSE	4.09	3.84	4.08	0.98
Dubinin– Radushkevich $q_e = q_{D-R} \exp(-B_{D-R}\varepsilon_{D-R}^2)$					

Models		Metal			
		Cadmium	Copper	Lead	Zinc
	q_{DR} (mg/g)	22.78	32.17	56.32	12.19
	B_{DR}	0.075	0.042	0.016	0.067
	SSE	13.94	32.99	33.5	7.81
	R^2	0.96	0.94	0.87	0.92
	RMSE	2.15	3.31	10.57	1.61
Three–parameter models					
Khan	$q_e = \dfrac{q_{m,K} b_K C_e}{(1+b_K C_e)^{a_K}}$				
	$q_{m,K}$(mg/g)	21.53	43.04	85.43	16.30
	a_K	0.013	0.23	0.09	0.68
	b_K(L/mg)	0.006	0.097	0.003	0.004
	SSE	15.2	1.02	28.66	1.39
	R^2	0.95	0.99	0.96	0.99
	RMSE	2.74	0.71	3.78	0.83
Redlich–Peterson	$q_e = \dfrac{K_{RP} C_e}{1+a_{RP} C_e^{\beta_{RP}}}$				
	β_{RP}	0.21	3.03	0.81	0.44
	K_{RP} (L/g)	0.08	0.20	4.17	0.18
	a_{RP}(L/mg)	0.67	0.02	0.15	0.41
	SSE	66.39	27.45	1.02	3.91
	R^2	0.79	0.95	0.99	0.97
	RMSE	5.76	3.70	0.71	1.21
Sips	$q_e = \dfrac{K_S C_e^{\beta_S}}{1+a_S C_e^{\beta_S}}$				
	β_S	3.56	1.80	0.77	1.13
	K_S (L/g)	0.028	0.017	4.457	0.051
	a_S (L/mg)	1.29	5.14	0.05	0.02
	SSE	7.59	15.01	0.43	1.45
	R^2	0.97	0.97	0.99	0.98
	RMSE	1.95	2.74	0.46	0.85

Table 4.5 Isotherm constants of two– and three–parameter models for Cd(II), Cu(II), Pb(II) and Zn(II) adsorption onto MMBB2(Initial pH 5.5±0.1, initial metal Conc.: 1–500 mg/L, contact time: 3 hr, rotary speed: 150 rpm, biosorbent dose: 5 g/L, particle size: 75–150μm)

Models	Metal			
	Cadmium	Copper	Lead	Zinc
Two–parameter models				
Langmuir $\quad q_e = \frac{q_{m,L} b_L C_e}{1 + b_L C_e}$				
$q_{m,L}$(mg/g)	31.73	41.06	76.25	26.63
b_L (L/mg)	0.005	0.010	0.034	0.005
SSE	2.24	4.52	65.03	3.89
R^2	0.99	0.99	0.97	0.97
RMSE	0.75	1.06	4.03	0.98
Freundlich $\quad q_e = K_F C_e^{1/n}$				
K_F	0.21	0.63	2.57	0.18
n	1.37	1.63	1.74	1.42
SSE	1.83	0.27	12.71	6.65
R^2	0.99	0.99	0.99	0.95
RMSE	0.67	0.25	1.78	1.29
Dubinin– Radushkevich $\quad q_e = q_{D-R} \exp(-B_{D-R} \varepsilon_{D-R}^2)$				
q_{D-R} (mg/g)	18.00	21.68	47.99	14.56
B_{D-R}	0.008	0.005	0.004	0.018
SSE	18.54	59.54	40.60	6.50
R^2	0.91	0.83	0.81	0.96
RMSE	2.15	3.85	10.07	1.27
Temkin $\quad q_e = \frac{RT}{b_{Te}} \ln(K_{Te} C_e)$				
K_{Te} (L/g)	0.15	0.21	1.16	0.08
b_{Te} (kJ/mol)	0.77	0.55	0.31	0.77
SSE	50.17	56.4	42.34	26.89
R^2	0.75	0.84	0.80	0.82
RMSE	3.54	3.75	10.29	2.59

Models	Metal			
	Cadmium	Copper	Lead	Zinc
Three–parameter models				

Radke–Prausnitz $q_e = \dfrac{a_{R-P} r_{R-P} C_e^{\beta_{R-P}}}{a_{R-P} + r_{R-P} C_e^{\beta_{R-P}-1}}$

	Cadmium	Copper	Lead	Zinc
a_{R-P} (L/g)	5.10	9.24	3.25	4.10
β_{R-P}	0.68	0.61	0.57	0.70
r_{R-P} (L/mg)	0.21	0.63	2.57	0.18
SSE	1.33	0.26	12.71	6.65
R^2	0.99	0.99	0.99	0.95
RMSE	1.52	0.99	2.05	1.48

Redlich–Peterson $q_e = \dfrac{K_{RP} C_e}{1 + a_{RP} C_e^{\beta_{RP}}}$

	Cadmium	Copper	Lead	Zinc
a_{RP} (L/mg)	1.25	0.10	2.09	5.39
β_{RP}	0.27	0.60	0.19	0.56
K_{RP} (L/g)	5.65	0.89	1.00	0.05
SSE	1.83	6.77	0.23	2.87
R^2	0.99	0.99	0.99	0.98
RMSE	0.78	4.75	0.27	0.97

Sips $q_e = \dfrac{K_S C_e^{\beta_S}}{1 + a_S C_e^{\beta_S}}$

	Cadmium	Copper	Lead	Zinc
a_S (L/mg)	0.001	0.004	0.063	0.001
β_S	0.83	0.59	0.38	1.72

Models	Metal			
	Cadmium	Copper	Lead	Zinc
K_S (L/g)	0.20	0.66	3.68	0.002
SSE	1.52	0.25	2.92	1.89
R^2	0.99	0.99	0.99	0.98
RMSE	0.23	0.29	0.98	0.79

The Sips isotherm is a combination of the Langmuir and Freundlich isotherm models and is expected to describe heterogeneous surfaces much better. At high sorbate concentrations it predicts a monolayer adsorption capacity characteristic of the Langmuir isotherm whereas at low sorbate concentrations it reduces to the Freundlich isotherm (Febrianto et al., 2009).

As the results given by Sips model, the experimental results of Cd(II), Cu(II) and Zn(II) biosorption onto MMBB2 are well fitted by all Sips better than Redlich–Peterson and Radke–Prausnitz models due to small RMSE and SSE as well as high R^2 close to 1.0.

Unlike Sips model, the Redlich–Peterson isotherm behaves like the Freundlich isotherm at high adsorbate concentrations and comes close the Henry's law at low amounts of concentration (Febrianto et al., 2009; Montazer–Rahmati et al., 2011).

β_{RP} is the Redlich–Peterson model exponent which lies between 0 and 1 (0.27, 0.60, 0.19 and 0.56 for Cd(II), Cu(II), Pb(II) and Zn(II), respectively). Pb(II) biosorption data is best correlated by the Redlich–Peterson as confirmed by the smallest values of RMSE, SSE and R^2 values very close to 1.0 (0.999).

Various kinds of agro–industrial wastes and by–products were studied for heavy metal removal. A comparison between maximum adsorptive capacities of MMBB and some other adsorbents is shown in Table 4.6. These study results are compatible with other adsorbents by higher or at least equal sorption potential for heavy metal removal from aqueous solutions. Furthermore, combination of several

types of low–cost agro–industrial waste might provide more selectivity as a result of increase in different effective functional groups involved in metal binding. Hence, this kind of adsorbent will be recommended for its significant advantages.

Moreover, the mean free energy of adsorption ($E = \frac{1}{\sqrt{2B_{D-R}}}$) calculated from Dubinin–Radushkevich isotherm which is applied to evaluate sorption properties and indicates if main mechanism is chemical reaction dominated by ion exchange or physical adsorption. Based on hypothesis of D–R isotherm, E values between 8 and 12 kJ/mol mean chemical adsorption by ion exchange process whereas E values less than 8 kJ/mol means physical adsorption. Hence, according to calculated B_{D-R} for Cd, Cu, Pb and Zn, E values show physical adsorption for cadmium and zinc removal (7.81 and 5.27 kJ/mol, for Cd and Zn, respectively) and ion exchange process for lead and copper biosorption (9.45 kJ/mol for Cu and 10.54 kJ/mol for Pb) when MMBB2 was examined. For MMBB1, calculated B_{D-R} for Cd, Cu, Pb and Zn and then E values showed physical adsorption or ion exchange for all metal removal process whose calculated values are 2.58, 3.45, 5.59 and 2.73 kJ/mol for Cd, Cu, Pb and Zn respectively which are all less than 8 kJ/mol.

Table 4.6 Biosorption capacities of various adsorbents

Adsorbent	Adsorbate	q_{max}(mg/g)	Reference
MMBB1	Cd(II)	41.48	Present study
	Cu(II)	39.48	
	Pb(II)	94.00	
	Zn(II)	27.23	
MMBB2	Cd(II)	31.73	Present study
	Cu(II)	41.06	
	Pb(II)	76.25	
	Zn(II)	26.63	
Cashew nut shell	Zn(II)	24.98	Kumar et al., 2012
Rice straw	Cd(II)	13.89	Ding et al., 2012
Sugarcane bagasse	Cd(II)	69.06	Garg et al., 2008
Sawdust	Cu(II)	6.88	Šćiban et al., 2007
	Zn(II)	0.96	
	Cd(II)	0.15	

Adsorbent	Adsorbate	q_{max}(mg/g)	Reference
Olive stone	Pb(II)	92.6	Fiol et al., 2006
	Cd(II)	77.3	
	Ni(II)	21.3	
	Cu(II)	20.2	
Orange peel	Pb(II)	113.5	Feng et al., 2011
	Cd(II)	63.35	
	Ni(II)	9.82	
Tea waste	Cu(II)	48	Amarasinghe and
	Pb(II)	65	Williams, 2007

Comparison between maximum adsorptive capacities of some adsorbents investigated by other researchers is shown in Table 4.6. This study results are compatible with other adsorbents by higher or at least equal sorptive potential for heavy metal removal from aqueous solutions. Besides, combination of several types of low–cost agro–industrial waste provides more selectivity as a result of increase in different effective functional groups (also confirmed by FTIR characterizations) involved in metal binding. As a consequence, these kinds of adsorbent combinations will be recommended for their significant advantages.

4.8   *Desorption studies*

The ability of biosorbent regeneration and batch sorption and desorption studies were conducted using four eluting agents (0.1 M NaCl, 0.1 M CaCl$_2$, 0.1 M CH$_3$COOH and Milli–Q water) for MMBB2 and five desorbing agents (0.1 M NaCl, 0.1 CaCL$_2$, 0.1 M NaOH, 0.1 M HCl and also Milli–Q water) for MMBB1. The biosorption capacity of eluted biosorbent was tested in five repeated cycles at optimum pH 5.5±0.1 and 50 mg/L initial metal concentrations. The contact time was 3 hours for sorption and desorption in each cycle. The biosorption capacity of MMBB1 and MMBB2 for Cd(II), Cu(II), Pb(II) and Zn(II) removal in the five cycles are indicated in Figure 4.5. To evaluate level of significance in the sorption and desorption cycles on the biosorption capacity, SPSS software was used for statistical testing of the model in the form of analysis of variance (ANOVA) and the one–sample t–test were done. For a 5% level of significance, the ANOVA data are given in Table 4.7 and Table 4.8.

From Table 4.7, for a 5% level of significance, the ANOVA data are for Cd(II) Cu(II) and Zn(II) adsorbed on MMBB1, P value is higher than 0.05 and also the values of F are lower than the critical F: 2.74 < 3.89 for Cd(II) (P value: 0.25), 2.32 < 3.80 for Cu(II) (P value: 0.34) and . F: 2.55 < 3.89 for Zn(II) (P value: 0.19). These values indicate the region of acceptance with 95% confidence; in other words, the variation of sorption capacities of the five desorbents is not significant after five cycles. But for Pb(II), the P value is lower than 0.05 (0.009) and the F value is higher than the critical F: 5.16> 3.89. Therefore, the type of desorbent affects the sorption capacity and there is significant difference between the five desorbing agents in Pb(II) removal.

For a 5% level of significance, T values for NaCl, CaCl$_2$, HCl, NaOH and Milli–Q water are listed in Table 4.7. For all heavy metals, the P value is higher than 0.05 and also the values of T are lower than the critical T (3.28): 2.16, 2.44, 1.86, 2.83 and 2.55 for Cd(II), 1.85, 1.91, 3.13, 2.78 and 3.02 for Cu(II), 4.23, 5.44, 4.42, 4.18 and 5.35 for Pb(II) and 1.57, 2.20, 1.60, 1.85 and 2.16 for Zn(II), respectively. It is obvious from the t–tests that for 0.1 M NaCl, 0.1 CaCL$_2$, 0.1 M NaOH, 0.1 M HCl and also Milli–Q water, the number of desorption times does not change the biosorption process efficiency. Biosorption results show that the effect of HCl and CaCl$_2$ on the biosorbent is significant with the highest increase in the sorption capacity.

From Table 4.8, for all metals, P value is less than 0.05 and also the values of F are higher than the critical F. Therefore, the type of eluent affects the sorption capacity and there is significant difference between the four desorbing agents in Cd(II), Cu(II), Pb(II) and Zn(II) removal. In this case, a P value less than 0.05 would result in the rejection of the null hypothesis at the 5% (significance) level. In addition, for a 5% level of significance T values for NaCl, CH$_3$COOH and CaCl$_2$, for all Zn(II) and Cd(II), the P value is higher than 0.05 and also the values of T are lower than the critical T (2.13).

	0.1 M NaCl	0.1 M CaCl2	0.1 M HCl	0.1 M NaOH	Milli-Q water
Cd	2.79	3.01	3.19	2.4	1.45
Cu	4.02	4.49	6.64	4.69	4.28
Pb	8.41	9.32	9.85	7.2	5.4
Zn	2.09	1.93	2.21	1.55	0.93

MMBB1

	0.1 M NaCl	0.1 M CaCl2	0.1 M CH3COOH	Milli-Q water
Cd	2.36	2.23	1.41	0.68
Cu	5.67	5.05	3.09	2.91
Pb	8.22	7.82	5.94	5.13
Zn	2.12	2.07	0.85	0.40
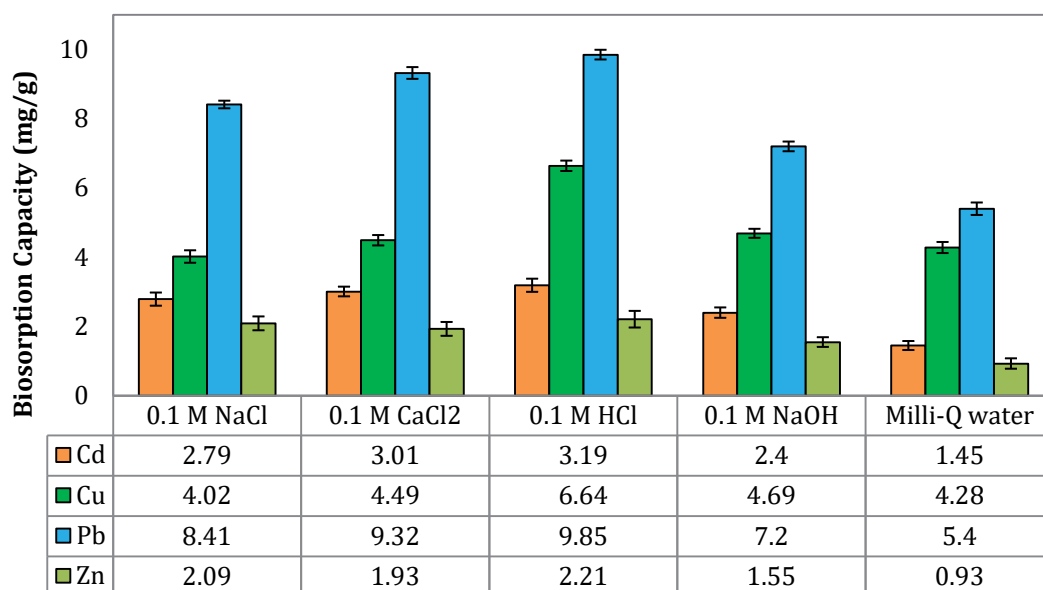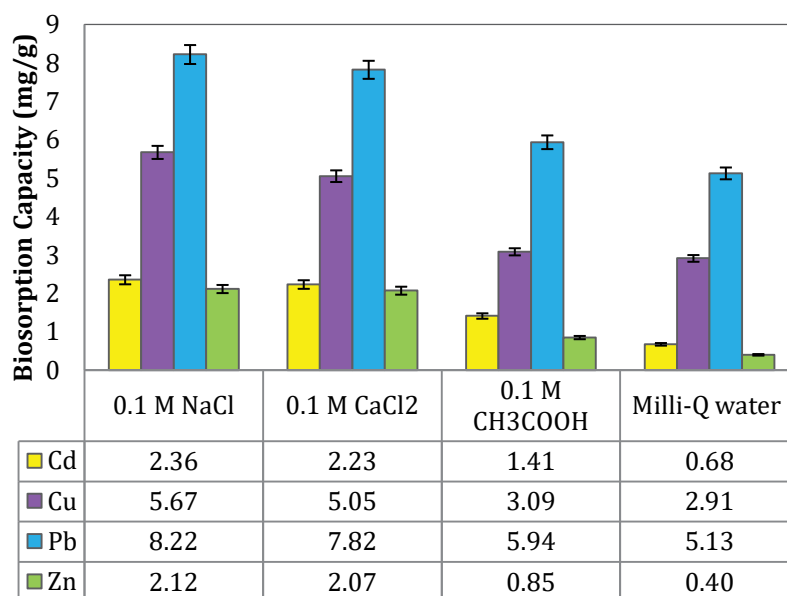
MMBB2

Figure 4.5 Biosorption capacity of Cd(II), Cu(II), Pb(II) and Zn(II) onto MMBB1 and MMBB2 washed by eluting agents (optimum pH 5.5±0.1; room temperature: 22±1 °C; sorption time: 3 hr ; desorption time: 3 hr; 5 cycles; initial metal conc.: 50 mg/L)

In other word, it is obvious from the t–tests that for these eluents, the number of elution times does not affect the biosorption process. However, biosorption results show that the effect of $CaCl_2$ and NaCl on the biosorbent is significant and causes higher increase in the sorption capacity in comparison with CH_3COOH and Milli–Q water when MMBB2 was used. Hence, these two chemicals are recommended as elution agents and desorption of cadmium, copper, lead and zinc from the biosorbent for MMBB2. Of course the much lower cost of NaCl should also be taken into consideration.

Table 4.7 ANOVA and One sample t–test data for sorption and desorption experiments of Cd(II), Cu(II), Pb(II) and Zn(II) biosorption onto MMBB1 (optimum pH 5.5±0.1; room temperature: 22±1 ℃; sorption time: 3 hr ; desorption time: 3 hr; 5 cycles; initial metal conc.: 50 mg/L)

Statistical Analysis Method	Metal			
	Cd	Cu	Pb	Zn
One–way ANOVA for NaCl, $CaCl_2$, HCl, NaOH and Milli–Q water				
F factor	2.74	2.32	5.16	2.55
$F_{critical}$ factor	3.29	3.29	3.29	3.29
Standard deviation	1.14	1.50	0.85	0.78
P value	0.25	0.34	0.009	0.19
One–sample T for NaCl				
T factor	2.16	1.85	4.23	1.57
$T_{critical}$ factor	3.28	3.28	3.28	3.28
P	0.18	0.15	0.24	0.28
One–sample T for $CaCl_2$				
T factor	2.44	1.91	5.44	2.20
$T_{critical}$ factor	3.28	3.28	3.28	3.28
P	0.12	0.23	0.24	0.32
One–sample T for HCl				
T factor	1.86	3.13	4.42	1.66
$T_{critical}$ factor	3.28	3.28	3.28	3.28
P	0.29	0.26	0.72	0.19

Statistical Analysis Method	Metal			
	Cd	Cu	Pb	Zn
One–sample T for NaOH				
T factor	2.83	2.78	4.18	1.85
$T_{critical}$ factor	3.28	3.28	3.28	3.28
P	0.31	0.15	0.67	0.23
One–sample T for Milli–Q water				
T factor	2.55	3.02	5.35	2.16
$T_{critical}$ factor	3.28	3.28	3.28	3.28
P	0.43	0.26	0.46	0.29

Table 4.8 ANOVA and One sample t–test data for sorption and desorption experiments of Cd(II), Cu(II), Pb(II) and Zn(II) biosorption onto MMBB2 (optimum pH 5.5±0.1; room temperature: 22±1 ℃; sorption time: 3 hr ; desorption time: 3 hr; 5 cycles; initial metal conc.: 50 mg/L)

Statistical Analysis Method	Metal			
	Cd	Cu	Pb	Zn
One–way ANOVA for NaCl, $CaCl_2$, CH_3COOH and Milli–Q water				
F factor	12.23	4.66	4.86	4.59
$F_{critical}$ factor	3.23	3.23	3.23	3.23
Standard deviation	1.08	0.90	0.65	0.87
P value	0.0002	0.0158	0.0136	0.0166
One–sample T for NaCl				
T factor	2.31	4.08	4.66	0.02
$T_{critical}$ factor	2.13	2.13	2.13	2.13
P	0.04	0.007	0.004	0.49
One–sample T for $CaCl_2$				
T factor	0.64	4.92	4.47	1.19
$T_{critical}$ factor	2.13	2.13	2.13	2.13
P	0.27	0.004	0.005	0.15
One–sample T for CH_3COOH				
T factor	1.93	7.16	5.19	2.81
$T_{critical}$ factor	2.13	2.13	2.13	2.13

Statistical Analysis Method	Metal			
	Cd	Cu	Pb	Zn
P	0.06	0.001	0.003	0.02
One–sample T for Milli–Q water				
T factor	5.00	5.60	4.76	5.48
$T_{critical}$ factor	2.13	2.13	2.13	2.13
P	0.003	0.02	0.004	0.005

4.9 *Conclusion*

Two new multi–metal binding biosorbent containing tea waste, maple leaves and mandarin peel as MMBB1 and tea waste, corncob and sawdust as MMBB2 were found to be an effective and low–cost alternatives for detoxifying of heavy metals contaminated aqueous solutions. The pH, contact time, adsorbent dose and initial metal concentrations of the adsorbate significantly governed the overall process of cadmium, copper, lead and zinc cations adsorption. For both MMBBS, the sorption equilibrium time was reached within 3 hr and pseudo–second–order kinetic model well fitted the experimental data.

The maximum amounts of biosorption capacity of MMBB1 by monolayer adsorption assumption for Cd, Cu, Pb and Zn obtained from Langmuir equation are 41.48, 39.48, 94.00 and 27.23 mg/g, respectively. These amounts for MMBB2 were 31.73, 41.06, 76.25 and 26.63 mg/g for Cd(II), Cu(II), Pb(II) and Zn(II) sorption, respectively. Desorption studies showed that NaCl was successfully used as eluent without affecting its sorption capability after five cycles of sorption and desorption of MMBB2 and HCl was the best choice for MMBB1 according to statistical data. MMBB1 was selected to modify and being investigated for further optimization and characterization.

In addition, FTIR spectra analyses confirmed that carboxyl and hydroxyl were the main functional groups in the complexation of metal cations and ion exchange processes.

Chapter 5

Heavy metal biosorption from synthetic wastewater by modified MMBB, characterization and optimization: batch study

Chapter 5 Heavy metal biosorption from synthetic wastewater by modified MMBB, characterization and optimization: batch study

A major part of Chapter 5 was published in the following paper:

Abdolali, A., Ngo, H.H., Guo, W.S., Zhou, J.L., Du, B., Wei, Q., Wang, X.C., Nguyen, P.D., 2015. Characterization of a multi–metal binding biosorbent: chemical modification and desorption studies. Bioresource Technology 193, 477–487.

5.1   *Introduction*

5.1.1   *Research background*

Over the past decades of studying heavy metal biosorption, many attempts have been carried out to apply different types of biosorbents, to optimize the operation conditions, to improve the mechanical strength of lignocellulosic biosorbents and to reuse the biosorbents in successive cycles by different eluents (Bhatnagar et al. 2015; Nguyen, 2015). A successful adsorption process depends on the selection of a proper adsorbent. In view of importance of economy in process design, this chapter focuses on process optimization, biosorbent modification, characterization, reutilizing and regeneration of the biosorbents.

5.1.2   *Objectives*

This chapter mainly explored characterization of the selected new biosorbent (MMBB1 or shortened to MMBB hereinafter) to find the principal surface functional groups and possible biosorption mechanisms involved in the biosorption in terms of chemical modification and desorbing agents using Fourier Transform Infrared Spectroscopy (FTIR), Scanning Electron Microscopy (SEM) and Scanning Electron Microscopy/ Energy Dispersive X–ray Spectroscopy (SEM/EDS). Desorption studies were carried out in terms of eluent type, concentration and contact time of desorption process. The effect of regeneration step by $CaCl_2$ was taken into consideration as well.

5.2   ***Biosorption process optimization***

5.2.1   Influence of biosorbent ratio

The effect of proportions for each biosorbent in MMBB (TW:ML:MP combination) for heavy metal removal was fulfilled with different proportions (Figure 5.1). All materials were separately weighed and mixed for removing any error and inaccuracy. Apparently, there are no significant differences between the equal proportions of 1:1:1 and the others, especially for lead and copper.

Since the ratio of 3:2:1 for TW:ML:MP showed the highest metal biosorption capacity, this ratio therefore will be used for further studies. The pH, moisture content (%), loss of mass and bulk density (g/cm^3) of MMBB were 4.97, 18.86, 0.93 and 0.36, respectively.

5.2.2   Influence of biosorbent particle size

The particle size distribution of modified MMBB is given in Figure 5.2. This figure illustrates that MMBB had a wide range of particle sizes (75–2000 μm). In addition, the majority (72.5%) of MMBB was retained on the larger sieves in the range of 300μm to 1000 μm. The result suggests that this biosorbent combination may have a proper permeability when been used in a fixed–bed column.

The tests for studying the effect of particle size of biosorbent were conducted for 5 g/L adsorbent dose and an initial concentration of 50 mg/L. The results of different particle sizes of <75 μm, 75–150 μm, 150–300 μm and 300–425 μm 425–600 μm, 600–1000 μm and 1–2 mm are indicated in Figure 5.2. It was found that biosorption capacity slightly increased by decreasing particle size. The reason was that these particle size distributions were very small (less than 300μm). The smaller biosorbent size (<600 μm) exhibited better performance in regard with metal removal. Nonetheless, the smaller size provides a higher surface area for metal adsorption, the mechanical stability reduces particularly in column (Liu et al., 2012). Hence, the size of 75–150 μm MMBB was selected for the batch experiments.

	1:1:1	2:1:1	1:2:1	1:1:2	3:1:1	1:3:1	1:1:3	4:1:1	1:4:1	1:1:4	2:2:1	1:2:2	2:1:2	1:2:3	1:3:2	2:3:1	3:2:1
Cd	2.58	2.02	1.78	1.51	1.71	1.16	1.28	1.27	0.72	1.16	1.33	1.02	1.11	3.02	2.92	2.98	3.21
Zn	2.46	1.90	1.68	1.96	1.56	1.35	1.44	1.35	1.35	1.53	1.09	1.27	1.22	2.33	2.26	2.31	2.38
Cu	6.67	6.73	6.46	6.47	6.67	6.37	6.26	6.69	6.26	6.26	6.33	6.10	6.38	6.60	6.46	6.71	6.91
Pb	10.00	10.01	9.86	9.71	9.89	9.99	9.66	10.01	9.88	9.67	9.85	9.71	9.85	9.85	10.00	10.21	10.08
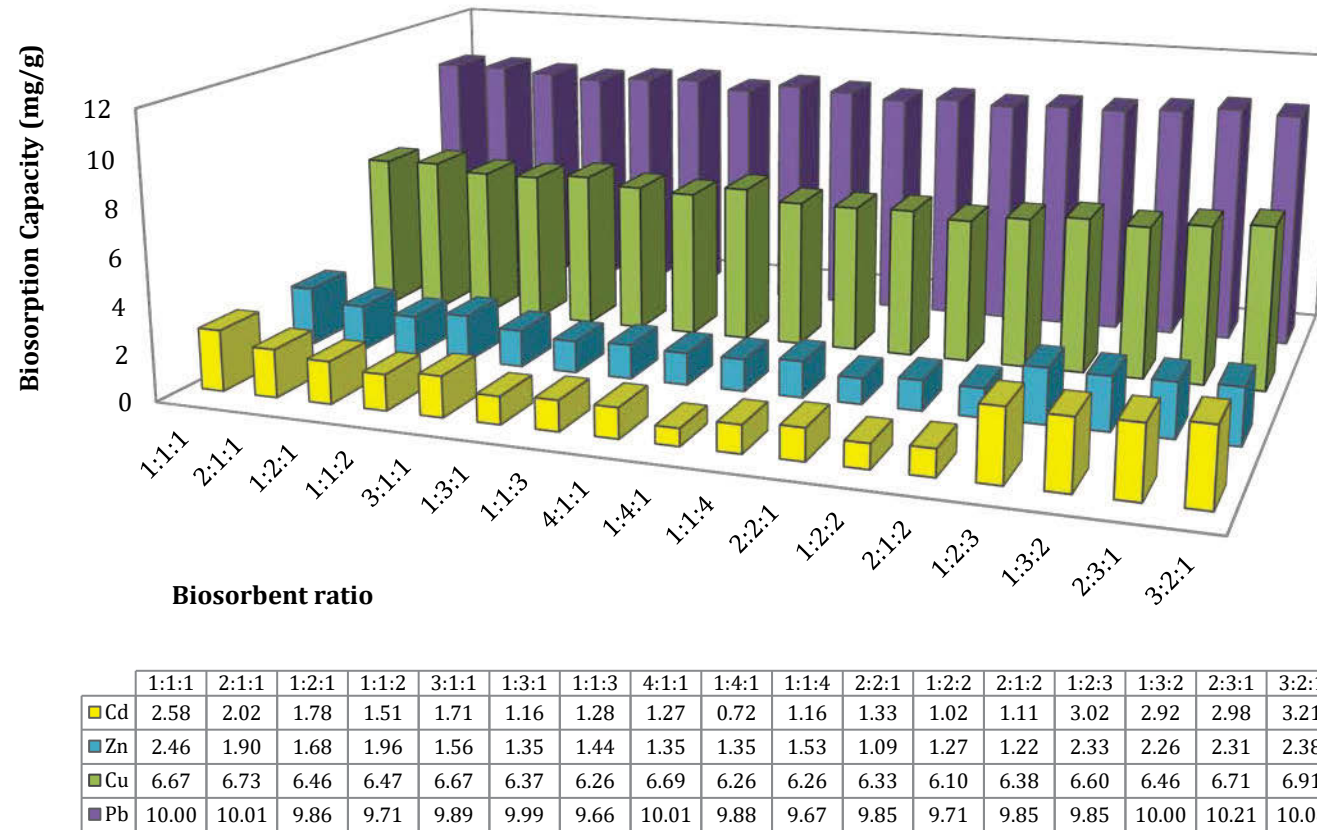
Figure 5.1 Effect of ratio of tea waste: maple leaves: mandarin peel on Cd(II), Cu(II), Pb(II) and Zn(II) adsorption(initial pH 5.0–5.5±0.1; room temperature, 22±1°C; contact time: 24 h r; initial metal conc.: 50 mg/L; biosorbent dose: 5g/L; rotary speed: 150 rpm; particle size: 75–150µm)
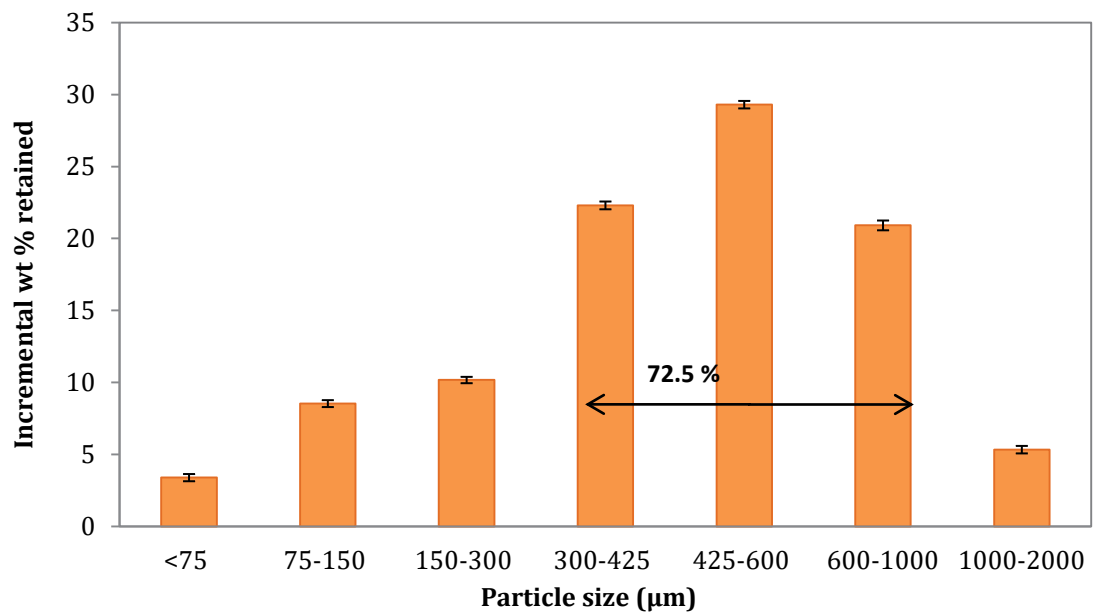
Figure 5.2 Particle size distribution of MMBB (<75 μm, 75–150 μm, 150–300 μm and 300–425 μm 425–600 μm, 600–1000 μm and 1000–2000 μm)
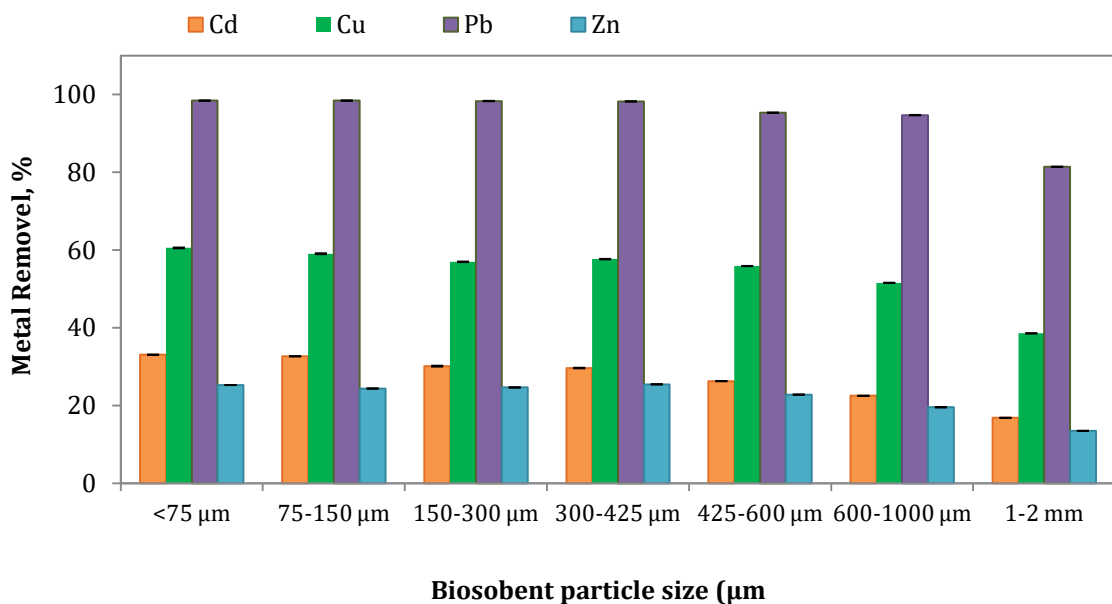
Figure 5.3 Effect of biosorbent particle size on Cd(II), Cu(II), Pb(II) and Zn(II) adsorption (Initial pH 5.0–5.5±0.1; room temperature, 22±1°C; initial metal Conc.: 50 mg/L; biosorbent dose: 5g/L; rotary speed: 150 rpm; the ratio of 3:2:1 for TW:ML:MP)

In column study, the larger particle size would be selected due to proper mechanical strength and good efficiency in column adsorption with high flow rate and also reusability (Chapter 6).

5.2.3   Influence of drying temperature

A few researchers investigated the effect of temperature of drying on biosorptive capacity of biosorbent for metal removal. In some literatures, biosorption performance was enhanced by increase in drying temperature. Thermal pretreatment can make larger surface sites and improve biosorbent surface activity and kinetic energy (Liu et al., 2012).

The drying time of tea leaves and mandarin peels have very similar pattern. For tea leaves, at $150^{\circ}C$ the remaining weight plateaued after 2 hr while at $75^{\circ}C$, the constant weight could be achieved within 6 hr. For maple leaves, due to low content of moisture, there were no remarkable differences between drying time in different drying temperature which were within 3 hr for lower drying temperatures and 2 hr for higher temperatures. However, when the temperature was higher than $105^{\circ}C$, there is no significant change in the drying rate for all three types of biosorbent after 2 hr of drying in oven.

All of biosorbents were dried at various temperatures to investigate the influence of drying temperature on drying rate and remaining weight. As can be expected, increasing drying temperature made a significant improvement of drying rate. The drying time was reduced remarkably with an increase in temperature within 50 to 150 $^{\circ}C$. However, in this study for metal concentration of 50 mg/L, the temperature did not affect the amount of Cd, Cu, Pb and Zn biosorption on MMBB (Figure 5.5).

Therefore, for low energy consumption in a short time of drying and also to avoid any physical damage of biosorbent structure, all biosorbent was dried at lower temperature (105 $^{\circ}C$) as an optimum temperature in this study.

5.2.4   Influence of chemical pretreatment

NaOH has been used to hydrolyse protein of biosorbents and methyl esters of cellulose, hemicellulose, pectin and lignin (Calero et al., 2013; Ronda et al., 2013; Feng et al., 2009a). Methyl ester bonds can be saponified to carboxyl (–COOH), carboxylate (–COO) and alcoholic (–OH) ligands. It also leads to a decrease in the degree of polymerization and crystallinity as follows:

$R-COOCH_3 + NaOH \rightarrow R-COO^- + CH_3OH + Na^+$
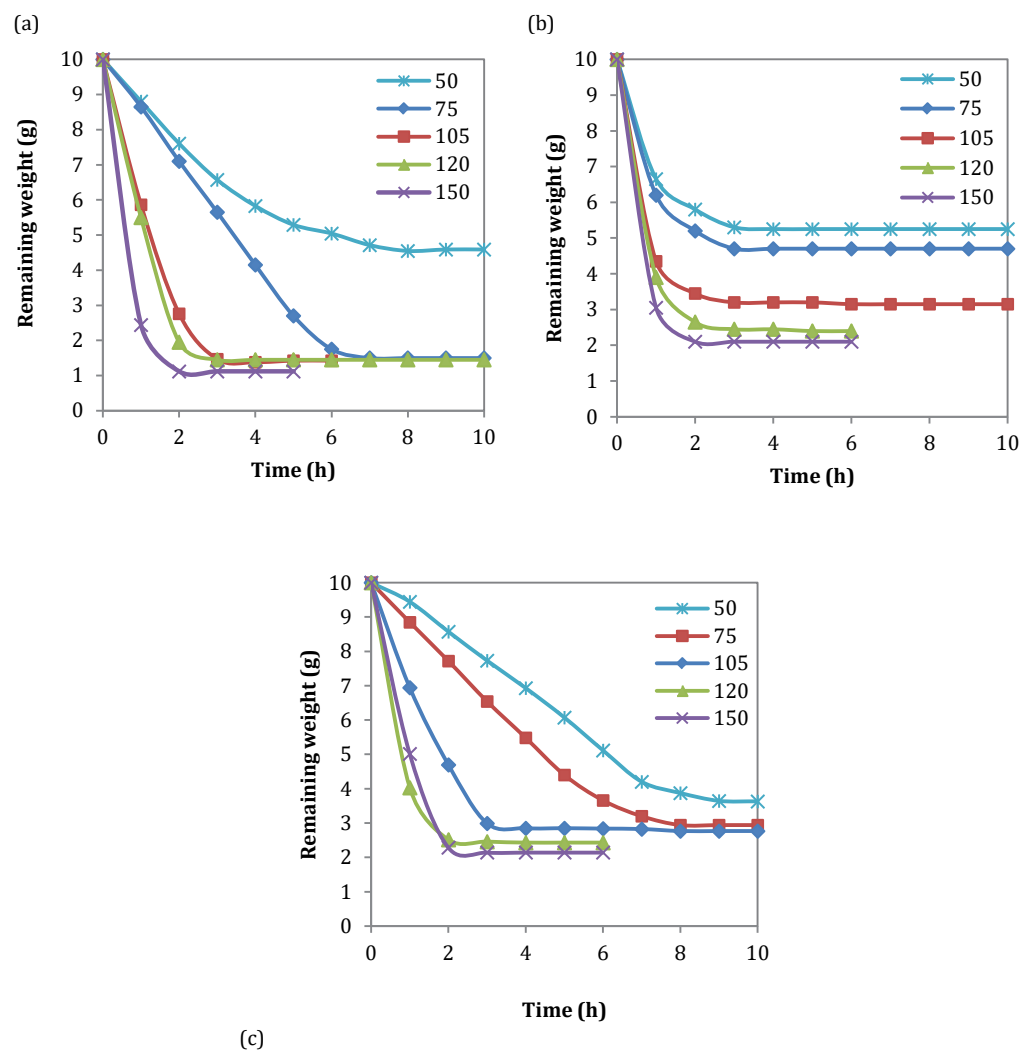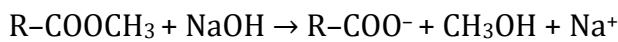
Figure 5.4 Drying rate of (a) tea leaves, (b) maple leaves and (c) mandarin peels at different drying temperature

Strong acids such as HCl, H_2SO_4 or HNO_3 can protonate unavailable functional groups in the structure of biosorbents by oxidizing functional groups and

transforming them to carboxylic groups (Chatterjee and Schiewer, 2014; Ronda et al., 2013; Schiewer and Balaria, 2009; Nadeem et al., 2008).
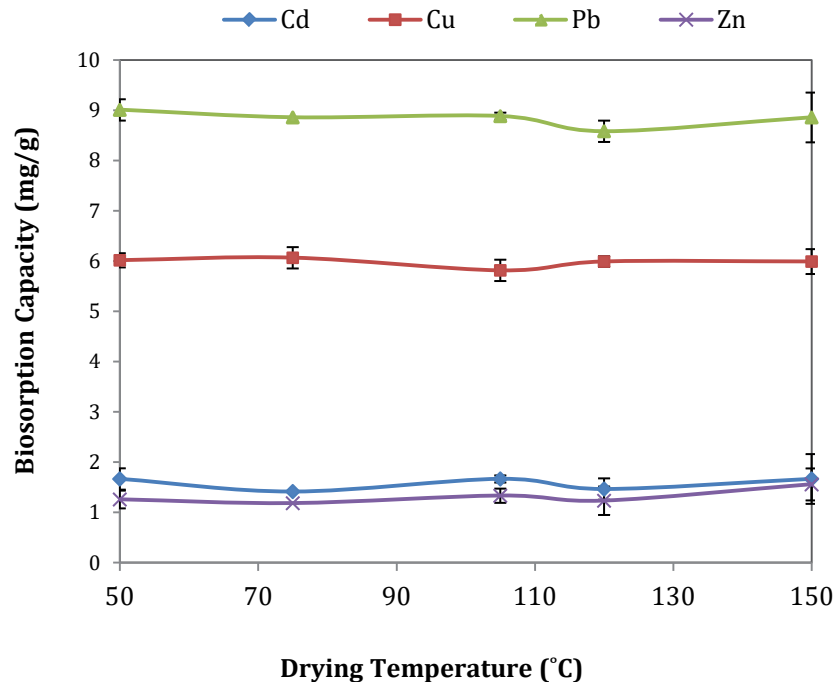
Figure 5.5 Effect of drying temperature on Cd(II), Cu(II), Pb(II) and Zn(II) adsorption(Initial pH 5.0–5.5±0.1; room temperature, 22±1°C; initial metal Conc.: 50 mg/L; biosorbent dose: 5g/L; rotary speed: 150 rpm)

Besides, alkali treatments in comparison with acidic ones at the same conditions were more effective on metal ion removal and made the functional groups denser and thermodynamically more stable (Velazquez–Jimenez et al., 2013). Dilute NaOH treatment leads to an increase in surface area, while treatment with nitric acid reduces the surface area and total pore volume (Ronda et al., 2013).

Formaldehyde can increase stability of the material and surface structure. It can be applied to pretreatment for prevention of organic leaching and metal uptake enhancement. Chen and Yang (2005) reported that formaldehyde reacts with the hydroxyl group of biosorbent to form acetyl groups and increase the structural stability of the biomass.

Pectin acid of lignocellulosic materials is precipitated by treating with calcium chloride and its solubility in solution decreases. In addition, $CaCl_2$ makes

biosorbent stable in term of mechanical structure by releasing organic compounds and volatiles (Feng et al., 2009a). It has been also reported that the formation of reactive carboxyl groups' cross–links with calcium might increase by adding a given amount of calcium ions (Sriamornsak, 2003).
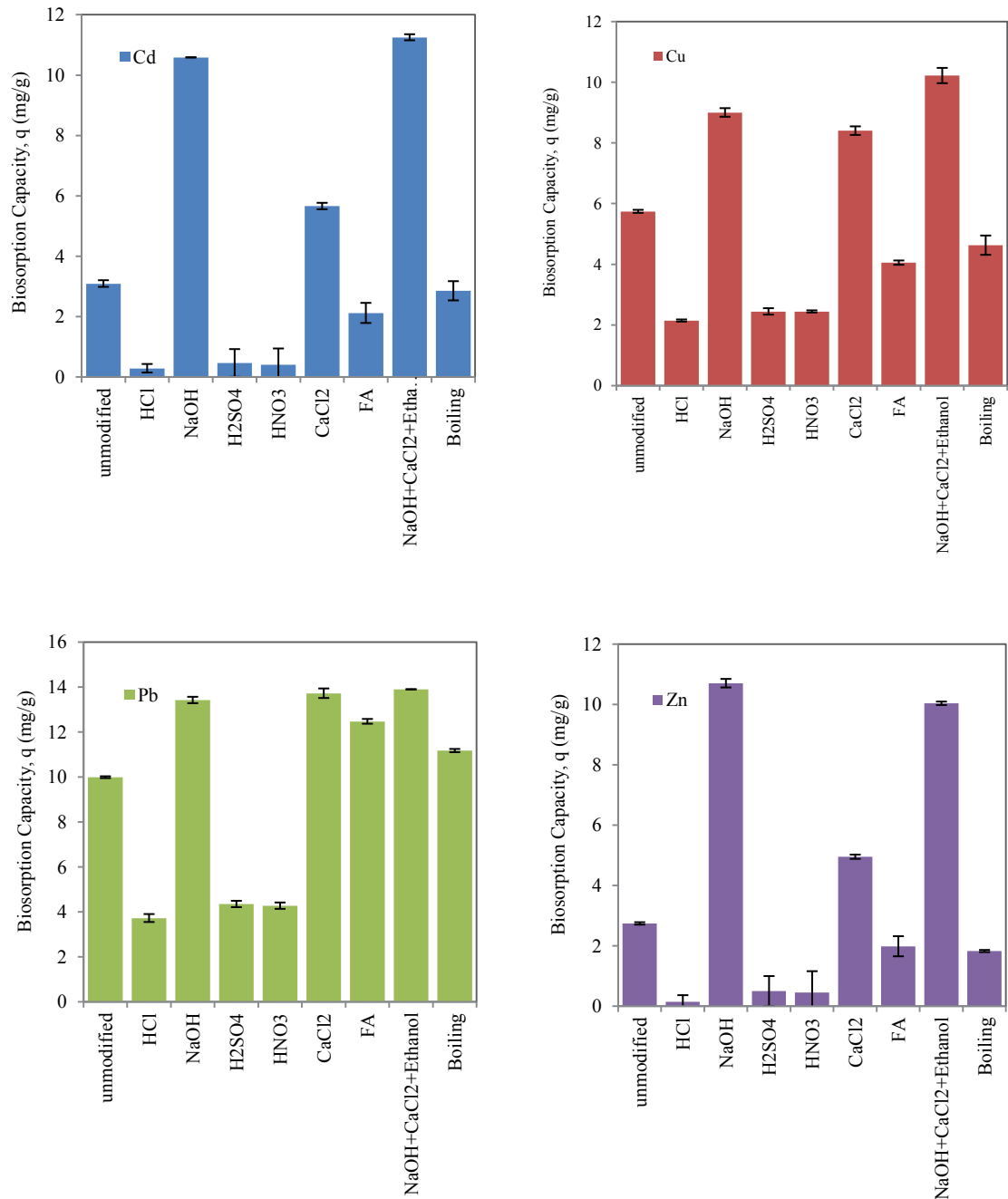
Figure 5.6 Biosorption capacity of modified MMBB by different chemical and physical methods (Initial pH 5.0–5.5±0.1; room temperature, 22±1 °C; initial metal Conc.: 50 mg/L; biosorbent dose: 5g/L; rotary speed: 150 rpm)

Finally, it should be noted that the enhancement obtained in biosorption capacity with pretreatments of MMBB by mineral acids was due to the functional groups replacement with more soluble compounds and improvements of surface characteristics (Velazquez–Jimenez et al., 2013; Ofomaja and Naidoo, 2011).

The calculated biosorption capacities for each metal ion were shown in Figure 5.6. The biosorption capacity of all metals increased after modification by NaOH which are 10.58, 9.00, 13.42 and 10.70 mg/g for Cd, Cu, Pb and Zn, respectively. HCl, HNO_3 and H_2SO_4 indicated reverse results due to probable damage of biosorbent structures by these mineral acids. $CaCl_2$ and formaldehyde improve lead removal whereas cadmium, copper and zinc removal decreased by formaldehyde–treated MMBB.

It can be concluded that, chemical modification by sodium hydroxide and the solution containing sodium hydroxide, calcium chloride and ethanol were more effective than the other chemical and physical pretreatment. Since calcium chloride made biosorbent structure more durable for reusing in successive and continuous processes, all biosorbents were pretreated by NaOH, $CaCl_2$ and ethanol.

5.2.5 Influence of ion strength

From FTIR, MMBB was characterized by negative charge due to dissociation of two weakly acidic active sites (carboxylic and amino acid). Another important parameter in biosorption is the ionic strength because of the nature of the active sites of biomasses and the type of physico–chemical interactions among these active sites and ionic species in the solution (Pagnanelli et al., 2014; Beolchini et al., 2006). Rather than hydroxide ions and the pH of solution, biosorption process is strongly dependent on water chemistry and presence of electrolyte ions.

Sodium as a common ion in wastewater competes with heavy metal ions for electrostatic binding to the biomass (Schiewer and Volesky, 1997). Therefore, the amount of heavy metals bound reduced by light metals (represented by ionic strength). Deprotonated functional groups are negatively charged; consequently they will electrostatically attract any cation. However, potassium and sodium ions do not compete directly with the covalent binding of heavy metals ions onto the

biosorbent surface. It is probably due to the poor complex with surface active sites (Vilar et al., 2005). The effect of Na^+ is more influential respecting the uptake of weakly bound heavy metals such as Zn or Ni, while strongly bound metals such as Pb and Cu are less affected by the ionic strength (Schiewer and Wong, 2000).

In this study, having investigated the effect of pH value and the presence of $[H_3O]^+$ ions, the effect of ionic strength on biosorption is studied by performing equilibrium sorption tests in batch systems. The flasks contained heavy Cd, Cu, Pb and Zn with initial concentrations of 10, 50 and 100 mg/L. Ionic strength of solutions varied by adding $NaNO_3$ with concentrations of 0.1 and 0.2 M. These relatively high concentrations were chosen for simulating the real wastewaters. For comparison with lower ionic strength level, there was a reference case with no addition of $NaNO_3$ to the heavy metal solution. The results are shown in Figure 5.7. Respecting covalent heavy metal speciation, in the studied pH range (2.5–6.0±0.1), the main form of Me^{2+} and its speciation are not remarkably influenced by the presence of Na^+ (Beolchini et al., 2006). The ionic strength only has a slight effect on cadmium, copper, lead and zinc ion uptake capacity at lower Na^+ concentration (0.1 M) by modified MMBB regardless of heavy metal concentrations. Besides, increasing of heavy metal concentration can cover the effect of ionic strength effect of high sodium concentration (0.2 M). Hence, it can be concluded that electrostatic binding of MMBB has nontangible contribution of covalent binding within biosorption process. In other study, it has been reported that strongly bound metals such as lead and copper are less affected by the ionic strength (Vilar et al. 2005).

5.3   *Characterization of adsorbents by FTIR*

FTIR analysis was performed to investigate the major functional group in cadmium, copper, lead and zinc binding process. The FTIR spectra of the unmodified and modified MMBB by NaOH, $CaCl_2$ and ethanol before and after metal loading were compared (Figure 5.8). The major band assignments and functional groups are as follows. A medium band at about 1051-1012 cm^{-1} corresponds to deformation vibration of groups C–N stretch of aliphatic amines. Broad bands at 1300-1000 cm^{-1} have been assigned to C–O stretching in acids,

alcohols, phenols, ethers and esters. Two bands (<200 cm^{-1} apart) were the appearance of N=O bend of nitro compounds between 1400–1300 cm^{-1}.
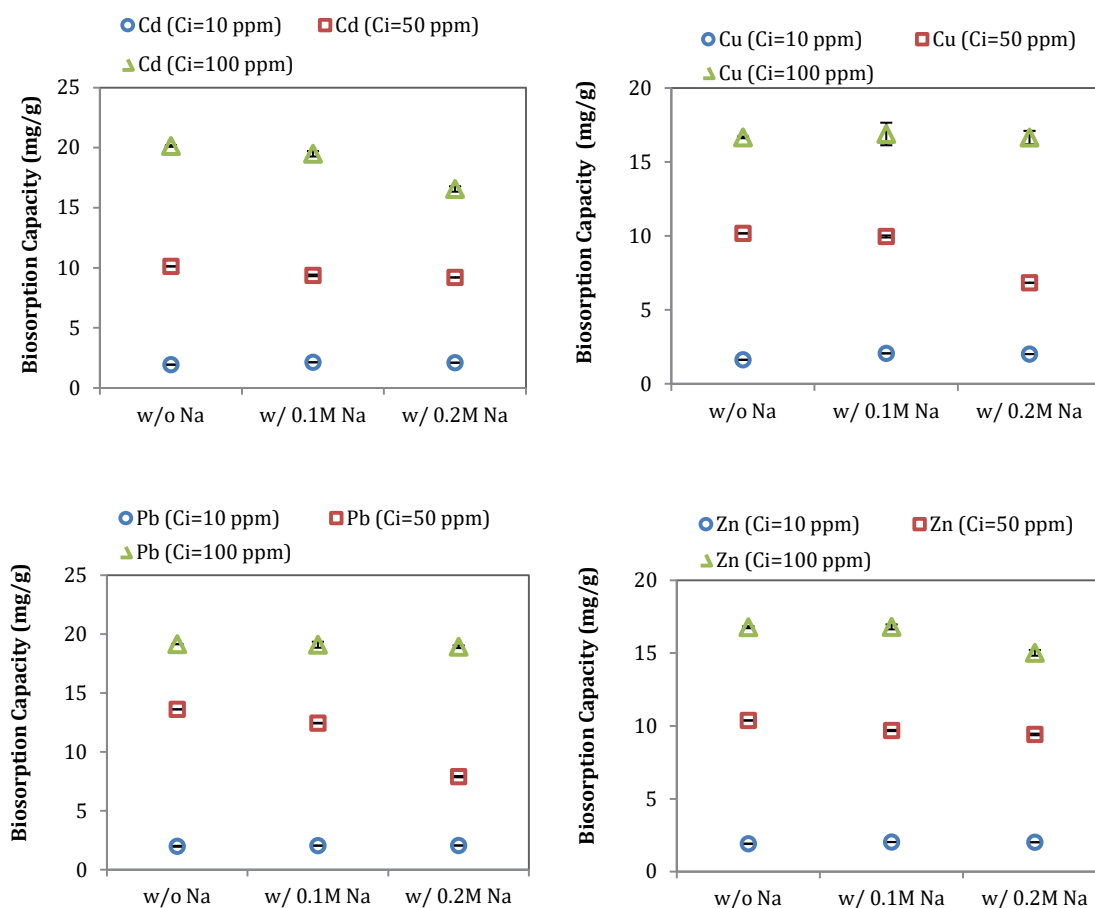
Figure 5.7 Experimental data for cadmium, copper, lead and zinc biosorption on modified MMBB at different ionic strength levels

The bands at 1579 and 1523 cm^{-1} for modified MMBB and at 1546 and 1533cm^{-1} for unmodified MMBB, respectively, correspond to stretching of carbonyl group and carboxylic acid (C=O) of primary amines (1̊ amine). The band at 1589 cm^{-1} corresponds to deformation vibration of N–H bends of primary amines (1° amine). The region between 2000 and 3000 cm^{-1} presents two major adsorption bands. At about 2341 and 2343 cm^{-1} for modified MMBB and at 2345 and 2353 cm^{-1} for unmodified MMBB, a doublet peak can be seen due to the existence of B–H stretch. The band around 2916 cm^{-1} was exhibited in presence of C–H stretching of CH$_2$ groups (asymmetric and symmetric stretches). Besides, a very broad weak band at

3144 and 3487 cm^{-1} might attribute to the presence of intermolecular hydrogen bonded O–H stretch of phenols and alcohols.

The changes after modification can be obviously seen in FTIR spectra as the fingerprint of sodium hydroxide pretreatment due to the formation of the intermolecular hydrogen bond and complexation of heavy metal ions by carboxylate groups. According to literature (Tan and Xiao, 2009; Gurgel and Gil, 2009), ester product and carboxyl acid compounds will have a strong sharp peak at ~2900 cm^{-1} (alkyl C–H) and a strong and sharp peak at ~1700 cm^{-1} (C=O). The absorption band wave number of the carboxylate groups (COO$^-$) is about 1670–1600 cm^{-1}, which shifted to low wave number because of the formation of the intermolecular hydrogen bond. This confirms that basic modification of biosorbent makes methyl ester hydrolyse, ester groups decrease and subsequently carboxylate groups increase. The FTIR analysis of the chemically modified MMBB in comparison with unmodified form also confirmed that carboxylate groups play an important role in heavy metal adsorption.

5.4   *Effect of contact time and kinetic study*

It is evident from Figure 5.9 that the rate of metal uptake was very fast within first 60 min for initial metal concentrations of 10 and 50 mg/L in comparison with 100 mg/L. The biosorption capacity levelled off after 120 min of contact time for cadmium, copper and zinc ions with initial concentration of 100 mg/L while for lead, there is no difference between metal removal in different initial content.

The experimental kinetic results were fitted to pseudo first–order and pseudo second–order kinetic models. The kinetic model parameters, residual root mean square error (RMSE), error sum of square (SSE) and correlation of determination (R^2) were measure and presented in Table 5.1. According to calculated kinetic and fitting parameters and also comparison between adsorption rate constants, the estimated q_e and the coefficients of correlation associated with the Lagergren pseudo–first–order and the pseudo–second–order kinetic models, cadmium, copper, lead and zinc biosorption process followed pseudo second–order kinetic model.

It is obvious that chemical reaction would be presumably the rate limiting step of Cd, Cu, Pb and Zn biosorption on both modified and unmodified MMBB. The calculated values of q_e for pseudo–second–order kinetic model (modified MMBB) are 10.94, 10.75, 13.56 and 9.68 mg/g for Cd(II), Cu(II), Pb(II) and Zn(II), respectively, approximately close to the experimental values (11.69, 11.63, 13.75 and 10.33 mg/g).
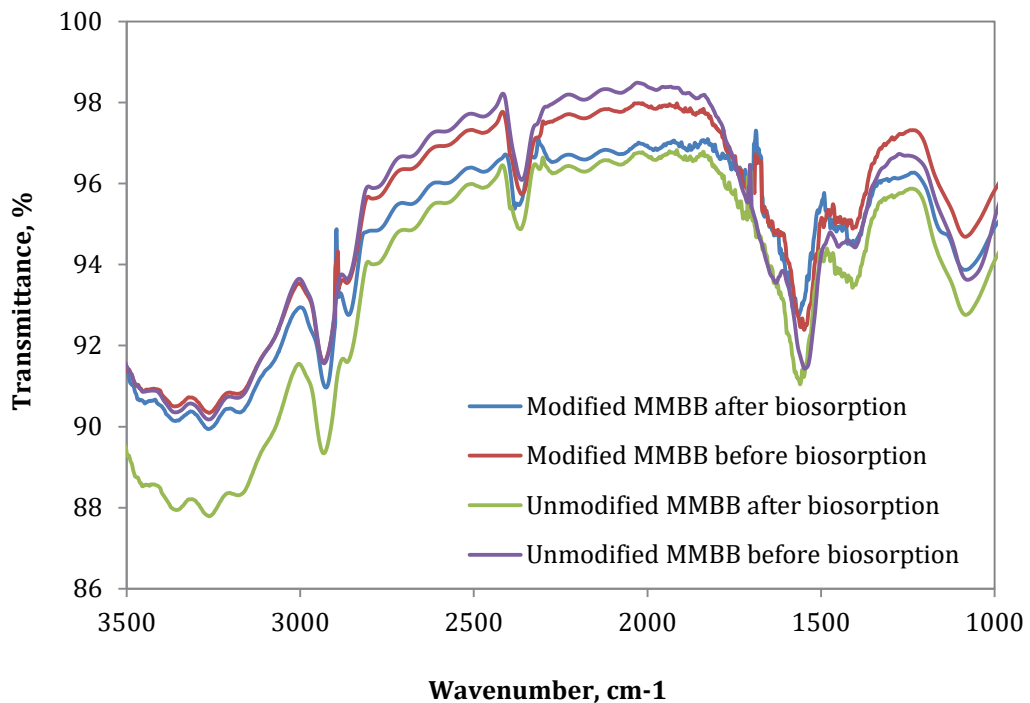
Figure 5.8 FTIR spectra of unmodified and modified MMBB before and after metal biosorption
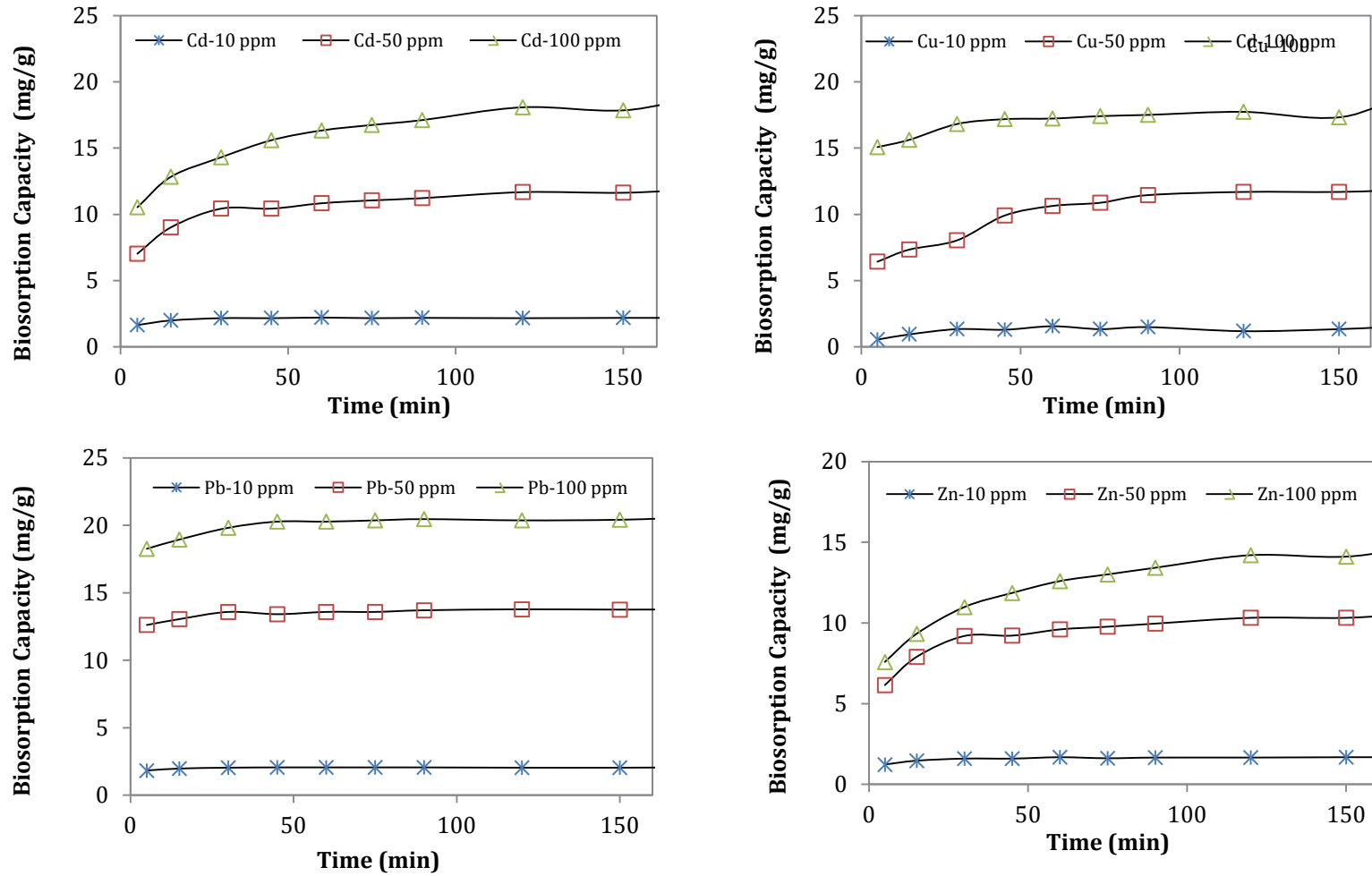
Figure 5.9 Effect of contact time on Cd(II), Cu(II), Pb(II) and Zn(II) adsorption

5.5   *Adsorption isotherm*

The correlation between the adsorbed and the aqueous metal concentrations at equilibrium was described by the Langmuir and Freundlich (Table 5.2). The Langmuir equation describes the equilibrium condition better than Freundlich model (R^2: 0.99 and small RMSE values). The maximum amounts of biosorption capacity by monolayer adsorption assumption for Cd, Cu, Pb and Zn obtained from Langmuir equation are 41.48, 39.48, 94.0 and 27.23 mg/g, respectively, for unmodified MMBB. These amounts were 69.56, 127.70, 345.20 and 70.55 mg/g for Cd(II), Cu(II), Pb(II) and Zn(II), respectively, for modified MMBB. Furthermore, it was understood that the Langmuir isotherm corresponded to a dominant ion exchange mechanism while the Freundlich isotherm showed adsorption–complexation reactions taking place at the outer heterogeneous surface of the adsorbent (Cay et al., 2004).

Table 5.3 summarizes the q_m values of various biosorbents for the comparison purpose. Table 5.3 reveals that this modified MMBB possessed relatively high q_m values, which were favourably comparable to most of the biosorbents in the literature for heavy metal removal from aqueous solutions. As found hereinbefore, combination of several types of low–cost agro–industrial waste might provide more selectivity as a result of increase in different effective functional groups involved in metal binding.

5.6   *Adsorption thermodynamics*

The biosorptive potential of modified MMBB for Cd(II), Cu(II), Pb(II) and Zn(II) removal was studied at the temperatures of 25, 30, 40 and 50 °C. The experimental results indicated dependency of adsorption on the temperature and are listed in Table 5. The thermodynamic parameters for the adsorption process such as Gibbs free energy change ($\Delta G°$), enthalpy change ($\Delta H°$), and entropy change ($\Delta S°$) were calculated to evaluate thermodynamic feasibility of the sorption process and to confirm its nature.

Table 5.1 Comparison between adsorption rate constants, the estimated q_e and the coefficients of correlation associated with the Lagergren pseudo–first–order and the pseudo–second order kinetic models (Initial metal Conc.: 50 ppm)

Kinetic models	Parameter	Metal							
		Cd[a]	Cd[b]	Cu[a]	Cu[b]	Pb[a]	Pb[b]	Zn[a]	Zn[b]
Experiment	q_e(mg/g)	3.30	11.63	6.40	11.69	9.02	13.75	2.88	10.33
Pseudo–first–order	$q_t = q_e[1 - exp\,(-K_1 t)]$								
	q_e(mg/g)	3.36	10.94	6.39	10.75	9.06	13.56	2.64	9.68
	K_1(hr^{-1})	10.70	11.02	8.047	5.95	8.93	3.33	5.17	10.62
	R^2	0.99	0.99	0.99	0.88	0.99	0.99	0.99	0.97
	SSE	0.10	3.47	0.005	13.99	0.354	0.37	0.007	2.91
	RMSE	0.08	0.65	0.006	1.32	0.165	0.21	0.02	0.60
Pseudo–second–order	$q_t = \dfrac{K_2 q_e^2 t}{1 + K_2 q_e t}$								
	q_e(mg/g)	3.40	11.63	6.39	11.74	8.99	13.7	2.68	10.32
	K_2 (mg g^{-1}hr^{-1})	11.08	1.46	3.32	0.78	0.72	9.83	0.08	1.57
	R^2	0.99	0.99	0.99	0.95	0.98	0.99	0.98	0.99
	SSE	0.04	0.62	0.53	6.27	1.14	0.12	0.07	0.53
	RMSE	0.05	0.28	0.006	0.88	0.29	0.12	0.76	0.25

(a)   Un–modified MMBB

(b)   Modified MMBB

Table 5.2 Isotherm constants of non–linear Langmuir and Freundlich models for Cd(II), Cu(II), Pb(II) and Zn(II) adsorption on unmodified and modified MMBB

Isotherm models	Metal							
	Cd[a]	Cd[b]	Cu[a]	Cu[b]	Pb[a]	Pb[b]	Zn[a]	Zn[b]
Langmuir $q_e = \frac{q_{m,L} b_L C_e}{1 + b_L C_e}$								
$q_{m,L}$ (mg/g)	41.48	69.56	39.48	127.70	94.00	245.20	27.23	70.55
b_L (L/mg)	0.001	0.004	0.004	0.001	0.007	0.060	0.002	0.004
R^2	0.99	0.98	0.99	0.99	0.99	0.99	0.99	0.99
RMSE	3.45	2.59	4.56	2.87	2.12	0.71	0.53	2.25
Freundlich $q_e = K_F C_e^{1/n}$								
K_F	0.92	1.24	1.64	0.75	7.80	0.37	0.46	1.17
n	1.88	1.71	1.96	1.40	2.38	1.15	1.80	1.67
R^2	0.79	0.95	0.92	0.97	0.98	0.99	0.97	0.95
RMSE	4.09	4.49	3.84	4.26	4.08	1.36	0.98	9.06

[a]   Un–modified MMBB

[b]   Modified MMBB

Table 5.3 Maximum biosorption capacities of various adsorbents

Adsorbent	Adsorbate	$q_{m,L}$(mg/g)	Reference
Tomato waste [b]	Cu(II)	34.48	Yargıç et al., 2014
Olive tree pruning [a]	Pb(II)	33.90	Anastopoulos et al., 2013
Olive tree pruning [b]	Pb(II)	82.64	Anastopoulos et al., 2013
Cabbage waste [a]	Cd(II)	20.56	Hossain et al., 2014
Cabbage waste [a]	Cu(II)	10.31	Hossain et al., 2014
Cabbage waste [a]	Pb(II)	60.56	Hossain et al., 2014
Cabbage waste [a]	Zn(II)	8.97	Hossain et al., 2014
Orange peel [b]	Pb(II)	113.5	Feng et al., 2011
Orange peel [b]	Cd(II)	63.35	Feng et al., 2011
Cashew nut shell [a]	Zn(II)	24.98	Kumar et al., 2012
Rice straw [a]	Cd(II)	13.89	Ding et al., 2012

[a] Unmodified MMBB

[b] Modified MMBB

The Gibbs free energy indicates the degree of spontaneity of sorption process, and the higher negative value reflects a more energetically favourable sorption. $\Delta H°$ and $\Delta S°$ were obtained from the slop and intercept of the Van't Hoff plots (Figure 5). The negative values of ($\Delta G°$) for all metal ions indicate the spontaneous nature of metal biosorption on modified MMBB. The negative value of $\Delta H°$ showed that the sorption process was exothermic in nature.

Except for zinc, calculated $\Delta S°$ values for cadmium, copper and lead were positive, reflecting the increased randomness at the solid/solution interface during sorption. It also indicates an affinity of the sorbent towards Cd, Cu and Pb ions. In

addition, the low value of $\Delta S°$ may imply that no remarkable change in entropy occurred during the sorption of Cd, Cu, Pb and Zn ions on modified MMBB.

5.7   ***Desorption studies***

It is desirable to desorb and recovered the adsorbed metals and also regenerate the adsorbent materials for another cycle of application. The regeneration of the adsorbent can be achieved by washing loaded adsorbent with an appropriate desorbing solution. Desorbing agent must be cheap, effective, non–polluting and non–damaging to the adsorbent structure (Ozdes et al. 2009).

In Figure 5.11, the desorption potential of the eluents is compared for first cycle of sorption/ desorption to select the best desorbing agent. It is apparently that Milli–Q water was very ineffective for releasing bonded metal onto MMBB. Sodium chloride and sodium hydroxide showed very weak potential for detaching adsorbed metal in comparison with the acids. It is well known that under acidic conditions the adsorbent surface is protonated by $[H_3O]^+$ ions to make possible desorption of positively charged metal ions from the adsorbent surface (Ozdes et al., 2009). Among these three mineral acids, HCl was slightly better than HNO_3 and H_2SO_4 for all metals.

Copper was almost completely desorbed with 0.1M HCl. Other metal ions recovery cannot thoroughly fulfilled by desorption. This might be due to heavy metal ions being trapped in the adsorbent porous structure and therefore difficult to release (Ozdes et al. 2009).

According to the Langmuir parameter presented in Table 5.2, lead biosorption presented the highest affinities for modified MMBB, therefore desorbed in longer time than other metals. The lead recovery was the lowest and copper showed the highest amounts which were 76.26 and 99.93 %, respectively by applying HCl as he desorbing agent. Cadmium and zinc desorption efficiency were 96.33 % and 91.93 % respectively for HCl, and 96.90 % and 92.90 %, respectively for HNO_3.
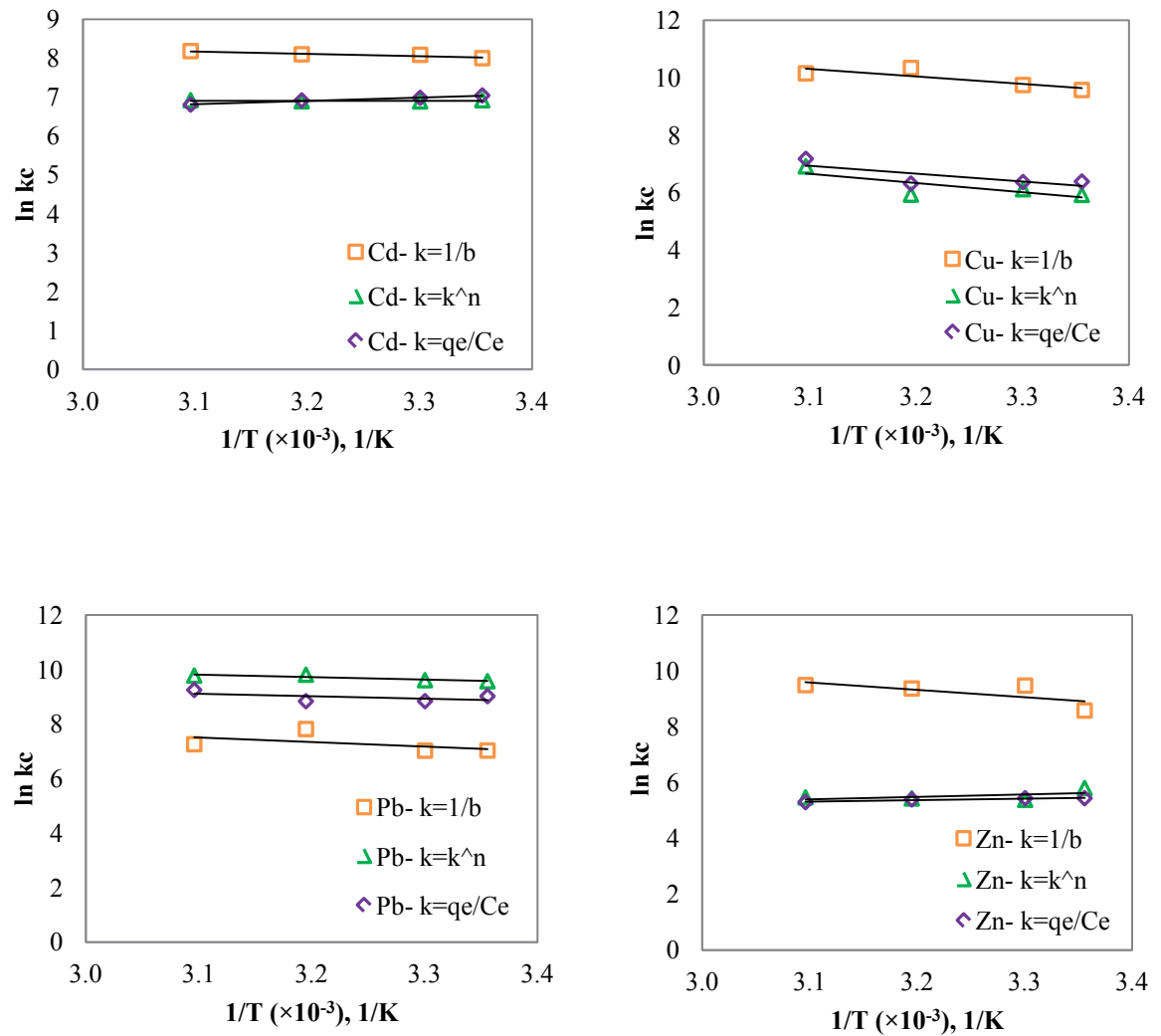
Figure 5.10 Van't Hoff plots for Cd(II), Cu(II), Pb(II) and Zn(II) adsorption(initial pH 5.5±0.1; initial metal Conc.: 1–50 mg/L; contact time: 3 h; biosorbent dose: 5 g/L

Generally, desorption efficiency of all metals did not tangibly change by using these three acids. It is necessary to note that because of low solubility of lead sulphate, H_2SO_4 could not be utilized for lead recovery.

For desorption study, the optimum conditions were determined and metal–loaded modified MMBB was desorbed using HCl, HNO_3 and H_2SO_4 (0.1M) for enough time within that the outlet metal concentration remained constant and equal or close to zero.

Table 5.4 Thermodynamic parameters, ΔG°(kJ/mol), ΔH° (kJ/mol) and ΔS°(kJ/mol K), for adsorption of Cd(II), Cu(II), Pb(II) and Zn(II) adsorption(Initial metal Conc.: 1–50 mg/L)

Metal	T (K)	$k_c=q_e/C_e$	ΔG°	ΔH°	ΔS°	$k_c=1/b_L$	ΔG°	ΔH°	ΔS°	$k_c=K_F^n$	ΔG°	ΔH°	ΔS°
Cd	298	1.14	−17.44	−4.11	0.87	2.97	−19.81	−10.06	0.61	1.01	−17.13	−6.95	0.02
	303	1.07	−17.57			3.24	−20.36			0.98	−17.34		
	313	1.00	−17.98			3.28	−21.07			0.98	−17.92		
	323	0.90	−18.27			3.56	−21.96			1.01	−18.57		
Cu	298	0.59	−15.81	−15.45	2.75	14.29	−23.70	−18.30	2.58	0.37	−14.66	−16.58	3.20
	303	0.58	−16.03			17.01	−24.54			0.45	−15.40		
	313	0.55	−16.42			30.77	−26.89			0.37	−15.42		
	323	1.3	−19.25			25.51	−27.25			1.00	−18.55		
Pb	298	8.29	−22.35	−11.93	0.90	1.13	−17.41	−12.65	1.65	14.35	−23.71	−12.68	0.92
	303	6.91	−22.27			1.12	−17.70			14.92	−24.21		
	313	6.89	−23.00			2.48	−20.34			18.25	−25.53		
	323	10.43	−24.85			1.42	−19.50			17.65	−26.26		
Zn	298	0.23	−13.47	−3.64	−0.54	5.32	−21.26	−17.72	2.62	0.33	−14.38	−2.57	−0.91
	303	0.23	−13.70			13.00	−23.86			0.22	−13.55		
	313	0.22	−14.04			11.72	−24.38			0.23	−14.13		
	323	0.2	−14.23			13.23	−25.48			0.24	−14.68		
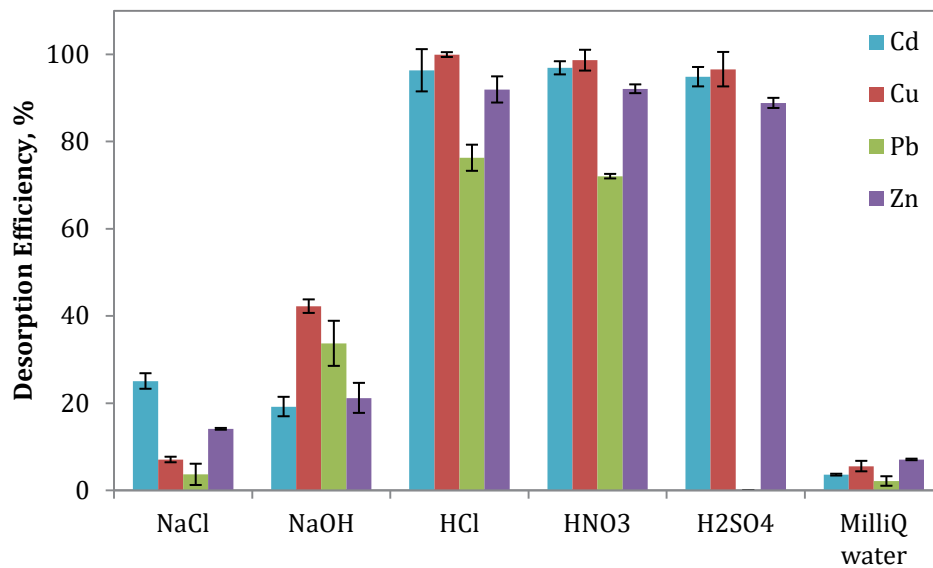
Figure 5.11 Comparison between Cd, Cu, Pb and Zn elution from metal–loaded modified MMBB using different desorbing agents (C_i: 50 ppm)

Figure 5.12 shows the elution curves of metal–loaded modified MMBB with HCl, HNO_3 and H_2SO_4 until desorption efficiency amount levelled off. Lead desorption by HCl was slower than other metal desorption. The lead desorption equilibrium took place within 3 hr whereas other metal desorption efficiency reach equilibrium state in 2 hr.

The effect of HCl concentration was indicated in Figure 5.13. Metal desorption efficiency increased by about 9, 47, 70 and 26 % for Cd, Cu, Pb and Zn, respectively, when HCl concentration increased from 0.01M to 0.1M. Higher acid concentration might damage the biosorbent structure and reduce the sorption and desorption efficiency due to biosorbent mass loss.

The metal–desorbed modified MMBB was used as the regenerated sorbent in five repeated sorption and desorption cycles and five successive cycles of sorption, desorption and regeneration to determine reusability potential of the adsorbent. After adsorption, the metal–loaded modified MMBB were filtered, oven dried, weighed and soaked in 0.1M HCl desorption solution with biosorbent concentration of 5 g/L. After each desorption step, biosorbents was washed

properly by distilled water, then contacted with 1M $CaCl_2$ for 12 hr at 4°C to be regenerated. In each cycle, the biosorbent was repeatedly washed with distilled water after each desorption to eliminate any excess chemical. Biosorbent stability or any probable weight loss was controlled by weighing MMBB after drying in oven.
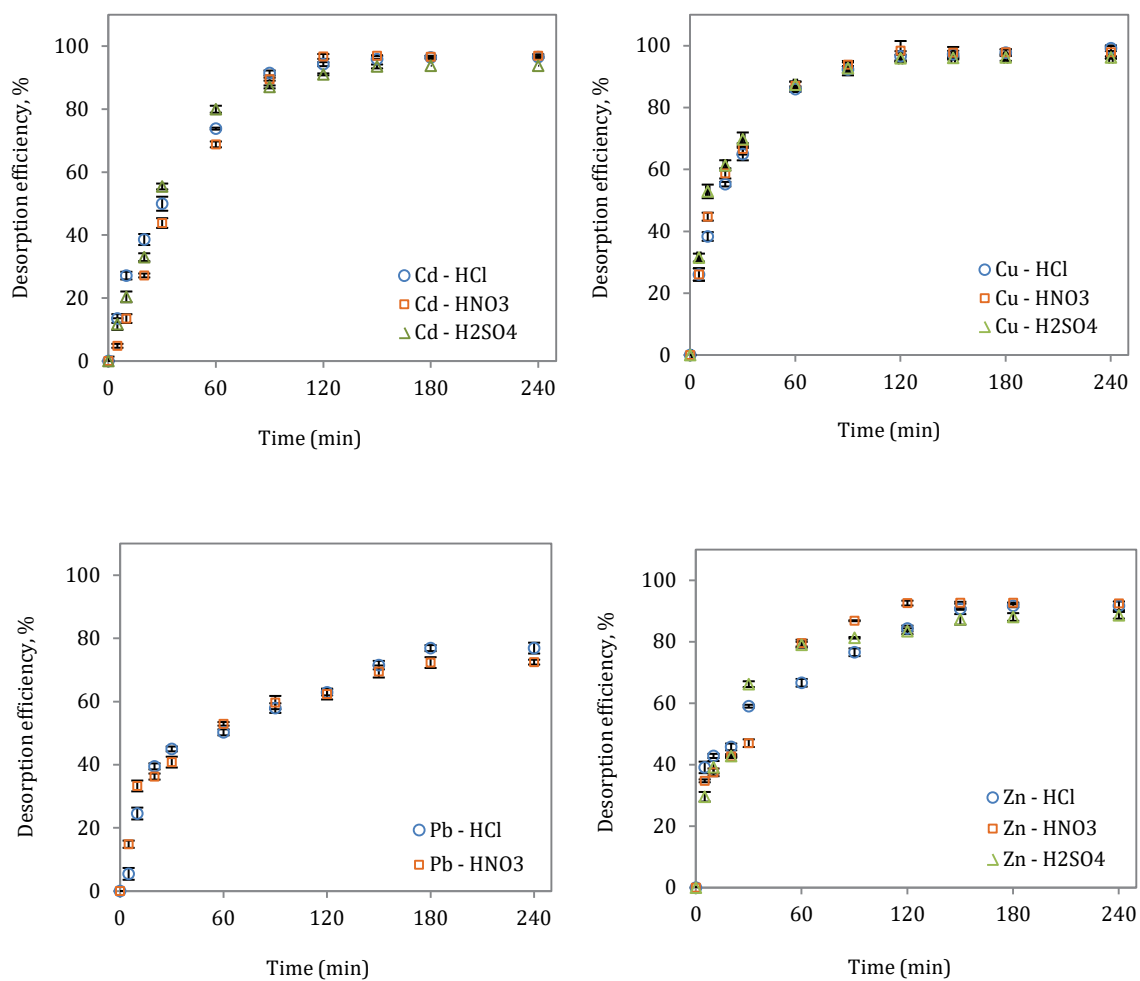
Figure 5.12 Elution of Cd, Cu, Pb and Zn from metal–loaded modified MMBB using different mineral acids: 0.1M HCl, H_2SO_4 and HNO_3
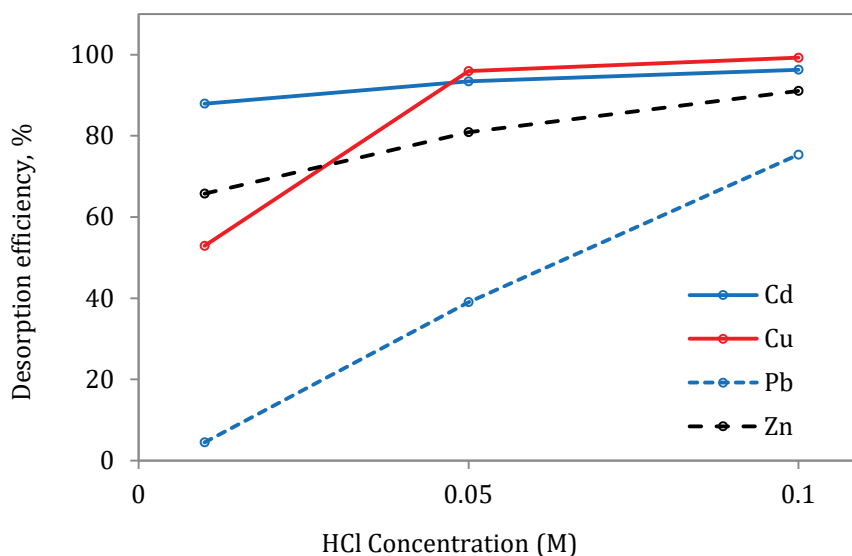
Figure 5.13 Effect of HCl concentration on desorption efficiency of metal–loaded modified MMBB

The results were very promising. Calcium chloride can increase the stability and reusability of MMBB and repairing the damage caused by the desorbing agents and removing the excess protons after each elution providing new binding sites. HCl was the best eluent for the reutilization of MMBB among all studied chemicals without destroying its sorption capability. MMBB were successfully reused (5 cycles) without any significant loss in both biosorption capacity and biosorbent mass. Metals uptake levelled off or increased after using a 1M $CaCl_2$ regeneration step after each desorption. After the fifth step of sorption and desorption, for Cd and Pb ions, biosorption capacity increased from 10.95 mg/g to 11.90 mg/g and 8.78mg/g to 9.20 mg/g, respectively, while Cu and Zn removal decreased by 3.76 and 8.57 mg/g, respectively (Figure 5.14).

The results were very promising. Calcium chloride can increase the stability and reusability of MMBB and repairing the damage caused by the desorbing agents and removing the excess protons after each elution providing new binding sites. HCl was the best eluent for the reutilization of MMBB among all studied chemicals without destroying its sorption capability. MMBB were successfully reused (5 cycles) without any significant loss in both biosorption capacity and biosorbent mass. Metals uptake levelled off or increased after using a 1M $CaCl_2$ regeneration

step after each desorption. After the fifth step of sorption and desorption, for Cd and Pb ions, biosorption capacity increased from 10.95 mg/g to 11.90 mg/g and 8.78mg/g to 9.20 mg/g, respectively, while Cu and Zn removal decreased by 3.76 and 8.57 mg/g, respectively (Figure 5.14).

Figure 5.14 Biosorption capacity of modified MMBB after each sorption/ desorption step without and with regeneration step by $CaCl_2$

Desorption efficiency of cadmium, copper, lead and zinc decreased by about 26, 37, 29 and 36 %, respectively (Figure 5.15). During desorption by hydrochloric acid, biosorbent can become swollen in the acid and the mass loss of MMBB was the result of this damage that was observed between the first and fifth cycles. After five cycles, however, biosorbent mass decreased by 32%, without regeneration by $CaCl_2$.

The biosorbent surface remained coarsely porous to entrap the metal ions, $CaCl_2$ could repair the damage caused by the acid during desorption and remove the excess protons remaining from that step (Mata et al. 2010; Mata et al. 2009). In addition, it was seen that the metal desorption efficiency and biosorption capacity remained constant or increased to a slight extent for all metals. This might be as a result of slightly chemical modification by $CaCl_2$. Similarly, Mata et al. (2009 and 2010) using 0.1M HNO_3 as desorbing agent and 1M $CaCl_2$ as regenerating agent for pectin gel beads in order to Cd, Cu and Pb uptake. It was very successful to reuse pectin gel beads after nine cycles of sorption/ desorption/ regeneration. In other study, calcium chloride was successfully applied as an eluent to desorbed cadmium, lead and nickel adsorbed on brown algae of *Cystoseira indica*. In that investigation, calcium chloride was compared with sodium chloride and acetic acid for five consecutive cycles of sorption and desorption (Montazer–Rahmati et al., 2011).
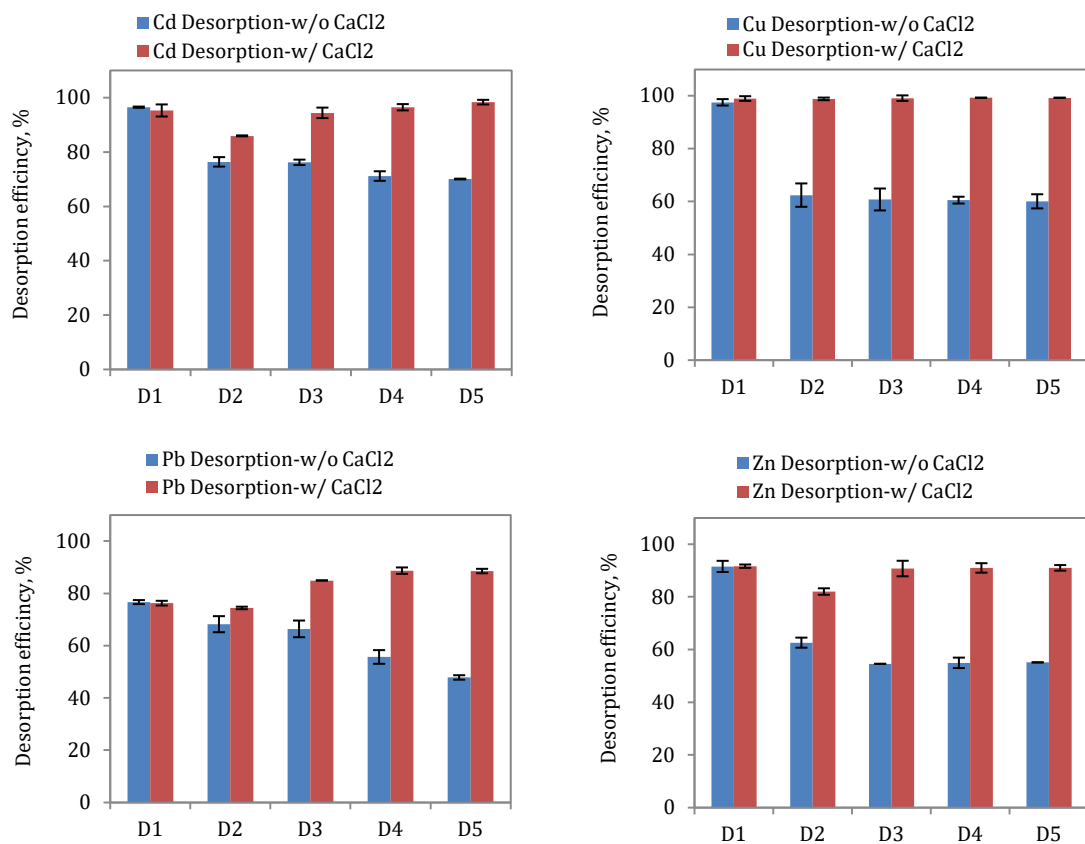
Figure 5.15 Desorption efficiency of modified MMBB after each sorption/ desorption step without and with regeneration by $CaCl_2$

Therefore, when regeneration step by calcium chloride added to sorption and desorption experiments, the mass loss of biosorbent decreased only 18%. It was obvious that after five cycles of sorption/ desorption/ regeneration, the biosorbent appearance, visible structure and mechanical stability did not demolish at all.

5.8   *SEM/EDS analysis*

SEM analysis (Figure 5.16) depicts the morphology changes of unloaded and loaded biosorbent. After biosorption of heavy metal ions, the surface became smoother with less porosity with probable metal entrapping and adsorbing on biosorbent.

The electron micrograph of the biosorbent before and after modification by NaOH and $CaCl_2$ after metal adsorption presents several sites on MMBB. The EDS graphs of MMBB samples (Figure 5.17) clearly show a strong peak of Ca and a moderate peak of Na after chemical modification. The distribution of peaks changed in element and intensity. Besides, after metal adsorption the strong peaks attributing to Cd, Cu, Pb and Zn appeared significantly. The variance in intensity of K, Na and Ca peaks might be due to ion exchange mechanism of metal uptake. Overall, the Cd(II), Cu(II), Pb(II) and Zn(II) intake by biosorbent was confirmed by SEM/EDS analysis.

5.9   *Biosorption mechanism*

The metal binding takes place as a passive mechanism based on the chemical properties of surface functional groups. The mechanisms involved in metal bioaccumulation are complicated; therefore the interpretation is very difficult. Usually these mechanisms are related to electrostatic interaction, surface complexation, ion–exchange, and precipitation, which can occur individually or in combination (Oliveira et al., 2014).
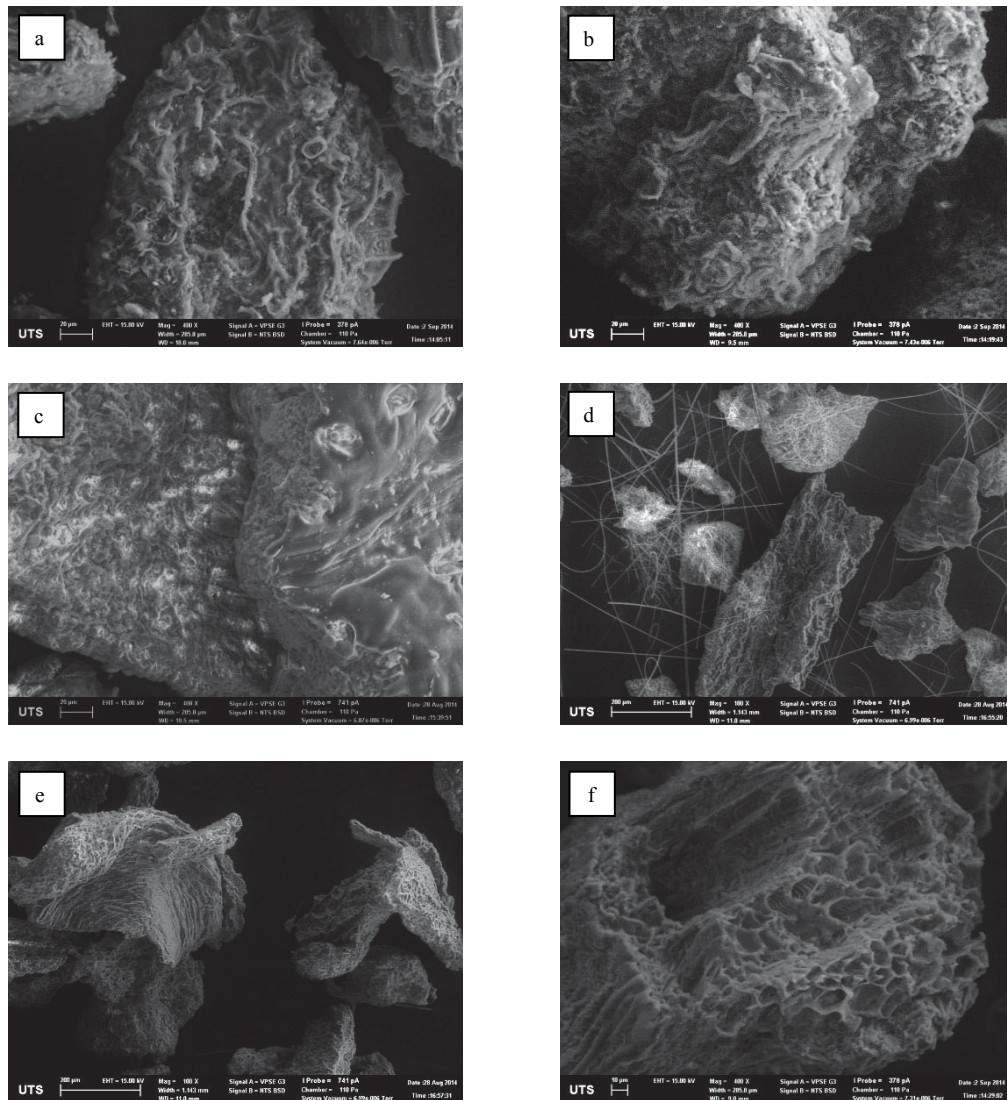
Figure 5.16 SEM images of (a) unmodified MMBB before metal adsorption (b) modified MMBB before metal adsorption, (c) unmodified MMBB after metal adsorption, (d) modified MMBB after metal adsorption (e) modified MMBB after 5 cycles of cycles of sorption/ desorption and (f) modified MMBB after five cycles of sorption/ desorption/ regeneration by $CaCl_2$

The main mechanisms are known for metal sorption on lignocellulosic biosorbents are chelating, ion exchanging and making complexion with functional groups and releasing $[H_3O]^+$ into aqueous solution. Ionic exchange is known as a mechanism which involves electrostatic interaction between positive metallic cations and the negatively charged groups in the cell walls. The ion exchange reaction could be represented as (Fiol et al., 2006):

$$\equiv S - M_{2/n}(s) + Me^{2+}(aq) \Leftrightarrow \equiv S - Me\ (s) + \frac{2}{n}M^{n+}(aq)$$
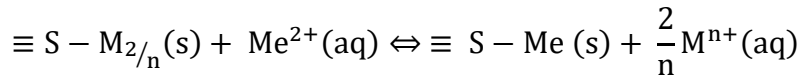
Where M^{n+} represents Na^+, K^+, Mg^{2+} or Ca^{2+} and Me^{2+} is heavy metal ions like Pb^{2+}, Cd^{2+}, Ni^{2+}, Cu^{2+}, etc. On the other hand, many characterization studies confirmed that ion exchange mechanism was included in heavy metal biosorption process rather than complexation with functional groups on the biosorbent surface and also showed the role of sodium, potassium, calcium and magnesium present in the adsorbent in ion exchange mechanism (Ding et al., 2012; Akar et al., 2012).
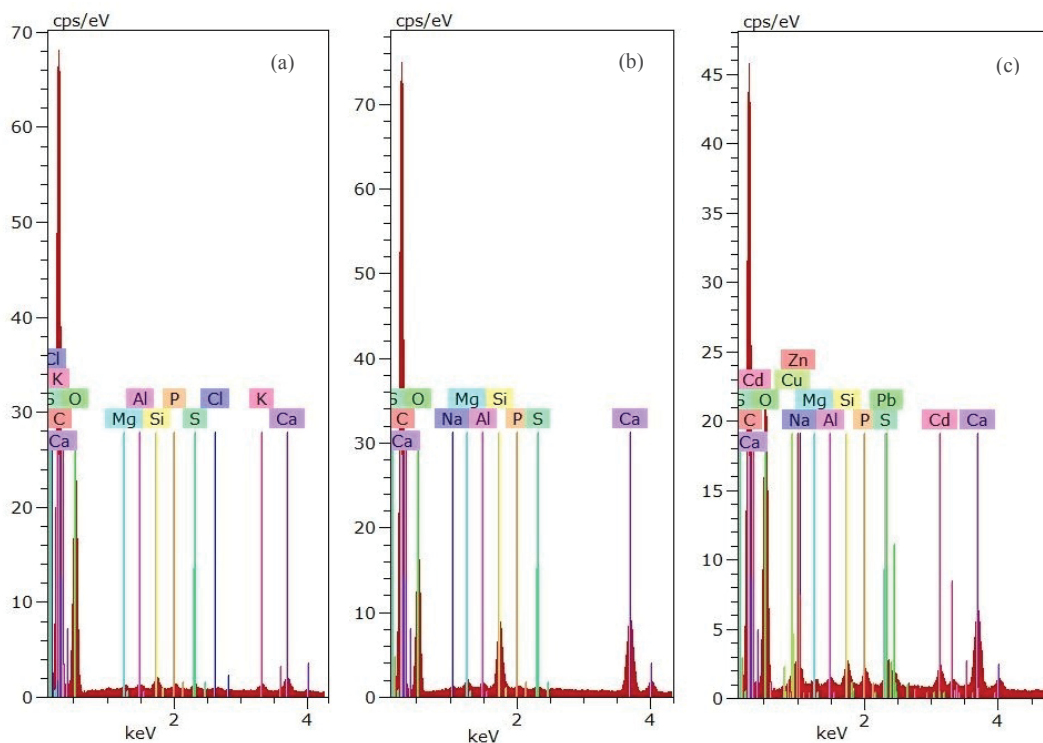
Figure 5.17 EDS spectra of (a) unmodified MMBB, (b) modified MMBB before biosorption and (c) modified MMBB after biosorption

The amount of adsorbed heavy metal ions and released alkali ions (Na^+, K^+, Mg^{2+} and Ca^{2+}) concentration (mg/L) is shown in Figure 5.18. Apparently, metal adsorption on biosorbent surface made Na^+, K^+, Mg^{2+} and Ca^{2+} ions release in aqueous medium. It confirmed the possibility of ion exchange mechanism in biosorption process by comparing total amount of adsorbed heavy metal ions (1.43 mmol/L) and released alkali ions (1.51 mmol/L) which were approximately

equal. SEM/EDS analysis confirmed that the variance in intensity of K, Na and Ca peaks might be due to ion exchange mechanism of metal uptake.
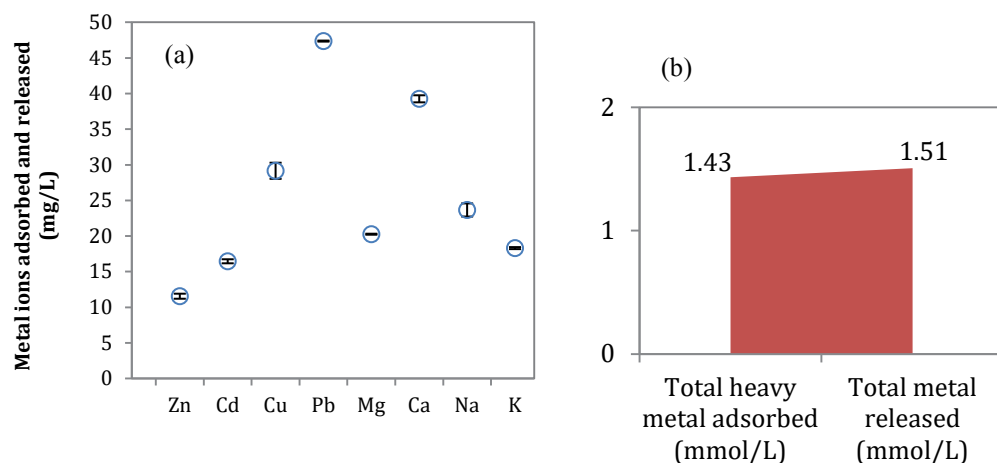
Figure 5.18 Comparison of (a) individual and (b) total metal ions adsorbed and released in biosorption process (Initial heavy metal conc.: 50 mg/L)

In addition, according to calculated B_{D-R} for Cd, Cu, Pb and Zn, E values show physical adsorption or ion exchange for four metal removal process whose calculated values are 2.58, 3.45, 5.59 and 2.73 kJ/mol for Cd, Cu, Pb and Zn respectively which are all less than 8 kJ/mol.

5.10   *Conclusions*

The results of this chapter show that modified MMBB may be efficiently used as a renewable biosorbent to remove Cd^{2+}, Cu^{2+}, Pb^{2+} and Zn^{2+} ions from aqueous solutions. As shown in FTIR studies, unmodified and modified MMBB have similar surface functional groups where by carboxylic acid groups involved in heavy metal binding. Modified MMBB revalues as an agricultural based biosorbent for heavy metal removal from a multi–component synthetic solution. In order to improve the biosorptive potential of MMBB, a solution containing sodium hydroxide, calcium chloride and ethanol were more effective than the other chemical and physical pretreatment. The maximum biosorption capacity calculated by Langmuir equation increased from 41.48 to 69.56 mg/g, 39.48 to 127.70 mg/g, 94.0 to

345.20 mg/g and 27.23 to 70.55 mg/g for Cd(II), Cu(II), Pb(II) and Zn(II), respectively when MMBB was chemically modified.

It was proven to have excellent desorption performance by metal desorption of 0.1M HCl for reutilization by following regeneration step with $CaCl_2$ in five cycles. SEM represents biosorbent surface remained coarsely porous to entrap the metal ions after five cycles of sorption/ desorption/ regeneration. Thermodynamic parameters revealed that heavy metal removal was spontaneous and feasible with negative Gibbs free energy and enthalpy changes for all metals.

Chapter 6

Heavy metal biosorption from synthetic wastewater by modified MMBB: column study

Chapter 6 Heavy metal biosorption from synthetic wastewater by modified MMBB: column study

A major part of Chapter 6 was published in the following paper:

6.1   *Research background*

Although numerous studies on biosorption of heavy metals in batch systems have been reported in the literature, in order to evaluate the feasibility of biosorption processes for real applications, continuous biosorption studies in packed bed columns would be more useful (Bhatnagar et al. 2015). In addition, a large volume of wastewater can be continuously treated using a defined quantity of adsorbent in the column. Reuse of biosorbent is also possible which makes the treatment process cheaper and more sustainable (Aksu et al., 2007)

6.2   *Objectives*

The biosorptive capacity of MMBB was investigated in term of biosorbent particle size, bed height, flow rate and inlet metal concentration in a fixed–bed column.

The general target of the present study was to develop a continuous heavy metal biosorption process in a fixed–bed column to investigate the applicability of MMBB in situations closer to reality. The specific objectives were investigating the effect of different operating variables (flow rate, bed depth, feed concentration, adsorbent particle size and influent pH) on the performance of MMBB packed bed column. The results were used to estimate the dynamic adsorption capacity and to examine the possibility of using common mathematical models (Thomas, Yoon–Nelson, Dose Response and Bed Depth Service time or BDST) for predicting the

breakthrough curves of heavy metal biosorption. Finally, the experimental data of lab–scale MMBB packed bed column was employed for sale–up calculations.

6.3 *Continuous biosorption experiments*

One of the most important factors in measuring the feasibility of a biosorbent in a real and practical application is the performance of biosorption process in a continuous fixed–bed column. In fact, the results from batch studies only present the biosorption equilibrium and kinetics (Shanmugaprakash and Sivakumar, 2015), therefore, in order to predict the performance of MMBB to remove Cd(II), Cu(II), Pb(II) and Zn(II) ions in the continuous mode, the experiments were carried out in a continuous reactor. The column internal radius was 22 mm and the height of 100 cm. The performance of the fixed–bed column was studied by varying the efficiency of the flow rate, influent concentration, pH, bed height and biosorbent particle size.

Based on the results obtained from batch studies, metal adsorption onto modified MMBB was strongly pH dependent and the optimum pH value was observed at 5.5±0.1. Thus in the continuous mode experiments, the pH value of the synthetic solution was adjusted to 5.5±0.1. The breakthrough curve showed the relative concentrations (C_t/C_i) on the y–axis versus time (t in min) on the x–axis. All the breakthrough curves followed the typical S–shape curve for column operation as the ratio of the effluent concentration at time t (C_t) to the influent concentration (C_i) versus time or throughput volume. The breakthrough curve's shape is determined by the shape of the equilibrium isotherm and any individual transport process can change it (Long et al., 2014). The most efficient adsorption performance will be obtained when the shape of the breakthrough curve is as sharp as possible (Chu, 2004). Results show that the adsorption of each metal ion onto the biomass surface strongly depended on the flow rate (Acheampong et al., 2013; Cruz–Olivares et al., 2013; Aksu et al., 2007). Initially each metal ion was rapidly adsorbed on the biomass due to the high availability of active sites. In consequence, the metal ions were captured around or inside the cells; meanwhile the effluent from the bottom of the bed was almost free of solute. As the solution continued to flow, due to the gradual occupancy of the available active sites, the

uptake became less effective and, accordingly, the outlet concentration started to increase until the saturation point was reached or at least until the outlet concentration was 90% of inlet concentration.

It is necessary to note that in a packed–bed column, channelling is often reported to be of great importance in process design despite there has been a shortage of theoretical and experimental works connected with channelling effects on column performance. However, it can be assumed that the wall effects play no role in adsorber performance in cases where cylindrical apparatus diameter to particulate biosorbent diameter ratio is greater than 20 (Saha et al., 2017; Tobis and Vortmeyer,1991; Tobis and Vortmeyer, 1988). Therefore the wall effect was assumed negligible in this column study.

6.3.1   Influence of flow rate

The breakthrough curves at three different flow rates (10, 20 and 30 mL/min) or HLR of 1.578, 3.156 and 4.734 m^3/m^2 hr are shown in Figure 6.1. The bed height was constant at 21 cm and the initial metal concentration at 20 mg/L. An increase in the flow rate reduced the volume of effluent treated before the bed became saturated and decreased the service time of the bed and vice versa. The slower flow rate provides more residence time for mass transfer into the pores, subsequently lets metals ions to access more active sites. Increasing the flow rate increased the steepness of the breakthrough curves. Also, the breakpoint time as well as saturation occurred faster with a higher flow rate. In other words, by increasing the flow rate the external film diffusion mass transfer resistance decreases, culminating in fast saturation and early breakthrough time. Moreover, with decrease in linear flow rate, the intra–particle diffusion becomes more effective due to longer residence time. An increase in the contact time between metal containing solution and the biosorbent in a packed–bed column at lower influent flow rates explained this result. The best performance was obtained at the lowest flow rate.

Generally, the column's removal efficiency fell when the flow rate increased, and the mass transfer zone decreased when the flow rate ebbed (Riazi et al., 2016). The

biosorption capacity in flow rate of 10 mL/min was 23.72, 43.32, 54.53 and 19.36 mg/g for Cd, Cu, Pb and Zn, respectively, which was higher than the other two flow rates of 20 and 30 mL/min. These findings agree with those documented in another study (Acheampong et al., 2013).

6.3.2   Influence of bed depth

Figure 6.2 presents the breakthrough curves of Cd(II), Cu(II), Pb(II) and Zn(II) biosorption onto MMBB obtained at various bed depths with a metal concentration of 20 mg/L and a constant flow rate of 10 mL/min (HLR = 1.578 m^3/m^2 hr). Three bed depths of 9.5, 21 and 31 cm, corresponding to 5, 10 and 15 g dry weight of MMBB, respectively, were investigated. The breakthrough curves (Figure 6.2) indicate that the breakthrough time and exhaustion (or saturation) time increased remarkably with an increase in bed depth from 9.5 to 31 cm. Breakthrough occurred at 77, 48, 32 and 45 min for 9.5 cm and 172, 180, 150 and 105 min for 31 cm bed height within Cd, Cu, Pb and Zn biosorption, respectively.

A Similar raising pattern can be obtained for saturation time. This was attributed to the more adsorbent specific surface and more available metal binding sites at higher bed height, which meant that consequently the total adsorbed metal ions increased. Moreover, an increase in the bed depth resulted in a wide mass transfer zone, which made the breakthrough curves moderately steeper.

In fact when the bed depth increased the diffusion mass transfer predominated in comparison with the axial dispersion phenomenon. For that reason, an enormous increase in the breakthrough time was observed. As Riazi et al. (2016) and Acheampong et al. (2013) reported for better performance of a fixed–bed column, the biosorbent's higher bed height would be more desirable if more active binding sites are to be provided.
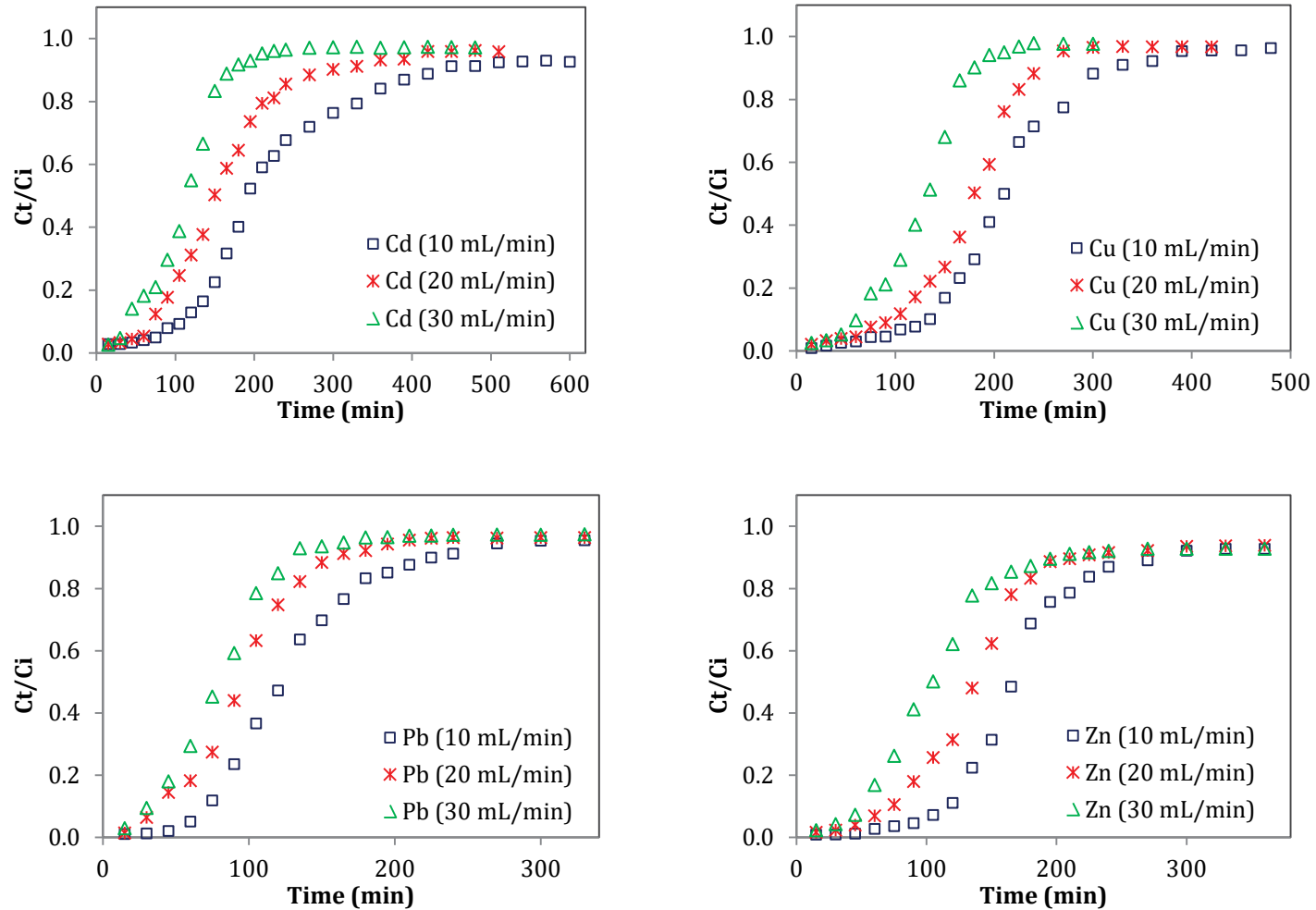
Figure 6.1 Effect of influent flow rate on the breakthrough curve of Cd, Cu, Pb and Zn adsorption onto modified MMBB (pH 5.5±0.1, bed height = 21 cm, influent metal concentration = 20 mg/L, particle size = 425–600 µm, room temperature)

6.3.3   Influence of inlet metal concentration

The Effect of initial concentration on the breakthrough curves is shown in Figure 6.3, using a bed depth of 21 cm at flow rate of 10 mL/min (HLR = 1.578 m^3/m^2 hr). The breakthrough curves of Cd^{2+}, Cu^{2+}, Pb^{2+} and Zn^{2+} were obtained from variations in the metal concentration in the column influent over time.

As can be seen in Figure 6.3 the shape and the gradient of the breakthrough curves changed significantly with an increase in metal concentration. The higher influent metal concentration resulted in the faster breakthrough and saturation and as a consequence the sharper breakthrough curves shifted to the left. This earlier exhaustion might be a result of two things: firstly the greater concentration gradient; and secondly, smaller mass transfer resistance at a higher metal concentration. The breakthrough times were 281.6, 279.2, 171.0 and 221.6 min for Cd, Cu, Pb and Zn, respectively using an influent metal concentration of 10 mg/L.

When the influent metal concentration increased to 30 mg/L, breakthrough took place in about 127.5, 158.3, 94.1 and 125 min for Cd, Cu, Pb and Zn, respectively. As presumed, an increase in inlet metal concentration (10 to 30 mg/L) gave an earlier saturation time from 510 to 225, 420 to 250, 277.5 to 165 and 430 to 195 for Cd, Cu, Pb and Zn, respectively.

These results demonstrated that the diffusion process of metal removal is highly concentration dependent (Bennani et al., 2015). Due to higher influent concentrations, higher driving force for mass transfer and also larger concentration gradient was expected.
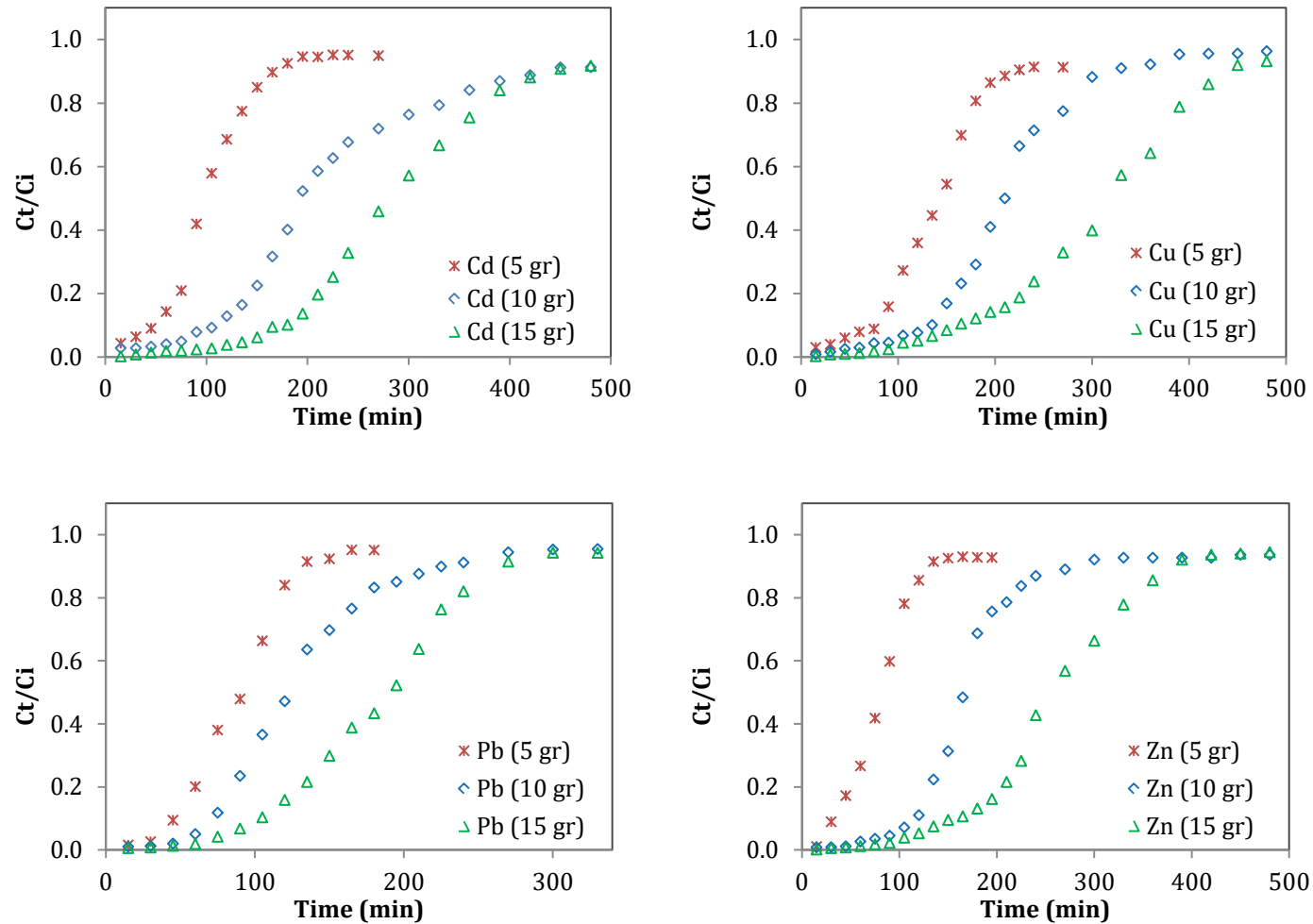
Figure 6.2 Effect of bed height (MMBB weight = 5, 10 and 15 gr) on the breakthrough curve of Cd, Cu, Pb and Zn adsorption onto modified MMBB (pH 5.5±0.1, influent flow rate = 10 mL/min or HLR = 1.578 m^3/m^2 hr, influent metal concentration = 20 mg/L, particle size = 425–600 μm, room temperature)

In addition, a decrease in the diffusion coefficient or mass transfer coefficient led to a lower concentration gradient and a slower mass transport of heavy metal ions from the film layer to the adsorbent's surface. These results confirmed that the change of initial concentration as a driving force affects the saturation rate, breakthrough time and adsorption zone length (Chen et al., 2012; Baral et al., 2009; Aksu et al., 2007). The dynamic adsorption capacities of cadmium, copper, lead and zinc was raised from 13.04, 28.90, 32.73 and 11.73 mg/g to 35.96, 47.51, 81.92 and 33.05mg/g respectively by elevating the inlet metal concentration from 10 to 30 mg/L.

6.3.4   Influence of biosorbent particle size

The other important parameter in a fixed–bed column with downward flow is the particle size distribution of packing materials. It is because of the handling and channelling problems during the operation which should be studied. As 425–600 μm was the most common particle size (Figure 5.2), the main physical characteristics of modified MMBB at this particle size were investigated. The particle density and bulk density of this particle size were 0.86 and 0.42 g/L, and a porosity of 80.26%. Thus MMBB possessed a low density but a high porosity and was appropriate for being applied in the packed bed column and continuous mode experiments.

Beside, according to the BET analysis, MMBB has a specific surface area of 1.3 m^2/g with an average pore diameter of 5.55 nm. The atomic and ionic radius of Cd, Cd^{2+}, Cu, Cu^{2+}, Pb, Pb^{2+}, Zn and Zn^{2+} is 152, 95, 128, 73, 175, 119, 137 and 74pm (1000pm = 1nm), respectively. Then the sorption process can take place on the surface and inside the pores.

In current work, the particle size of 300–425, 425–600 and 600–1000 μm were used for Cd, Cu, Pb and Zn removal. The bed depths corresponded to 10 g of MMBB were 17, 19.5 and 21 cm for 300–425, 425–600 and 600–1000 μm, respectively.
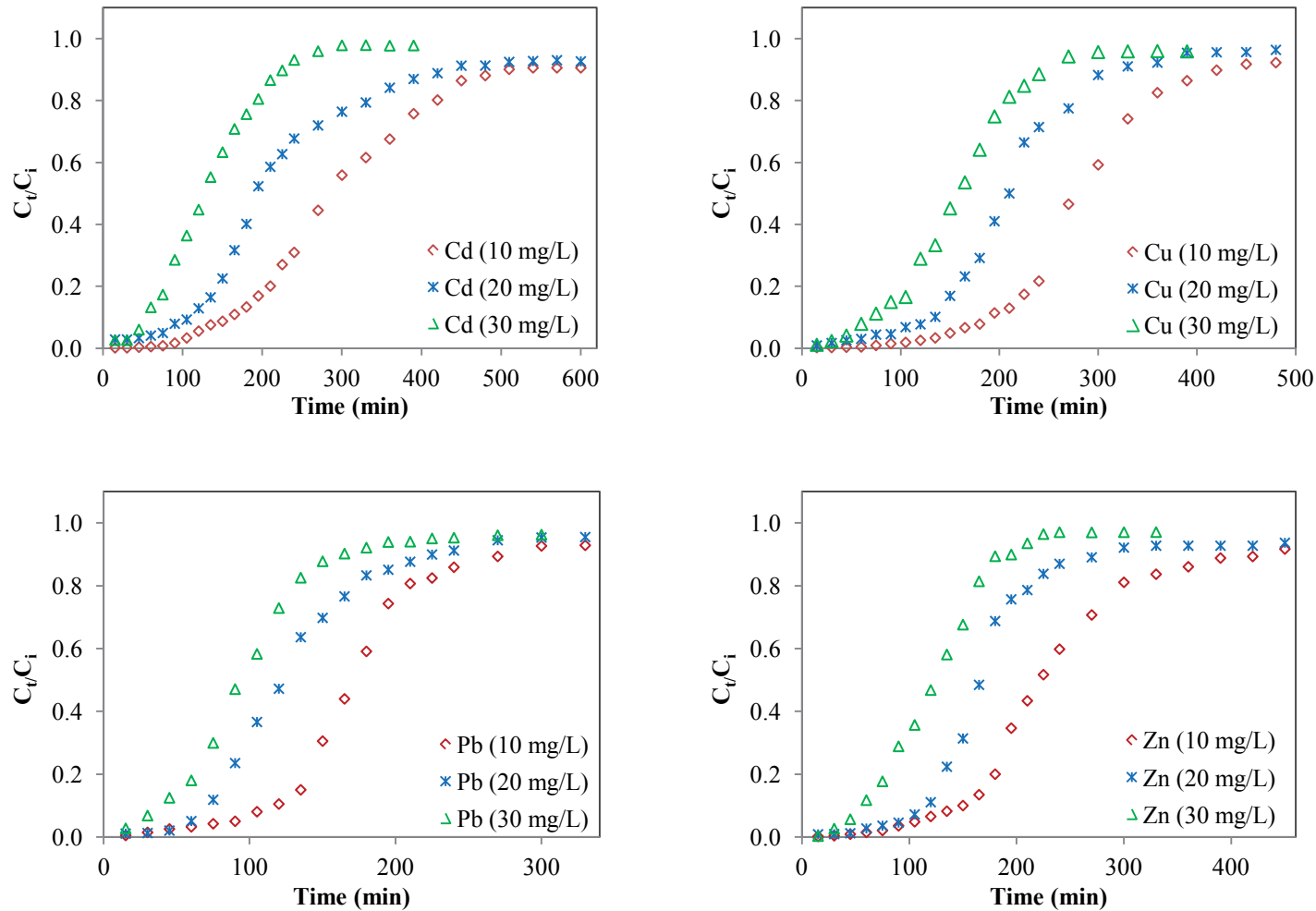
Figure 6.3 Effect of influent metal concentration on the breakthrough curve of Cd, Cu, Pb and Zn adsorption onto modified MBB (pH 5.5±0.1, bed height = 21 cm, influent flow rate = 10 L/min or HLR = 1.578 m^3/m^2 hr, particle size = 425–600 μm, room temperature)
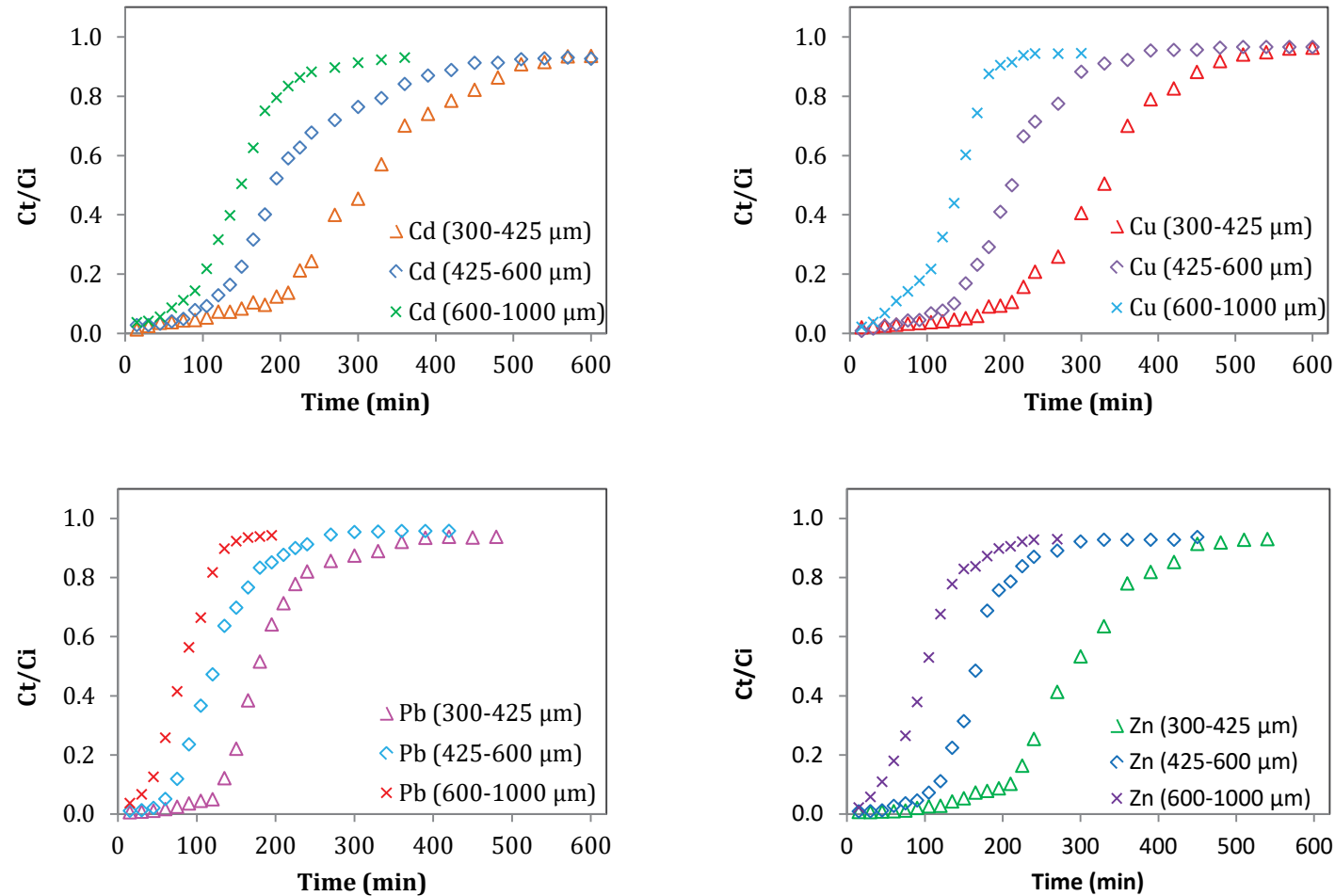
Figure 6.4 Effect of particle size on the breakthrough curve of Cd, Cu, Pb and Zn adsorption onto modified MMBB (pH 5.5±0.1, bed heights = 17, 19.5 cm and 21 cm, influent flow rate = 10 mL/min or HLR = 1.578 m^3/m^2 hr, influent metal concentration = 20 mg/L, room temperature)

The effect of biosorbent particle size on the shape of the breakthrough curves of cadmium, copper, lead and zinc on modified MMBB is illustrated in Figure 6.4. It is shown that the breakthrough time decreased with decreasing the biosorbent particle size for constant metal concentration of 20 mg/L. At larger particle size distribution, the breakthrough curves were dispersed and breakthrough took place slowly. As the biosorbent with smaller particle was packed in the column, sharper and steeper breakthrough curves and earlier breakthrough time were received from the experiments for all heavy metal ions.

These results demonstrate that the change in the particle size affects the saturation rate and breakthrough time in continuous mode while no significant change was seen in the batch biosorption process.

6.3.5   Influence of pH

As obtained from batch experiments, the pH of solution is one of important controlling factors in the heavy metal adsorption process; hence the synthetic solutions at different pH, namely 4.5 and 5.5 were monitored for observing the column behaviour in term of this parameter. Because of hydroxide formation of cadmium, copper, lead and zinc, the experiments were carried out within the acidic range.

The effect of influent pH value on cadmium, copper, lead and zinc removal by modified MMBB packed–bed column is presented in Figure 6.5. As can be seen, shorter breakthrough time or steeper breakthrough curve occurred at pH 4.5. The breakthrough time was about 81, 72, 51 and 85 min for Cd, Cu, Pb and Zn, respectively. Likewise, the exhaustion or saturation time took place faster at 322.5, 288, 150 and 210 min for Cd, Cu, Pb and Zn, respectively when influent pH remained at 4.5. Hence, higher pH value of the feed solution results in a more effective operation of the column or higher maximum metal adsorption capacity as well as longer breakthrough time. This result was in agreement with previous batch adsorption experiments as well as other studies (Christoforidis et al. 2015; Antunes et al., 2003).

6.4   ***Breakthrough curve modeling***

As Nur (2014) reported, a well–researched model can be used as a reliable solution to design, optimise and predict the breakthrough curves of fixed–bed columns because an appropriate numerical solution can help to reduce the number of experiments associated with new operating conditions. Table 6.1 listed the calculated parameters of Thomas, Yoon–Nelson and Dose Response models derived from the experimental data when initial influent concentration, flow rate and bed depth were varied. The best results for adsorption capacity were obtained at a flow rate of 10 mL/min and height of the bed of 31 cm.

All parameters and the models' correlation coefficient values were generated by MATLAB non–linear curve fitting tools. The correlation coefficient values indicate a proper agreement between the experimental data and column data generated using the models (Table 6.1).

From Table 6.1, for Thomas and Dose Response models the values of the calculated adsorption capacity increased as initial concentration rose. This is because at a higher concentration, mass transfer is enhanced due to the mass gradient's higher driving force, and led to an improvement in the adsorption capacity. Where external and internal mass diffusion steps are not the limiting steps, Thomas and Dose Response models are suitable for describing the adsorption processes (Cruz–Olivares et al., 2013). Moreover, the values of maximum biosorption capacities calculated from fitting the experimental data to Thomas and Dose Response models were also very similar.

The results showed that the Yoon–Nelson model less adequately matches the experimental data (the values of R^2). The time required to reach 50% of the retention decreases when the inlet concentration increased, due to rapid saturation in the higher concentration.
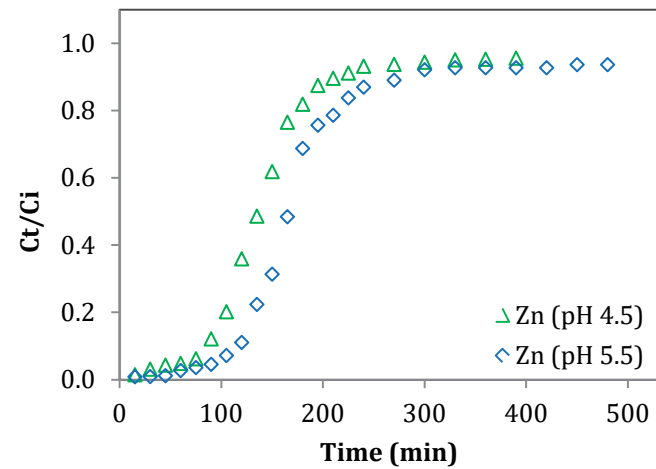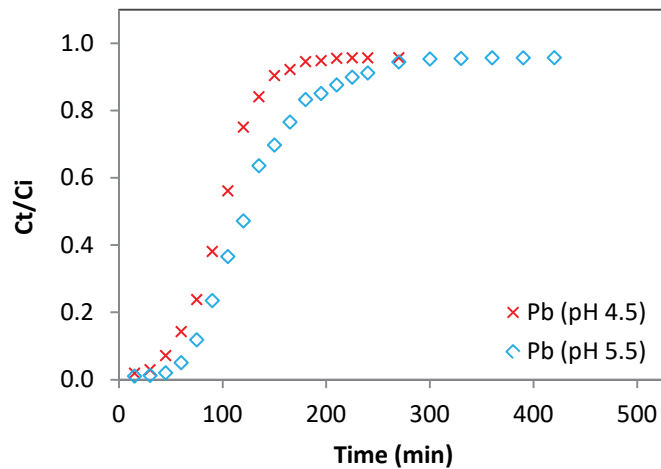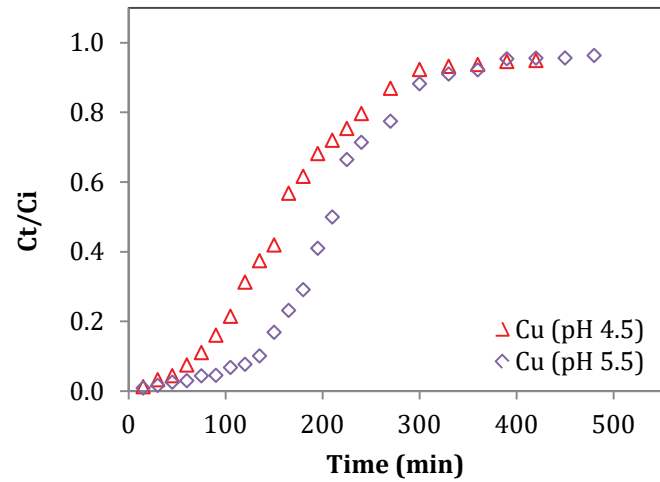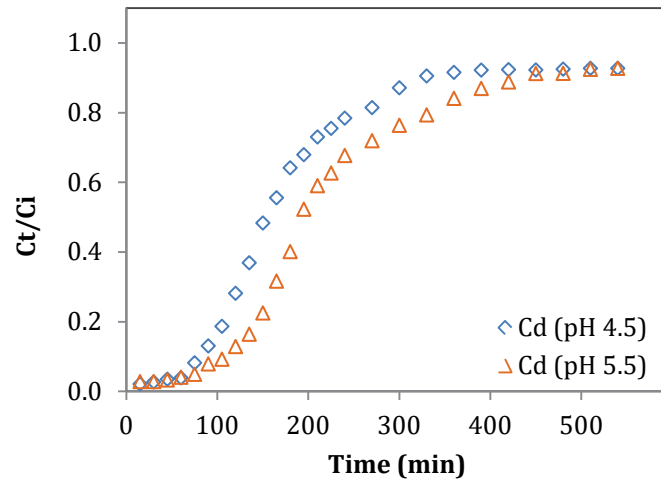
Figure 6.5 Effect of influent pH on the breakthrough curve of Cd, Cu, Pb and Zn adsorption onto modified MMBB (bed height = 21 cm, influent flow rate = 10 mL/min or HLR = 1.578 m³/m² hr, influent metal concentration = 20 mg/L, particle size = 425–600 μm, room temperature)

6.5   *Comparative study*

From Table 6.1, the highest metal adsorption capacities of modified MMBB at the exhaustion times were 38.25, 63.37, 108.12 and 35.23 mg/g for Cd, Cu, Pb and Zn, respectively. The maximum adsorption capacity values were achieved for a bed height of 31 cm, flow rate of 10 mL/min and initial metal concentration of 20 mg/L, particle size of 425–600 µm, and influent pH of 5.5. Biosorption capacity of Pb was the highest in comparison to those of other metals due to better affinity towards biosorbents. This phenomenon can be confirmed by calculating the Langmuir parameter of b_L representing this attraction. In addition, thermodynamic study revealed that except for zinc, calculated $\Delta S°$ values for cadmium, copper and lead were positive, reflecting the increased randomness at the solid/solution interface during sorption. It also indicates an affinity of the sorbent towards Cd, Cu and Pb ions. Biosorption capacities of some biosorbents with reference to Cd(II), Cu(II), Pb(II) and Zn(II) removal in a packed–bed column study are summarised in Table 6.2. As observed, the biosorption capacity of modified MMBB is comparable with the reported biosorption capacities. . It is, however, too difficult to conclude which adsorbent performed better since experimental operating conditions were completely different.

If behaviour in batch reactors is compared to performance in a fixed–bed column, maximum biosorption capacities of copper, lead and zinc which were calculated by Langmuir and Thomas models, respectively were higher when biosorption process was carried out in a fixed–bed column with the same conditions. According to Gupta et al. (2004) a higher column capacity can result from a large concentration gradient continuously present at the interface zone as the metal solution passes through the column, whereas the concentration gradient decreases with time in batch experiments. However, shorter contact time because of high influent flow rate through a column might cause less biosorption efficiency in continuous mode. In this study, the initial metal concentration changed in the batch experiments from 1 to 500 mg/L while in the column, the influent metal concentration did not exceed 30 mg/L. As a result, the maximum biosorption capacities calculated by Langmuir and Thomas cannot indicate any rational comparison in this regard.

Table 6.1 Thomas, Yoon–Nelson and Dose Response model constants for Cd, Cu, Pb and Zn adsorption onto modified MMBB column (pH 5.5±0.1, particle size = 425–600 μm, room temperature)

Metal	Conditions				Thomas			Yoon–Nelson			Dose Response		
	Q	Bed height	C_i	q	k_{Th}	q_{Th}	R^2	k_{Y-N}	τ	R^2	a	q_{D-R}	R^2
Cd	10	21	20	23.72	0.485	23.66	0.991	0.016	210.7	0.971	3.128	23.53	0.989
	20	21	20	12.43	0.572	12.36	0.998	0.023	155.2	0.987	3.271	11.95	0.991
	30	21	20	4.55	0.768	4.52	0.994	0.034	127.8	0.993	4.393	4.46	0.988
	10	21	10	13.04	1.358	13.03	0.999	0.027	282.4	0.986	3.768	12.81	0.988
	10	21	30	35.96	0.483	35.93	0.996	0.025	130.9	0.996	3.265	34.74	0.985
	10	9.5	20	14.10	1.921	14.03	0.992	0.038	101.6	0.987	3.941	13.61	0.984
	10	31	20	38.25	0.238	38.07	0.994	0.029	283.2	0.990	4.575	37.76	0.989
Cu	10	21	20	43.32	0.615	43.18	0.994	0.025	210.6	0.991	4.962	42.43	0.991
	20	21	20	24.30	0.751	24.23	0.996	0.029	178.6	0.992	5.334	24.03	0.990
	30	21	20	14.42	1.191	14.38	0.995	0.036	128.0	0.994	5.328	14.14	0.989
	10	21	10	28.90	2.123	28.88	0.999	0.033	279.5	0.985	5.656	28.38	0.993
	10	21	30	47.51	0.879	47.46	0.997	0.026	158.2	0.997	4.081	46.99	0.993
	10	9.5	20	28.25	1.525	28.03	0.992	0.034	142.7	0.985	4.222	27.26	0.990
	10	31	20	63.37	0.773	63.14	0.991	0.038	321.7	0.988	4.668	63.27	0.992
Pb	10	21	20	54.53	0.749	54.48	0.996	0.032	126.1	0.985	3.739	54.25	0.995

Metal	Conditions				Thomas			Yoon–Nelson			Dose Response		
	Q	Bed height	C_i	q	k_{Th}	q_{Th}	R^2	k_{Y-N}	τ	R^2	a	q_{D-R}	R^2
	20	21	20	27.74	0.988	27.64	0.993	0.039	95.9	0.989	3.686	26.91	0.991
	30	21	20	12.67	1.549	12.54	0.994	0.045	79.9	0.993	3.543	11.78	0.991
	10	21	10	32.73	0.871	32.61	0.995	0.032	174.1	0.986	5.722	32.41	0.992
	10	21	30	81.92	0.168	81.87	0.992	0.037	196.2	0.991	5.799	81.19	0.990
	10	9.5	20	19.02	2.36	17.88	0.992	0.047	89.4	0.984	4.074	17.84	0.992
	10	31	20	108.12	0.295	107.27	0.991	0.026	186.3	0.990	4.418	103.64	0.989
Zn	10	21	20	19.36	0.542	19.18	0.993	0.033	178.6	0.982	5.572	19.24	0.987
	20	21	20	10.95	0.855	10.89	0.998	0.034	136.7	0.986	4.431	10.33	0.988
	30	21	20	3.68	1.710	3.50	0.993	0.032	105.9	0.972	3.134	3.60	0.987
	10	21	10	11.73	1.684	11.56	0.993	0.035	218.6	0.984	4.401	11.54	0.991
	10	21	30	33.05	0.068	32.93	0.997	0.032	123.1	0.987	3.905	32.47	0.992
	10	9.5	20	16.32	2.263	16.25	0.997	0.045	81.23	0.985	3.492	15.55	0.989
	10	31	20	35.23	0.153	35.15	0.995	0.041	256.3	0.989	5.132	34.79	0.987

Notation: bed depth (cm); Q, flow rate (mL/min); C_i, influent metal concentration (mg/L); q, adsorption capacity (mg/g); k_{Th}, Thomas model rate constant (mL/mg min), q_{Th}, Thomas sorption capacity (mg/g); k_{Y-N}, Yoon–Nelson model rate constant (1/min); τ, the time required for 50% breakthrough (min), a is a constant and q_{D-R} is Dose Response model adsorption capacity of heavy metal ions (mg/g)
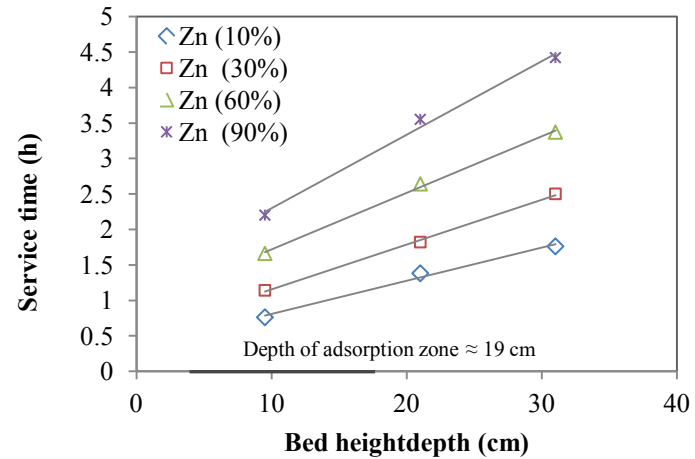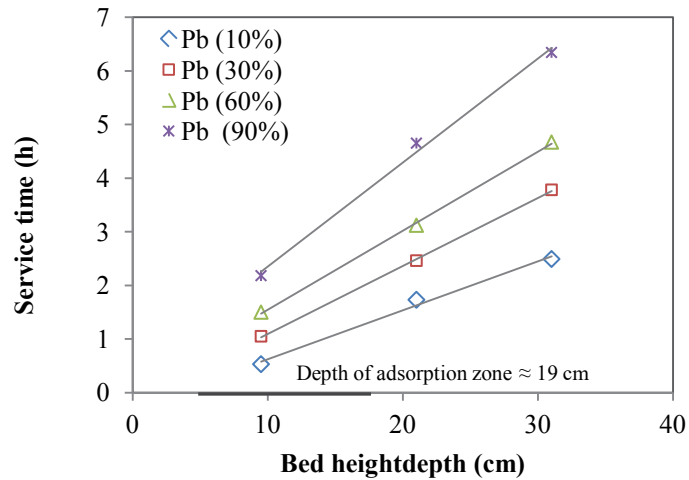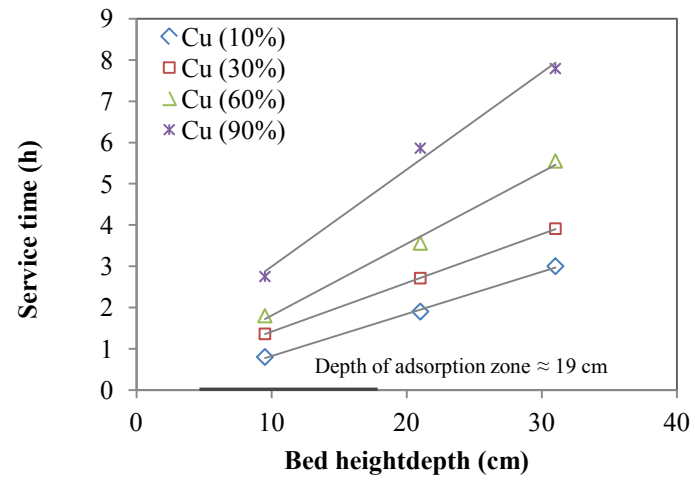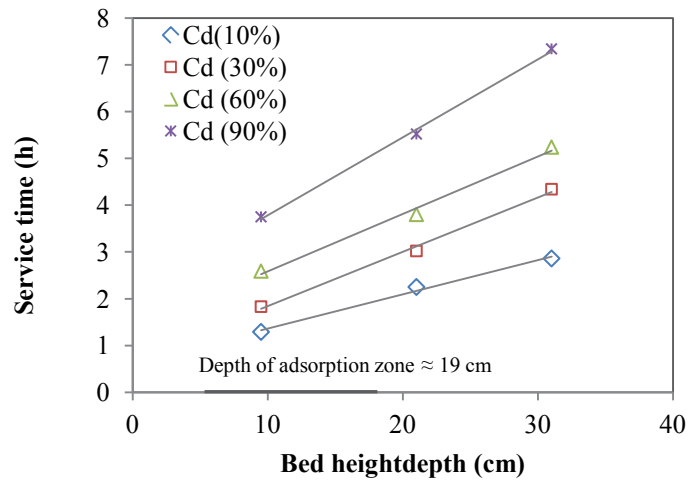
Figure 6.6 BDST model of different MMBB weight = 5, 10 and 15 g (9.5, 21 and 31 cm) (pH 5.5±0.1, influent flow rate = 10 mL/min, influent metal concentration = 20 mg/L, particle size = 425–600 μm, room temperature)

Table 6.2 Dynamic adsorption capacity of cadmium, copper, lead and zinc onto different adsorbents

Adsorbent/adsorbate	C_i (mg/L)	Bed depth (cm)	Q (mL/min)	q_{Th} (mg/g)	q_{exp} (mg/g)	Reference
Pongamia oil cake /Zn	100	15	5	49.7	84.2	Shanmugaprakash and Sivakumar, 2015
Citrus Maxima peel/Cd	300	2	3	144	–	Chao et al., 2014
Citrus Maxima peel/Cu	300	2	3	98.1	–	Chao et al., 2014
Citrus Maxima peel/Pb	300	2	3	173	–	Chao et al., 2014
Passion fruit shell/Cd	300	2	3	55.8	–	Chao et al., 2014
Passion fruit shell /Cu	300	2	3	36.3	–	Chao et al., 2014
Passion fruit shell /Pb	300	2	3	59.4	–	Chao et al., 2014
Sugarcane bagasse/Cd	300	2	3	26.7	–	Chao et al., 2014
Sugarcane bagasse /Cu	300	2	3	22.2	–	Chao et al., 2014
Sugarcane bagasse /Pb	300	2	3	31.8	–	Chao et al., 2014
Agaricus bisporus/Pb	35	2	3	67.7	67	Long et al., 2014
Allspice residue/ Pb	15	15	20	14.3	16.2	Cruz–Olivares et al., 2013
Allspice residue/ Pb	25	15	20	13.4	15.9	Cruz–Olivares et al., 2013
Sunflower waste/Cd	10	30	1	–	23.6	Jain et al., 2013
Coconut shell/Cu	10	20	10	53.5	7.2	Acheampong et al., 2013
Wheat straw/Cd	100	50	300	12.13	16.9	Muhamad et al., 2010

Table 6.3 Parameters predicted from the BDST model for biosorption of Cd, Cu, Pb and Zn on MMBB (5, 10 and 15 g or 9.5, 21 and 31 cm) in a fixed–bed column

	Breakpoint (%)	Slope (hr/cm)	Intercept (hr)	N_{BDST} (mg/L)	K_{BDST} (L/mg h)	MTZ (cm)	$L_{critical}$ (cm)	R^2
Cd	10	0.073	0.631	51.63	0.167	6.23	8.64	0.992
	30	0.09	0.676	63.65	0.060	12.44		0.995
	60	0.102	1.359	72.14	0.014	18.92		0.991
Cu	10	0.102	–0.194	74.39	0.528	6.74	1.90	0.998
	30	0.118	0.229	86.06	0.172	14.19		0.999
	60	0.153	0.072	111.59	0.262	19.06		0.994
Pb	10	0.091	–0.292	66.99	0.347	7.19	3.21	0.992
	30	0.126	0.17	92.75	0.230	13.19		0.999
	60	0.147	0.077	108.21	0.243	18.82		0.999
Zn	10	0.046	0.342	32.00	0.314	6.22	7.43	0.993
	30	0.063	0.525	43.83	0.079	12.84		0.998
	60	0.079	0.923	54.96	0.021	18.66		0.998

While on the subject, taking into consideration the results from Table 6.1 and the parameters influencing metal adsorption in a fixed–bed column as discussed previously (Sections 6.3.1–6.3.5), the optimal conditions for all heavy metal ions were obtained at flow rate of 10 mL/min or HLR of 1.578 m^3/m^2 hr, bed depth of 31 cm and inlet metal concentration of 20 mg/L.

6.6 *Scale–up study*

Iso–concentration lines for removing Cd, Cu, Pb and Zn ions in a fixed–bed at C_t/C_i= 10%, 30%, 60% and 90% were determined (Figure 6.6).

As presented in Table 6.3, a consistent increase in slopes and a subsequent increase in the corresponding dynamic sorption capacity, N_{BDST}, were observed for C_t/C_i ratios of 10–90%. Apart from this, the rate constant, k_{BDST}, outlined the rate of solute transfer from the fluid phase to the solid phase.

The k_{BDST} value declined at higher C_t/C_i ratio due to progressive binding sites saturation during heavy metal removal. Moreover, at 50% breakthrough, C_t/C_i = 2,

therefore reducing the logarithmic term of the BDST equation to zero with a good correlation coefficient suggested the BDST model's conformity with the sorption of Cd, Cu, Pb and Zn by modified MMBB. The critical bed depth, $L_{critical}$, is calculated by setting t = 0 and $C_t = C_b$. The critical bed depths of Cd, Cu, Pb and Zn adsorption were 8.64, 1.90, 3.21 and 7.43 cm, respectively.

This value presents the minimum theoretical bed height of the adsorbent in a packed–bed column which is sufficient such that the effluent concentration at t = 0 will not exceed the breakthrough concentration, C_b. In addition, the calculated depth of the adsorption zone for all metals was about 19 cm and the Empty Bed Contact Time (EBCT) was 8.0 min.

The data obtained from laboratory and pilot scale is used as the basis for the designing a full or industrial scale adsorption column. One of the most important design parameters is bed depth for a specific adsorption service time.

6.6.1   Column Scale–up calculation

According to scale–up principles that Okochi reported (2013), the column adsorption system can be easily scaled–up to pilot–scale and then to full industrial–scale by using the data obtained from lab–scale column. As a matter of fact, the similarity in mass transfer and hydrodynamic features between the lab–scale column and the pilot–scale column makes similar breakthrough curves. It can be assumed because there is no change in the boundary conditions, dimensionless parameters and mechanisms when the size of the system changes. The scale–up does not affect some dynamic parameters of adsorption system such as empty bed contact time (EBCT) and also superficial velocity (Ohura et al., 2011; Nguyen, 2015). On the other hand, the ratio of the internal diameter to the bed depth remains constant while the column size increases. BDST model parameters can be helpful for developing an applicable heavy metal biosorption process in larger scale. Based on the scale–up principles, the design parameters for a pilot–scale column are listed in Table 6.4.

Estimate superficial velocity for the pilot–scale column;

Note: LC goes for lab–scale column and PC for pilot–scale column.

$$v_{LC} = v_{PC} = \frac{Q_{LC}}{A_{LC}} = \frac{10 \text{ cm3/min}}{3.80 \text{ cm2}} = 2.63 \text{ cm/min} = 1.578 \text{ m}^3/\text{m}^2 \text{ hr}$$

$\rightarrow v_{PC} = 2.63 \text{ cm/min} = 1.578 \text{ m}^3/\text{m}^2 \text{ hr}$

Estimate bed depth for the pilot–scale column;

$$\frac{D_{LC}}{H_{LC}} = \frac{D_{LC}}{H_{LC}} \rightarrow H_{PC} = \frac{H_{LC}}{D_{LC}} \times D_{PC} = \frac{21}{2.2} \times 5 = 47.72 \text{ cm}$$

$\rightarrow H_{PC} = 47.72 \text{ cm}$

Estimate bed volume for the pilot–scale column;

$$V_{EPC} = A_{PC} \times H_{PC} = \pi \times (\frac{5}{2})^2 \times 47.72 = 937.12 \text{ cm}^3$$

$\rightarrow V_{EPC} = 937.12 \text{ cm}^3$

Estimate biosorbent amount for the pilot–scale column;

$$d_{PC} = \frac{m_{PC}}{V_{PC}}, \ m_{PC} = V_{PC} \times d_{PC} = V_{PC} \times d_{LC} = V_{PC} \times \frac{m_{LC}}{V_{LC}} = 937.12 \text{cm}^3 \times 0.42 \frac{g}{\text{cm}^3} = 393.6 \text{ g}$$

$\rightarrow m_{PC} = 393.6 \text{ g}$

Estimate volumetric flow rate for the pilot–scale column;

$$v_{PC} = \frac{Q_{PC}}{A_{PC}}, \ Q_{PC} = v_{PC} \times A_{PC} = 2.63 \times \pi \times 2.5^2 = 51.64 \text{ cm}^3/\text{min} = 3.09 \text{ L/hr}$$

$\rightarrow Q_{PC} = 3.09 \text{ L/hr}$

Estimate empty bed contact time (EBCT) for the pilot–scale column;

$$EBCT_{PC} = \frac{H_{PC}}{v_{PC}} = 47.72 \div 2.63 = 18.14 \text{ min}$$

$\rightarrow EBCT_{PC} = 18.14 \text{ min}$

Estimate service time at 10% breakthrough for the pilot–scale column;

From $\frac{C}{C_i} = \frac{1}{1+\exp\left[k_{BDST}C_i\left(\frac{N_{BDST}}{C_i v}L-t\right)\right]}$; $t_{PC} = \frac{H_{PC} \times N_{BDST}}{C_i \times v_{PC}} - \frac{1}{K_{BDST} \times C_i}\ln\left(\frac{C_i}{C_b}-1\right)$

$\rightarrow t_{PC,Cd}$ = 46.2 h

$\rightarrow t_{PC,Cu}$ = 67.3 h

$\rightarrow t_{PC,Pb}$ = 60.5 h

$\rightarrow t_{PC,Zn}$ = 28.6 h

N_{BDST} and K_{BDST} are recalled from Table 6.3 for cadmium, copper, lead and zinc at 10% breakthrough.

Estimate the volume of treated water at 10% breakthrough for the pilot–scale column;

$V_{WPC} = Q_{PC} \times t_{PC} = 3.09 \times t_{PC}$ (for each metal ion)

$\rightarrow V_{WPC,Cd}$ = 142.4 L

$\rightarrow V_{WPC,Cu}$ = 207.9 L

$\rightarrow V_{WPC,Pb}$ = 186.8 L

$\rightarrow V_{WPC,Zn}$ = 88.5 L

Estimate biosorbent exhaustion rate for the pilot–scale column;

$AER = \frac{m_{PC}}{V_{WPC}} = \frac{393.6}{V_{WPC}}$ (for each metal ion)

$\rightarrow AER_{Cd}$ = 2.76 g/L

$\rightarrow AER_{Cu}$ = 1.89 g/L

$\rightarrow AER_{Pb}$ = 2.11 g/L

$\rightarrow AER_{Zn}$ = 4.44 g/L

Table 6.4 Proposed pilot–scale column parameters

Parameters	Lab–scale column	Pilot–scale column	Scale–up ratio
Column design criteria			
Inner diameter, D_i (cm)	2.2	5.0	0.44
Column area, A (cm²)	3.80	19.63	0.19
Biosorbent weight, m (g)	10	337.36	0.03
Operation conditions			
Influent concentration, C_i (mg/L)	20	20	1
Superficial velocity, v (m³/m² hr) [a]	1.578	1.578	1
Volumetric flow rate, Q (L/hr)	0.6	3.09	0.19
Empty bed contact time, EBCT (min)	8.0	18.1	0.44
Service time, t_b (hr) [b,c]	2.25, 1.9, 1.38 and 1.73	46.2, 67.3, 60.5 and 28.6	0.05, 0.03, 0.02 and 0.06
Treated water volume, $V_{W,b}$ (L) [b,c]	1.35, 1.15, 0.83 and 1.04	142.4, 207.9, 186.8 and 88.5	9.5, 5.5, 4.4 and 11.7 [d]
Adsorbent exhaustion rate, AER (g/L) [c]	7.41, 8.70, 12.05 and 9.61	2.76, 1.89, 2.11 and 4.44	2.7, 4.6, 5.7 and 2.2

[a] Hydraulic Loading Rate (HLR = Q/A)

[b] Service time and treated water volume were calculated at 10% breakthrough.

[c] For Cd, Cu, Pb and Zn, respectively

[d] (Scale–up ratio for Cd, Cu, Pb and Zn) ×10³

6.7 *Conclusions*

The effect of column design parameters, such as flow rate, inlet metal concentration, bed depth, biosorbent particle size distribution and influent pH was examined. The results revealed that lower flow rate, higher bed depth, smaller feed concentration, smaller particle size and lower influent pH facilitated the adsorption performance of the column, which was evidenced by longer service time and higher treated volume. The highest dynamic adsorption capacity of modified MMBB for Cd, Cu, Pb and Zn was obtained at flow rate of 10 mL/min, bed depth of 31 cm, pH 5.5±0.1, MMBB particle size of 425–600 and inlet metal concentration of 20 mg/L (Table 6.1) from Synthetic solution. The highest metal adsorption capacity of modified MMBB at the exhaustion time was 38.25, 63.37, 108.12 and 35.23 mg/g for Cd, Cu, Pb and Zn, respectively.

Although all of the predictive models explained the dynamic behaviour of the breakthrough curves fairly well, the Thomas model strongly correlated the experimental data, as deduced from the statistical calculated parameters (i.e. $R^2 > 0.99$). Furthermore, the BDST model fitted well the experimental data ($R^2 > 0.99$) and successfully described the linear relationship between bed depth and column service time. The depth of adsorption was predicted accurately about 19 cm by the BDST model. Besides, this model was applied for column scale–up calculation from a mini lab–scale column to a pilot–scale one. The competitively high values of column capacity and the low cost of these biosorbents make this new multi–metal binding biosorbent a better choice for continuous treatment of effluents polluted with heavy metal ions.

Chapter 7

Application of modified MMBB for real wastewater and desorption study

Chapter 7 Application of modified MMBB for real wastewater and desorption study

    7.1   *Objectives*

The purpose of the biosorption process is to remove pollutants from industrial wastewater effluents which regularly contain other anions and cations rather than specified heavy metal ions. For this reason, continuous biosorption process experiments were also done under identical experimental conditions utilising a semi–simulated real wastewater as the column feed. Desorption, regeneration and reuse properties of MMBB packed bed column were evaluated by selected desorbing and regenerating agents from batch studies.

    7.2   *Applicability of modified MMBB packed–bed column in treating a real wastewater*

As mentioned before, the real wastewater used in this study was the primary effluent, downstream of the Malabar WWTP sedimentation tanks collected from Sydney Water plant, NSW, Australia. Prior to the adsorption test, the sewage was settled for 24 hr, filtered using a 150 μm sieve, and used for column adsorption tests without any pH alterations.

The municipal wastewater was collected from Sydney Water was not contaminated by Cd, Cu, Pb and Zn, and therefore an appropriate amount of metallic nitrate salts was added to provide the desired initial concentrations of 20 mg/L of each metal ion. The pH of this semi–simulated real wastewater was 5.9±0.1 (above the optimal pH) and no change in pH value was required for the actual application of modified MMBB in a fixed–bed column.

The municipal wastewater composition was determined as follows: pH 7.37±0.1, salinity 0.45%, turbidity 83.5 NTUs, electrical conductivity 863 μS/cm, total dissolved solids (TDS) 567 mg/L, total suspended solids (TSS) 97 mg/L, ammonium 62 mg/L, nitrate 3.45 mg/L, orthophosphate 5.4 mg/L, total organic carbon (TOC) 21.55 mg/L, chemical oxygen demand (COD) 246 mg/L, chloride 118.32 mg/L, calcium 28.62 mg/L, magnesium 9.67 mg/L, iron 0.29 mg/L, copper

0.2 mg/L, lead 0.35 mg/L, manganese 0.05 mg/L, nickel 0.03 mg/L, also zinc and cadmium were undetectable. Obviously, the concentration of heavy metals was negligible in municipal wastewater. Hence an appropriate amount of metallic nitrate salts were added to provide the desired initial concentrations of 20 mg/L of each metal ion. The concentrations of Cd, Cu, Pb and Zn and major quality parameters of the solutions before and after passing through the column were determined according to standard procedures. All the laboratory experiments were conducted in accordance with national and institutional guidelines for the protection of human subjects and animal welfare.

The results presented in Figure 7.1 indicate that the modified MMBB packed–bed column removed more than 90% of Cd(II), Cu(II), Pb(II) and Zn(II) ions from 3227, 2617, 1714 and 2019 mL municipal wastewater in 322, 261, 171 and 201 minutes, respectively. From Figure 7.1, the breakthrough time and the dynamic biosorption capacity of cadmium, copper, lead and zinc eliminated from the municipal wastewater were quite similar to those from the synthetic solution. Moreover, by using a column packed with only 10 g of modified MMBB, the levels of copper, lead and zinc concentrations in the effluent were within the recommended standard discharge limit of heavy metal ions (about 5, 10 and 10 mg/L, respectively).

Cadmium has been identified as the major heavy metal of concern which needs to be remediated using another treatment method. As a result of successful metal removal by modified MMBB column, the effect of co–existing ions in the municipal wastewater on the continuous adsorption process could be negligible. It is also proven that modified MMBB can remove heavy metal ions from real municipal wastewater in the dynamic adsorption system as a final remark. However, if behaviour in batch reactors is compared to performance in a fixed–bed column utilising the same operating conditions, biosorption capacities of copper and lead are higher when the biosorption process is carried out in a fixed–bed column. According to Gupta et al. (2004), because a large concentration gradient continuously presents at the interface zone as the metal solution passes through the column, a higher column capacity can be obtained whereas the concentration gradient decreases with time in batch experiments.

### 7.3   *Continuous sorption and desorption experiments*

Regeneration of metal–loaded adsorbent, subsequent reuse of the biosorbent and recovery of adsorbate(If possible) would make the wastewater treatment process economically feasible, reasonable and sustainable (Jain et al., 2013; Naddafi et al., 2007). The main factors for choosing suitable eluents and regenerating agents are the type of biosorbent and the biosorption mechanism (Bhatnagar et al., 2015).

In batch studies, desorption of Cd, Cu, Pb and Zn ions was evaluated by applying different desorbing agents and the best eluent was hydrochloric acid The results showed that 0.1 M HCl was noted to most effectively desorbed 96.33%, 99.93%, 76.26% and 91.93% respectively for cadmium, copper, lead and zinc. The spent adsorbent was regenerated by 1 M $CaCl_2$.

 Calcium chloride can increase the stability and reusability of MMBB and repairing the damage caused by the desorbing agents. It can also remove the excess protons after each elution and thereby provide new binding sites. This observed mechanical stability and stiffness of the modified MMBB make it suitable for fixed–bed column applications. Thus the reusability of modified MMBB for removing heavy metal from real wastewater was conducted using 0.1 M HCl (10 mL/min) within three successive cycles of alternating sorption and desorption in a continuous system , supplemented by a solution of cadmium, copper, lead and zinc. The influent concentration of each metal was adjusted to 20 mg/L for each metal.

The desorption of Cd(II), Cu(II), Pb(II) and Zn(II) from loaded modified MMBB took place rapidly. Actually the breakthrough curves of these three cycles showed no tangible change for three adsorption times especially in the first three cycles. A negligible loss in bed height and mass of modified MMBB was observed after three cycles, and the obtained results for biosorption and desorption are presented in Figure 7.2 and Figure 7.3.

For the first adsorption step, the breakthrough of Cd(II), Cu(II), Pb(II) and Zn(II) was 82.4, 75, 51.6 and 83.8 min, while the exhaustion taking place at 423, 261.7, 171.4 and 201.7 min, respectively.
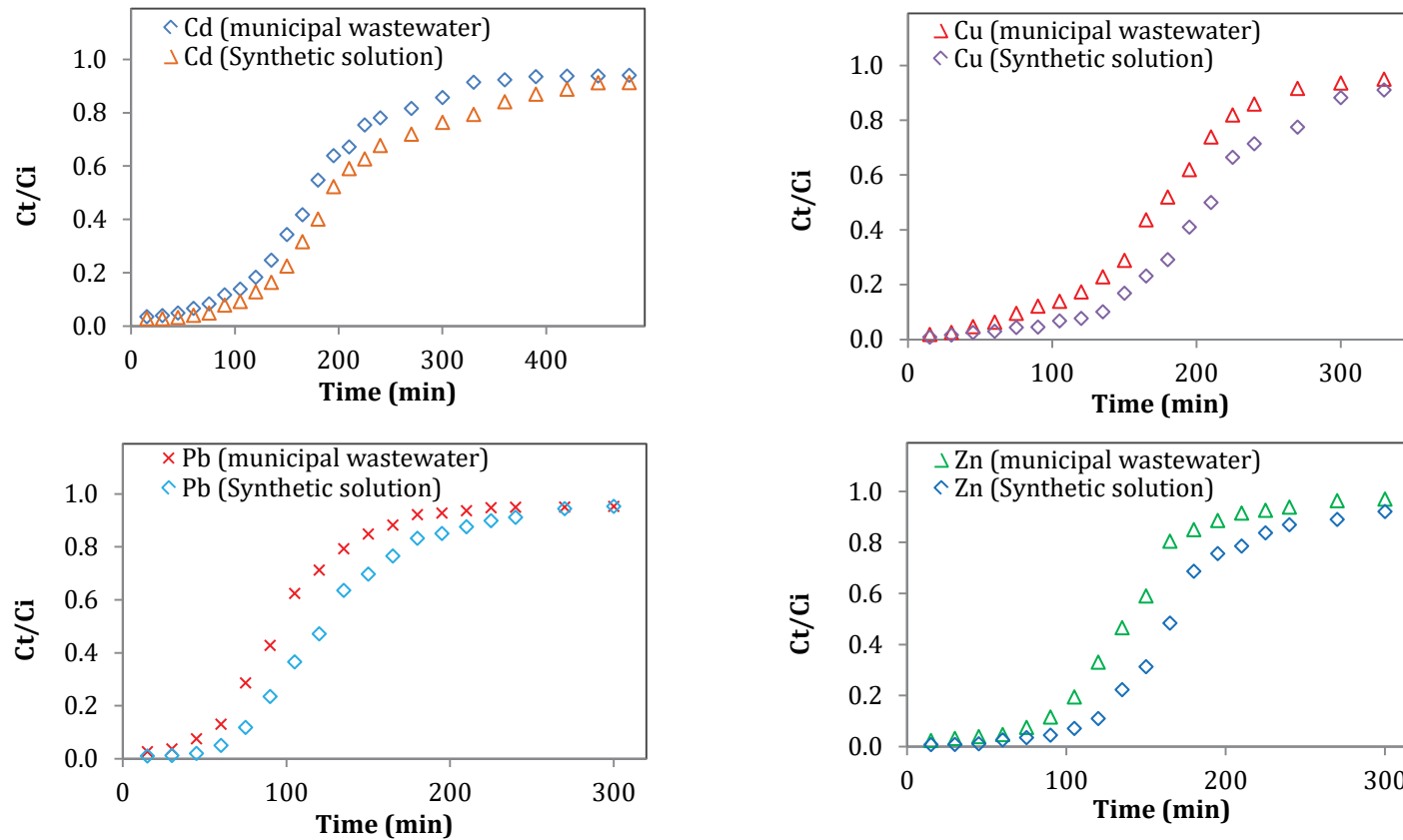
Figure 7.1 Breakthrough curves of Cd, Cu, Pb and Zn adsorption onto modified MMBB from synthetic and real municipal wastewater (bed height = 21 cm, influent flow rate = 10 mL/min or HLR = 1.578 m^3/m^2 hr, influent each metal concentration = 20 mg/L, particle size = 425–600 μm, room temperature)
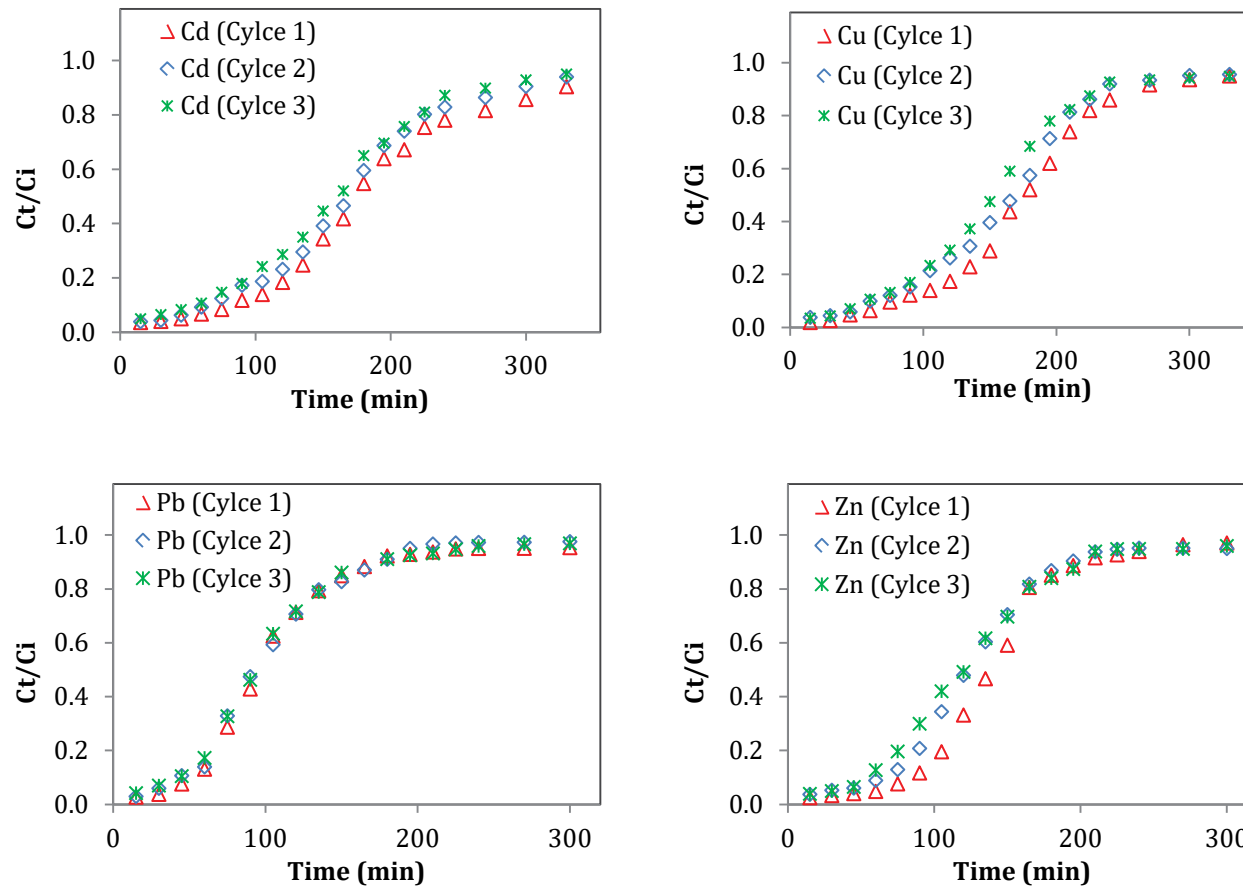
Figure 7.2 Breakthrough curves for Cd, Cu, Pb and Zn adsorption from municipal wastewater by modified MMBB in three cycles of sorption/ desorption/ regeneration (pH 5.5±0.1, bed height = 21 cm, flow rate = 10 mL/min or HLR = 1.578 m³/m² hr, influent metal concentration = 20 mg/L, particle size = 425–600 µm, room temperature)

For the third time, the breakthrough time achieved at was 55, 56.2, 42.3 and 53.6 min and exhaustion time occurred at 270, 231, 157.5 and 186.4 min. After three cycles of sorption, desorption and regeneration, there was a modest decline in the metal uptake at the exhaustion times which were 49.94, 50.76, 56.38 and 53.87 % for Cd, Cu, Pb and Zn, respectively. It means the regenerated modified MMBB was still able to remove heavy metal ions even after the third cycle with moderately similar removal efficiency (Table 7.1). Nonetheless a decrease in the total amount of heavy metal removal was probably due to possible biosorbent damage.

Table 7.1 also shows that some heavy metal ions are irreversibly bound to the surface of modified MMBB. The desorption efficiency amounts decreased when the the number of cycles rose from 48.08, 47.61, 57.37 and 45.88 % in the first cycle to 22.80, 23.69, 34.44 and 23.80 % in the third cycle for Cd, Cu, Pb and Zn. Biosorption and desorption efficiency progressively decreased, as the biosorption and desorption cycles continued as reported by Bulgariu and Bulgariu (2016).

Figure 7.4 indicates the desorption curves obtained for Cd, Cu, Pb and Zn. These unsymmetrical–shaped desorption curves are very similar. The initial metal concentration increase is followed by a flatter reduction in that within the first 30 min, the maximum concentration peak was achieved for all heavy metal ions in the first 10 min. The advantage of applying acidic eluent with a higher desorption rate was reported by Martín–Lara et al. (2016). Moreover, from these desorption profiles, the maximum concentration peak, C_p (mg/L), in which the eluted metal concentration reached to its maximum value at the time of t_p (min) can be measured. The peak information provides a clue to the elution rate. Besides, the overall sorption process concentration factor (CF_p) is calculated as C_p divided by the inlet metal concentration. This term implies the factor by which the metal concentration increases compared to its initial concentration in the influent. Therefore, in order to desorb the maximum quantity of metal within a short time or a low effluent volume, CF_p should be high as possible (Martín–Lara et al., 2016).
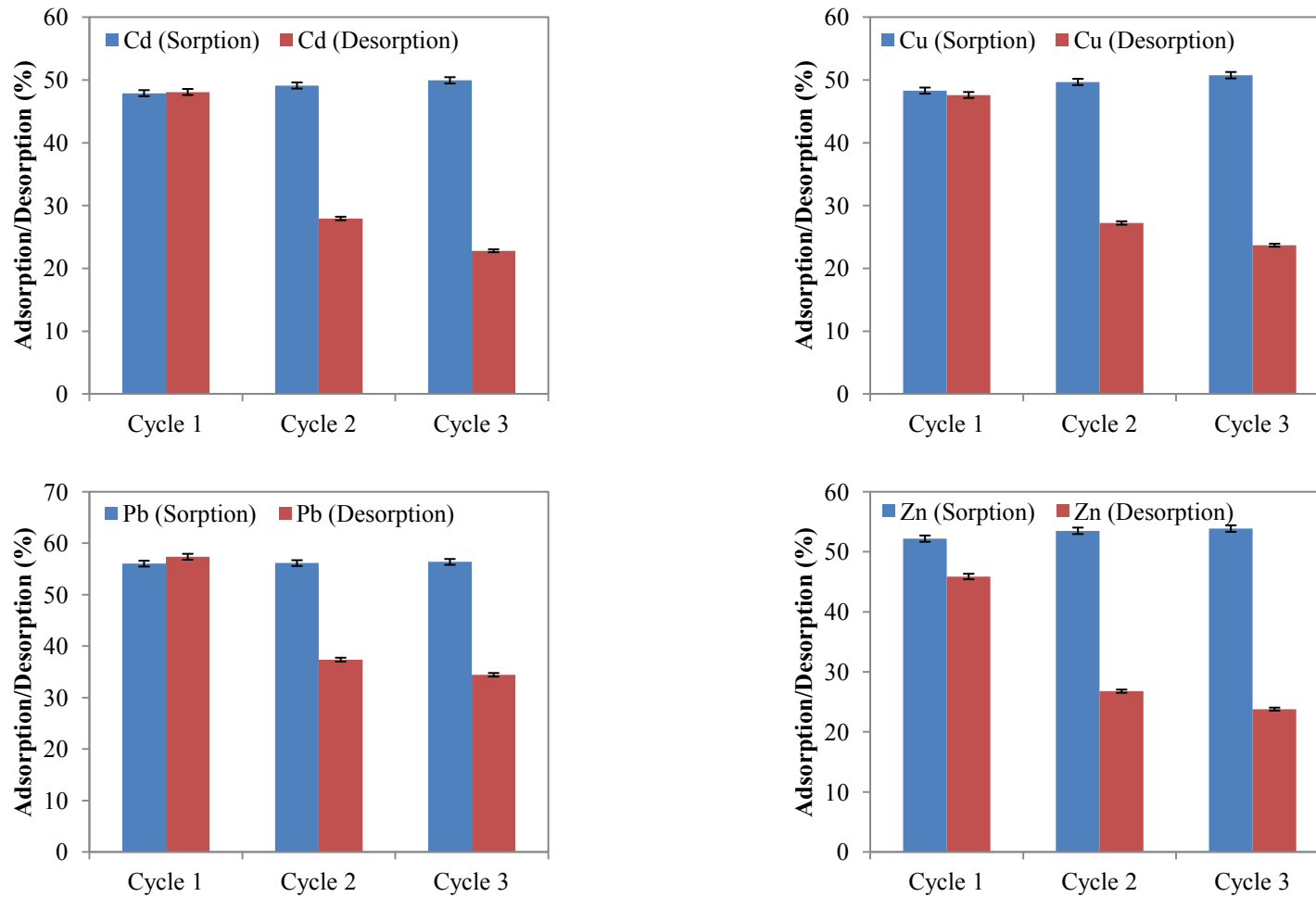
Figure 7.3 Performance of modified–MMBB packed–bed column in three successive cycles of sorption, desorption and regeneration (sample size N = 2)
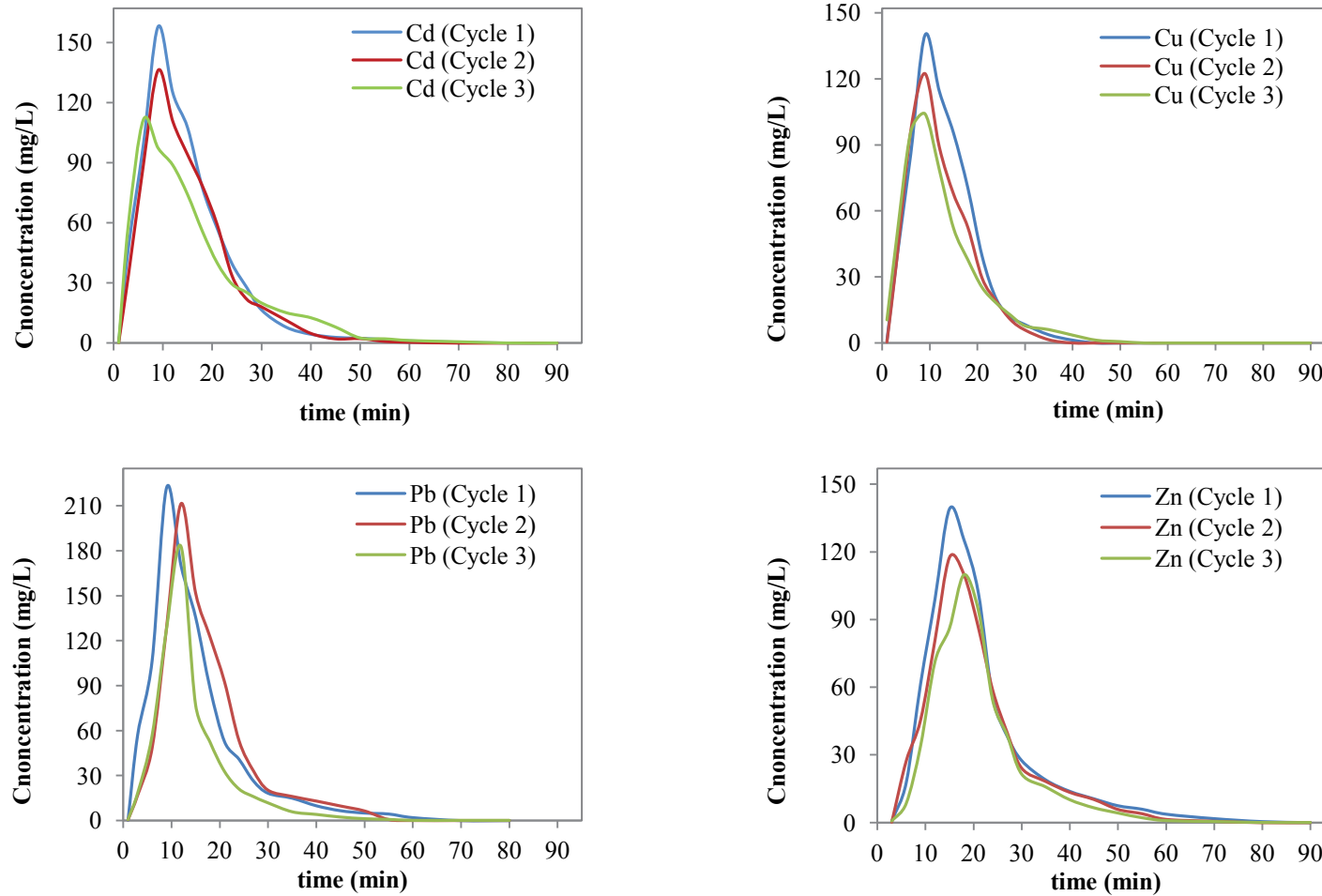
Figure 7.4 Desorption kinetic of Cd, Cu, Pb and Zn adsorbed on modified MMBB (10 g , desorption solution = 0.1 M HCl, flow rate = 10 mL/min)

Table 7.1 Desorption parameters for three cycles of biosorption and desorption cycles with municipal wastewater

Metal	Cycle	t_b (min)	t_{sat} (min)	q_i (mg/g)	q_c (mg/g)	$q_{e,d}$ (mg/g)	%R	%E	t_p (min)	C_p (mg/L)	CF_p*
Cd	1	82.4	423	0	9.58	4.61	47.90	48.08	9	157.94	8.08
	2	65	322.7	4.97	9.82	4.13	49.12	27.94	9	129.16	6.61
	3	55	270	5.69	9.90	3.57	49.94	22.80	7	111.35	5.70
Cu	1	75	261.7	0	9.66	4.60	48.30	47.61	9	139.82	7.05
	2	60	235	5.06	9.94	4.08	49.69	27.22	10	124.33	6.27
	3	56.2	231	5.85	10.15	3.79	50.76	23.69	9	117.6	5.93
Pb	1	51.6	171.4	0	11.21	6.43	56.04	57.37	8	223.40	10.99
	2	48	166.2	4.78	11.23	5.98	56.14	37.38	12	211.42	10.40
	3	42.3	157.5	5.24	11.28	5.69	56.38	34.44	11	182.67	8.99
Zn	1	83.8	201.7	0	10.44	4.79	52.20	45.88	15	139.07	6.63
	2	63.7	195	5.65	10.70	4.38	53.50	26.79	14	117.61	5.61
	3	53.6	186.4	6.32	10.77	4.07	53.87	23.80	18	109.82	5.23

*$CF_p = C_p/C_i$

7.4   *Conclusions*

Chapter 7 investigated heavy metal removal by modified MMBB fixed–bed column from real wastewater. The results clearly demonstrated that it was feasible to eliminate Cd, Cu, Pb and Zn from municipal wastewater in a dynamic adsorption system.

Desorption studies by 0.1M HCl showed that the reusability of modified MMBB is feasible. After three cycles of sorption, desorption and regeneration of metal–loaded modified–MMBB, the metal uptake at the exhaustion time slightly decreased from 49.94, 50.76, 56.38 to 53.87 % for Cd, Cu, Pb and Zn, respectively. Column regeneration experiment by using 0.1M $CaCl_2$ within three successive cycles of sorption, desorption and regeneration demonstrated that modified MMBB could serve as a viable low–cost potential biosorbent for the removal of Cd(II), Cu(II), Pb(II) and Zn(II) ions from aqueous solution in a continuous column mode. Calcium chloride can increase the stability and reusability of MMBB.

Chapter 8

Conclusions and Recommendations

Chapter 8 Conclusions and recommendations

The previous Chapters provide insights into different aspects of developing a lignocellulosic multi–metal binding biosorbent (MMBB) for cadmium, copper, lead and zinc removal from multi–metal solutions in both batch and continuous modes. Initially two different biosorbent combinations were used for heavy metal biosorption and then the better MMBB with considering its maximum batch biosorption capacity was selected for detailed analyses on further optimization, characterization and application in continuous fixed–bed column for real wastewater. The overall concluding remarks of this thesis, the unsolved problems, and the direction for future studies are major contents of Chapter 8.

8.1   *Conclusion remarks*

A novel multi–metal binding biosorbent (MMBB) was developed by combining a group of three from the selective natural lignocellulosic agro–industrial wastes and by–products for effectively eliminating cadmium, copper, lead and zinc from aqueous solutions. Two MMBBs with different combinations (MMBB1: tea waste, maple leaves, mandarin peels and MMBB2: tea waste, corncob and sawdust) were selected among eighteen lignocellulosic biosorbents. Both combinations indicated the highest biosorption capacity at pH of 5.5±0.1 when the other conditions were similar. FTIR analysis for characterizing the MMBBs explored that these MMBBs contains more functional groups available and mainly carboxyl and hydroxyl groups were responsible for metal binding. Comparing these two MMBBs for heavy metal removal from synthetic solution revealed that MMBB1 showed higher maximum biosorption capacities of 41.48, 39.48, 94.00 and 27.23 mg/g for Cd(II), Cu(II), Pb(II) and Zn(II), respectively. The monolayer adsorption capacity of MMBB2 were 31.73, 41.06, 76.25 and 26.63 mg/g for Cd(II), Cu(II), Pb(II) and Zn(II), respectively. In addition, the kinetic study demonstrated that heavy metal biosorption onto MMBB1 and MMBB2 was rapid, and the equilibrium reached within first hour. The Pseudo–second order model most satisfactorily described the kinetic data, suggesting the dominance of chemisorptions mechanism. Furthermore, NaCl and HCl were successfully used as eluent for desorption process of metal–loaded MMBB1 and MMBB2, respectively. Their sorption

capability after five cycles of sorption and desorption still remained excellent without remarkable change.

MMBB1 was selected for further experiments on optimization in terms of terms of influence of temperature, chemical modification, biosorbent ratio in the combination, biosorbent drying temperature, ionic strength in the solution and biosorbent particle size. The results helped to understand the possible mechanism and characterization analysis before and after metal sorption. The solution containing sodium hydroxide, calcium chloride and ethanol were more effective than the other chemical and physical pretreatment to improve the biosorptive potential of MMBB1. Its maximum biosorption capacity which calculated by Langmuir isotherm were 69.56, 127.70, 345.20 and 70.55 mg/g for Cd(II), Cu(II), Pb(II) and Zn(II), respectively. The ionic strength only has a slight effect on cadmium, copper, lead and zinc removal at lower Na^+ concentration (0.1 M) by modified MMBB regardless of heavy metal concentrations. The calculated thermodynamic parameters showed feasible, spontaneous and exothermic biosorption process. Desorption studies by more eluent agents confirmed 0.1M HCl was more effective for desorption and $CaCl_2$ could successfully regenerate and improve the biosorbent structural damage after each desorption step. Moreover, mass loss of biosorbent decreased only 18% with regeneration while without regeneration step, it was 32%. SEM/EDS analysis confirmed that the variance in intensity of K, Na and Ca peaks might be due to ion exchange mechanism of metal uptake. According to calculated B_{D-R} for Cd, Cu, Pb and Zn, E values show physical adsorption or ion exchange for four metal removal process whose calculated values are 2.58, 3.45, 5.59 and 2.73 kJ/mol for Cd, Cu, Pb and Zn respectively which are all less than 8 kJ/mol.

Continuous biosorption system in a fixed–bed column found to performs feasible to eliminate Cd, Cu, Pb and Zn from synthetic and real wastewater. Thomas, Dose Response and Yoon–Nelson models satisfactorily interpret the experimental breakthrough curves under varying conditions of effluent flow rate, feed concentration and biosorbent bed height. Taking into account the results from Thomas model, it would seem that the dynamic adsorption capacity of modified–MMBB fixed–bed column increased with a lower flow rate, a higher bed

depth, and a higher feed metal concentration. The highest metal adsorption capacity of modified MMBB at the exhaustion time was 38.25, 63.37, 108.12 and 35.23 mg/g for Cd, Cu, Pb and Zn, respectively. The bed depth service time (BDST) model was used to scale–up the continuous sorption experiments as well. The critical bed depth of Cd, Cu, Pb and Zn uptake were 8.64, 1.90, 3.21 and 7.43 cm, respectively. Also, the depth of adsorption was predicted accurately about 19 cm by BDST model. The results obtained from column regeneration showed that the reusability of modified MMBB was feasible and modified MMBB could efficiently remove cadmium, copper, lead and zinc from industrial wastewater after three cycles of sorption/ desorption/ regeneration.

The batch and column experiments presented that the alkaline treated multi–metal binding biosorbent can be successfully used for large scale treatment of industrial wastewater due to the abundant availability worldwide, low cost, simple processing and unique physical characteristics.

8.2   *Future outlook*

The present research provided an initial glimpse into the possibilities of using a novel multi–metal binding biosorbent combining different types of biomasses for heavy metal removal from aqueous solutions. Furthermore, it identified the influences of operation conditions on biosorbents' performance in batch and continuous experiments for synthetic and real municipal wastewater.

Process improvements via optimization of influential factors, characterization and kinetic, thermodynamic and equilibrium isotherm studies are necessary. This is not only for finding how suitable, efficient and economically friendly this breakthrough biosorbent is but also for further studies in a column for real wastewater and to verify the experimental models. Then the following improvements are suggested for future work:

- Future research needs to explore other combinations of agro–industrial wastes and by–products for the removal of heavy metal ions that have good adsorption capacities.

- Rather than chemical surface modifications, biological surface modifications can be considered to improve the biomass bindings in the combination and to improve the surface structure and selectivity

- More studies on characterization approaches can be took into account to help understanding the biosorption mechanism.

- More trials need to extend the application of multi–metal binding biosorbents in pilot–scale fixed–bed columns which have more relevance to real operating systems. The reason is dealing with several problems such as non–uniform distribution of the flow, selective flow path or uneven packing in a large packed–bed column.

- A technique can develop this kind of studies for efficient extraction methods and heavy metal recovery after desorption and biosorbent regeneration (e.g. through electrochemical techniques such as electro–winning).

References

References

Abbas, S.H., Ismail, I.M., Mostafa, T.M., 2014. Abbas H. Sulaymon, 2014. Biosorption of Heavy Metals: A Review. Journal of Chemical Science and Technology 3, 74–102.

Abdel–Raouf, M.S., Abdul–Raheim, A.R.M., 2017. Removal of Heavy Metals from Industrial Waste Water by Biomass-Based Materials: A Review, Journal of Pollution Effects and Control 5 180–193.

Achak, M., Hafidi, A., Ouazzani, N., Sayadi, S., Mandi, L., 2009. Low cost biosorbent "banana peel" for the removal of phenolic compounds from olive mill wastewater: Kinetic and equilibrium studies. Journal of Hazardous Materials 166, 117–125.

Acheampong, M.A., Pakshirajan, K., Annachhatre, A.P., Lens P.N.L., 2013. Removal of Cu(II) by biosorption onto coconut shell in fixed–bed column systems Journal of Industrial and Engineering Chemistry 19, 841–848.

Adamczuk, A., Kołodynska, D., 2015. Equilibrium, thermodynamic and kinetic studies on removal of chromium, copper, zinc and arsenic from aqueous solutions onto fly ash coated by chitosan. Chemical Engineering Journal 274, 200–212.

Ahmad, A., Rafatullah, M., Sulaiman, O., Ibrahim, M.H., Hashim, R., 2009. Scavenging behaviour of meranti sawdust in the removal of methylene blue from aqueous solution. Journal of Hazardous Materials 170, 357–365.

Ahmed, M.J.K., Ahmaruzzaman, M., 2016. A review on potential usage of industrial waste materials for binding heavy metal ions from aqueous solutions. Journal of Water Process Engineering 10, 39–47.

Akar, S.T., Arslan, S., Alp, T., Arslan, D., Akar, T., 2012. Biosorption potential of the waste biomaterial obtained from *Cucumis melo* for the removal of Pb^{2+} ions from aqueous media: Equilibrium, kinetic, thermodynamic and mechanism analysis. Chemical Engineering Journal 185–186, 82–90.

Akar, T., Tosun, I., Kaynak, Z., Ozkara, E., Yeni, O., Sahin, E.N., Akar, S.T., 2009. An attractive agro–industrial by–product in environmental cleanup: Dye biosorption potential of untreated olive pomace. Journal of Hazardous Materials 166, 1217–1225.

Aksu, Z., Çağatay, Ş.Ş., Gönen F., 2007. Continuous fixed–bed biosorption of reactive dyes by dried *Rhizopus arrhizus*: Determination of column capacity. Journal of Hazardous Materials 143, 362–371.

Alencar, W.S., Acayanka, E., Lima, E.C., Royer, B., de Souza, F.E., Lameira, J., Alves, C.N., 2012. Application of Mangifera indica (mango) seeds as a biosorbent for removal of Victazol Orange 3R dye from aqueous solution and study of the biosorption mechanism. Chemical Engineering Journal 209, 577–588.

Alomá, I., Martín–Lara, M.A., Rodríguez, I.L., Blázquez, G., Calero, M., 2012. Removal of nickel(II) ions from aqueous solutions by biosorption on sugarcane bagasse. Journal of the Taiwan Institute of Chemical Engineers 43, 275–281.

Amarasinghe, B.M.W.P.K., Williams, R.A., 2007. Tea waste as a low cost adsorbent for the removal of Cu and Pb from wastewater. Chemical Engineering Journal 132, 299–309.

Anastopoulos, I., Massas I., Ehaliotis, C., 2013. Composting improves biosorption of Pb^{2+} and Ni^{2+} by renewable lignocellulosic materials. Characteristics and mechanisms involved. Chemical Engineering Journal 231, 245–254.

Ansari, A.A., Gill, S.S., Gill, R., Lanza, G.R., Newman, L., 2014. Phytoremediation: Management of Environmental Contaminants, Springer.

Antunes, W., Luna, A., Henriques, C., da Costa, A.C., 2003. An evaluation of copper biosorption by a brown seaweed under optimized conditions. Electronic Journal of Biotechnology 6, 174–184.

Asadi, F., Shariatmadari, H., Mirghaffari, N., 2008. Modification of rice hull and sawdust sorptive characteristics for remove heavy metals from synthetic solutions and wastewater. Journal of Hazardous Materials 154, 451–458.

Asberry, H.B., Kuo, C.Y., Gung, C.H., Conte, E.D., Suen, S.Y., 2014. Characterization of water bamboo husk biosorbents and their application in heavy metal ion trapping. Microchemical Journal 113, 59–63.

Asgher, M., Bhatti, H.N., 2012. Removal of reactive blue 19 and reactive blue 49 textile dyes by citrus waste biomass from aqueous solution: equilibrium and kinetic study. The Canadian Journal of Chemical Engineering 90, 412–419.

Aydın, H., Bulut, Y., Yerlikaya, Ç., 2008. Removal of copper(II) from aqueous solution by adsorption onto low–cost adsorbents. Journal of Environmental Management 87, 37–45.

Bansal, M., Garg, U., Singh, D., Garg, V.K., 2009. Removal of Cr(VI) from aqueous solutions using pre–consumer processing agricultural waste: A case study of rice husk. Journal of Hazardous Materials 162, 312–320.

Baral, S.S., Das, N., Ramulu, T.S., Sahoo, S.K., Das, S.N., Chaudhury, G.R., 2009. Removal of Cr(VI) by thermally activated weed *Salvinia cucullata* in a fixed–bed column. Journal of Hazardous Materials 161, 1427–1435.

Batzias, F.A., Sidiras, D.K., 2007. Simulation of methylene blue adsorption by salts–treated beech sawdust in batch and fixed–bed systems. Journal of Hazardous Materials 149, 8–17.

Belala, Z., Jeguirim, M., Belhachemi, M., Addoun, F., Trouvé, G., 2011. Biosorption of basic dye from aqueous solutions by Date Stones and Palm–Trees Waste: Kinetic, equilibrium and thermodynamic studies. Desalination 271, 80–87.

Bennani, K.A., Mounir, B., Hachkar, M., Bakasse, M., Yaacoubi, A., 2015. Adsorption of cationic dyes onto Moroccan clay: Application for industrial wastewater treatment, Journal of Materials and Environmental Science 6, 2483–2500.

Beolchini, F., Pagnanelli, F., Toro, L., Veglio, F., 2006. Ionic strength effect on copper biosorption by Sphaerotilusnatans: equilibrium study and dynamic modeling in membrane reactor. Water Research 40, 144–152.

Bernardo, G.R., Rene R.M., Ma Catalina, A.D.T., 2009. Chromium(III) uptake by agro–waste biosorbents: chemical characterization, sorption–desorption studies, and mechanism. Journal of Hazardous Materials 170, 845–854.

Bhatnagar, A., Sillanpää, M., Witek–Krowiak A., 2015. Agricultural waste peels as versatile biomass for water purification – A review. Chemical Engineering Journal 270, 244–271.

Bhatnagar, A., Sillanpää, M., 2010. Utilization of agro–industrial and municipal waste materials as potential adsorbents for water treatment—A review. Chemical Engineering Journal 157, 277–296.

Bilal, M., Shah, J.A., Ashfaq, T., Gardazi, S.M.H., Tahir, A.A., Pervez, A., Haroon, H., Mahmood, Q., 2013. Waste biomass adsorbents for copper removal from industrial wastewater—A review. Journal of Hazardous Materials 263, 322–333.

Blázquez, G., Calero, M., Hernáinz, F., Tenorio, G., Martín–Lara, M.A., 2010. Equilibrium biosorption of lead(II) from aqueous solutions by solid waste from olive–oil production. Chemical Engineering Journal 160, 615–622.

Blázquez, G., Hernáinz, F., Calero, M., Martín–Lara, M.A., Tenorio, G., 2009. The effect of pH on the biosorption of Cr(III) and Cr (VI) with olive stone. Chemical Engineering Journal 148, 473–479.

Brandão, P.C., Souza, T.C., Ferreira, C.A., Hori, C.E., Romanielo, L.L., 2010. Removal of petroleum hydrocarbons from aqueous solution using sugarcane bagasse as adsorbent. Journal of Hazardous Materials 175, 1106–1112.

Bulgariu, D., Bulgariu L., 2016. Potential use of alkaline treated algae waste biomass as sustainable biosorbent for clean recovery of cadmium(II) from aqueous media: batch and column studies. Journal of Cleaner Production 112, 4525–533.

Bulut, Y., Tez, Z., 2007. Removal of heavy metals from aqueous solution by sawdust adsorption. Journal of Environmental Sciences, 19, 160–166.

Bulut, Y., Baysal, Z., 2006. Removal of Pb(II) from wastewater using wheat bran. Journal of Environmental Management 78, 107–113.

Cagnon, B., Py, X., Guillot, A., Stoeckli, F., Chambat, G., 2009. Contributions of hemicellulose, cellulose and lignin to the mass and the porous properties of chars and steam activated carbons from various lignocellulosic precursors. Bioresource Technology 100, 292–298.

Calero, M., Pérez, A., Blázquez, G., Ronda, A., Martín–Lara, M.A., 2013. Characterization of chemically modified biosorbents from olive tree pruning for the biosorption of lead. Ecological Engineering 58, 344–354.

Carolin, C.F., Kumar, P.S., Saravanan, A., Joshiba, G.J., Naushad, M., 2017. Efficient techniques for the removal of toxic heavy metals from aquatic environment: A review. Journal of Environmental Chemical Engineering 5, 2782–2799.

Cay, S., Uyanik, A., Ozasik, A., 2004. Single and binary component adsorption on copper(II) and cadmium(II) from aqueous solution using tea industry waste. Seperation and Purification Technology 38, 273–280.

Chao, H.P., Chang, C.C., Nieva, A., 2014. Biosorption of heavy metals on Citrus maxima peel, passion fruit shell, and sugarcane bagasse in a fixed–bed column. Journal of Industrial and Engineering Chemistry 20, 3408–3414.

Chatterjee, A., Schiewer, S., 2014. Multi–resistance kinetic models for biosorption of Cd by raw and immobilized citrus peels in batch and packed–bed columns. Chemical Engineering Journal 244, 105–116.

Chen, S., Yue, Q., Gao, B., Li, Q., Xu, X., Fu, K., 2012. Adsorption of hexavalent chromium from aqueous solution by modified corn stalk: A fixed–bed column study. Bioresource Technology 113, 114–120.

Chen, J.P., Yang, L., 2005. Chemical modification of *Sargassum* sp. for prevention of organic leaching and enhancement of uptake during metal biosorption. Industrial and Engineering Chemistry Research 44, 9931–9942.

Christoforidis, A.K., Orfanidis, S., Papageorgiou, S.K., Lazaridou, A.N., Favvas, E.P., Mitropoulos, A.Ch., 2015. Study of Cu(II) removal by Cystoseira crinitophylla biomass in batch and continuous flow biosorption. Chemical Engineering Journal 277, 334–340.

Chu, K.H., 2004. Improved fixed–bed models for metal biosorption. Chemical Engineering Journal 97, 233–239.

Crini, G., 2006. Non–conventional low–cost adsorbents for dye removal: A review. Bioresource Technology 97, 1061–1085.

Cruz–Olivares, J., Pérez–Alonso, C., Barrera–Díaz, C., Ureña–Nuñez, F., Chaparro–Mercado, M.C., Bilyeu, B., 2013. Modeling of lead(II) biosorption by residue of allspice in a fixed–bed column. Chemical Engineering Journal 228, 21–27.

Cui, J., Zhang, L., 2008. Metallurgical recovery of metals from electronic waste: a review. Journal of Hazardous Materials 158, 228–256.

Das, N., Das, D., 2013. Recovery of rare earth metals through biosorption: An overview. Journal of Rare Earths 31 (10), 933–943.

Ding, D., Zhao, Y., Yang, S., Shi, W., Zhang, Z., Lei, Z., Yang, Y., 2013. Adsorption of cesium from aqueous solution using agricultural residue e Walnut shell: Equilibrium, kinetic and thermodynamic modeling studies. Water Research 47, 2563–2571.

Ding, Y., Jing, D., Gong, H., Zhou, L., Yan, X., 2012. Biosorption of aquatic cadmium(II) by unmodified rice straw. Bioresource Technology 114, 20–25.

Farooq, U., Kozinski, J. A., Ain Khan, M., Athar M., 2010. Biosorption of heavy metal ions using wheat based biosorbents – A review of the recent literature. Bioresource Technology 101, 5043–5053.

Febrianto, J., Kosasih, A.N., Sunarso, J., Ju, Y.–H., Indraswati, N., Ismadji, S., 2009. Equilibrium and kinetic studies in adsorption of heavy metals using biosorbent: A summary of recent studies. Journal of Hazardous Materials 162, 616–645.

Feng, N., Guo, X., Liang, S., Zhu, Y., Liu, J., 2011. Biosorption of heavy metals from aqueous solutions by chemically modified orange peel. Journal of Hazardous Materials 185, 49–54.

Feng, N., Guo, X., Liang, S., 2009a. Adsorption study of copper(II) by chemically modified orange peel. Journal of Hazardous Materials 164, 1286–1292.

Feng, N., Guo, X., Liang, S., 2009b. Kinetic and thermodynamic studies on biosorption of Cu(II) by chemically modified orange peel. Transactions of Nonferrous Metals Society of China 19, 1365–1370.

Fiol, N., Villaescusa, I., Martínez, M., Miralles, N., Poch, J., Serarols, J., 2006. Sorption of Pb(II), Ni(II), Cu(II) and Cd(II) from aqueous solution by olive stone waste. Separation and Purification Technology, 50, 132–140.

Fu, H.Z., Wang, M.H., Ho, Y.S., 2013. Mapping of drinking water research: A bibliometric analysis of research output during 1992–2011. Science of The Total Environment 443, 757–65.

Fu, F., Wang, Q., 2011. Removal of heavy metal ions from wastewaters: A review. Journal of Environmental Management 92, 407–418.

Gadd, GM., 2009a. Heavy metal pollutants: environmental and biotechnological aspects. In:Schaechter M (ed) Encyclopedia of microbiology, 3rd ed. Elsevier, Oxford, 321–334.

Gadd, G.M., 2009b. Biosorption: critical review of scientific rationale, environmental importance and significance for pollution treatment. Journal of Chemical Technology and Biotechnology 84 (1), 13–28.

Garg, U., Kaur, M.P., Jawa, G.K., Sud, D., Garg, V.K., 2008. Removal of cadmium(II) from aqueous solutions by adsorption on agricultural waste biomass. Journal of Hazardous Materials 154, 1149–1157.

Gautam, R.K., Mudhoo, A., Lofrano, G., Chattopadhyaya, M.C., 2014. Biomass–derived biosorbents for metal ions sequestration: Adsorbent modification and activation methods and adsorbent regeneration. Journal of Environmental Chemical Engineering 2, 239–259.

Gong, R., Ding, Y., Liu, H., Chen, Q., Liu, Z., 2005. Lead biosorption and desorption by intact and pretreated *spirulina maxima* biomass. Chemosphere 58, 125–130.

Guimarães Gusmão, K.A., Alves Gurgel, L.V., Sacramento Melo, T.M., Gil, L.F., 2012. Application of succinylated sugarcane bagasse as adsorbent to remove methylene blue and gentian violet from aqueous solutions – Kinetic and equilibrium studies. Dyes and Pigments, 92, 967–974.

Gundogdu, A., Ozdes, D., Duran, C., Bulut, V.N., Soylak, M., Senturk, H.B., 2009. Biosorption of Pb(II) ions from aqueous solution by pine bark (*Pinus brutia* Ten.). Chemical Engineering Journal 153, 62–69.

Guo, W.S., Ngo, H.H., 2012.Chapter 6: Membrane Processes for Wastewater Treatment,in: Zhang, T.C., Surampalli, R.Y., Vigneswaran, S., Tyagi, R.D., Ong, S.L. and Kao, C.M. (Eds.), Membrane Technology and Environmental Applications.American Society of Civil Engineers (ASCE), USA, pp. 169–216.

Gupta, V.K., Carrott, P.J.M., Carrott, M.M.L.R., Suhas., 2009. Low–Cost Adsorbents: Growing Approach to Wastewater Treatment—a Review. Critical Reviews in Environmental Science and Technology 39, 783–842.

Gupta, V.K., Imran, Ali S., Saini, V.K., 2004. Removal of rhodamine B, fast green, andmethylene blue from wastewater using red mud, an aluminum industry waste. Industrialand Engineering Chemistry Research 43, 1740–1747.

Gurgel, L.V.A., Gil, L. F., 2009. Adsorption of Cu(II), Cd(II) and Pb(II) from aqueous single metal solutions by succinylated twice–mercerized sugarcane bagasse functionalized with triethylenetetramine. Water Reseach 43, 4479–4488.

Gutiérrez–Segura, E.,Solache–Ríos, M., Colín–Cruz, A., Fall, C., 2014. Comparison of Cadmium Adsorption by Inorganic Adsorbents in Column Systems. Water, Air, & Soil Pollution 225, 1–9.

Hameed, B.H., 2008. Equilibrium and kinetic studies of methyl violet sorption by agricultural waste. Journal of Hazardous Materials 154, 204–212

Hameed, B.H., 2009a. Grass waste: A novel sorbent for the removal of basic dye from aqueous solution. Journal of Hazardous Materials 166, 233–238.

Hameed, B.H., 2009b. Spent tea leaves: A new non–conventional and low–cost adsorbent for removal of basic dye from aqueous solutions. Journal of Hazardous Materials 161, 753–759.

Han, R., Wang, Y., Yu, W., Zou, W., Shi, J., Liu, H., 2007. Biosorption of methylene blue from aqueous solution by rice husk in a fixed–bed column. Journal of Hazardous Materials 141, 713–718.

Haq, I., Bhatti, H.N., Asgher, M., 2011. Removal of solar red BA textile dye from aqueous solution by low cost barley husk: equilibrium, kinetic and thermodynamic study. The Canadian Journal of Chemical Engineering 89, 593–600.

Homagai, P.L., Ghimire, K.N., Inoue, K., 2010. Adsorption behavior of heavy metals onto chemically modified sugarcane bagasse. Bioresource Technology 101, 2067–2069.

Hossain, M.A., Ngo, H.H., Guo, W.S., Nghiem, L.D., Hai, F.I., Vigneswaran, S., Nguyen, T.V., 2014. Competitive adsorption of metals on cabbage waste from multi–metal solutions. Bioresource Technology 160, 79–88.

Hossain, M.A., Ngo, H.H., Guo, W.S., Setiadi, T., 2012. Adsorption and desorption of copper(II) ions onto garden grass. Bioresource Technology 121, 386–395.

Huang, J., Yuan, F., Zeng, G., Li, X., Gu, Y., Shi, L., Liu, W., Shi, Y., 2017. Influence of pH on heavy metal speciation and removal from wastewater using micellar-enhanced ultrafiltration. Chemosphere 173, 199–206.

Izquierdo, M., Gabaldón, C., Marzal, P., Álvarez–Hornos F.J., 2010, Modeling of copper fixed–bed biosorption from wastewater by *Posidonia oceanica.* Bioresource Technology 101, 510–517.

Jain, M., Garg, V.K., Kadirvelu, K., 2013. Cadmium(II) sorption and desorption in a fixed–bed column using sunflower waste carbon calcium–alginate beads. Bioresource Technology 129, 242–248.

Kalavathy, M.H., Miranda, L.R., 2010. Moringa oleifera–A solid phase extractant for the removal of copper, nickel and zinc from aqueous solutions. Chemical Engineering Journal 158, 188–199.

Khan, M.A., Ngabura, M., Choong, T.S.Y., Masood, H., Chuah, L.A., 2012. Biosorption and desorption of Nickel on oil cake: Batch and column studies. Bioresource Technology 103, 35–42.

Kazemipour, M., Ansari, M., Tajrobehkar, S., Majdzadeh, M., Kermani, H.R., 2008. Removal of lead, cadmium, zinc, and copper from industrial wastewater by carbon developed from walnut, hazelnut, almond, pistachio shell, and apricot stone. Journal of Hazardous Materials 150, 322–327.

Khoramzadeh, E., Nasernejad, B., Halladj, R., 2013. Mercury biosorption from aqueous solutions by Sugarcane Bagasse. Journal of the Taiwan Institute of Chemical Engineers 44, 266–269.

Kim, N., Park, M., Park, D., 2014. A new efficient forest biowaste as biosorbent for removal of cationic heavy metals. Bioresource Technology 175C, 629–632.

Krishnani, K.K., Meng, X., Christodoulatos, C., Boddu, V.M., 2008. Biosorption mechanism of nine different heavy metals onto biomatrix from rice husk. Journal of Hazardous Materials 153, 1222–1234.

Kubicek, C.P., 2012. Fungi and Lignocellulosic Biomass. Wiley–Blackwell, John Wiley & Sons, Inc., Publication, New Jersey.

Kumar, R., Sharma, R.K., Singh, A. P., 2017. Cellulose based grafted biosorbents – Journey from lignocellulose biomass to toxic metal ions sorption applications – A review. Journal of Molecular Liquids 232, 62–93.

Kumar, P.S., Ramalingam, S., Abhinaya, R.V., Kirupha, S.D., Vidhyadevi, T., Sivanesan, S., 2012. Adsorption Equilibrium, Thermodynamics, Kinetics, Mechanism and Process Design of Zinc(II) ions onto Cashew Nut Shell. The Canadian Journal of Chemical Engineering 90, 973–982.

Kumar, P.S., Ramalingam, S., Kirupha, S.D., Murugesan, A., Vidhyadevi, T., Sivanesan, S., 2011. Adsorption behavior of nickel(II) onto cashew nut shell: Equilibrium, thermodynamics, kinetics, mechanism and process design. Chemical Engineering Journal 167, 122–131.

Leyva–Ramos, R., Landin–Rodriguez, L.E., Leyva–Ramos, S., Medellin–Castillo, N.A., 2012. Modification of corncob with citric acid to enhance its capacity for adsorbing cadmium(II) from water solution. Chemical Engineering Journal 180, 113–120.

Liang, S., Guo, X., Feng, N., Tian, Q., 2009a. Adsorption of Cu^{2+} and Cd^{2+} from aqueous solution by mercapto–acetic acid modified orange peel. Colloids and Surfaces B: Biointerfaces 73, 10–14.

Liang, S., Guo, X., Feng, N., Tian, Q., 2009b. Application of orange peel xanthate for the adsorption of Pb^{2+} from aqueous solutions. Journal of Hazardous Materials 170, 425–429.

Liu, C., Ngo, H.H., Guo, W., Tung, K.L., 2012. Optimal conditions for preparation of banana peels, sugarcane bagasse and watermelon rind in removing copper from water. Bioresource Technology 119, 349–354.

Long, Y., Lei, D., Ni, J., Ren, Z., Chen, C., Xu H., 2014. Packed bed column studies on lead(II) removal from industrial wastewater by modified *Agaricus bisporus*. Bioresource Technology 152, 457–463.

Loukidou, M.X., Zouboulis, A.I., Karapantsios, T.D., Matis, K.A., 2004. Equilibrium and kinetic modeling of chromium(VI) biosorption by *Aeromonas caviae*. Colloids and Surfaces A: Physicochemal and Engineering Aspects 242, 93–104.

Madrakian, T., Afkhami, A., Ahmadi, M., 2012. Adsorption and kinetic studies of seven different organic dyes onto magnetite nanoparticles loaded tea waste and removal of them from wastewater samples. Spectrochimica acta Part A: Molecular and Biomolecular Spectroscopy 99, 102–109.

Martín–Lara, M.A., Blázquez, G., Calero, M., Almendros, A.I., Ronda, A., 2016. Binary biosorption of copper and lead onto pine cone shell in batch reactors and in fixed–bed columns. International Journal of Mineral Processing 148, 72–82.

Martín–Lara, M.A., Blázquez, G., Ronda, A., Rodríguez, I.L., Calero, M., 2012. Multiple biosorption–desorption cycles in a fixed–bed column for Pb(II) removal by acid–treated olive stone. Journal of Industrial and Engineering Chemistry 18, 1006–1012.

Martín–Lara, M.Á., Rico, I.L.R., Vicentem, I.d.l.C.A., García, G.B., de Hoces, M.C., 2010. Modification of the sorptive characteristics of sugarcane bagasse for removing lead from aqueous solutions. Desalination 256, 58–63.

Mata, Y.N., Blázquez, M.L., Ballester, A., González, F., Munoz, J.A., 2010. Studies on sorption, desorption, regeneration and reuse of sugar–beet pectin gels for heavy metal removal. Journal of Hazardous Materials 178, 243–248.

Mata, Y.N., Blázquez, M.L., Ballester, A., González, F., Munoz, J.A., 2009. Sugar–beet pulp pectin gels as biosorbent for heavy metals: Preparation and determination of biosorption and desorption characteristics. Chemical Engineering Journal 150, 289–301.

Mehta, K., Gaur, J.P., 2005. Use of algae for removing heavy metal ions from wastewater: progress and prospects. Critical Reviews in Biotechnology 25, 113–152.

Mavioglu Ayan, E., Secim, P., Karakaya, S., Yanik, J., 2012. Oreganum Stalks as a New Biosorbent to Remove Textile Dyes from Aqueous Solutions. CLEAN – Soil, Air, Water, 40, 856–863.

Miretzky, P., Cirelli, A.F., 2010. Cr(VI) and Cr(III) removal from aqueous solution by raw and modified lignocellulosic materials: A review. Journal of Hazardous Materials 180, 1–19.

Montazer–Rahmati, M.M., Rabbani, P., Abdolali, A., Keshtkar, A.R., 2011. Kinetics and equilibrium studies on biosorption of cadmium, lead, and nickel ions from aqueous solutions by intact and chemically modified brown algae. Journal of Hazardous Materials 185, 401–407.

Muhamad, H., Doan, H., Lohi, A., 2010. Batch and continuous fixed–bed column biosorption of Cd^{2+} and Cu^{2+}. Chemical Engineering Journal 158, 369–377.

Naddafi, K., Nabizadeh, R., Saeedi, R., Mahvi, A.H., Vaezi, F., Yaghmaeian, K., Ghasri, A., Nazmara, S., 2007. Biosorption of lead(II) and cadmium(II) by protonated *Sargassum glaucescens* biomass in a continuous packed bed column. Journal of Hazardous Materials 147, 785–791.

Nadeem, R., Hanif, M.A., Shaheen, F., Perveen, S., Zafar, M.N., Iqbal, T., 2008. Physical and chemical modification of distillery sludge for Pb(II) biosorption. Journal of Hazardous Materials 150, 335–342.

Nguyen, T.A.H, 2015. Removal and recovery of phosphorus from municipal wastewater by adsorption coupled with crystallization by (Doctor of Philosophy thesis). University of Technology, Sydney (UTS), Sydney, Australia.

Nguyen, T.A.H., Ngo, H.H., Guo, W.S, Nguyen, T.V., Zhang, J., Liang, S., Chen, S.S., Nguyen, N.C. 2014. A comparative study on different metal–loaded soybean milk by–product 'okara' for biosorption of phosphorus from aqueous solution. Bioresource Technology 169, 291–298.

Njikam, E., Schiewer, S., 2012. Optimization and kinetic modeling of cadmium desorption from citrus peels: A process for biosorbent regeneration. Journal of Hazardous Materials 213–214, 242–248.

Nur, T., 2014. Nitrate, phosphate and fluoride removal from water using adsorption process (Doctor of Philosophy thesis). University of Technology, Sydney, NSW, Australia.

O'Connell, D.W., Birkinshaw, C., O'Dwyer, T.F., 2008. Heavy metal adsorbents prepared from the modification of cellulose: A review. Bioresource Technology 99, 6709–6724.

Ofomaja, A.E. Naidoo, E.B., 2011. Biosorption of copper from aqueous solution by chemically activated pine cone: A kinetic study. Chemical Engineering Journal 175, 260–270.

Ofomaja, A.E., 2011. Kinetics and pseudo–isotherm studies of 4–nitrophenol adsorption onto mansonia wood sawdust. Industrial Crops and Products 33, 418–428.

Ohura, S., Harada, H., Biswas, B.K., Kondo, M., Ishikawa, S., Kawakita, H., Ohto, K., Inoue, K., 2011. Phosphorus recovery from secondary effluent and side–stream liquid in a sewage treatment plant using zirconium–loaded saponified orange waste. Journal of Material Cycles and Waste Management 13, 293–297.

Okochi, N.C., 2013. Phosphorus removal from storm water using electric ARC furnace steel slag (Doctor of Philosophy thesis). University of Regina, Saskatchewan, Canada.

Oliveira, R.C., Hammer, P., Guibal, E., Taulemesse, J.M., Garcia Jr.,O., 2014. Characterization of metal–biomass interactions in the lanthanum(III) biosorption on *Sargassum* sp. using SEM/EDX, FTIR, and XPS: Preliminary studies. Chemical Engineering Journal 239, 381–391.

Ozdes, D., Gundogdu, A., Kemer, B., Duran, C., Senturk, H.B., Soylak, M., 2009. Removal of Pb(II) ions from aqueous solution by a waste mud from copper mine industry: Equilibrium, kinetic and thermodynamic study. Journal of Hazardous Materials 166, 1480–1487.

Pagnanelli, F., Jbari, N., Trabucco, F., Martínez, M.E., Sánchez, S., Toro, L., 2014. Biosorption–mediated reduction of Cr(VI) using heterotrophically–grown Chlorella vulgaris: Active sites and ionic strength effect, Chemical Engineering Journal 231, 94–102.

Palumbo, A. J., Daughney, C.J., Slade, A. H., Glover, C. N., 2013. Influence of pH and natural organic matter on zinc biosorption in a model lignocellulosic biofuel biorefinery effluent. Bioresource Technology 146, 169–175.

Pan, B., Pan, B., Zhang, W., Lv, L., Zhang, Q., Zheng, S., 2009. Development of polymeric and polymer–based hybrid adsorbents for pollutants removal from waters. Chemical Engineering Journal 151, 19–29.

Parab, H., Sudersanan, M., Shenoy, N., Pathare, T., Vaze, B., 2009. Use of Agro–Industrial Wastes for Removal of Basic Dyes from Aqueous Solutions. CLEAN – Soil, Air, Water, 37, 963–969.

Patil, D.S., Chavan, S.M., Oubagaranadin, J.K.U., 2016. A review of technologies for manganese removal from wastewaters. Journal of Environmental Chemical Engineering 4, 468–487.

Pehlivan, E., Altun, T., Parlayici, Ş., 2012. Modified barley straw as a potential biosorbent for removal of copper ions from aqueous solution. Food Chemistry 135, 2229–2234.

Pehlivan, E., Tran, H.T., Ouédraogo, W.K.I., Schmidt, C., Zachmann, D., Bahadir, M., 2013. Sugarcane bagasse treated with hydrous ferric oxide as a potential adsorbent for the removal of As(V) from aqueous solutions. Food Chemistry 138, 133–138.

Pehlivan, E., Altun, T., Parlayici, Ş., 2012. Modified barley straw as a potential biosorbent for removal of copper ions from aqueous solution. Food Chemistry 135, 2229–2234.

Peng, W., Li, H., Liu, Y., Song, S., 2017. A review on heavy metal ions adsorption from water by graphene oxide and its composites. Journal of Molecular Liquids 230, 496–504.

Pereira, F.V., Gurgel, L.V.A., Gil, L.F., 2010. Removal of Zn^{2+} from aqueous single metal solutions and electroplating wastewater with wood sawdust and sugarcane bagasse modified with EDTA dianhydride (EDTAD). Journal of Hazardous Materials 176, 856–863.

Pérez Marín, A.B., Aguilar, M.I., Meseguer, V.F., Ortuño, J.F., Sáez, J., Lloréns, M., 2009. Biosorption of chromium(III) by orange (Citrus cinensis) waste: Batch and continuous studies. Chemical Engineering Journal 155, 199–206.

Pessoa deFranca, F., Tavares, A.P.M., Augusto daCosta, A.C., 2002. Calcium interference with continuous biosorption of zinc by Sargassum sp. (*Phaeophyceae*) in tubular laboratory reactors. Bioresource Technology 99, 1896–1903.

Prado, A.G.S., Moura, A.O., Holanda, M.S., Carvalho, T.O., Andrade, R.D.A., Pescara, I.C., de Oliveira, A.H.A., Okino, E.Y.A., Pastore, T.C.M., Silva, D.J., Zara, L.F., 2010. Thermodynamic aspects of the Pb adsorption using Brazilian sawdust samples: Removal of metal ions from battery industry wastewater. Chemical Engineering Journal 160, 549–555.

Rangabhashiyam, S., Anu, N., Selvaraju, N. 2013. Sequestration of dye from textile industry wastewater using agricultural waste products as adsorbents. Journal of Environal Chemal Engineering 1, 629–641.

Raval, N.P., Shah, P.U., Shah, N.K., 2016. Adsorptive removal of nickel(II) ions from aqueous environment: A review. Journal of Environmental Management 179, 1–20.

Reddy, D.H.K., Seshaiah, K., Reddy, A.V.R., Lee, S.M., 2012. Optimization of Cd(II), Cu(II) and Ni(II) biosorption by chemically modified *Moringa oleifera* leaves powder. Carbohydrate Polymers 88, 1077– 1086.

Riazi, M., Keshtkar, A.R., Moosavian M.A., 2016. Biosorption of Th(IV) in a fixed–bed column by Ca–pretreated *Cystoseira indica*. Journal of Environmenta Chemical Engineering 4, 1890–1898.

Rocha, C.G., Zaia, D.A.M., Alfaya, R.V.d.S., Alfaya, A.A.d.S., 2009. Use of rice straw as biosorbent for removal of Cu(II), Zn(II), Cd(II) and Hg(II) ions in industrial effluents. Journal of Hazardous Materials 166, 383–388.

Ronda, A., Calero, M., Blázquez, G., Pérez, A., Martín–Lara, M.A., 2015. Optimization of the use of a biosorbent to remove heavy metals: Regeneration and reuse of exhausted biosorbent A. Journal of the Taiwan Institute of Chemical Engineers 51, 109–118.

Ronda, A., Martín–Lara, M.A., Calero, M., Blázquez, G., 2013. Analysis of the kinetics of lead biosorption using native and chemically treated olive tree pruning, Ecological Engineering 58, 278– 285.

Roy, A., Chakraborty, S., Kundu, S.P., Adhikari, B., Majumder, S.B., 2013. Lignocellulosic jute fibre as a bioadsorbent for the removal of azo dye from its aqueous solution: Batch and column studies. Journal of Applied Polymer Science 129, 15–27.

Rudnicki, P., Hubicki, Z., Kołodynska, D., 2014. Evaluation of heavy metal ions removal from acidic waste water streams. Chemical Engineering Journal 252, 362–373.

Saad, S.A., Isa, K.M., Bahari, R., 2010. Chemically modified sugarcane bagasse as a potentially low–cost biosorbent for dye removal. Desalination 264, 123–128.

Safa, Y., Bhatti, H.N., Bhatti, I.A., Asgher, M., 2011. Removal of direct Red–31 and direct Orange–26 by low cost rice husk: Influence of immobilisation and pretreatments. The Canadian Journal of Chemical Engineering 89, 1554–1565.

Santos, S., Ungureanu, G., Boaventura, R., Botelho, C., 2015. Selenium contaminated waters: An overview of analytical methods, treatment options and recent advances in sorption methods. Science of the Total Environment 521–522, 246–260.

Saha, T., Kumar, S., Bhaumik, S.K., 2017. Slip–enhanced flow through thin packed column withsuperhydrophobic wall. Sensors and Actuators B: hemical 240, 468–476.

Saha, P.D., Chakraborty, S., Chowdhury, S., 2012. Batch and continuous (fixed–bed column) biosorption of crystal violet by Artocarpus heterophyllus (jackfruit) leaf powder. Colloids and Surfaces B: Biointerfaces 92, 262–270.

Schiewer, S., Balaria, A., 2009. Biosorption of Pb^{2+} by original and protonated citrus peels: Equilibrium, kinetics, and mechanism. Chemical Engineering Journal 146, 211–219.

Schiewer, S., Patil, S.B., 2008. Pectin–rich fruit wastes as biosorbents for heavy metal removal: Equilibrium and kinetics. Bioresource Technology 99, 1896–1903.

Schiewer, S., Wong, M.H., 2000. Ionic strength effects in biosorption of metals by marine algae. Chemosphere, 41, 271–282.

Schiewer, S., Volesky, B., 1997. Ionic strength and electrostatic effects in biosorption of divalent metal ions and protons. Environmental Science and Technology 31, 2478–2485.

Šćiban, M., Radetić, B., Kevrešan, Ž., Klašnja, M., 2007. Adsorption of heavy metals from electroplating wastewater by wood sawdust. Bioresource Technology 98, 402–409.

Sha, L., Xueyi, G., Ningchuan, F., Qinghua, T., 2009. Adsorption of Cu^{2+} and Cd^{2+} from aqueous solution by mercapto–acetic acid modified orange peel. Colloids and Surfaces B: Biointerfaces73, 10–14.

Shanmugaprakash, M., Sivakumar, V., 2015. Batch and fixed–bed column studies for biosorption of Zn(II) ions onto pongamia oil cake (*Pongamia pinnata*) from biodiesel oil extraction. Journal of Environmental Management 164, 161–170.

Singha, B., and Das, S.K., 2011. Biosorption of Cr (VI) ions from aqueous solutions: Kinetics, equilibrium, thermodynamics and desorption studies. Colloids and Surfaces B: Biointerfaces 84, 221–232.

Sousa, F.W., Oliveira, A.G., Ribeiro, J.P., Rosa, M.F., Keukeleire, D., Nascimento, R.F., 2010. Green coconut shells applied as adsorbent for removal of toxic metal ions using fixed–bed column technology. Journal of Environmental Management 91, 1634–1640.

Sriamornsak, P., 2003. Chemistry of pectin and its pharmaceutical uses: A review. Silpakorn University International Journal 3(1–2), 206–228.

Stasinakis, A.S., Elia, I., Petalas, A.V., Halvadakis, C.P., 2008. Removal of total phenols from olive–mill wastewater using an agricultural by–product, olive pomace. Journal of Hazardous Materials 160, 408–413.

Sud, D., Mahajan, G., Kaur, M.P., 2008. Agricultural waste material as potential adsorbent for sequestering heavy metal ions from aqueous solutions –A review. Bioresource Technology 99, 6017–6027.

Tan, G., Yuan, H., Liu, Y., Xiao, D., 2010. Removal of lead from aqueous solution with native and chemically modified corncobs. Journal of Hazardous Materials 174, 740–745.

Tan, G., Xiao, D., 2009. Adsorption of cadmium ion from aqueous solution by ground wheat stems. Journal of Hazardous Materials 164, 1359–1363.

Tang, Y., Chen, L., Wei, X., Yao, Q., Li, T., 2013. Removal of lead ions from aqueous solution by the dried aquatic plant, Lemna perpusilla Torr. Journal of Hazardous Materials 244–245, 603–612.

Tobis, J., Vortmeyer, D., 1991. Scale–up Elects due to near–wall channelling in isothermal adsorption columns: on the limitations in the Use of Plug Flow Models. Chemical Engineering and Proressing 29, 147–153.

Tobis, J., Vortmeyer, D., 1988. The near-wall channelling effect on isothermal constant-pattern adsorption. Chemical Engineerng Science 43 (6), 1363–1369.

Torab–Mostaedi, M., Asadollahzadeh, M., Hemmati, A., Khosravi, A., 2013. Equilibrium, kinetic, and thermodynamic studies for biosorption of cadmium and nickel on grapefruit peel. Journal of the Taiwan Institute of Chemical Engineers 44, 295–302.

Tunali Akar, S., Arslan, S., Alp, T., Arslan, D., Akar, T., 2012. Biosorption potential of the waste biomaterial obtained from Cucumis melo for the removal of Pb^{2+} ions from aqueous media: Equilibrium, kinetic, thermodynamic and mechanism analysis. Chemical Engineering Journal 185–186, 82–90.

Tunali Akar, S., Gorgulu, A., Akar, T., Celik, S., 2011. Decolorization of Reactive Blue 49 contaminated solutions by Capsicum annuum seeds: Batch and continuous mode biosorption applications. Chemical Engineering Journal 168, 125–133.

Velazquez–Jimenez, L.H., Pavlick, A., Rangel–Mendez, J.R., 2013. Chemical characterization of raw and treated agave bagasse and its potential as adsorbent of metal cations from water. Industrial Crops and Products, 43, 200–206.

Vargas–García, M.C., López, M.J., Suárez–Estrella, F., Moreno, J., 2012. Compost as a source of microbial isolates for the bioremediation of heavy metals: *Invitro* selection. Science of the Total Environment 431, 62–67.

Vijayaraghavan, K., Balasubramanian, R., 2015. Is biosorption suitable for decontamination of metal-bearing wastewaters? A critical review on the state-of-the-art of biosorption processes and future directions. Journal of Environmental Management 160, 283–296.

Vilar, V.J.P., Botelho C.M.S., Boaventura, R.A.R. 2005. Influence of pH, ionic strength and temperature on lead biosorption by Gelidiumand agar extraction algal waste. Process Biochemistry 4, 3267–3275.

Volesky, B., 2007. Biosorption and me. Water Research 41, 4017–4029.

Wahab, M.A., Jellali, S., Jedidi, N., 2010. Ammonium biosorption onto sawdust: FTIR analysis, kinetics and adsorption isotherms modeling. Bioresource Technology 101, 5070–5075.

Wan Ngah, W.S., Hanafiah, M.A.K.M., 2008. Removal of heavy metal ions from wastewater by chemically modified plant wastes as adsorbents: A review. Bioresource Technology 99, 3935–3948.

Wang, Y., Gao, B.Y., Yue, W.W., Yue, Q. Y., 2007. Adsorption kinetics of nitrate from aqueous solutions onto modified wheat residue. Colloids and Surfaces A: Physicochemal and Engineering Aspects 308, 1–5.

Witek–Krowiak, A., 2012. Analysis of temperature–dependent biosorption of Cu^{2+} ions on sunflower hulls: Kinetics, equilibrium and mechanism of the process. Chemical Engineering Journal 192, 13–20.

Witek–Krowiak, A., Szafran, R.G., Modelski, S., 2011. Biosorption of heavy metals from aqueous solutions onto peanut shell as a low–cost biosorbent. Desalination 265, 126–134.

Won, S.W., Kotte, P., Wei, W., Lim, A., Yun, Y.S., 2014. Biosorbents for recovery of precious metals. Bioresource Technology 160, 203–212.

Xu, F., Zhu, T.T., Rao, Q.Q., Shui, S.W., Li, W.W, He, H.B., Yao, R.S., 2017. Fabrication of mesoporous lignin–based biosorbent from rice straw and its application for heavy–metal–ion removal. Journal of Environmental Sciences 53, 132–140.

Xu, C., Arancon, R.A.D., Labidi, J.,Luque, R., 2014. Lignin Depolymerisation Strategies: Towards Valuable Chemicals and Fuels. Chemical Society Reviews 43 (22), 7485–7500.

Xu, X., Gao, Y., Gao, B., Tan, X., Zhao, Y.–Q., Yue, Q., Wang, Y., 2011. Characteristics of diethylenetriamine–crosslinked cotton stalk/wheat stalk and their biosorption capacities for phosphate. Journal of Hazardous Materials 192, 1690–1696.

Xu, X., Gao, B.Y., Yue, Q.Y., Zhong, Q. Q., 2010. Preparation of agricultural by–product based anion exchanger and its utilization for nitrate and phosphate removal. Bioresource Technology 101, 8558–8564.

Yao, L., Ye, Z.F., Tong, M.P., Lai, P., Ni, J.R., 2009. Removal of Cr^{3+} from aqueous solution by biosorption with aerobic granules. Journal of Hazardous Materials 165, 250–255.

Yargıç, A.S., R.Z., Yarbay Sahin, Ozbay, N., Onal, E., 2014. Assessment of toxic copper(II) biosorption from aqueous solution by chemically–treated tomato waste (*Solan*um lycopersicum). Journal of Cleaner Production 88,152–159.

Zafar, M.N., Aslam, I., Nadeem, R., Munir, S., Rana, U.A., Khan, S.U.D., 2014. Characterization of chemically modified biosorbents from rice bran for biosorption of Ni(II). Journal of Taiwan Institute of Chemical Engineers 46(1), 82–88.

Curriculum Vitae

ATEFEH ABDOLALI

School of Civil and Environmental Engineering, University of Technology, Sydney (UTS)
P.O. Box 123 Broadway, Ultimo, NSW 2007, Australia
Email: [   ]@gmail.com

EDUCATION

University of Technology Sydney (UTS), Sydney, Australia   **2012–2016**
PhD in Environmental Engineering
Thesis Subject: Detoxification of heavy metal ions from aqueous solutions using a novel lignocellulosic multi–metal binding biosorbent

University of Tehran, Tehran, Iran   **2006–2008**
Master of Science in Chemical Engineering
Thesis Subject: Biosorption of heavy metal ions from aqueous solutions by different species of brown algae of the Oman Sea

University of Tehran, Tehran, Iran   **2001–2006**
Bachelor of Science in Chemical Engineering
Thesis Subject: The principles of scale–up and design of fluidized bed from bench scale to pilot scale

WORK HISTORY

ASYN Steel Engineering Co, Tehran, Iran   **2009–2011**
Junior process engineer

Iran Mineral Research and Application Company, Tehran, Iran   **2008–2009**
Graduate engineer

Tehran Refinery, Tehran, Iran   **2004**
Trainee in ISOMAX Unit

PROFESSIONAL MEMBERSHIP

- Life member of International Forum on Industrial Bioprocesses (IFIBiop)
- Centre for Technology in Water and Wastewater (CTWW), University of Technology, Sydney (UTS)

LANGUAGE AND COMPUTER SKILLS

- Native Farsi language
- Proficient in written and oral English
- Satisfactory knowledge of speaking and reading French
- Proficient in MS Office (Word, Excel, Power Point, visio), Hysys, Aspen Plus, AutoCAD, EndNote, C++ and MATLAB

PUBLICAIONS

Book chapter
- Book Chapter: Water production and wastewater treatment, ISBN 978–1–61728–503–5, Chapter 4; Biosorption of Cd(II) and Ni(II) from aqueous solutions by *Cystoseira indica*, Nova Science Publishers, Inc. (2010).

Journal papers
- Application of a breakthrough biosorbent for removing heavy metals from synthetic and real wastewaters in a lab–scale continuous fixed–bed column. Bioresource Technology 229, 2017, 78–87.
- A breakthrough biosorbent in removing heavy metals: equilibrium, kinetic, thermodynamic and mechanism analyses in a lab–scale study. Science of the Total Environment 542, 2016, 603–611.
- Characterization of a multi–metal binding biosorbent: chemical modification and desorption studies. Bioresource Technology, 2015,193, 477–487.
- Typical lignocellulosic wastes and by–products for biosorption process in water and wastewater treatment: a critical review. Bioresource Technology, 160, 2014, 57–66
- Development and evaluation of new multi–metal biding biosorbent. Bioresource Technology, 160, 2014, 98–106.
- Kinetics and equilibrium studies on biosorption of cadmium, lead, and nickel ions from aqueous solutions by intact and chemically–modified brown algae, Journal of Hazardous Materials, 185 (1), 2011, 401–407.
- Biosorption of Cd(II) and Ni(II) ions from aqueous solution by raw and pre–treated *Cystoseira indica* algae, Journal of Chemical and Petroleum Engineering, University of Tehran, 43 (1), 2009, 37–45.

Conference papers
- Poster presentation in ESBES–IFIBiop Conference, Lille, France (2014)
- Oral presentation in the 6[th]International Conference on the Challenges in Environmental Science and Engineering (CESE–2013), Daegu, Korea (2013)
- Oral presentation in Proceedings of Iran International Aluminium Conference, Arak, Iran (2012)
- Oral presentation in 8th World Congress of Chemical Engineering, Montreal, Canada (2009)
- Oral presentation in First International Conference on Advances in Wastewater Treatment and Reuse, Tehran, Iran (2009)

HOBBIES

Painting (oil color and water color), running and reading book

REFERNCES

- Prof. Dr. Huu Hao Ngo
  School of Civil and Environmental Engineering, University of Technology, Sydney (UTS), Australia
  Email: HuuHao.Ngo@uts.edu.au

- A/Prof. Dr Manouchehr Haghighi
  University of Adelaide, Australia
  Email: mhaghighi@asp.adelaide.edu.au